AD-A178 625 COORDINATED RESEARCH PROGRAM IN PULSED POWER PHYSICS (U) TEXAS TECH UNIV LUBBOCK DEPT OF ELECTRICAL ENGINEERING 16 FEB 87 ARO-21056.34-PH AFOSR-84-0032 1/2

UNCLASSIFIED F/G 10/2 NL

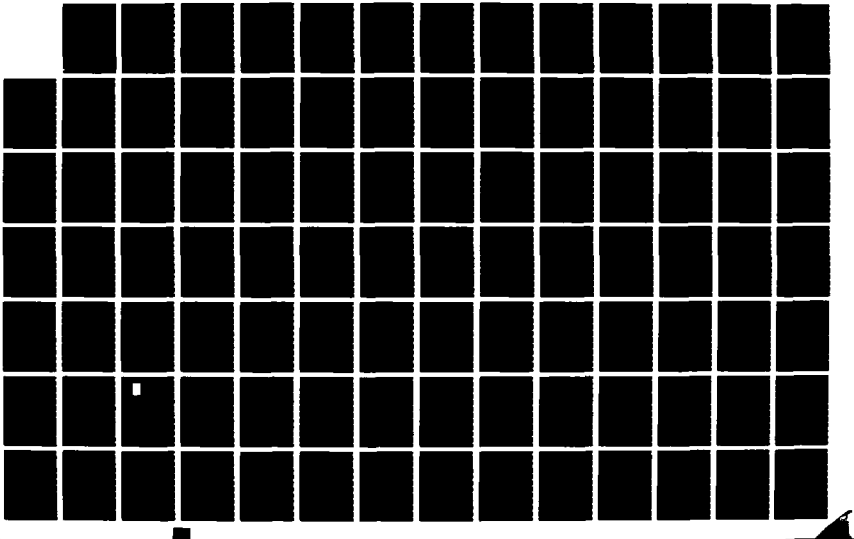

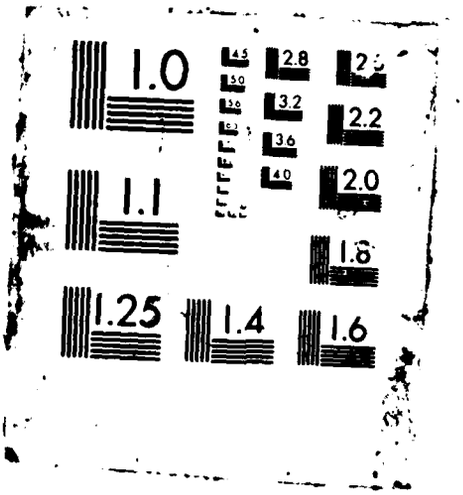
1.0
1.1
1.25
1.4
1.6
2.8
3.2
3.6
4.0
2.2
2.0
1.8

FINAL REPORT
on

# COORDINATED RESEARCH PROGRAM
# in
# PULSED POWER PHYSICS



February 16, 1987

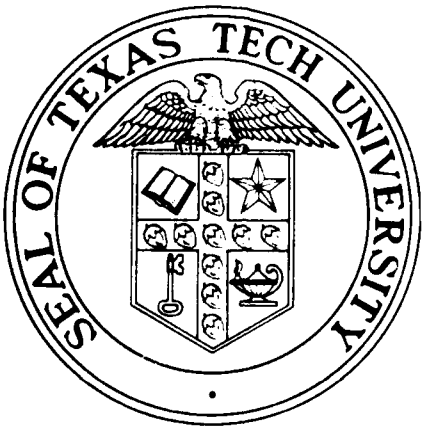


Air Force Office of Scientific Research
Grant No. 84-0032
and
U.S. Army Research Office
MIPR/ARO 100-86





PULSED POWER LABORATORY

Department of Electrical Engineering
TEXAS TECH UNIVERSITY

Lubbock, Texas 79409

UNCLASSIFIED

SECURITY CLASSIFICATION OF THIS PAGE (When Data Entered)

| REPORT DOCUMENTATION PAGE | | READ INSTRUCTIONS BEFORE COMPLETING FORM |
|---|---|---|
| 1. REPORT NUMBER<br>ARO 21056.34-PH | 2. GOVT ACCESSION NO.<br>N/A | 3. RECIPIENT'S CATALOG NUMBER<br>N/A |
| 4. TITLE (and Subtitle)<br>Coordinated Research Program in Pulsed Power Physics | | 5. TYPE OF REPORT & PERIOD COVERED<br>Final Technical Report<br>Sept. 30, 1985 - Sept. 30, 1986 |
| | | 6. PERFORMING ORG. REPORT NUMBER |
| 7. AUTHOR(s) | | 8. CONTRACT OR GRANT NUMBER(s)<br>Proposal No. 21056-PH<br>Funding Doc. MIPR-ARO 100-86 |
| 9. PERFORMING ORGANIZATION NAME AND ADDRESS<br>Texas Tech University<br>Dept. of Electrical Engineering<br>Lubbock, TX 79409-4439 | | 10. PROGRAM ELEMENT, PROJECT, TASK AREA & WORK UNIT NUMBERS |
| 11. CONTROLLING OFFICE NAME AND ADDRESS<br>U. S. Army Research Office<br>Post Office Box 12211<br>Research Triangle Park, NC 27709 | | 12. REPORT DATE<br>16 February, 1987<br>13. NUMBER OF PAGES<br>185 |
| 14. MONITORING AGENCY NAME & ADDRESS(if different from Controlling Office)<br>N/A | | 15. SECURITY CLASS. (of this report)<br>Unclassified<br>15a. DECLASSIFICATION/DOWNGRADING SCHEDULE |

16. DISTRIBUTION STATEMENT (of this Report)

Approved for public release; distribution unlimited.

17. DISTRIBUTION STATEMENT (of the abstract entered in Block 20, if different from Report)

NA

18. SUPPLEMENTARY NOTES

The view, opinions, and/or findings contained in this report are those of the author(s) and should not be construed as an official Department of the Army position, policy, or decision, unless so designated by other documentation.

19. KEY WORDS (Continue on reverse side if necessary and identify by block number)

Pulsed Power, Diffuse Discharges, Opening Switches, Laser Triggering, Surface Discharges, Field Distortion, Streak Photography, X-Ray Triggering.

20. ABSTRACT (Continue on reverse side if necessary and identify by block number)

The work on three program elements, related to pulsed power research, is described. The program is a multi-investigator program whose main emphasis is on gaining a better understanding of repetitive opening and closing switch phenomena. Some effort has been given to studies of electrode erosion and insulator damage in high power closing switches. A few exploratory ideas and concept were also investigated.

DD FORM 1 JAN 73 1473 EDITION OF 1 NOV 65 IS OBSOLETE

UNCLASSIFIED

SECURITY CLASSIFICATION OF THIS PAGE (When Data Entered)

# Final Report

# on

# COORDINATED RESEARCH PROGRAM

# IN

# PULSED POWER PHYSICS

AFOSR Grant #84-0032
MIPR/ARO 100-86

February 16, 1987



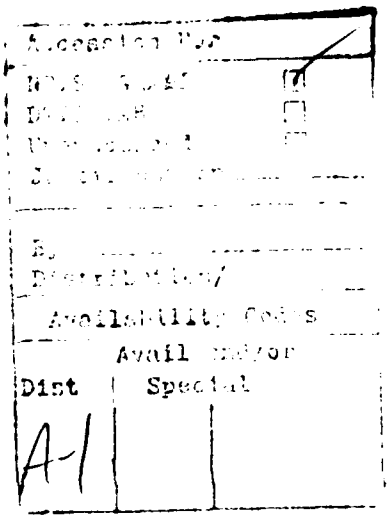


Program Director: M. Kristiansen

Principal Investigators:
K. Ikuta
M. Kristiansen
H. Krompholz
G. Schaefer
K. Schoenbach
P.F. Williams

Associate Investigator: L. Hatfield

Research Associate: K. Zinsmeyer

Administrative Secretary: M. Byrd

Technician: K. Rathbun

Graduate Students:
R. Cooper
R. Curry
A. Donaldson
H. Harjes
G. Hutcheson
M. Ingram
R. Korzekwa
B. Pashaie
P. Ranon
D. Skaggs
E. Strickland
L. Thurmond

## TABLE OF CONTENTS

## INTRODUCTION

The Coordinated Research Program in Pulsed Power Physics is a multi-investigator program involving 6 Principal Investigators, 1 Associate Investigator and 11 Graduate Students. Other faculty investigators from Electrical Engineerings, Physics and Chemistry, also interacted and cooperated at various times. The program is jointly sponsored by AFOSR and ARO. Some 8 refereed journal articles and 16 conference proceedings papers were published during the 27 month contract period. Several other papers were prepared and two Journal papers have recently been submitted for publication. All of the papers listed in the Faculty Publication section are reproduced in the Appendices. The main projects are Opening Switches, Spark Gap and Arc Discharge Investigations, and Exploratory Concepts.

# SUMMARY OF RESEARCH OBJECTIVES

for

October 1984 - January 1987

## OPENING SWITCHES

I. Investigation of repetitive e-beam controlled discharges with respect to the influence of different gas properties such as attachment rate coefficient, drift velocity, and Penning ionization. - Modeling of diffuse discharges, including control mechanisms.

II. Investigations of the interaction of discharge and circuit for discharge pulses with short risetimes.

III. Investigation of optogalvanic effects with respect to their use as discharge control mechanisms.

IV. Studies of concepts for optically assisted, externally sustained, diffuse discharge switches.

## SPARK GAP AND ARC DISCHARGE INVESTIGATIONS

V. Studies of the limitations on high current, high energy switches resulting from electrode erosion.

VI. Investigation of x-ray ionization of switch gases.

VII. Investigation of insulator performance when subjected to repetitive surface discharge switching.

## EXPLORATORY CONCEPTS

VIII. A new approach to field distortion triggering of spark gaps.

IX. Design, construction, and testing of two different high voltage line-type pulsers.

X. An electromagnetic method for injecting a projectile into a mass driver.

# OPENING SWITCHES

(G. Schaefer, K.H. Schoenbach, H. Krompholz,
M. Kristiansen, B.E. Strickland, R.A. Korzekwa,
D. Skaggs, G.Z. Hutcheson, and K.R. Rathbun)

## I. Summary of the Investigations of Repetitive E-Beam Controlled Discharges

The primary objective of this work is to study control processes in externally sustained or controlled diffuse discharges, with respect to their application as opening switches. Concepts for diffuse discharge opening switches have been developed, experimental facilities have been assembled and experiments have been performed to investigate the applicability of these concepts. Computer codes have been developed and applied to different systems to allow optimization and scaling.

The major research areas during the research period 1984/87 in the field of diffuse discharge opening switches were:

- concepts for diffuse discharge opening switches (Section II)
- the electron-beam sustained diffuse discharge (Section III)
- the optically controlled diffuse discharge, where optical control either means increased conductivity of the discharge by means of laser radiation or optical stimulation of loss processes (Section IV).

For the investigation of the electron-beam sustained discharge an apparatus was designed, operated, and improved, which allows investigations of repetitive opening in the time range of 100 ns at current levels of up to 10 kA.

Experiments performed with this device concentrated on investigation on the influence of specific gas properties on the characteristic and the transient behavior of the discharges.

The investigations on optical control processes concentrated on two mechanisms:

1) photodetachment

2) photoenhanced attachment

and their influence on the characteristics of externally and self sustained discharges.

## II. Opening Switch Concepts

(G. Schaefer and K.H. Schoenbach)

The development and evaluation of new switch concepts and the utilization of new processes for external discharge control was a permanent issue during the entire research period. Individual processes considered in the last two years are presented in the next two sections. A general overview of the field of diffuse discharge opening switches is presented in a review article which has been published in IEEE Transactions on Plasma Sciences (Appendix A). A short review was also presented at the IEEE Pulsed Power Conference, 1985 (Appendix B).

## III. E-Beam Controlled Diffuse Discharge Switch

(G. Schaefer, K.H. Schoenbach, H. Krompholz, M. Kristiansen, B.E. Strickland, R.A. Korzekwa, D. Skaggs, and G. Hutcheson)

The work on electron beam sustained discharges for switching applications concentrated on three gas properties of the gas mixtures used in diffuse discharge switches: 1) the attachment rate coefficient, 2) the drift velocity, and 3) Penning ionization.

1) To achieve low losses during conduction (at low E/N) and fast opening and high hold-off voltage (at high E/N) attachers have to be used with an attachment rate coefficient increasing with E/N. Gas mixtures containing such attachers show an increased resistivity with increasing E/N. If the attachment rate increases strongly with E/N, a negative differential conductivity is also found. This effect was, for example, found in gases recommended by the group of L.G. Christophorou at Oak Ridge National Laboratories, such as gas mixtures with Argon and $CH_4$ as buffer gases and admixtures of attachers, such as $CF_4$, $C_2F_6$, and $C_3F_8$. The experimental results with these gases were presented at two conferences (Appendices C and D).

Although such a characteristic has advantages for the closed phase and for the opening phase, it can cause several problems. One is the development of striations in the intermediate E/N range. This effect is discussed in a 1985 IEEE Pulsed Power Conference presentation (Appendix E).

Another effect is the interaction of an element with negative differential conductivity with a high impedance circuit. Investigations concerning this effect were presented in one of the 1985 IEEE Pulsed Power Conference presentations (Appendix B) and in a paper in Applied Physics Letters (Appendix F). The most recent results have also been presented at the BEAMS '86 Conference (Appendix G).

An additional possibility to shape the discharge characteristic is to use two attachers with attachment cross sections at different energies. Several gas mixtures were proposed and investigated (Appendices H and I).

A third effect investigated is the interaction of the electron source (e-beam) with the attachers used in the gas discharge. This effect is discussed in two conference proceedings papers (Appendices B and C).

2) The influence of the drift velocity on the switch performance was investigated in gas mixtures containing Argon, Nitrogen and an attacher. These results are submitted for presentation at the ICPIG 1987 (Appendix J).

3) The addition of a Penning additive to the switch gas can increase the ionization efficiency of the electron beam. The Penning additive, however, was also found to reduce the breakdown strength of the gas mixture. These results will be presented at the 1987 Gaseous Dielectrics Conference (Appendix K).

We are also preparing a comprehensive paper on the "Optimization of Gas Mixtures for Electron Beam Sustained Diffuse Discharge Switches" which can be used as a design guideline for switches for different applications (Appendix L).

## IV. Optically Controlled Discharges

(G. Schaefer, K.H. Schoenbach, and G.Z. Hutcheson)

The optical control mechanisms, considered to be most suitable for external discharge control, are photodetachment and optically enhanced attachment (Appendices A and B). The influence of these effects on the discharge characteristic has to be investigated over the full E/N range of interest, which means mainly for externally sustained discharges at low values of E/N and the transition region to the self sustained discharge. The experimental setup used for these investigations is a transverse electrode configuration with a UV source incorporated into one of the electrodes, similar to a TEA laser. Such configurations can also be used as optically sustained discharge opening switches. This setup in combination with a dye laser was used to investigate the influence of photodetachment on the characteristics of an externally sustained discharge. Strong resistance changes were observed under the influence of photodetachment. Photodetachment was also found to improve the discharge stability significantly. A paper has been submitted to the Journal of Applied Physics (Appendix M).

# SPARK GAP AND ARC DISCHARGE INVESTIGATIONS

(A.L. Donaldson, M. Ingram, P. Ranon,
H. Krompholz, and M. Kristiansen)

Electrode erosion is one of the main limiting features of high current switches, such as spark gaps. The erosion leads to erratic behavior of the switch and quantitative information for engineering design is essentially non-existent. Most available data are single point data, i.e. data taken for a specific application, and are very difficult to extrapolate to other parameter regimes with any level of confidence.

## V. ELECTRODE EROSION

(A.L. Donaldson, H. Krompholz, and M. Kristiansen)

The work performed during this contract period has primarily focused on addressing the limitations on relatively high current (<200 kA), high energy switches resulting from electrode erosion. As a result of the work summarized here, investigations at still higher current levels (200-600 kA) were performed with support from an SDIO-DNA contract. At these levels the erosion process is much more interesting since a larger variety of phenomena are occurring simultaneously and the need for reducing the erosion rate is much more acute. Nevertheless, it was the results obtained under the AFOSR contract which enabled a clear and concise frame work of the erosion processes to be obtained, which could be extended to higher current levels.

The goals for the combination of both research efforts consisted of:

1) produce an annotated bibliography including recent translations of Soviet work,
2) determine the detailed role of various variables of interest,
3) clarify the discrepancies of previous experimental results,
4) use the above to determine scaling relations for parameters of interest,
5) use the above to select materials for a particular application,
6) develop from the above and from our own experimental studies, a systematic framework from which the electrode erosion could be described,
7) design and test "new" state-of-the-art materials.

The strategies used to accomplish these goals were:

- identify/classify/describe both thermal and material removal mechanisms,
- examine solutions to the appropriate equations which adequately describe these mechanisms (e.g. thermal conduction, magneto-hydrodynamics, etc.)
- determine the implication of these solutions on the electrode erosion as a function of engineering variables,
- identify areas for further model development,
- use the above to design "new" materials for use as electrodes,
- measure electrode erosion under a wide number of conditions (peak current, charge transfer, electrode material, gas pressure, gap spacing, electrode diameter).

Specific results are summarized in the following paragraphs:

An extensive library has been compiled on arc erosion (over 350 papers to date), including numerous translations from the Soviet literature (provided by the U.S. Army FSTC, Mr. Larry Turner, and the U.S. Air Force FTD, Mr. Barry Ballard). Considerable interest for this collection has been expressed by the scientific community and an annotated bibliography is currently nearing completion. Not only have these papers provided the information necessary to design the experiments needed to accomplish our goals but they also served to bring to our attention many well documented aspects of the erosion process which have been overlooked in the West.

Materials testing took place for both low current (10-100 kA) and high current (100-500 kA) regimes. Material rankings were obtained in both of these regimes for a large number of materials, including CuC, CuMo, CuNb, CuW, $CuWLaB_6$, C, Mo, CuZr, CuCrZr, $CuAl_2O_3$, Cu, and Al. Explanations were also developed for changes in relative material performance occurring in the transition from low to high current.

Several surface damage mechanisms were investigated in the low current regime, including crack formation in stainless steel due to the presence of manganese stringers and thermal stress (see Appendix N).

The discontinuity effect (a rapid transition in the electrode erosion rate as a function of peak current, charge, etc.) was investigated as a function of pressure, gap spacing, electrode area, material, and relative initial charging polarity. Its

qualitative location as a function of these variables was determined, as well as the physical basis for its existence. These results are reported as part of a DNA/SDIO contract.

In the high current regime, the significance of vapor jet heating of the opposite electrode as one of the major energy sources leading to electrode erosion was also confirmed.

## VI. X-RAY IONIZATION OF SWITCH GASES

(M. Ingram and M. Kristiansen)

Novel trigger mechanisms for spark gaps are always of interest. In a large array of spark gaps, one can conceive of using a wide area burst of x-rays to trigger the gaps with low relative jitter. A cold emission flash x-ray tube was, therefore, used to investigate spark gap triggering at switch pressures of 1, 3, and 5 atmosphere of various gases (Air, $N_2$, and $SF_6$). The available x-ray flux was quite low and the results were inconclusive. The delay times (> 100 ns) and jitter (> 10 ns) were quite high but it was not possible to increase the x-ray flux or energy with the available resources (M. Ingram, M.S. Thesis, Texas Tech University, 1985).

## VII. SURFACE DISCHARGE SWITCHING

(P. Ranon, M. Kristiansen, and L. Hatfield)

Insulators in the vicinity of high current discharges (e.g. in switches and mass drivers) are subject to intense heat and

radiation fluxes. This often leads to insulator degradation and/or catastrophic failures.

A dielectric surface discharge switch with peak currents in excess of 100 kA and a repetition rate of 1/3 pulse per second was used to evaluate various possible insulators. It was found that some insulators quickly developed permanent damage, whereas others recovered their dielectric strength if allowed to cool off. These insulators (e.g. Delrin and Teflon) typically decreased their surface voltage hold-off strength to about 50-75% of the initial value after about 20 shots. These results are described further in Appendix O.

# EXPLORATORY CONCEPTS

(G. Schaefer, B. Pashaie, P.F. Williams, K.H. Schoenbach, H. Krompholz, J.R. Cooper, K. Ikuta, and M. Kristiansen)

The "Exploratory Concepts" part of this research program was intended to enable investigations of promising concepts and ideas which arose during the investigations. The expectation was to enable short studies to determine the feasibility of these ideas which invariably occur during such a multi-investigator program.

## VIII. Field Distortion Triggering

(G. Schaefer, B. Pashaie, P.F. Williams, K.H. Schoenbach, and H. Krompholz)

A new approach to field distortion triggering of spark gaps has been investigated. Unlike in common field distortion triggered gaps, field enhancement at the surface of one of the main electrodes is utilized .

A common gap using field distortion triggering is initially designed to provide optimum performance. A trigger electrode is then added, shaped and located on an equipotential surface. When a trigger pulse is applied, field enhancement occurs at an edge of this trigger electrode and in most cases cascade breakdown is initiated.

Field enhancement at one of the main electrodes can be utilized if the trigger electrode shields this electrode in the hold-off state and direct breakdown between the main electrodes in initiated. An experimental set-up to prove this trigger concept has been designed and constructed. Test experiments showed the feasibility of this concept (Appendix P). Field calculations for different spark gap parameters allow the optimization of the gap geometry for this new method which is discussed in Appendix Q.

## IX. SLOW WAVE LINE PULSERS

(H. Krompholz, J.R. Cooper, J. Doggett,
K.H. Schoenbach, and G. Schaefer)

The advantages of using a coaxial line with helical inner conductor as a pulse generator, compared to the usual pulse forming networks (LC-chains) or cable discharges, are

- rectangular output pulse without oscillations inherent to LC-chains
- small physical length as compared to ordinary coaxial lines designed to produce the same pulse duration.

Theoretical investigations on the limiting factor for helical slow wave structures (dispersion) where first performed for a transmission line current sensor and unit step response, which is equivalent to an initially charged waveguide pulse generator (see Appendix R).

Two experimental set-ups were built to prove the theoretical results as discussed in Appendix S.

## X. PROJECTILE INJECTION INTO A MASS DRIVER

(K. Ikuta and M. Kristiansen)

A novel concept for injecting projectiles into a mass driver was conceived and studied. The main idea is to utilize a conical liner implosion to push an incompressible fluid which acts on the projectile. The concept is outlined in a publication (Appendix T).

## FACULTY PUBLICATIONS

### Journal Papers and Conference Proceeding Papers
### Published with AFOSR/ARO Support
### (10-1-84 through 1-14-87)


1. H.C. Harjes, K.H. Schoenbach, G. Schaefer, M. Kristiansen, H. Krompholz, and D. Skaggs, "An Electron Beam Tetrode for Multiple, Submicrosecond Pulse Operation," Rev. Sci. Instr., vol. 55, pp. 1684-1685, Oct. 1984.
2. G. Schaefer, P. Husoy, K.H. Schoenbach, and H. Krompholz, "Pulsed Hollow-Cathode Discharge with Nanosecond Risetime," IEEE Trans. Plasma Sci. vol. PS-12, pp. 271-274, Dec. 1984.
3. K.H. Schoenbach, G. Schaefer, M. Kristiansen, H. Krompholz, H.C. Harjes, and D. Skaggs, "An electron-Beam Controlled Diffuse Discharge Switch," J. Appl Phys., vol. 57, pp. 1618-1622, March 1985.
4. H. Krompholz, K.H. Schoenbach, and G. Schaefer, "Transmission Line Current Sensor," Proc. IEEE Conf. Instrumentation/ Measurement Technology, Tampa, FL, March 1985.
5. G. Schaefer, B. Pashaie, P.F. Williams, K.H. Schoenbach, and H. Krompholz, "A New Design Concept for Field Distortion Trigger Spark Gaps," J. Appl. Phys., vol. 57, pp. 2507-2511, April 1985.
6. G. Schaefer and K.H. Schoenbach, "External Control of Diffuse Discharge Switches," Proc. 5th IEEE Pulsed Power Conf. Arlington, VA, pp. 644-647, June 1985.

7. K.H. Schoenbach, G. Schaefer, M. Kristiansen, H. Krompholz, D. Skaggs, and E. Strickland, "An E-Beam Controlled Diffuse Discharge Switch," Proc. 5th IEEE Pulsed Power Conf., Arlington, VA, pp. 640-643, June 1985.

8. M.R. Wages, G. Schaefer, K.H. Schoenbach, and P.F. Williams, "Streak Photographic Studies of Trigatron Triggered Breakdown," Proc. 5th IEEE Pulsed Power Conf., Arlington, VA, pp. 414-417, June 1985.

9. A.L. Donaldson, M. Kristiansen, H. Krompholz, M.O. Hagler, L.L. Hatfield, G.R. Leiker, P.K. Predecki and G.L. Jackson, "Analysis of electrode Surface Damage in High Energy Spark Gaps", Proc. 5th IEEE Pulsed Power Conf., Arlington, VA, pp. 457-460, June 1985.

10. P.M. Ranon, H. Krompholz, M. Kristiansen, and L.L. Hatfield, "High Current Surface discharge Switch", Proc. 5th IEEE Pulsed Power Conf., Arlington, VA, pp. 276-279, June 1985.

11. B. Maas, H. Krompholz, M. Kristiansen, and M. Hagler, "Arc Current, Voltage, and Resistance in a High Energy, Gas-Filled Spark Gap", Proc. 5th IEEE Pulsed Power Conf., Arlington, VA, pp. 99-101, June 1985.

12. G. Schaefer, K.H. Schoenbach, M. Kristiansen, and H. Krompholz, "An Electron-Beam Controlled Diffuse Discharge Switch," Proc. XVIIth Int. Conf. on Phenomena in Ionized Gases, pp. 626-628, Budapest, Hungary, July 1985.

13. M.R. Wages, G. Schaefer, K.H. Schoenbach, and P.F. Williams, "Physical Triggering Mechanisms of Trigatron Spark Gaps," Proc. XVIIth Conf. on Phenomena in Ionized Gases, pp. 638-640, Budapest, Hungary, July 1985.

14. Kazunari Ikuta and M. Kristiansen, "Conical Liner Implosion as a Projectile Injector for Mass Drivers," Japanese J. Appl. Phys., vol. 25, pp. L198-L199, March 1986.

15. G. Schaefer, K.H. Schoenbach, M. Kristiansen, B.E. Strickland, R.A. Korzekwa, and G.Z. Hutcheson, "The Influence of the Circuit Impedance on an Electron Beam Controlled Diffuse Discharge with a Negative Differential Conductivity," Appl. Phys. Lett. vol. 48, pp. 1776-1778, June 1986.

16. G. Schaefer, K.H. Schoenbach, M. Kristiansen, B.E. Strickland, and R.A. Korzekwa, "Negative Differential Conductivity in an Electron Beam Controlled Diffuse Discharge for Switching Applications," presented at the International Conference on Plasma Science and Technology (ICPST), Beijing, China, June 1986.

17. G. Schaefer, K.H. Schoenbach, M. Kristiansen, B.E. Strickland, R.A. Korzekwa, G.Z. Hutcheson, and K.R. Rathbun, "Interaction of Discharge and Circuit in an Electron-Beam Controlled Diffuse Discharge opening Switch", Proc. of the Sixth Int. Conf. on High Power Particle Beams, Kobe, Japan, June 1986.

18. G. Schaefer, K.H. Schoenbach, M. Kristiansen, R.A. Korzekwa, and G.Z. Hutcheson, "Optimization of Gas Mixtures for Electron-Beam Controlled Diffuse Discharge Opening Switches," Proc. 1986 Seventeenth Power Modulator Symp., Seattle, WA, June 1986.

19. H. Krompholz, J.R. Cooper, J. Doggett, K.H. Schoenbach, and G. Schaefer, "Slow Wave Line-Type Pulsers," Proc. Seventeenth Power Modulator Symp., Seattle, WA, June 1986.

20. G. Schaefer and K.H. Schoenbach, "A Review of Diffuse Discharge Opening Switches," IEEE Trans. Plasma Sci., vol. PS-14, pp. 561-578, October 1986.

21. G. Schaefer, G.Z. Hutcheson, K.H. Schoenbach, and P.F. Williams, "The Influence of Photodetachment on the J-E/N Characteristics of Diffuse Discharges Containing Oxygen," J. Appl. Phys., submitted January 1987.

22. B. Pashaie, G. Schaefer, K.H. Schoenbach, and P.F. Williams, "Field Enhancement Calculations for a Field Distortion Triggered Spark Gap," J. Appl. Phys. pp. 790-792, vol. 61, No. 2, January 1987.

23. G. Schaefer, K.H. Schoenbach, M. Kristiansen, and R. Korzekwa, "Penning Ionization Gas Mixtures for Diffuse Discharge Opening Switches," in Gaseous Dielectrics V, L.G. Christophorou (ed.), Pergamon Press, to be published in 1987.

24. R.A. Korzekwa, G. Schaefer, M. Kristiansen, and K.H. Schoen-4bach, "The Influence of $N_2$ on Argon Based Gas Mixtures for an Electron Beam Controlled Diffuse Discharge," to be presented at the Int. Conf. on Phenomena in Ionized Gases, University College of Swansea, University Wales, Singleton Park, Swansea, U.K., July 13-17, 1987.

25. G. Schaefer, R.A. Korzekwa, K.H. Schoenbach, and M. Kristiansen, "Methane-Attacher Mixtures in an Electron Beam Controlled Diffuse Discharge Opening Switch," to be presented at the 6th IEEE Pulsed Power Conf., June 29-July 1, 1987.

26. G. Schaefer, R.A. Korzekwa, M. Kristiansen, and K.H. Schoen-bach, "Optimization of Gas Mixtures for Electron-Beam Controlled Diffuse Discharge Opening Switches," to be submitted to the J. Appl. Physics.

## INTERACTIONS

### a) Papers Presented

During the contract period (October 10, 1984 - January 14, 1987), the following papers were presented, in addition to those listed as conference proceeding papers:

1. J.R. Cooper, K.H. Schoenbach, G. Schaefer, J.M. Proud, and W.W. Byszewski, "Magnetic control of Low Pressure Glow Discharges," 37th Gaseous Electronics Conference, Boulder, CO. CO, Oct. 1984.
2. M.R. Wages, P.F. Williams, G. Schaefer, and K.H. Schoenbach, "Streak Photographic Studies of Trigatron Triggered Breakdown," 37th Gaseous Electronics Conference, Boulder, CO, Oct. 1984.
3. -Invited- K.H. Schoenbach and G. Schaefer, "External Control of Diffuse Discharge Switches," 12 IEEE Int. Conf. Plasma Sci., Pittsburgh, PA, June 1985.
4. G. Reinking, G. Schaefer, K.H. Schoenbach, and G. Hutcheson, "Attachment of Initial Secondary Electrons in an Electron Beam Sustained Discharge," 12th IEEE Int. Conf. Plasma Sci., Pittsburgh, PA, June 1985.
5. J.R. Cooper, K.H. Schoenbach, and G. Schaefer, "Magnetic Control of Low Pressure Diffuse Discharges," Joint Symp. Swarm Studies and Inelastic Electron Molecule Collisions, Lake Tahoe, NV, July 1985.

6. A.L. Donaldson, A. Watson, and M. Kristiansen, "Investigation of the Discontinuity effect in High Energy Spark Gap Erosion," 27th Annual Meeting, APS Division of Plasma Physics, San Diego, CA, Nov. 1985.
7. G. Schaefer, K.H. Schoenbach, M. Kristiansen, and E. Strickland, "Negative Differential Conductivity in E-Beam Sustained Discharges," 27th Annual Meeting Division of Plasma Physics, American Physical Society, San Diego, CA, Nov. 1985.
8. A.L. Donaldson, A. Watson, and M. Kristiansen, "Scaling Laws for High Energy Gap Erosion as a Function of Peak Current," 28th Annual Meeting of the Plasma Physics Division, American Physical Society, Nov. 1986, Baltimore, MD.

b) Consultative and Advisory Functions

During the contract period, the following functions were undertaken:

1. Dr. Kristiansen served on the USAF Scientific Advisory Board.
2. Dr. Kristiansen served on the USAF Ad Hoc Committee on "High Power Microwave Systems".
3. Dr. Kristiansen served on the USAF Ad Hoc Committee on the "Effects of HEMP on Military $C^3$".
4. Dr. Kristiansen served on the USAF Ad Hoc Committee on "Basic Science".
5. Dr. Kristiansen was a member of the NASA Workshop on "Plasma Physics and Fusion Scientific Activity for the Space Station".

6. Dr. Kristiansen served as a consultant to LANL and LLNL.
7. Dr. Kristiansen worked with personnel from Maxwell Labs, WPAFB, and Boeing Co. to resolve a critical problem related to an Air Force project (see Appendix U).

c) Other Interactions

Numerous interactions with other universities, industry and government laboratories were carried out during the contract period. Our group effectively served as a coordination point for much of the ongoing work in high power gas discharges for switching applications in the U.S.

1. Prof. M. Kristiansen co-chaired the ARO supported workshop on Foreign Switch Technology (Tamarron V), March 6-8, 1984.
2. Prof. M. Kristiansen attended the Technical Program Review Meeting for the 5th IEEE Pulsed Power Conference, Wash., DC, Jan. 1985
3. Prof. M. Kristiansen visited with Dr. B. Kulp, the Air Force Systems Command, Wash., DC, Jan. 1985.
4. Prof. M. Kristiansen attended, by invitation, a NASA Workshop, and also met with Mr. L. Webster of the U.S. Army Ballistic Missile Defense, May 1985.
5. Prof's. G. Schaefer and K.H. Schoenbach attended the 12th IEEE Int. Plasma Sci. Conf., Pittsburgh, PA, June 1985.
6. Prof. G. Schaefer visited the Department of Physics, University of Pittsburgh, PA, (Prof's. F. Biondi and R. Johnsen) June 1985.

7. Prof. G. Schaefer visited the Westinghouse Research Laboratory, Pittsburgh, PA, (Dr's. P. Chantry and L. Kline) June 1985.
8. Prof. G. Schaefer visited Oak Ridge National Laboratory, TN, (Prof. L. Christophorou) June 1985.
9. Prof's M. Kristiansen, L. Hatfield, K.H. Schoenbach, and G. Schaefer attended the 5th IEEE Pulsed Power Conference in Arlington, VA, June 1985.
10. Prof's. M. Kristiansen and G. Schaefer attended the Int. Conf. on Phenomena in Ionized Gases, Budapest, Hungary, July 1985.
11. Prof. G. Schaefer visited the Karlsruhe Nuclear Research Center, West Germany (Prof's. W. Schmidt and Citron), July 1985.
12. Prof. G. Schaefer visited the Department of Electrical Engineering, Technical University Darmstadt, West Germany (Prof. W. Pfeiffer), July 1985.
13. Prof. G. Schaefer visited the High Voltage Institute, Technical University Braunschweig, West Germany (Prof. J. Salge), July 1985.
14. Prof. G. Schaefer visited the Air Force Weapons Laboratory, Albuquerque, NM (Chief Scientist Dr. A. Guenther) August 1985.
15. Prof. G. Schaefer participated in the Organizing Committee meeting for the Workshop "Research Issues in Power Conditioning", Los Angles, CA (Prof. M. Gundersen) Sept. 1985.

16. Prof. Kristiansen visited with personnel at Eglin AFB, Oct. 1985.
17. Prof. Kristiansen co-chaired the Eglin AFB support workshop on Opening switches for Railguns (Tamarron VI), March 11-13, 1986.
18. Prof. Kristiansen and Schaefer attended the International Conference on Plasma Science and Technology, Beijing, China, June 1986 and the BEAMS '86 Conf. in Kobe, Japan, June 1986.
19. Prof. M. Kristiansen attended the 17th Power Modulator Symposium and presented two research papers (work supported by AFOSR/ARO), Seattle WA, June 1986.
20. Prof. M. Kristiansen worked with Dr. A. Guenther, Chief Scientist of the AFWL, on research issues related to AFOSR research contract, Albuquerque, NM, August 1986.
21. Prof. M. Kristiansen gave an invited paper at the Inaugural Meeting of the United Kingdom Pulsed Power Club, London, UK, September 1986
22. Prof. M. Kristiansen attended the American Physical Society Plasma Physics Division Meeting, chaired one session and presented two research papers, Baltimore, MD, November 1986.

## ADVANCED DEGREES AWARDED

(1984-1987)

1. Henry Charles Harjes, Ph.D., "An Electron Beam Controlled Diffuse Discharge Switch," May 1985.

2. Leo Erasmus Thurmond, M.S., "Photodetachment as a Discharge Control Mechanism in Gases Containing Oxygen," May 1985.

3. Brian Lee Maas, M.S., "Arc Current, Voltage, and Resistance in a High Energy, Gas-Filled Spark Gap," May 1985.

4. Randy Dale Curry, M.S., "Triggering of Surface Discharge Switches," August 1985.

5. Michael Ingram, M.S., "X-Ray Preionization for Triggering Spark Gaps," May 1986.

6. Brian Edward Strickland, M.S., "Negative Differential Conductivity in E-Beam Sustained Diffuse Discharges for Switching Applications," May 1986.

7. George Zohn Hutcheson, Ph.D., "Optically Controlled Diffuse Discharges for Switching Applications," August 1986.

8. James Randall Cooper*, Ph.D., "Magnetic Field Control of Low Pressure diffuse Discharges," December 1986.

9. Douglas S. Skaggs, M.S., "Current-Voltage Characteristics of Electron-Beam Controlled Diffuse Discharges," May 1987.

10. Courtney Holmberg+, M.S., "Optically Enhanced Attachment Processes in Diffuse Discharges," May 1987.

11. Peter Miyagi Ranon+, M.S., "Insulator Degradation Resulting from High Current Surface Discharges," May 1987.

---

+ (AFIT) Graduate Student

* Also supported by other contracts

## SEMINARS
1984 - 1987

| | | |
|---|---|---|
| 1. | Wayne W. Hofer | "High Power Microwave Research"<br>October 3, 1984<br>Lawrence Livermore National Laboratory<br>Livermore, CA |
| 2. | Osamu Ishihara | "Nonlinear Evolution of Two-Stream Instabilities"<br>December 17, 1984<br>University of Saskatchewan<br>Saskatchewan, Canada |
| 3. | William C. Nunnally | "Photo-Conducting Power Switches"<br>February 18, 1985<br>Los Alamos National Laboratory<br>Los Alamos, NM |
| 4. | William M. Moeny | "Experimental Investigations of a Radial Opening Switch"<br>March 27, 1985<br>Tetra Corporation<br>Albuquerque, NM |
| 5. | James A. Ionson | "The Policy and Technology of the Strategic Defense Initiative"<br>May 2, 1985<br>Director, Innovative Science and Technology Office, SDIO<br>Washington, DC |
| 6. | William G. Dunbar | "Insulating Materials Applications" and "Space Applications of Insulating Materials"<br>May 13, 1985<br>"Materials Testing"<br>May 14, 1985<br>Boeing Aerospace Company<br>Seattle, WA |
| 7. | Malcolm Buttram | "Spark Gap Stability"<br>July 22, 1985<br>Sandia National Laboratories<br>Albuquerque, NM |
| 8. | Giyuu Kido | "Generation and Application of Megagauss Fields"<br>August 21, 1985<br>Tohoku University<br>Sendai, Japan |

9. **Alan Watson**

"Electrode Damage from Strong Transient Sparks by Surface Material Displacement in Hydromagnetic Flow"
September 12, 1985
University of Windsor
Windsor, Ontario, Canada

10. **Andrew K. Jonscher**

"Dielectric Spectroscopy of Semi-Insulating Gallium Arsenide"
October 10, 1985
"Surface Conduction on Humid Insulators"
October 11, 1985
King's College
London, UK

11. E.R. Menzel
T.W. Sinor

"Laser Spectroscopy: Applications to Forensic Science and Semiconductor Device Fabrication"
October 24, 1985
Physics Department
Texas Tech University
Lubbock, TX

12. Martin Gundersen

"Recent Progress in High Power Switch Research"
October 25, 1985
University of Southern California
Los Angles, CA

13. Klaus Zieher

"Investigation of a Self-Magnetically Insulated High Current Ion Source"
November 21, 1985
Chemical and Nuclear Engineering
University of New Mexico
Albuquerque, NM

14. Hriar S. Cabayan

"High Power Microwave Activities at Lawrence Livermore National Laboratory"
November 26, 1985
Lawrence Livermore National Laboratory
Livermore, CA

15. Gerhard Schaefer

Fast Plasma Mixing - A New Excitation Method for CW Gas Lasers"
December 6, 1985
Dept. Electrical Engineering
Texas Tech University
Lubbock, TX

16. W.M. Moeny — "Experimental and Theoretical Investigations of Planar and UV-Sustained Glow Discharge Opening Switches"
April 15, 1986
Tetra Corporation
Albuquerque, NM

17. Nino R. Pereira — "X-Radiation from Plasma Z-Pinches"
August 1, 1986
Berkeley Research Associates, Inc.
Springfield, VA

18. Hidenori Akiyama — "Characteristics of a High-Current Pulsed Discharge"
September 10, 1986
Kumamoto University
Kumamoto, Japan

19. R.E. Voshall — "Experimental Analysis of Fast Closing Surface Discharge Switches"
September 16, 1986
Westinghouse R&D Center
Pittsburgh, PA

20. J.L. Wu — "An Overview of Research Topics Related to Railgun Plasma Armature"
September 16, 1986
Westinghouse R&D Center
Pittsburgh, PA

21. M. Kristiansen — "Pulsed Power in the U.S.A."
September 25, 1986
Dept. Electrical Engineering
Texas Tech University
Lubbock, TX

## GUESTS OF THE PLASMA AND SWITCHING LABORATORY
October 1984 - January 1987

| | |
|---|---|
| **December 17, 1984** | |
| Osamu Ishihara | University of Saskatchewan<br>Saskatoon, Canada |
| **March 7, 1985** | |
| Jan P. Jansen | Norwegian State TV, Oslo, Norway |
| **May 2, 1985** | |
| James A. Ionson | SDIO, Washington, DC |
| Emanuel Honig | LANL, Los Alamos, NM |
| **May 13, 1985** | |
| William G. Dunbar | Boeing Aerospace Co., Seattle, WA |
| **July 19, 1985** | |
| James Thompson<br>William Nunnally | University of Texas at Arlington<br>Arlington, TX |
| **August 21, 1985** | |
| Mami and Giyuu Kido | Tohoku University, Sendai, Japan |
| Hwang Changsing | Taiwan, Republic of China |
| **September 24, 1985** | |
| Joe Brown | Mississippi State University<br>Starkville, MS |
| **September 25, 1985** | |
| Satoru Yanabu | Toshiba Corp., Kawasaki, Japan |

October 8, 1985

| | |
|---|---|
| Lloyd Gordon<br>Wayne Hofer<br>Ted Wilson | Lawrence Livermore National Laboratory<br>Livermore, CA |

October 10, 1985

| | |
|---|---|
| Andrew K. Jonscher | Kings College, London, UK |

February 28, 1986

| | |
|---|---|
| Edmond Y. Chu<br>Mike Montogomery | Maxwell Laboratories<br>San Diego, CA |

April 15, 1986

| | |
|---|---|
| William M. Moeny<br>Chris Young | Tetra Corporation<br>Albuquerque, NM |

April 25, 1986

| | |
|---|---|
| Hermann Krompholz | H.K. Fraunhofer Institut fuer Laser-technik Federal Republic of Germany |
| Leo Thurmond | Computer Science and Applications<br>Fort Walton Beach, FL |

June 21, 1986

| | |
|---|---|
| Lt. Gen. James Abrahamson | Strategic Defense Initiative |
| Dwight Dustin | SDIO/IST |
| U.S. Sen. Phil Grahmn | (R. Texas) |
| U.S. Rep. Larry Combest | (R. Texas) |

June 30, 1986

| | |
|---|---|
| Erich Kunhardt<br>Gerhard Schaefer | Weber Research Institute<br>Polytechnic University<br>Farmingdale, NY |
| Karl Schoenbach | Old Dominion University<br>Norfolk, VA |

July 1, 1986

| | |
|---|---|
| Barry Ballard | Wright-Patterson Air Force Base<br>Dayton, Ohio |

September 17, 1986

| | |
|---|---|
| Roy E. Voshall<br>J.L. Wu | Westinghouse R&D Center<br>Pittsburgh, PA |

October 17, 1986

| | |
|---|---|
| E. Igenberger<br>Sebastian Aigner<br>Axel Hudepahl<br>Martin Rott | Lehrstuhl fur Raumfahrttechnik (LRT)<br>University of Munich<br>Federal Republic of Germany |

October 30, 1986

| | |
|---|---|
| Andrew K. Jonscher | Kings College London, U.K. |

November 12, 1986

| | |
|---|---|
| Shannon Wells Lucid | Nasa, JSC, Houston, Texas |

November 25, 1986

| | |
|---|---|
| A.H. Guenther | Kirtland Air Force Base<br>Albuquerque, NM |
| T.H. Martin | Sandia National Laboratory<br>Albuquerque, NM |

January 7, 1987

| | |
|---|---|
| A.R. Cole<br>E.A. Lopez | Maxwell Laboratories, Inc.<br>Albuquerque, NM |

# APPENDICES

(OTHER FACULTY PUBLICATIONS)

IEEE TRANSACTIONS ON PLASMA SCIENCE, VOL. PS-14, NO. 5, OCTOBER 1986

# A Review of Diffuse Discharge Opening Switches

G. SCHAEFER, SENIOR MEMBER, IEEE, AND K. H. SCHOENBACH, SENIOR MEMBER, IEEE

*Abstract*—**The basic operation principles of externally controlled diffuse discharges with respect to their application as opening switches are discussed. Discharge sustainment by electron and UV ionization and additional control mechanisms, such as photodetachment and optically enhanced attachment, are considered. Special emphasis is given electron-beam (e-beam) controlled switches. For such systems, design criteria are discussed and a summary of experimental switch results is presented.**

## I. Introduction

INDUCTIVE energy storage is attractive in pulsed power applications because of its intrinsic high-energy density compared to capacitive storage systems. The key technological problem in developing inductive energy storage systems, especially for repetitive operation, is the development of opening switches. Promising candidates for repetitive opening switches are electron-beam (e-beam) or laser-controlled diffuse discharges.

In a "diffuse discharge opening switch," the switch medium is an externally sustained discharge. Most of the research on externally sustained high-pressure ($>1$ atm), diffuse discharges has been performed with respect to its application for molecular lasers. The most common sustainment method, the e-beam controlled discharge technique, was used by Daugherty *et al.* in 1971 [1] to operate large-volume high-energy $CO_2$ lasers. The use of diffuse discharges as fast closing and opening switches was first proposed in 1974 by Hunter [2], [3] and Koval'chuk and Mesyats [4], [5].

A schematic diagram of an externally controlled opening switch as part of an inductive energy storage system is shown in Fig. 1. When the gas between the electrodes is ionized by an e-beam or by radiation, it becomes conductive, the diffuse discharge switch closes, and the inductor is charged. During conduction, the reduced electric field strength $E/N$ is kept in a range where ionization through the discharge electrons is negligible. When the external ionization source is turned off, electron attachment and recombination processes in the gas cause the conductivity to decrease and the switch opens. Consequently, the current through the inductor is commutated into the load, and the voltage across the load increases according to the impedance ratio of load and storage system.

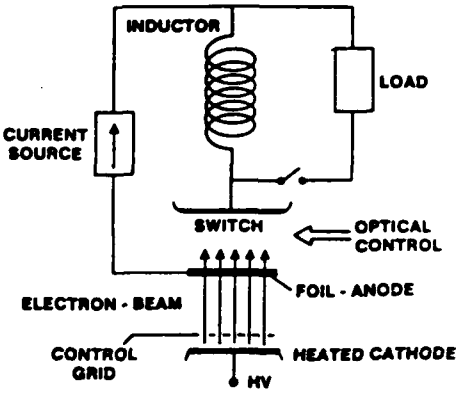


Fig. 1. Schematic of an externally controlled opening switch as part of an inductive energy storage system.

The most efficient method at this time to provide for plasma conductivity is the e-beam controlled discharge technique. Up to 50 percent of the e-beam energy can be converted directly into ionization energy [6]. The remaining energy mainly goes into excitation. The ionization efficiency can be increased further by using Penning gas mixtures, where part of the excitation energy is converted into ionization through Penning collisions [7]. The only way to reduce the conductivity in an e-beam sustained discharge is to reduce or to turn off the e-beam. Optical control of diffuse discharges, on the other hand, allows changing of the conductivity in either direction [8]. By irradiating a discharge with radiation in the wavelength range corresponding to an atomic or molecular transition, the electric properties of the plasma can be modified through optogalvanic effects [9]. An attractive concept for an externally controlled diffuse discharge switch is to combine the advantages of both the e-beam and optical control to create an e-beam sustained optically assisted switch [10].

## II. Discharge Analysis

### A. General Considerations

The goal of a discharge analysis of an externally sustained discharge for switching applications is to evaluate the time-dependent impedance of the discharge for a given time-dependent electron source in a given circuit. Such an analysis will allow the optimization of gas mixtures and operation conditions. A complete discharge model must consider the bulk of the discharge and the fall regions, especially the cathode sheath. It must provide for

Manuscript received January 23, 1986; revised June 16, 1986. This work was supported by AFOSR and ARO.

G. Schaefer is with the Department of Electrical Engineering, Texas Tech University, Lubbock, Texas 79409-4439, and with Polytechnic University of New York, Farmingdale, New York 11735-3995.

K. H. Schoenbach is with the Department of Electrical Engineering, Old Dominion University, Norfolk, Virginia 23508.

IEEE Log Number 8610254.

steady-state solutions and the transient behavior, and should include a stability analysis of the discharge.

Model calculations aimed toward discharge applications for opening switches have concentrated mainly on the bulk of the discharge (zero-dimensional), on the influence of the proposed optimum gas properties (*E/N* dependence of attachment coefficient and mobility), and on the transient behavior (time dependence) of the discharge in an inductive energy storage circuit [10]–[15]. Bulk discharge models are based on solving a set of rate equations for the charged particles and those excited particles that contribute to ionization. The steady-state solution of the set of rate equations gives the *V–I* characteristics of the discharge. For the evaluation of its transient behavior in a given circuit, the set of time-dependent rate equations and the circuit equation must be solved simultaneously.

To solve the set of rate equations, the rate constants have to be known for all processes contributing to the charged particle balance, depending on the reduced field strength *E/N*. In some cases, these rate constants are directly available from experiments. If only cross sections are known, the rate constants have to be calculated using the electron energy distribution functions. These distribution functions have to be calculated for a specific gas mixture, with *E/N* as the variable parameter, using a Bolzmann code or a Monte Carlo code.

In externally sustained discharges, also, the electrons produced by the external source have to be considered. The energies of the initial secondary electrons for a UV sustained discharge, for example, are low ($\leq 1$ eV) and do not influence the electron energy distribution at low values of *E/N*.

The initial secondary electrons produced by an electron beam, however, are spread over a wide energy range [16]–[19] and, especially at low values of *E/N*, electrons are produced at high energies where otherwise no electrons are found. The relaxation of these electrons has been calculated for several gases, especially with relevance to gas discharge lasers [20]–[25]. The relaxation of fast electrons, their influence on the electron energy distribution, and the consequences on an e-beam sustained discharge as a switch have been calculated for nitrogen containing different attachers [25]. The relaxation time was found to be very short ($< 1$ ns for atmospheric pressure $N_2$). This time was exclusively spent in the energy range from 4 to 8 eV where $N_2$ does not have any significant inelastic cross sections. This effect causes a secondary maximum in the distribution function as shown in Fig. 2. The source function of an e-beam sustained discharge at low *E/N* is therefore significantly reduced if attachers are used which have their attachment cross section in the energy range of this secondary maximum, while optically sustained discharges are not affected [26].

A simplified model of a spatially homogeneous discharge considers only the charged particles [14]. All ionization processes by the discharge electron are neglected, and two-body dissociative attachment is considered to be the dominant attachment process. The rate equations are

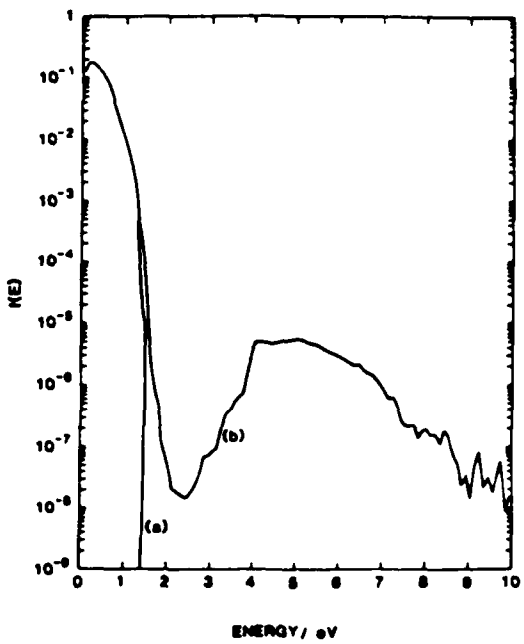


Fig. 2. Electron energy distribution in an externally sustained discharge in $N_2$ at $E/N = 1$ Td: (a) for electron generation at low energies; and (b) for an e-beam sustained discharge, with a source function of $S = 5 \cdot 10^{16}$ $cm^{-3}\,s^{-1}$ [26].

then given as

$$\frac{dn_e}{dt} = S - k_{re} n_+ n_e - k_a N_a n_e \tag{1}$$

$$\frac{dn_+}{dt} = S - k_{re} n_+ n_e - k_r n_+ n_- \tag{2}$$

$$\frac{dn_-}{dt} = k_a N_a n_e - k_r n_+ n_- \tag{3}$$

where $k_{re}$ and $k_r$ are the electron–ion and ion–ion recombination rate coefficients, respectively, $k_a$ is the attachment rate coefficient, $N_a$ is the attacher concentration in the gas mixture, and $S$ is the source function (rate of electron–ion pair production by the e-beam). Assuming charge neutrality in the discharge so that $n_+ = n_e + n_-$, and with the assumption that $k_{re} = k_r = k_r$, the rate equation can be solved for the *steady-state* electron density $n_{eo}$:

$$n_{eo} = \frac{S}{k_a N_a + \sqrt{S k_r}} \tag{4}$$

and for the *steady-state* positive ion density $n_{+o}$:

$$n_{+o} = \sqrt{S/k_r}\,. \tag{5}$$

For electrons that are the dominant current carriers, the conductivity is given as

$$\sigma = \frac{e\mu S}{k_a N_a + \sqrt{S k_r}} \tag{6}$$

where $\mu$ is the electron mobility. This solution reduces to the attachment dominated solution for $k_a N_a \gg k_r n_+$:

$$\sigma_a = \frac{e\mu S}{k_a N_a} \tag{7}$$

and the recombination dominated solution for $k_a N_a << k_r n_+$:

$$\sigma_r = \mu e \sqrt{\frac{S}{k_r}}. \tag{8}$$

Since the diffuse discharge is considered to be used as a switch, that means as an element which controls the energy flow from an energy storage into a load, the power dissipated in the discharge should ideally be negligible compared to the power commutated to the load. This requires a high conductivity at a low reduced field strength $E/N$. The desirable gas properties for the conduction phase are therefore, according to (6), a large electron mobility and small attachment and recombination rate coefficients at low $E/N$.

In order to minimize losses during the transition from the conductive to the nonconductive state (opening phase) the switch conductance should decay as fast as possible. A simplified analysis of the opening phase is given by considering the rate of change in electron density (1) for either recombination or attachment-dominated discharges. For a nonattaching gas ($k_a = 0$), the relative change of electron density $n_e$ (and the switch conductivity $\sigma$) is proportional to the instantaneous value of $n_e$:

$$\frac{dn_e/dt}{n_e} = -k_r n_e \tag{9}$$

i.e., the relative rate of change slows down with reduced electron density. In an attachment-dominated discharge ($k_a N_a >> k_r n_+$), on the other hand, the relative rate of decay is *not* dependent on the electron density:

$$\frac{dn_e/dt}{n_e} = -k_a N_a. \tag{10}$$

It can be controlled completely by the type and concentration of the electronegative gas added to the buffer gas.

In order to achieve opening times of less than 1 ms at initial electron densities $n_e < 10^{14}$ cm$^{-3}$, the dominant loss mechanism *must* be attachment. That means that the switch gas mixture must contain an electronegative gas. On the other hand, additives of attaching gases increase the power loss during conduction. Both low forward voltage drop and fast opening can be obtained by considering the $E/N$ dependence of rate coefficients and transport coefficients, and choosing gases or gas mixtures that satisfy the following conditions [8], [10], [27], [28].

a) For low values of the reduced field strength $E/N$, characteristic for the conduction phase, the electron drift velocity $w$ should be large and the attachment rate coefficient $k_a$ should be small in order to minimize losses.

b) With increasing $E/N$, characteristic for the opening phase of a switch in an inductive energy storage system, the attachment rate coefficient should increase and the electron drift velocity should decrease in order to support the switch opening process.

c) Additionally, the gas should have a high dielectric strength to hold off the expected high voltage across the switch when it opens.

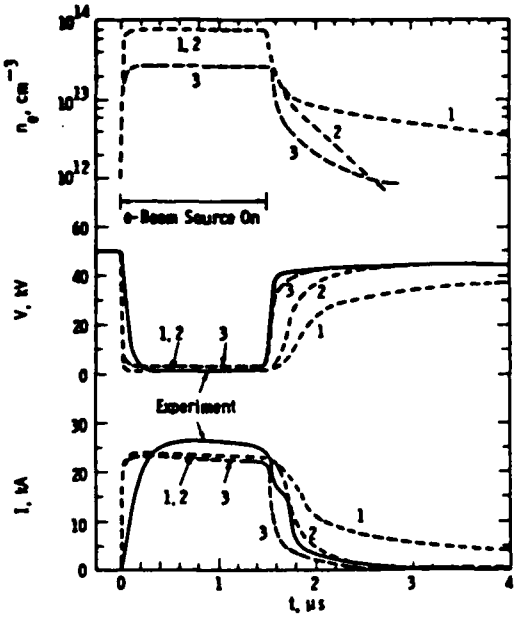


Fig. 3. Measured and predicted e-beam switch waveforms in methane [3], [14]. Impurity attachment rates: (1) $k_a N_a = 0$; (2) $k_a N_a = 7.2 \cdot 10^5$ s$^{-1}$; (3) $k_a N_a = 2.2 \cdot 10^6$ s$^{-1}$.

## B. Specific Gas Mixtures

Calculations on the discharge behavior of specific gas mixtures have been performed by several authors. Fernsler *et al.* [12] studied the influence of an admixture of an attacher ($O_2$) to a buffer gas ($N_2$) during the opening phase of the discharge. The attachment rate of the three-body attachment process ($e + O_2 + N_2 \rightarrow O_2^- + N_2$) was considered to be dominant and independent of $E/N$. Shortening of switch opening with increasing attacher concentration was demonstrated.

Kline [14] presented calculations on discharges in $N_2$, Ar, $N_2$:Ar mixtures, and $CH_4$ for the operation range of small e-beam current densities (some mA/cm$^2$). The steady-state analysis presents the discharge characteristic, the switch characteristic, and the current gain. The current gain in an e-beam sustained discharge is considered a figure of merit for the control efficiency of the diffuse discharge switch. It is defined as the ratio of switch current to sustaining e-beam current.

Kline's transient analysis of the diffuse discharge [14] incorporates the influence of an attacher; however, an attachment rate independent of $E/N$ was considered. As a result of the calculations, methane was found to be the best of the switch gases studied since it exhibits a high electron drift velocity at low values of $E/N$. Fig. 3 shows the measured and predicted e-beam switch waveforms in methane for the experimental conditions of Hunter [3]. The three different predictions result from different values for the attachment rates used in the calculations.

Schaefer *et al.* [10] presented calculations on discharges in $N_2$ with $N_2O$ as an attacher. These calculations

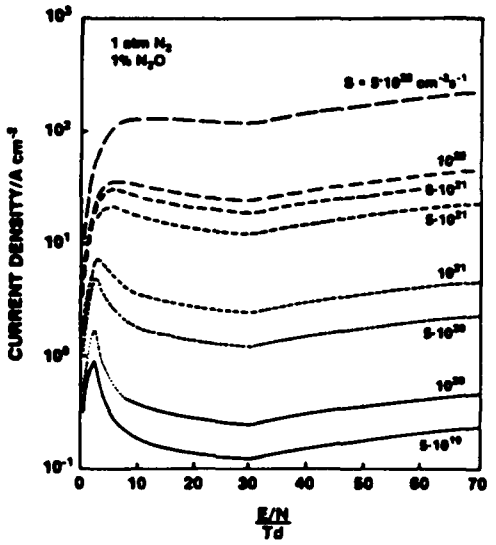


Fig. 4. Calculated steady-state $E/N - j$ characteristics for an e-beam sustained discharge in $N_2$ with an $N_2O$ fraction of 1 percent. The variable parameter is the electron generation rate [10].

concentrate on the influence of an attacher with an attachment rate increasing with $E/N$. It was demonstrated that such an attacher with sufficient concentration generates a discharge characteristic with a negative differential conductivity (NDC) in an intermediate $E/N$ range. This behavior has also been predicted for discharges in $N_2$ with admixtures of $CO_2$ or $O_2$ as attachers [29]. Fig. 4 shows the steady-state $E/N$-$j$ characteristic with the source function $S$ as the variable parameter for an $N_2/N_2O$ discharge [10]. Below $\sim 3$ Td, the discharge is recombination dominated. Above $\sim 3$ Td, the attachment rate increases, causing the conductivity to decrease (NDC). At high values of the source functions, the electron density will be high enough so that recombination is significant also in the $E/N$ range with a high attachment rate, and the negative differential conductivity disappears.

The transient analysis shows that such a discharge characteristic allows the operation of the discharge with low losses during the conduction phase in the $E/N$ range below the threshold for attachment and to achieve fast opening times. Fig. 5 shows the calculated time dependence of $E/N$ and the current density $j$ with the attacher concentration as the variable parameter. For the three smaller values of the attacher concentration (0.1–0.75 percent), the discharge reaches the same low value of $E/N$ where it is recombination dominated. The opening time decreases with attacher concentration; however, the closing time increases. For the higher values of the attacher concentration ($\geq 1$ percent) the discharge is obstructed to reach the low $E/N$ range and stays attachment dominated, causing high losses. These results demonstrate that the desired attachment rate for low losses during conduction and for fast opening obstructs switch closing. Photodetachment is therefore discussed as an additional control mechanism to overcome attachment during switch closure (see Section IV).

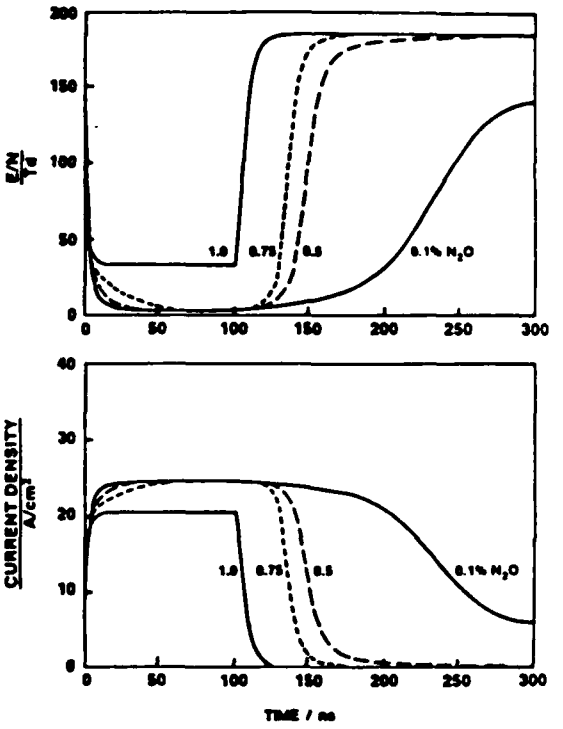


Fig. 5. Time dependence of $E/N$ (top) and current density (bottom) of an e-beam sustained discharge in 1 atm $N_2$ with admixtures of $N_2O$. The e-beam is on for $0 \leq t \leq 100$ ns. The variable parameter is the $N_2O$ fraction in percent [10].

## III. Boundary Effects and Instabilities

The voltage drop across e-beam sustained diffuse discharges reaches from several hundred volts to several kilovolts, depending on operation conditions. An appreciable amount of the total voltage may be the cathode fall voltage [30]–[34]. The cathode fall voltage is a function of e-beam current, discharge current, gas type and pressure, and electrode material [34]. For atmospheric pressure discharges and small gap distances, it can be considerably larger than the voltage across the bulk of the discharge. The addition of an attaching gas does not seem to increase the cathode fall voltage very much.

A theoretical investigation of the cathode fall in high-pressure e-beam controlled discharges included secondary emission from the cathode and electron-impact ionization of metastable states [33]. The results showed that the cathode fall of an e-beam ionized discharge is very sensitive to the value of the cathode secondary emission coefficient, demonstrating the importance of the electrode properties.

Instabilities which lead to a glow-to-arc transition usually originate near the electrodes, a region of higher electric-field intensity and lower electron density. Streamer formation is considered to begin with the formation of a filament of gas, heated to a temperature adequate to provide sufficient thermal ionization to become significantly conductive. Streamers can grow from cathode layer hot spots, and have been observed to originate on cathode protrusions [35], [36]. The streamers subsequently propagate at speeds close to sonic, generally progressing with

increasing velocity across the gap. An important feature of streamers in discharge gases is therefore that arcing can occur a considerable time after the e-beam current has been turned off [37].

The development of plasma instabilities in the bulk of the diffuse discharge was addressed by Haas [38], [39], Nighan [40], and Bychkov *et al.* [11]. Two general models of bulk instabilities have been proposed: thermal and ionization. The thermal instability is due to local heating and dilution of the gas with subsequent increase in *E/N*, which in turn causes increased local energy deposition, etc. The ionization instabilities occur when in high field regions of the discharge, preferentially close to the electrodes, the regenerative ionization becomes comparable to the ionization caused by the external source. The initiation of instabilities has also been attributed to nonuniform ionization through the external source [13]. The times for the development for these instabilities range from hundreds of nanoseconds to milliseconds, depending on discharge parameters and filling pressure [41].

Discharges in mixtures containing electronegative gases can exhibit an attachment instability, if the attachment rate coefficient $k_a$ is a rapidly increasing function of *E/N* [42], [43]. A small local increase in the electric-field intensity in such a gas mixture causes an increase in attachment which leads to a decrease of the electron density and therefore to a further increase in electric field. Ultimately, waves of high electric field in electron-depleted regions move across the discharge, resulting in current waves. Oscillatory waveforms are also observed in gases where the drift velocity decreases with decreasing *E/N* [44], [45]. The relevance of these instabilities is that the high local fields caused by the electron loss will greatly increase local heating, and streamers are initiated, growing toward both electrodes.

A problem related to instabilities in diffuse discharges is power loading [46]. The electrical energy density deposited in the gas is the product of discharge current density and electric field integrated over time. This energy is deposited in the form of kinetic energy of the gas molecules (gas heating) and in the internal degrees of freedom of the gas molecules. Experimental investigations have led to the conclusion that a uniform discharge can be sustained until the gas temperature has increased to approximately 500° K [37]. After that point the uniform glow goes over to an arc.

There are attempts to quantify the fraction of the electrical energy input which results in gas heating as a function of *E/N* for timescales short compared to vibrational relaxation [47]. A major fraction of the energy input to molecular gases is consumed by vibrational excitation. Shirley and Hall [48] determined vibrational temperatures in $H_2$ as a function of energy density deposited in the gas. They found vibrational temperatures of 1500°–1800° K for power loadings of several kJ/mole, or about 0.1 J/cm$^3$ atm at 30 Td. The changes due to enhanced population in the high-energy states of the gas molecules will affect the behavior of the diffuse discharge switch, especially if attachers are used where the attachment cross section changes drastically with vibrational excitation as in HCl or $H_2$ [49], [50].

## IV. Optical Control of Diffuse Discharges

External control of a diffuse gas discharge means to make use of some mechanisms to influence the charge carrier balance in the discharge, in addition to those processes solely caused by the applied electric field. A control mechanism can increase or decrease the conductivity by controlling the electron generation or depletion mechanism.

For opening switches, mainly externally sustained discharges are considered, operated in the *E/N* range where the ionization coefficient is negligible. Besides electron beams, UV radiation has been used to sustain TEA-laser discharges [51]–[53] and discharges for switching applications [54]–[56]. The advantage is that the design and operation of a UV flashboard is significantly simpler than an e-beam gun. Problems at this time are to achieve a fast cutoff of the ionization source and short discharge opening times [54], [57].

An alternative is to use lasers that allow a very precise timing. Due to the high costs of laser photons, however, it seems to be inefficient at this time to use lasers to sustain the discharge. Lasers, on the other hand, offer the unique possibility of influencing the density of specific states, and subsequently the generation and depletion mechanisms of electrons [9], [57]. Laser discharge control for switching application is therefore considered only as an *additional* control for a specific switch phase, where other means do not allow the optimization of the discharge properties. Laser control of diffuse discharges for opening switches is a very recent research field. Besides papers on concepts [8], [9], [58], [59], model calculations on certain proposed systems [10], [15], and investigations of basic processes [60], [61], there are no results on operational switching devices available.

One concept discussed is optical quenching of metastables (excitation into higher lying states with short radiative lifetimes), which significantly reduces the ionization rate and consequently the conductivity of self-sustained discharges [59]. The influence of metastables, however, is reduced in externally sustained discharges and discharges with molecular additives.

As discussed in Section II, attachers have to be used to achieve fast opening. Concepts on additional optical control therefore concentrate on attachment and its control in one of the transition phases. Methods for optically controlling attachment are: a) photodetachment to overcome attachment [58]; and b) optically induced attachment in gases which otherwise do not have a strong attachment rate in the *E/N* range of interest [8].

### A. Photodetachment

Just like photoionization, photodetachment is a nonresonant process which in general requires much lower pho-

ton energies. The cross sections usually are not very high, requiring a high laser power.

A negative ion considered for photodetachment as a control mechanism is $O^-$ [58]. The photodetachment cross section has a threshold at a photon energy of 1.47 eV and reaches a plateau of $6.3 \cdot 10^{-18}$ cm$^2$ at approximately 2 eV [62]–[64]. Several molecules, such as $O_2$, NO, CO, $N_2O$, $CO_2$, and $SO_2$, undergo dissociative attachment producing $O^-$ (example: $e^- + O_2 \rightarrow O^- + O$).

In all these gases or gas mixtures with these gases, competitive attachment processes exist or reactions of $O^-$ will occur, producing molecular negative ions which, in general, have lower cross sections for photodetachment. In discharges in $O_2$ at low $E/N$ (< 10 Td) and at high pressure [65], [66], for example, the dominant molecular negative ion is $O_2^-$ and its cross section for photodetachment is smaller by a factor of approximately 5 at 2 eV.

Photodetachment experiments in low-pressure $O_2$ discharges and flowing afterglows showed that a fraction of 50 percent of the negative ions could be detached with laser pulses with an energy flux of 35 mJ/cm$^2$ and a photon energy of 2.2 eV [58]. This value may be higher by a factor of up to 5 in high-pressure systems at an $E/N$ below 50 Td. Photodetachment experiments of $F^-$ in a hollow cathode discharge containing $NF_3$ demonstrated that the negative ion density reached up to 50 times the steady-state electron density [67].

### B. Optically Enhanced Attachment

Optically enhanced attachment means to use a gas mixture with an additive of molecules, which in their initial state are very weak attachers, and to transfer these molecules through optical excitation and maybe some subsequent process into a species which acts as a strong attacher [8].

Certain attachers have a drastically increased attachment cross section in their rotationally and/or vibrationally excited states. This effect was first observed for dissociative attachment of $SF_6$ producing $SF_5^-$ [68], [69]. An attachment rate constant $k_a(T)$, increasing with temperature $T$, is the clearest indication for such a behavior [70], [71].

As yet, there are no known measurements of attachment cross sections for individual vibrational states. However, it was demonstrated that monoenergetic electrons at least allow the excitation of specific modes of vibration, and subsequently the measurement of attachment cross sections of a special group of vibrational states [72]. Bardsley and Wadehra [49] have calculated the cross section for the vibrational states ($v$ = 0–3) of HCl (Fig. 6) from cross-section measurements at different gas temperatures [71]. These data show that the attachment rate can be increased drastically, but this advantage disappears in HCl if the electron energy is larger than 0.5 eV. For switching application, attachers are needed, having their maximum attachment cross section in the ground state at a somewhat higher energy.

For application in diffuse discharges, one must consider

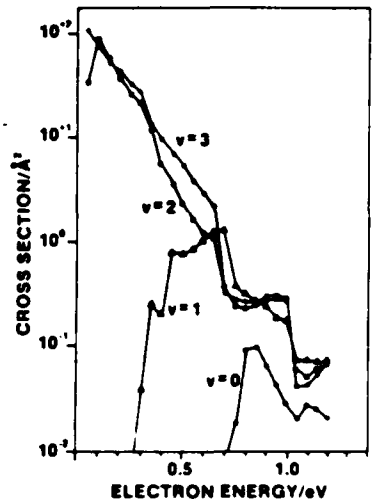


Fig. 6. Theoretical cross section for $e + HCL \rightarrow H + Cl^-$, depending on electron energy for the vibrational states ($v$ = 0–3), assuming a Boltzmann distribution over rotational states at $T$ = 300 K [49].

TABLE I
PHOTOENHANCED ELECTRON ATTACHMENT

| |
|---|
| (1) VIBRATIONAL EXCITATION |
| (a) Single-Photon Excitation plus Energy Transfer |
| (b) Overtone and Combination Band Excitation |
| (c) Multi-Photon Excitation |
| (2) PHOTODISSOCIATION |
| (a) Single-Photon - UV |
| (b) Multi-Photon - IR |
| (3) ELECTRONIC EXCITATION |
| (a) E -> V,R Collisions |
| (b) E -> V,R Transitions, Radiative |

that vibrational excitation also will result from electron collisions. In cold discharges at low $E/N$, molecules in the excited state with the lowest excitation energy are the only excited species at considerable densities. Thus an external control mechanism will work efficiently only if the significant increase of the attachment cross section in the considered electron energy range occurs for states with energies well above that of the lowest lying excited state. Some possible mechanisms to produce such molecules are listed in Table I.

a) Optical vibrational excitation of higher lying states can be accomplished through vibration–vibration energy transfer, through overtone excitation or excitation of combination states, and through multiphoton excitation. Such mechanisms can be found as excitation mechanisms of numerous optically pumped IR lasers. Examples are lasers, optically pumped with a $CO_2$ laser, in molecules such as $CF_4$, NOCl, $CF_3I$, and $NH_3$ [73]. To date, experiments have failed to demonstrate a significant increase of the attachment rate in an e-beam sustained discharge after irradiation with a pulsed $CO_2$ laser [61]. In low-current dc charges containing $C_2H_3F$, sustained by helium plasma

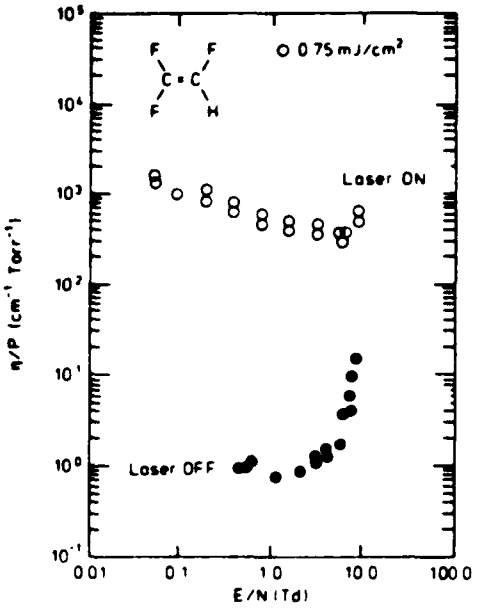


Fig. 7. Attachment coefficient for trifluoroethylene. The solid dots give the values for the unexcited sample (200 mtorr of $C_2F_3H$ in 200 torr helium). The open circles represent the data for the excited sample (100 mtorr of $C_2F_3H$ in 100 torr helium). The attachment coefficients are expressed in terms of the unexcited trifluorethylene pressure [60].

injection, small increases of the resistivity (~2 percent) have been found during irradiation with a very low power ($< 5$ W · cm$^{-2}$) $CO_2$ laser [74].

b) Single-photon and multiphoton dissociation of large molecules producing molecules in vibrationally excited states have been used as excitation mechanisms for molecular gas lasers. Photoelimination of HF from $CH_2CF_2$, $CH_2CHF$, and other halogenated hydrocarbons using UV flashlamps, generates a significant fraction of the HF molecules in states $v > 1$ [75], [76]. Some of these processes have significant cross sections at 193 nm (ArF lasers). Rossi *et al.* [60] performed drift tube experiments to demonstrate the feasibility of these processes for controlling the electron balance. In mixtures of helium with $C_2HF_3$ at low values of *E/N*, they obtained an increase of the attachment rate of up to $10^3$ with an ArF laser at 193 nm (Fig. 7). Similar experiments were performed in $C_2H_3Cl$. Schaefer *et al.* [77] performed measurements in dc discharges at low values of *E/N* (1–10 Td), which were externally sustained by helium plasma injection. In a gas mixture of 60-torr helium and 3-percent $C_2H_3Cl$, pulsed resistance changes of a factor of 0.35 were measured after irradiating the discharge with a UV spark source through a quartz window.

c) Electronic excitation can be transferred into vibrational excitation either through collisions or radiative processes (for a review see [78]). Optical excitation of bromine and subsequent collisional energy transfer to $CO_2$ have, for example, been used to operate a $CO_2$ laser ($Br_2 + h\nu \rightarrow Br + I^*$ and $Br^* + CO_2 \rightarrow Br + CO_2^{\dagger} + \Delta E$) [79].

Electronic excitation of $I_2$ and subsequent radiative transitions into highly vibrationally excited states (Fig. 8)

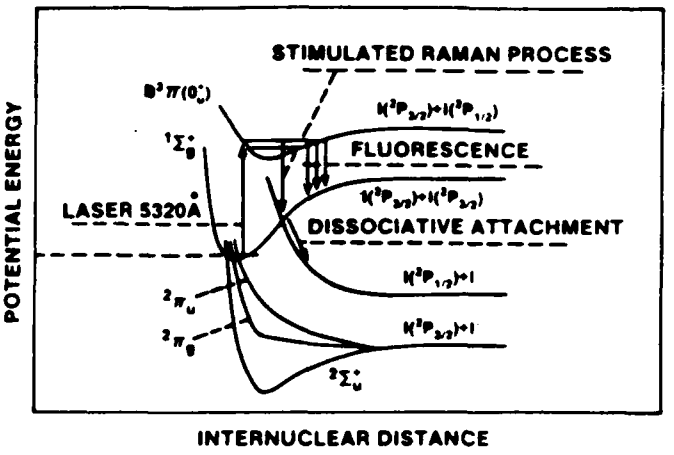


Fig. 8. Some potential curves for $I_2$ and $I_2^-$ and the scheme of excitation of vibrational levels [80].

have been used by Beterov and Fatayev [80] to show that vibrational excitation of $I_2$ can increase the attachment rate for dissociative attachment by three to four orders of magnitude. The radiation from a frequency doubled Nd:YAG laser ($\lambda = 532$ nm) was used to excite the *B* state. Intense Stokes fluorescence indicated a subsequent transition into highly vibrationally excited states. Vibrational relaxation to provide the population of the optimum vibrational states required times on the order of some 10 $\mu$s. It was suggested to use a stimulated resonant Raman process to excite the optimum vibrational states directly.

It has also been suggested to use attachers, which have an increased attachment cross section in an electronically excited metastable state [81]. The maximum attachment cross section of the metastable state of $O_2$ ($a\ ^1\Delta_g$), for example, is approximately 3.5 times higher than for the ground state [82]. Such states have the advantage that their energy is high and, consequently, the collisional excitation rate is low. Metastable states with higher attachment rates can be produced by optical excitation and subsequent internal energy conversion. For some aromatic molecules, conversion quantum yields close to 100 percent were observed [83].

For all proposed processes of optically enhanced attachment, it is very important to consider the attachment properties of the starting molecules. A real advantage of optically enhanced attachment can be achieved only if the attachment rate is significantly increased over a wide *E/N* range, and if the starting molecules are stable with respect to collisional processes in the e-beam sustained discharge. One also must consider other energy exchange processes that may compete with the desired attachment process. Processes producing new species in the discharge may also require changing the switch gas between shots.

## V. E-Beam Control of Diffuse Discharges

### A. E-Beam Considerations

E-beams are the most commonly used ionization sources for externally sustained diffuse discharges. Typically,

TABLE II
PROPERTIES OF FOIL MATERIAL CANDIDATES [84]

| FOIL MATERIAL | ADVANTAGE | DISADVANTAGE |
|---|---|---|
| Beryllium | Very Low Z<br>High Conductivity | Highly Toxic<br>Available only in Small Pieces, Expensive (~ $50/in$^2$) |
| Kapton | Low Z | Very Low Conductivity<br>Disintegrates from Electron Radiation |
| Aluminum | Relatively Low Z<br>High Conductivity | Low Strength at T > 200° C |
| Titanium (Pure and Alloy) | High Strength | Low Conductivity<br>Relatively High Z |
| Stainless Steel | High Strength | Low Conductivity<br>High Z |
| Inconel 718 | Very High Strength | Low Conductivity<br>High Z |
| Composite<br>E.G. Cu or Al Clad Ti | Combines High Strength with High Conductivity | Difficulty to Fabricate in Uniform Layers with Good Bonding |

beam energies are in the 100-300 keV range with current densities up to several amperes per square centimeter. In order to generate the e-beam, it is necessary to have the electrodes in a vacuum of $>10^{-3}$ torr for cold cathode operation and $>10^{-6}$ torr for thermionic cathodes.

The electron-generation mechanism at cold cathodes is usually field emission. With field-emitting cathodes, current densities of several hundred amperes per square centimeter can be obtained [84] at the expense, however, of limited pulse duration due to "diode closure" [85]. Diode closure is caused by plasma formation at the cathode. The plasma moves with velocities of 2-5 $10^6$ cm/s toward the anode and "closes" the diode gap in typically 2-5 $\mu$s.

Another cold cathode used for electron generation in e-beam controlled diffuse discharges is the wire-ion-plasma (WIP) electron gun [86]-[88]. The WIP gun cavity is filled with helium, typically at 10-20 mtorr. A positive pulse applied to the wire anode ionizes the helium in the plasma chamber. Helium ions are extracted and accelerated by the dc high voltage applied to the e-beam cathode. On helium impact, electrons are emitted from the cathode and accelerated by a high voltage. The e-beam current obtained in this device is typically 10 A over a cross section of 100 cm$^2$.

Thermionic emitters offer the advantage of decoupling electron generation and electron acceleration with unlimited pulse length. The generation of pulse trains is possible by using a triode or tetrode configuration. In a tetrode with thoriated tungsten electrodes, current densities of up to 4 A/cm$^2$ were obtained [89]. With dispenser-type thermionic cathodes, values of 300 A/cm$^2$ were reached [90], [91].

The interface between electron gun and switch chamber is generally a thin (20-50 $\mu$m) foil backed by a support structure. The foil material should have low electron-stopping power, and good thermal and mechanical properties. In Table II, properties of different foil materials are listed [84]. A severe constraint for long e-beam pulses and/or repetitive operation is foil heating. In order to avoid structural fractures, the foil temperature must be limited. A foil heating analysis has been performed by Daugherty [92].

### *B. Design of an E-Beam Controlled Diffuse Discharge Switch*

Because of the limited conduction time of an e-beam sustained discharge due to the development of instabilities and the time constraints of the e-beam source, it is proposed to use it as the main switch in a two-loop inductive energy storage circuit [10]. Fig. 9 shows the schematic circuit with the charging loop and the discharge loop having only the inductor in common. The inductor is charged through the initially closed switch *A*. The e-beam is turned on when the current through the inductor has reached its maximum steady-state value. Switch *A* now can open the charging circuit at relatively low switch voltage and commutate the current into the e-beam controlled discharge. If switch gases with low losses at low *E/N* are used, the efficiency of this commutation can be very high. Once the current is transferred into the diffuse discharge switch, the circuit can generate either a single pulse by closing switch *B* and simultaneously opening the diffuse discharge, or a pulse train by repetitively closing and opening the diffuse discharge with switch *B* closed. In order to prevent loss currents in the load when the diffuse discharge is conducting (if the load impedance is comparable to the diffuse discharge impedance), switch *B* could be replaced by a second e-beam controlled switch which opens and closes a countermode to the first switch.

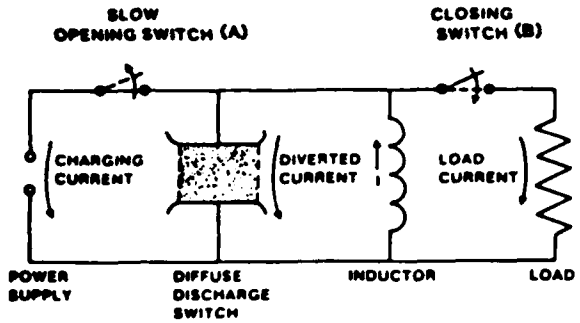


Fig. 9. Schematic circuit for an e-beam sustained discharge switch in an inductive energy storage system [10].

The following design criteria for the e-beam sustained switch in such a circuit are based on a group report in the *Proceedings of the ARO Workshop on Diffuse Discharge Opening Switches* [93]. For an efficient switch, the major electron loss in the conduction state will occur through recombination. Attachment is important only in onset and cutoff, steepening the current pulse. In steady state the electron density is well described by (4) with $k_a$ being neglected. The conductivity therefore is given by (8):

$$\sigma = e\mu\sqrt{\frac{S}{k_r}}, \quad \text{with} \quad \mu = \frac{v_d}{E_s} \quad \text{and} \quad S = \frac{J_B}{eW_i}\left(\frac{dW}{dx}\right) \tag{11}$$

where $v_d$ is the electron drift velocity, $E_s$ is the electric-field intensity in the diffuse discharge, $J_B$ is the e-beam current density, $dW/dx$ is the spatial rate of e-beam energy loss in the gas [94], [95], and $eW_i$ is the beam ionization energy of the gas [96].

In order to avoid glow-to-arc transition, the temperature in a molecular gas should not exceed $T_0 = 500$ K. Assuming that any increase in gas temperature $\Delta T$ is caused by Joule heating, leads to the relation

$$\rho c_v \Delta T = \frac{J^2\tau}{\sigma} \tag{12}$$

$\rho$ being the gas density, $c_v$ the specific heat, and $\tau$ the conduction time. This relation allows estimation of an upper limit for the current density:

$$J_{max} = \sqrt{(T_0 - T_i)\frac{\rho c_v \sigma}{\tau}} \tag{13}$$

where $T_i$ is the initial temperature.

For a given total current $I$, this determines the switch diameter. The discharge gap length $d$ is determined by the required switch holdoff voltage $V_0$:

$$d = \frac{V_0}{E_{crit}}. \tag{14}$$

Critical field strengths $E_{crit}$ are in the order of 6–12 kV/cm at a pressure of 1 atm.

Calculations along this line were performed for a switch which carries 10 kA for a time of 50 $\mu$s to charge a capacitor of 400 nF to a voltage of 250 kV [93]. A switch gas pressure of 10 atm in 90-percent $CH_4$ and 10-percent Ar was assumed. The standoff capability of this mixture is $E_{crit} = 5$ kV/cm at 1 atm. For a holdoff voltage of 250 kV, the gap length $d$ must be at least 5 cm at a pressure of 10 atm. With an assumed e-beam current density of $J_B = 140$ mA/cm$^2$ and an e-beam energy of 200 keV after passing the foil which separates e-beam gun and diffuse discharge switch, the discharge conductivity is $\sigma = 2.1 \cdot 10^{-2}$ $(\Omega\ \text{cm})^{-1}$ (11). The maximum current density is according to (13) $J_{max} \approx 19$ A/cm$^2$. For a total current of 10 kA, the switch area must be 531 cm$^2$.

Using these data, the transfer efficiency of the switch can be calculated. The energy transferred into the capacitor is $E_{cap} = 12.5$ kJ. The Joule losses in the diffuse discharge are $E_{dis} = 2.25$ kJ. The e-beam energy dissipated in the switch is 0.75 kJ. Allowing, conservatively, structure and foil e-beam losses to be 30 percent, the total required e-beam energy is $E_{eb} = 1.06$ kJ. The efficiency is then given as

$$\eta = \frac{E_{cap}}{E_{cap} + E_{eb} + E_{dis}} \tag{15}$$

which is about 80 percent for this diffuse discharge switch. This calculation allows a rough estimate of the geometry and the transfer efficiency of a diffuse discharge switch as part of a pulsed power circuit.

A more detailed design procedure which includes the energy consumption during opening of a repetitively operated switch was developed by Commisso *et al.* [13]. The energy transfer efficiency $\eta$ is defined as

$$\eta = \frac{I_L^0 V_L^0 \tau_L}{\langle I_{sw}V_{sw}\rangle_c\tau_c + \langle I_{sw}V_{sw}\rangle_0\tau_0 + I_L^0 V_L^0 \tau_L + I_{eb}V_{eb}\tau_c} \tag{16}$$

$I_{sw}$, $I_L$, and $I_{eb}$ are the switch, load, and e-beam currents; $V_{sw}$, $V_L$, and $V_{eb}$ are the corresponding voltages (the superscript 0 denotes peak values). $\tau_c$, $\tau_0$, and $\tau_L$ are the conduction time, the opening time, and the characteristic load pulsewidth, respectively. The terms in the denominator describe Joule losses in the switch during conduction and during opening, the energy transferred to the load, and the e-beam energy, necessary to sustain the discharge for the time of conduction.

For energy transfer efficiency comparable to capacitive store pulsed power generators, it is required that each of the losses in the switch is small compared to the energy transferred to the load. These conditions can be interpreted as restrictions for the switch opening time $\tau_0$, for the voltage drop across the discharge during conduction $V_{sw}$, and for the current gain $\epsilon = I_{sw}^0/I_{eb}$.

In [13] the system was optimized by requiring that the switch pressure be minimum. The result of this optimization is that each of the major energy losses—conduction, opening, and e-beam production—are roughly equal to each other.

TABLE III
SUMMARY OF DATA ON RELEVANT EXPERIMENTS ON E-BEAM CONTROLLED SWITCHES

| INSTUTUTE, REFERENCES | E-BEAM SYSTEM | E-BEAM CURRENT DENSITY $J_B$[A/cm$^2$] | E-BEAM ENERGY $E_B$(keV] | GASES | SWITCH CURRENT DENSITY $J_S$[A/cm$^2$] | CURRENT GAIN | OPENING TIME |
|---|---|---|---|---|---|---|---|
| High Current Electr. Dept., Tomsk, USSR (Koval'chuk and Mesyats [4,5]) | Cold Cathode | 1.5 | 330 | Natural Gas: $CH_4$:$C_2H_6$:$C_3H_8$: $O_2$:$CO_2$: other hydrocarbons | 15 | ~ 10 | 200 ns |
| (Efremov and Koval'chuk [99]) | Therminionic Cathode, Tetrode | 0.014 | 135 | $CO_2$:$N_2$:He | 30 | 1000 | 3 μs - 5 μs |
| Maxwell Labs San Diego, CA (Hunter [2,3]) | Cold Cathode | 2-5 | 250 | $CH_4$ | 27 | 5 | 400 ns |
| AFWL, Wright Patterson (Bletzinger [32,34]) | Hot Matrix Cathode | 0.02 | 175 | $N_2$,Ar,$CH_4$ with $C_2F_6$,$C_3F_8$,$NF_3$, $CF_4$,$CCl_4$ | 2 | 100-1000 | 10 μs - 1 μs |
| Westinghouse R&D Ctr. Pittsburgh, PA (Lowry et al. [45]) | WIP-gun | < 0.1 | 150 | $CH_4$ | 19 | 380 | > 1 μs (with inductor in switch loop) |
| Hughes Research Laboratories Malibu, CA (Gallagher & Harvey [88]) | WIP-gun | < 0.035 | 150 | $CH_4$ | 20 | < 1000 | > 1 μs (with inductor in switch loop) |
| Naval Research Lab, Washington, DC (Commisso et al. [103, 104]) | Cold Cathode, 200 ns and ~1 μs pulse durations | 0.2-5 | 200 | $CH_4$,$N_2$ $N_2$:$O_2$ Ar:$O_2$ $CH_4$:$C_2F_6$ | < 50 | 10-20 | 50 ns - 100 ns |
| Texas Tech University Lubbock, TX (Schoenbach et al. [109], Schaefer et al. [110]) | Thermionic Cathode, Tetrode, pulse train | 0.1-1.0 | 250 | $N_2$:$N_2O$ $N_2$:$SO_2$ $N_2$:$CO_2$ Ar:$C_2F_6$ | < 15 | ~ 15 | 50 ns |

The transfer efficiency calculated by using this formalism [13], which includes switch losses during opening, is smaller than the one obtained with the simple model discussed before (15). The design equations for the switch geometry in the two models become identical for the case that switch losses during opening can be neglected and all safety factors are of the order of unity.

### C. Experimental Results

A summary of relevant experiments on e-beam controlled switches is given in Table III. Listed are e-beam and switch parameters. The values for current gain and opening time are mostly approximate values which serve to define the range of operation for the respective experiment.

Early experiments on diffuse discharge switches were performed by Hunter [3] and Koval'chuk and Mesyats [5]. They used cold cathode e-beam emitters derived from laser experiments. With large e-beam current density, they achieved fast rise times and could afford to work with added attachers to get fast opening, at the expense of power gain. They did not use specially designed gases, however. Hunter [3] recognized the importance of having a gas with high electron drift velocity and therefore chose methane. Methane has an electron drift velocity peaking at more than $10^7$ cm/s at about 3 Td.

In later publications, several gas mixtures with optimized properties have been proposed for diffuse discharge opening switches [8], [28], [97]-[99]. Fig. 10 shows

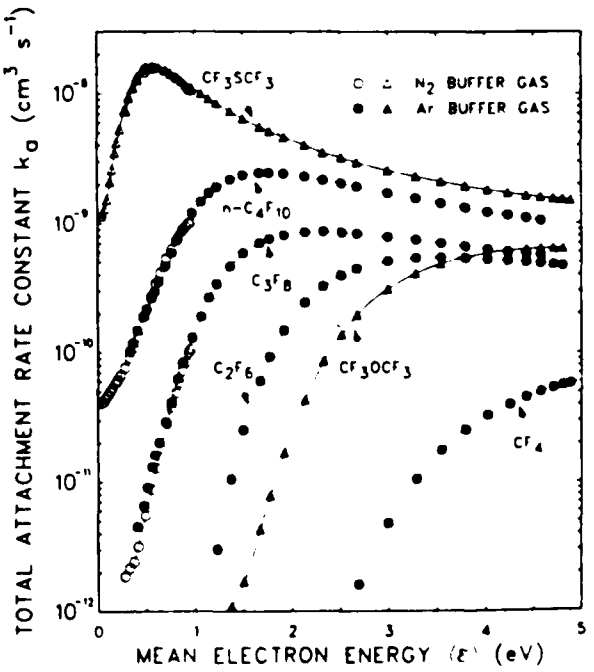


Fig. 10. Total electron attachment rate constants as a function of the mean electron energy ⟨ε⟩ for several perfluoroalkanes and perfluoroethers measured in buffer gases of $N_2$ and Ar [98].

electron attachment rate constants for several attachers in Ar and $CH_4$ as buffer gas [98]. These gas mixtures also exhibit a negative differential drift velocity region over a wide range of fractional concentrations of the attaching

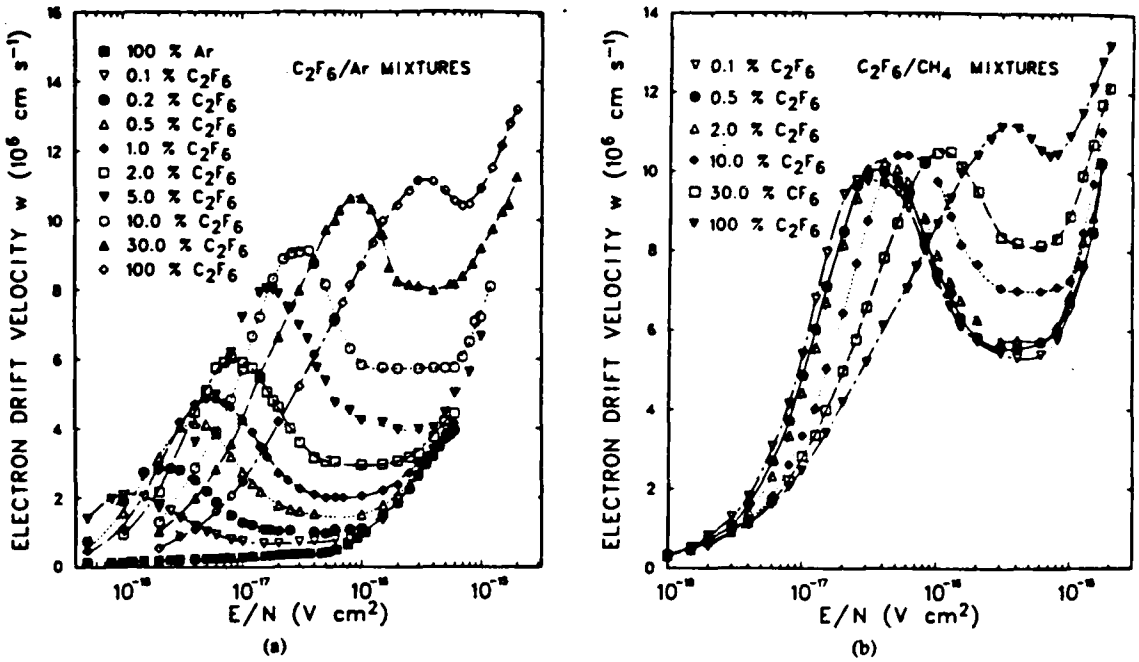


Fig. 11. Electron drift velocity $w$ versus $E/N$ for several (a) $C_2F_6$/Ar and (b) $C_2F_6$/$CH_4$ gas mixtures [98].

gas in the buffer gas as shown in Fig. 11 for $C_2F_6$ in Ar and $CH_4$, respectively [98]. Consequently, the current density-reduced field strength ($J$-$E/N$) characteristics of e-beam sustained discharges in gas combinations of this type exhibit a pronounced negative differential conductivity range [77], [100].

Another gas combination which was proposed as switch gas for e-beam sustained diffuse discharge opening switches is $N_2O$ in $N_2$ as buffer gas [8]. The gas mixture exhibits an $E/N$-dependent electron decay rate which increases by more than a factor of 20 in the $E/N$ range from 3–15 Td [101].

Work done at Wright-Patterson [31]–[34], Hughes Laboratories [88], and Westinghouse Laboratories [45] has concentrated on high-gain systems with opening times in the microsecond range. At Wright-Patterson [31]–[34], special consideration was given to the cathode region and its influence on the discharge characteristic. Work at the Naval Research Lab [102]–[106] and at Texas Tech University [100], [107]–[110] deals with repetitive or burst-mode opening switch operation. Both groups concentrate on switches with opening times in the submicrosecond range, but try to achieve reasonable current gains ($> 100$) by using suitable gas mixtures. At Texas Tech University, the interaction of discharge and circuit has been investigated for discharges with a strong negative differential conductivity such as in mixtures of Ar and $C_2F_6$. Fig. 12 shows such a characteristic and demonstrates that the maximum current cannot be utilized in the burst mode in a high-impedance system if the pulse separation is shorter than the discharge time of the inductor [110].

Opening switch experiments in discharge circuits including inductors have demonstrated the use of e-beam

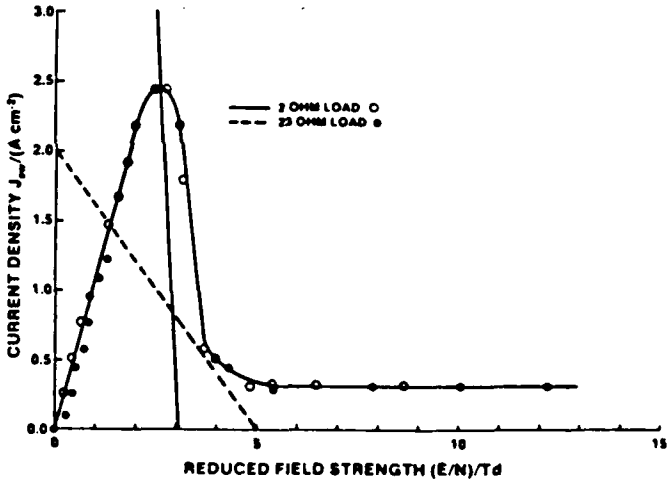


Fig. 12. Load lines and current density $j$ versus reduced electric field strength $E/N$ obtained with different load lines [110].

controlled diffuse discharges for the generation of high-voltage pulses. For an experiment performed at Wright-Patterson [111], [112], a capacitor discharge current of up to 135 A was commutated into an inductive load after opening of the e-beam controlled switch. A short microsecond voltage pulse was generated, with its peak voltage exceeding the static breakdown voltage of the e-beam controlled discharge by more than 50 percent with a $CH_4$/$C_2F_6$ gas mixture. An experiment performed at NRL [104] used an e-beam controlled diffuse discharge as the switch element in an inductive energy storage circuit. The storage inductor (1.5 $\mu$H) was energized by a capacitor charged to 26 kV. Upon termination of the ionizing e-beam, the 10-kA discharge was interrupted, thereby gen-

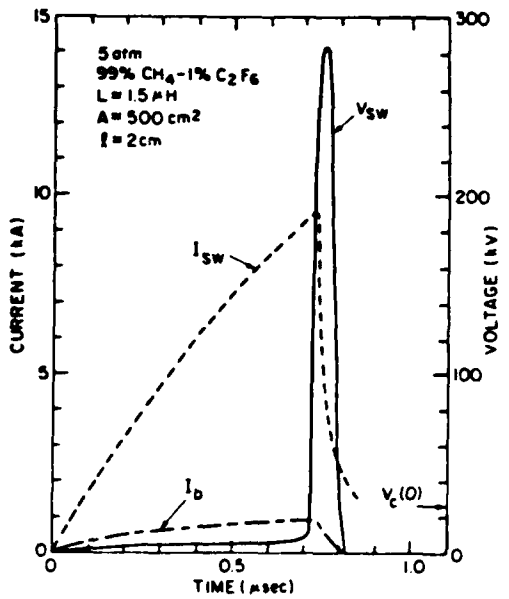


Fig. 13. System current, e-beam current, and switch voltage for an e-beam controlled switch using 5 atm of $CH_4$ with 1 percent $C_2F_6$ [104].

erating a 280-kV 60-ns voltage pulse across an open circuit (Fig. 13). The gas mixture in the e-beam controlled switch was $CH_4/C_2F_6$ at 5 atm. The current gain was about 10.

The experimental results demonstrate that diffuse discharge switches are suitable for the generation of high-power pulses. In order to improve the efficiency of these switches (low losses during conduction at high current gain) and to minimize the opening time, it is important to utilize electron-molecule interactions in gas mixtures. Using "gas engineering" as a means to design switch gases should lead to improved switch performance, with current gains on the order of 100 at opening times of less than 100 ns.

## Acknowledgment

The authors wish to express their appreciation for the very helpful comments and suggestions of the reviewers.

## References

[1] J. D. Daugherty, E. R. Pugh, and D. H. Douglas-Hamilton, *Bull. Amer. Phys. Soc.*, vol. 16, p. 399, 1971.
[2] R. O. Hunter, "Electron beam controlled low impedance discharges," *Bull. Amer. Phys. Soc.*, vol. 20, p. 255, 1975.
[3] R. O. Hunter, "Electron beam controlled switching," in *Proc. 1st IEEE Int. Pulsed Power Conf.* (Lubbock, TX), 1976, p. IC8-1.
[4] B. M. Koval'chuk and G. A. Mesyats, "Rapid cutoff of a high current in an electron-beam-excited discharge," *Sov. Tech. Phys. Lett.*, vol. 2, p. 252, 1976.
[5] B. M. Koval'chuk and G. A. Mesyats, "Current breaker with space discharge controlled by electron beam," in *Proc. 1st IEEE Int. Pulsed Power Conf.* (Lubbock, TX), 1976, p. IC7-1.
[6] D. R. Shure and J. T. Verdeyen, "Energy distributions in electron-beam produced nitrogen plasmas," *J. Appl. Phys.*, vol. 47, p. 4484, 1976.
[7] K. Nakanishi, L. G. Christophorou, J. G. Carter, and S. R. Hunter, "Penning ionization ternary gas mixtures for diffuse discharge switching applications," *J. Appl. Phys.*, vol. 58, p. 633, 1985.
[8] K. H. Schoenbach, G. Schaefer, M. Kristiansen, L. L. Hatfield, and A. H. Guenther, "Concepts for optical control of diffuse discharge opening switches," *IEEE Trans. Plasma Sci.*, vol. PS-10, p. 246, 1982.
[9] A. H. Guenther, "Optically controlled discharges," in *Proc. ARO Workshop on Repetitive Opening Switches* (Tamarron, CO), 1981, p. 48.
[10] G. Schaefer, K. H. Schoenbach, H. Krompholz, M. Kristiansen, and A. H. Guenther, "The use of attachers in electron-beam sustained discharge switches—Theoretical considerations," *Lasers and Particle Beams*, vol. 2, p. 273, 1984.
[11] Yu. I. Bychkov, Yu. D. Korolev, and G. A. Mesyats, "Pulse discharges in gases under conditions of strong ionization by electrons," *Sov. Phys.—Usp.*, vol. 21, p. 944, 1978.
[12] R. F. Fernsler, D. Conte, and I. M. Vitkovitsky, "Repetitive electron-beam controlled switching," *IEEE Trans. Plasma Sci.*, vol. PS-8, p. 176, 1980.
[13] R. J. Commisso, R. F. Fernsler, V. E. Scherrer, and I. M. Vitkovitsky, "High power electron beam controlled switches," *Rev. Sci. Instr.*, vol. 55, p. 1834, 1984.
[14] L. E. Kline, "Performance predictions for electron-beam controlled on/off switches," *IEEE Trans. Plasma Sci.*, vol. PS-10, p. 224, 1982.
[15] G. Schaefer, K. H. Schoenbach, P. Tran, J. Wang, and A. H. Guenther, "Computer calculations of the time dependent behavior of diffuse discharge switches," in *Proc. 4th IEEE Pulsed Power Conf.* (Albuquerque, NM), 1983, p. 714.
[16] C. B. Opal, W. K. Peterson, and E. C. Beaty, "Measurements of secondary-electron spectra produced by electron impact ionization of a number of simple gases," *J. Chem. Phys.*, vol. 55, pp. 4100-4106, 1971.
[17] A. E. S. Green and T. Sawada, "Ionization cross sections and secondary electron distributions," *J. Atmos. Terr. Phys.*, vol. 34, pp. 1719-1728, 1972.
[18] L. R. Peterson and J. E. Allen, Jr., "Electron impact cross sections for argon," *J. Chem. Phys.*, vol. 56, pp. 6068-6076, 1972.
[19] C. H. Jackson, R. H. Garvey, and A. E. S. Green, "Electron impact on atmospheric gases, I. Updated cross sections," *J. Geophys. Res.*, vol. 82, pp. 5081-5090, 1977.
[20] R. C. Smith, "Computed secondary-electron and electric field distributions in an electron-beam controlled gas-discharge laser," *Appl. Phys. Lett.*, vol. 21, pp. 352-355, 1972.
[21] J. N. Bass and A. E. S. Green, "Energy deposition of electrons in gas lasers," *J. Appl. Phys.*, vol. 44, pp. 3726-3728, 1973.
[22] C. J. Elliot and A. E. S. Green, "Electron energy distributions in e-beam generated Xe and Ar plasmas," *J. Appl. Phys.*, vol. 47, pp. 2946-2953, 1976.
[23] J. Bertagne, G. Delouya, J. Godart, and V. Puech, "High-energy electron distribution in an electron-beam-generated argon plasma," *J. Phys. D: Appl. Phys.*, vol. 14, pp. 1225-1239, 1981.
[24] J. Bertagne, J. Godart, and V. Puech, "Low-energy electron distribution in an electron-beam-generated argon plasma," *J. Phys. D: Appl. Phys.*, vol. 15, pp. 2205-2225, 1982.
[25] J. A. LaVerne and A. Mozumder, "Energy loss and thermalization of low-energy electrons," *Radiat. Phys. Chem.*, vol. 23, pp. 637-660, 1984.
[26] G. Schaefer, G. F. Reinking, and K. H. Schoenbach, "Monte Carlo calculations on the influence of attachment on the thermalization of secondary electrons in an electron beam sustained discharge," submitted to *J. Appl. Phys.*, 1986.
[27] K. H. Schoenbach, M. Kristiansen, E. E. Kunhardt, L. L. Hatfield, and A. H. Guenther, "Exploratory concepts of opening switches," in *Proc. ARO Workshop on Repetitive Opening Switches* (Tamarron, CO), 1981, p. 65.
[28] L. G. Christophorou, S. R. Hunter, J. G. Carter, and R. A. Mathis, "Gases for possible use in diffuse-discharge switches," *Appl. Phys. Lett.*, vol. 41, p. 147, 1982.
[29] A. D. Barkalov and G. G. Gladush, "Domain instability of a non-self-sustaining discharge in electronegative gases, I. Numerical calculations," *High Temp.*, vol. 20, p. 16, 1982
A. D. Barkalov and G. G. Gladush, "Domain instability of a non-self-sustaining discharge in electronegative gases, II. Theoretical analysis," *High Temp.*, vol. 20, p. 172, 1982
[30] J. J. Lowke and D. K. Davies, "Properties of electric discharges sustained by a uniform source of ionization," *J. Appl. Phys.*, vol 48, p. 4991, 1977.
[31] P. Bletzinger, "Electron beam switching experiments in the high current gain regime," in *Proc. 3rd Int. Pulsed Power Conf.* (Albuquerque, NM), 1981, p. 81.

[32] P. Bletzinger, "E-beam experiments—Interpretations and extrapolations," in *Proc. ARO Workshop on Diffuse Discharge Opening Switches* (Tamarron, CO), 1982, p. 112.
[33] M. R. Hallada, P. Bletzinger, and W. Bailey, "Application of electron-beam ionized discharges to switches—A comparison of experiment with theory," *IEEE Trans. Plasma Sci.*, vol. PS-10, p. 218, 1982.
[34] P. Bletzinger, "Scaling of electron beam switches," in *Proc. 4th IEEE Pulsed Power Conf.* (Albuquerque, NM), 1983, p. 37.
[35] Yu. I. Bychkov, Yu. D. Korolev, G. A. Mesyats, A. P. Khuzeev, and I. A. Shemyakin, "Volume discharge excited by an electron-beam in an Ar-$SF_6$ mixture, I. Beam controlled discharge," *Izv. Vyssh. Ucheb. Zaved.*, vol. 7, p. 898, 1979.
Yu. I. Bychkov, Yu. D. Korolev, G. A. Mesyats, A. P. Khuzeev, and I. A. Shemyakin, "Volume discharge excited by an electron-beam in an Ar-$SF_6$ mixture, II. Cascade ionization discharge," *Izv. Vyssh. Ucheb. Zaved.*, vol. 7, p. 77, 1979.
[36] Yu. D. Korolev, G. A. Mesyats, and A. P. Khuzeev, "Electrode phenomena preceding the transition of non-selfmaintaining diffuse discharge to a spark," *Sov. Phys.—Dokl.*, vol. 25, p. 573, 1980.
[37] D. H. Douglas-Hamilton, "Some instabilities in non-self-sustained gas discharges," in *Proc. US-FRG Joint Seminar on Externally Controlled Diffuse Discharges* (Bad Honnef, FRG), 1983, p. 43.
[38] R. A. Haas, "Plasma stability of electric discharges in molecular gases," *Phys. Rev. A*, vol. 8, p. 1017, 1973.
[39] R. A. Haas, "Stability of excimer laser discharges," in *Applied Atomic Collision Physics, Volume 3: Gas Lasers*, E. W. McDaniel and W. L. Nighan, Eds. New York: Academic, 1982.
[40] W. L. Nighan, "Stability of high-power molecular laser discharges," in *Principles of Laser Plasmas*, G. Bekefi, Ed. New York: Wiley, 1976.
[41] E. E. Kunhardt, "Basic topics of current interest to switching for pulsed power applications," in *Gaseous Dielectrics IV*, L. G. Christophorou and M. O. Pace, Eds. New York: Pergamon, 1983.
[42] D. H. Douglas-Hamilton and S. A. Mani, "An electron attachment plasma instability," *Appl. Phys. Lett.*, vol. 23, pp. 508–510, Nov. 1973.
[43] D. H. Douglas-Hamilton and S. A. Mani, "Attachment instability in an externally ionized discharge," *J. Appl. Phys.*, vol. 45, p. 4406, 1974.
[44] P. Bletzinger, "A review of some boundary effects in electron beam ionized discharges," in *Proc. US-FRG Joint Seminar on Externally Controlled Diffuse Discharges* (Bad Honeff, FRG), 1983, p. 148.
[45] J. F. Lowry, L. E. Kline, and J. V. R. Heberlein, "Electron-beam controlled on/off discharge characterization experiments," in *Proc. 4th IEEE Pulsed Power Conf.* (Albuquerque, NM), 1983, p. 94.
[46] L. C. Pitchford, "Power loading effects in gas discharge models," in *Proc. US-FRG Joint Seminar on Externally Controlled Diffuse Discharges* (Bad Honeff, FRG), 1983, p. 148.
[47] A. P. Napartovich, V. G. Naumov, and V. M. Shashkov, "Heating of gas in a combined discharge in a flow of nitrogen," *Sov. Phys.—Dokl.*, vol. 22, p. 35, 1977.
[48] J. A. Shirley and R. J. Hall, "Vibrational excitation in $H_2$ and $D_2$ electric discharges," *J. Chem. Phys.*, vol. 67, p. 2419, 1977.
[49] J. N. Bardsley and J. M. Wadehra, private communication, 1982.
[50] J. M. Wadehra, "Effect of rot-vibrational excitation on dissociative attachment of $H_2$," presented at the 35th Gaseous Elec. Conf., Dallas, TX, 1982, Abstr. NA-2.
[51] H. Seguin and J. Tulip, "Photoinitiated and photosustained laser," *Appl. Phys. Lett.*, vol. 21, p. 414, 1972.
[52] D. R. Shure and S. A. Wutzke, "UV sustained CO laser discharge, II. Dicharge studies," *J. Appl. Phys.*, vol. 52, p. 3858, 1981.
[53] D. R. Shure, "UV sustained CO laser discharge, I. Photoionization studies," *J. Appl. Phys.*, vol. 52, p. 3855, 1981.
[54] W. M. Moeny and M. von Dadelszen, "UV-sustained glow discharge opening switch experiments," in *Proc. 5th IEEE Pulsed Power Conf.* (Arlington, VA), 1985, p. 630.
[55] C. M. Young *et al.*, "Investigation of a UV-sustained radial glow discharge opening switch," in *Proc. 5th IEEE Pulsed Power Conf* (Arlington, VA), 1985, p. 633.
[56] G. Z. Hutchenson, J. R. Cooper, E. Strickland, G. Schaefer, and K. H. Schoenbach, "Time dependent emission from a spark array used as an ionization source for diffuse discharges," *IEEE Trans. Electron Devices*, submitted for publication.
[57] D. K. Doughty and J. E. Lawler, "Model of optogalvanic effects in the neon positive column," *Phys. Rev. A*, vol. 28, pp. 773–780, Aug. 1983.
[58] G. Schaefer, P. F. Williams, K. H. Schoenbach, and J. T. Moseley, "Photodetachment as a control mechanism for diffuse discharge switches," *IEEE Trans. Plasma Sci.*, vol. PS-11, p. 263, 1983.
[59] J. E. Lawler, and A. H. Guenther, "Applications of optogalvanic effects in opening switches," in *Proc. 3rd IEEE Int. Pulsed Power Conf.* (Albuquerque, NM), pp. 147–150, 1981.
[60] M. J. Rossi, H. Helm, and D. C. Lorents, "Photoenhanced electron attachment in vinylchloride and trifluorethylene at 193 nm," *Appl. Phys. Lett.*, vol. 47, pp. 576–578, Sept. 1984.
[61] F. L. Eisele, "Photon induced electron attachment," Final Rep. AFWAL-TR-85-2015, 1984.
[62] S. J. Smith, in *Proc. 4th Int. Conf. Ionization Phenomena in Gases*, 1960, p. IC-219.
[63] D. S. Burch, S. J. Smith, and L. M. Branscomb, "Photodissociation spectroscopy of $O_2^-$," *J. Chem. Phys.*, vol. 112, p. 171, 1958.
[64] L. M. Branscomb, S. J. Smith, and G. Tisone, "Oxygen metastable atom production through photodetachment," *J. Chem. Phys.*, vol. 43, p. 2906, 1965.
[65] J. L. Moruzzi and A. V. Phelps, "Survey of negative ion molecule reactions in $O_2$, $CO_2$, $H_2O$, CO, and mixtures of these gases," *J. Chem. Phys.*, vol. 44, pp. 4617–4627, Dec. 1966.
[66] R. Gruenberg, "Messungen des Anlagerungskoeffizienten von Electronen in Sauerstoff," *Z. Naturforsch.*, vol. 24a, pp. 1039-1048, 1969.
[67] K. E. Greenberg, G. A. Heben, and J. T. Verdeyen, "Negative ion densities in $NF_3$ discharges," *Appl. Phys. Lett.*, vol. 44, pp. 299–301, Feb. 1984.
[68] C. L. Chen and P. J. Chantry, "Photon-enhanced dissociative electron attachment in $SF_6$ and its isotopic selectivity," *J. Chem. Phys.*, vol. 71, p. 3897, 1979.
[69] R. Barbe, J. P. Astruc, A. Lagreze, and J. P. Schermann, "Spectral and temperature dependence of laser induced dissociative attachment in $SF_6$," *Laser Chem.*, vol. 1, p. 17, 1982.
[70] W. E. Wentworth, R. George, and H. Keith, "Dissociative thermal electron attachment of some alphatic chloro, bromo, iodo compounds," *J. Chem. Phys.*, vol. 51, p. 1791, 1969.
[71] M. Allan and S. F. Wong, "Dissociative attachment from vibrationally and rotationally excited HCl and HF," *J. Chem. Phys.*, vol. 74, p. 1687, 1981.
[72] S. K. Srivastava and O. J. Orient, "A double e-beam technique for collision studies from excited states: Application to vibrationally excited $CO_2$," *Phys. Rev. A*, vol. 27, p. 1209, 1983.
[73] J. J. Tiee and C. Wittig, "Optically pumped molecular lasers in the 11–17 micron region," *J. Appl. Phys.*, vol. 49, p. 61, 1978.
[74] G. Schaefer *et al.*, "Interaction of discharge and circuit in an electron-beam controlled diffuse discharge opening switch," in *Proc. BEAM's 86* (Osaka, Japan), June 1986.
[75] E. R. Sirkin and G. C. Pimentel, "HF rotational laser emission through photoelimination from vinyl fluoride and 1,1-difluorothene," *J. Chem. Phys.*, vol. 75, p. 604, 1981.
[76] M. J. Berry, "Chlorethylene photochemical lasers: Vibrational energy content of HCl molecular elimination products," *J. Chem. Phys.*, vol. 61, p. 3114, 1974.
[77] G. Schaefer and K. H. Schoenbach, "External control of diffuse discharge switches," in *Proc. 5th IEEE Pulsed Power Conf.* (Arlington, VA), p. 644, 1985.
[78] P. L. Houston, "Electronic to vibrational energy transfer from excited halogen atoms," in *Photoselective Chemistry—Part 2*, J. Jortner, R. D. Levine, and S. R. Rice, Eds. New York: Wiley, 1981.
[79] A. B. Peterson, C. Wittig, and S. R. Leone, "Electronic to vibrational pumped $CO_2$ laser operating at 4.3, 10.6, and 14.1 $\mu$m," *J. Appl. Phys.*, vol. 47, pp. 1051–1054, Mar. 1976.
[80] I. M. Beterov and N. V. Fatayev, "Optogalvanic demonstration of state-to-state dissociative electron capture rate in $I_2$," *Opt. Comm.*, vol. 40, p. 425, 1982.
[81] D. Lorents, in "Report on optically induced processes," in *Proc. ARO Workshop on Diffuse Discharge Opening Switches* (Tamarron, CO), 1982, p. 212.
[82] P. D. Burrow, "Dissociative attachment from the $O_2(a^1\Delta_g)$ state," *J. Chem. Phys.*, vol. 59, p. 4922, 1983.
[83] A. N. Dharamsi and J. Tulip, "Contact charge transfer lasers," *J. Appl. Phys.*, vol. 52, p. 4418, 1981.
[84] J. E. Eninger, "Broad area electron beam technology for pulsed high power gas lasers," in *Proc. 3rd IEEE Pulsed Power Conf.* (Albuquerque, NM), 1981, p. 499.
[85] T. J. Orzechowski and G. Bekefi, "Current flow in a high-voltage

diode subjected to a crossed magnetic field," *Phys. Fluids*, vol. 19, p. 43, 1976.
[86] W. M. Clark, "Ion plasma electron gun research," HRL Final Rep., ONR Contract N00014-77-C-0484, 1977.
[87] G. Wakalopulos and L. Gresko, "Pulsed WIP electron gun, Final Report—Design Phase," HAC Rep. FR-79-73-735, UCRL, 1979.
[88] H. E. Gallagher and R. J. Harvey, "Development of a 1-GW electron-beam controlled switch," in *Proc. 16th Power Modulator Symp.* (Arlington, VA), 1984, p. 158.
[89] C. H. Harjes *et al.*, "Electron-beam tetrode for multiple, submicrosecond pulse operation," *Rev. Sci. Instr.*, vol. 55, p. 1684, 1984.
[90] R. Petr, and M. Gundersen, "Field emission cathode for high current beams," *Lasers and Particle Beams*, vol. 1, p. 207, 1983.
[91] J. L. Cronin, "Modern dispenser cathodes," *Proc. Inst. Elec. Eng.*, vol. 128, p. 19, 1982.
[92] J. D. Daugherty, "Electron beam ionized lasers," in *Principles of Laser Plasmas*, G. Bekefi, Ed. New York: Wiley, 1976.
[93] D. H. Douglas-Hamilton, "Diffuse discharge production—Group report," in *Proc. ARO Workshop on Diffuse Opening Switches* (Tamarron, CO), 1982, p. 169.
[94] M. J. Berger and S. M. Seltzer, "Tables of energy-losses and ranges of electrons and positions," NAS-NRC Publ. 1133, p. 205, 1964.
[95] "Stopping powers for electrons and positrons, International Commission on Radiation Units and Measurements," ICRU Publications, Bethesda, MD, ICRU Rep. 37, 1984.
[96] D. C. Lorents and R. E. Olson, "Excimer formation and decay processes in rare gases," Stanford Res. Inst., Stanford, CA, SRI Semiannual Tech. Rep. 1, 1971.
[97] L. C. Lee and F. Li, "Shortening of electron conduction pulses by electron attachers $O_2$, $N_2O$, and $CF_4$," *J. Appl. Phys.*, vol. 56, p. 3169, 1984.
[98] S. R. Hunter, J. G. Carter, J. L. Christophorou, and V. K. Lakdawala, "Transport properties and dielectric strengths of gas mixtures for use in diffuse discharge opening switches," in *Gaseous Dielectrics IV*, L. G. Christophorou and M. O. Pace, Eds. New York: Pergamon, 1984.
[99] A. M. Efremov and B. M. Koval'chuk, "A non-self-consistent electron-beam controlled discharge in methane," *Izv. Vyssh. Ucheb. Zaved.*, vol. 4, p. 65, 1982.
[100] K. H. Schoenbach *et al.*, "An e-beam controlled diffuse discharge switch," in *Proc. 5th IEEE Pulsed Power Conf.* (Arlington, VA), 1985, p. 640.
[101] L. C. Lee, C. C. Chiang, K. Y. Tang, D. L. Huestis, and D. C. Lorents, "Gaseous electronic kinetics for e-beam excitation of $Cl_2$, NO and $N_2O$ in $N_2$," Dept. Elec. Eng., Texas Tech Univ., Lubbock, TX, 2nd Ann. Rep. Coord. Res. Program in Pulsed Power Physics, p. 189, 1981.
[102] R. J. Commisso, R. F. Fernsler, V. E. Scherrer, and I. M. Vitkovitsky, "Electron-beam controlled discharges," *IEEE Trans. Plasma Sci.*, vol. PS-10, p. 241, 1982.
[103] R. J. Commisso, R. F. Fernsler, V. E. Scherrer, and I. M. Vitkovitsky, "Application of electron-beam controlled diffuse discharges to fast switching," in *Proc. 4th IEEE Pulsed Power Conf.* (Albuquerque, NM), 1983, p. 87.
[104] R. J. Commisso, R. F. Fernsler, V. E. Scherrer, and I. M. Vitkovitsky, "Inductively generated, high voltage pulse using an electron beam controlled opening switch," *Appl. Phys. Lett.*, vol. 47, p. 1056, 1985.
[105] V. E. Scherrer, R. J. Commisso, R. F. Fernsler, L. Miles, and I. M. Vitkovitsky, "The control of breakdown and recovery in gases by pulsed electron beams," in *Gaseous Dielectrics III*, L. G. Christophorou, Ed. New York: Pergamon, 1982.
[106] V. E. Scherrer, R. J. Commisso, R. F. Fernsler, and I. M. Vitkovitsky, "Study of gas mixtures for e-beam controlled switches," in *Gaseous Dielectrics IV*, L. G. Christophorou and M. O. Pace, Eds. New York: Pergamon, 1984.
[107] K. H. Schoenbach *et al.*, "Investigations of e-beam controlled diffuse discharges," in *Gaseous Dielectrics IV*, L. G. Christophorou and M. O. Pace, Eds. New York: Pergamon, 1984.
[108] K. H. Schoenbach *et al.*, "An e-beam controlled diffuse discharge switch," in *Proc. 16th Power Modulator Symp.* (Arlington, VA), 1984, p. 152.
[109] K. H. Schoenbach *et al.*, "An electron-beam controlled diffuse discharge switch," *J. Appl. Phys.*, vol. 57, p. 1618, 1985.
[110] G. Schaefer *et al.*, "The influence of the circuit impedance on an electron beam controlled diffuse discharge with a negative differential conductivity," *Appl. Phys. Lett.*, vol. 48, p. 1776, 1986.
[111] P. Bletzinger, "Operation of externally ionized discharges at high electric fields," presented at GEC 1985, Monterey, CO, Abstr. H4, 1985.
[112] P. Bletzinger, "Determination of breakdown voltages and instabilities in electron beam ionized discharges," in *Proc. 5th IEEE Pulsed Power Conf.* (Arlington, VA), 1985, p. 58.

# EXTERNAL CONTROL OF DIFFUSE DISCHARGE SWITCHES

G. Schaefer and K. H. Schoenbach
Texas Tech University, Department of Electrical Engineering
Lubbock, Texas 79409

Abstract: Electron-beam sustained diffuse discharges have attracted considerable interest as submicrosecond opening switches for inductive energy storage systems. Opening is accomplished through turning off the ionizing e-beam. In order to increase the switch efficiency (switch current/e-beam current) at high hold-off voltages and to reduce the opening time attachers are used with a high attachment rate at high values of E/N and a low attachment rate at low values of E/N. These attachers will decrease the net source term and will obstruct the closing phase. Additional control through photodetachment and optically enhanced attachment will also allow to optimize the closing phase. The results of model calculations and experimental studies on various control mechanisms are discussed.

## Introduction

In recent years there has been an increasing interest in the development of fast, repetitive, opening switches which would allow the use of inductive energy storage in repetitively operated pulsed power systems. Opening switch concepts that show promise for fast repetitive operation are based on the external control of the electron generation and depletion mechanisms in a diffuse discharge. Such control mechanisms can be the sustainment by electron beams and radiation sources, optical control of the electron depletion mechanisms, or external magnetic field to control the internal ionization processes. This paper gives an overview of the mentioned control mechanisms and discusses the requirements for the optimization of such systems.

## Externally Sustained Discharges

An externally sustained discharge switch makes use of the electrons produced by an external source (electron-beam, UV radiation, or x-rays). The voltage across the gas discharge is always kept well below the value required for internal ionization. Figure 1 shows the general time dependence of some of the important discharge quantities through one full switch cycle, assuming that the time dependent source function has a trapezoidal shape with a steep rise and fall (Fig. 1a). The electron density (Fig. 1b), and consequently the current density will initially be zero and the switch is open. A constant source function S will then increase the electron density in the closing phase until it approaches a new steady state condition given by the balance of the electron generation and depletion mechanisms. In this state the current density reaches its maximum and the switch is closed. When the source is turned off the electron depletion mechanism will cause a decrease of the electron density and consequently of the current density in the opening phase until the initial state with approximately zero electron density is reached again. Since this device is operated in an inductive energy storage system the voltage and the reduced field strength E/N will drop to a lower value when the switch is conducting and will increase when the conduction is reduced (s. Figure 1c).

## Steady State Conditions

In the closed phase the switch is supposed to have a resistivity as low as possible at a low voltage drop across the switch and consequently at a low value of E/N. This requires a high electron mobility and an electron depletion rate as low as possible at low values of E/N. Recombination can not be controlled significantly except by keeping the electron density low, but any further losses such as attachment have to be avoided. In the opening phase the switch has to withstand a high voltage. This means that strong electron losses must occur at very low electron densities at high values of E/N. This can be accomplished by an attacher with a high attachment rate at high values of E/N. The mobility of the electrons in the high E/N range is of minor importance since the electron density approaches zero. A decreasing mobility with increasing E/N, however, will improve the transition into the high E/N range. The two steady state phases therefore require an E/N dependence of the mobility and attachment rate as shown in Figure 2a [1,2].

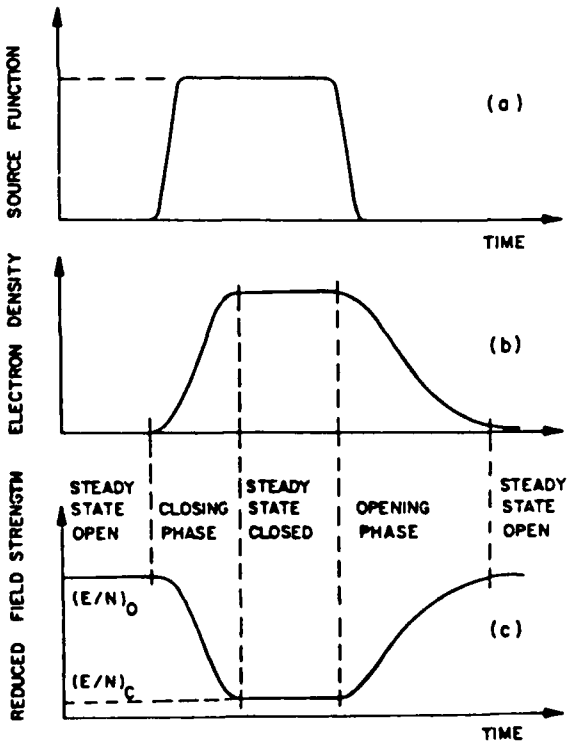


Fig. 1. Schematic time dependence of the electron source (a), electron density (b), and reduced electric field strength (c) in an externally sustained diffuse discharge for switching applications.

Although one never intends to operate the switch as an externally sustained discharge at high values of E/N one can calculate and measure the steady state resistivity and (J-E/N) characteristic for the full E/N range as shown in Figure 2b and c. The part of the discharge characteristic at high values of E/N has important consequences on the opening and closing phases as discussed later.

The required attachment characteristics can cause undesired losses if an electron beam is used as a discharge sustainment source. An attachment rate as shown in Figure 2a is given if the attachment cross section has its maximum above, but close to the energy range of the electron energy distribution function at the low value of the reduced field strength in the closed phase $(E/N)_c$, as shown in Figure 3. Since there is no overlap of the electron energy distribution function with the attachment cross section no attachment will occur. When E/N is increased, the electron energy distribution function is shifted towards higher energies and the attachment rate increases.

The initial secondary electrons produced by the high energy electron beam have an energy distribution over a wide energy range as shown in Figure 3 [3], and only a small fraction is produced in the energy range of the steady state electron energy distribution. A significant fraction (approximately 80% for the attacher $N_2O$ in a $N_2$ buffer gas) is generated above the energy range of the attachment cross section. These electrons will during their relaxation move through the energy range where attachment can occur. The probability for attachment of these electrons will

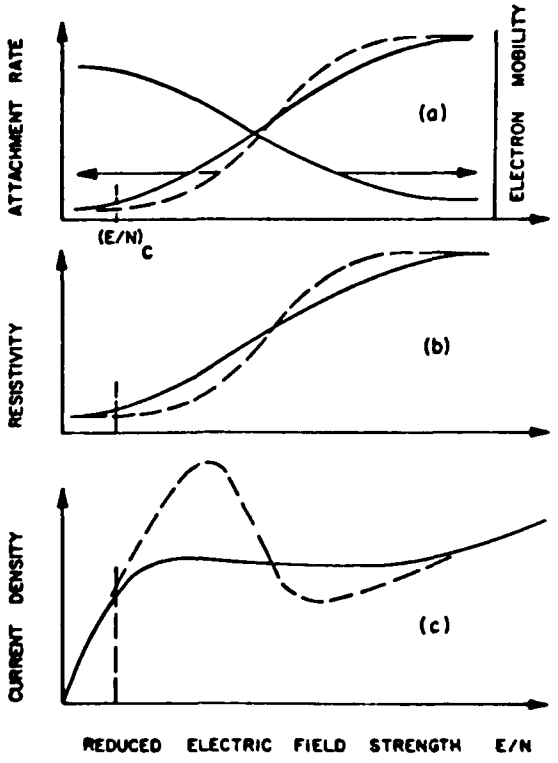


Fig. 2. Schematic E/N dependence of attachment rate and electron mobility (a), resistivity (b), and current density (c) in an externally sustained diffuse discharge for switching applications.

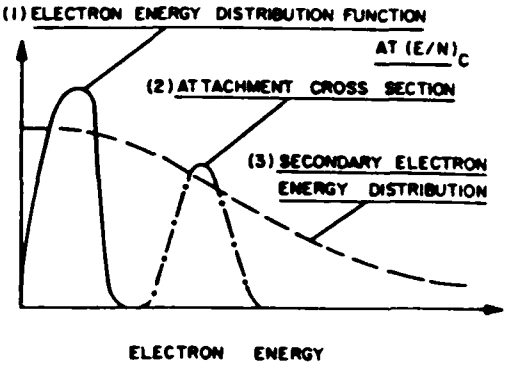


Fig. 3. Schematic electron energy dependence of the steady state electron energy distributions at low E/N, the attachment cross section, and the distribution function of the initial secondary electrons in an electron beam sustained discharge.

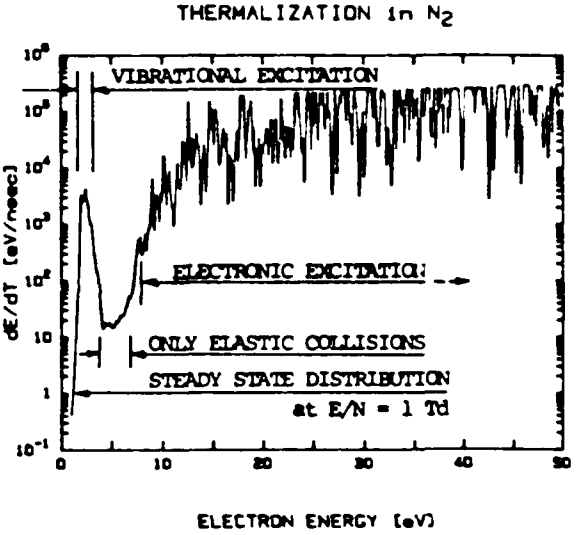


Fig. 4 Average velocity of relaxing electrons in energy space of relaxing electrons generated at 100 eV in $N_2$ at E/N = 1 Td.

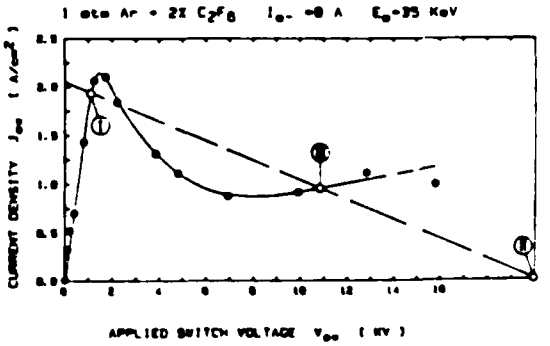


Fig. 5. Measured Current-Voltage characteristic of an electron beam sustained discharge in a mixture of 2% $C_2F_6$ in 1 atm Argon.

then depend on their velocity in energy space in the energy range where attachment is dominant. Figure 4 shows the calculated average velocity of the electrons in energy space, dE/dt, during relaxation in $N_2$ for initial energies of 100 eV [4]. This velocity is very high (> $10^3$ eV/ns) in energy ranges with strong inelastic cross section but significantly lower (10 eV/ns) in the 3-7 eV range where $N_2$ has no significant inelastic cross sections. Attachment of the initial secondary electrons in a $N_2$ buffer gas will therefore be significant if the attacher has its maximum cross section in the 3-7 eV range (example $SO_2$, approximately 10% are attached with 2% $SO_2$ in $N_2$) and much less significant if the maximum cross section is below 3 eV but above the steady state distribution (example $N_2O$) [4]. Attachment of the initial secondary electrons has therefore to be considered using a correction factor in the source function, and these losses can be minimized by using an appropriate mixture of an attacher with a buffer gas as discussed above.

## Opening and Closing Phases

The opening phase starts when the electron source is turned off. Since the opening phase starts at the $(E/N)_c$ value of the closed state, the electron depletion rate and consequently the rise of E/N will initially be slow until the system reaches the E/N regime where attachment dominates the electron losses. Since the performance of an inductive energy storage system strongly depends on the rise of the switch resistance dR/dt the attachment rate should have a steep rise with E/N (dashed line in Figure 2a). Such a gas mixture will cause a negative differential conductivity (d(E/N)/dJ) in an intermediate E/N range as shown in Figure 2c. Such a characteristic, however, can cause problems for the closing phase. Figure 5 shows the measured V-I characteristic of an electron beam sustained discharge in a mixture of 1 atm Ar and 2% $C_2F_6$ [5]. The optimum operation condition for the switch in the closed phase is at the maximum current in the low resistance regime at low values of E/N as indicated in condition (I). The suitable open condition (II) is given by a voltage of approximately 20 kV (at 1 atm and 1 cm discharge length), well below the hold-off voltage. In a good approximation an inductive energy storage system can be considered as having a transmission line characteristic. This means that the system will move on a straight line. When the source is turned on the system will therefore only approach condition (III) in Figure 5 with a lower current density and strong losses (high value of E/N) [6]. To avoid this problem different approaches can be taken. One approach is to compromise with respect to the closing and opening phase using a gas mixture with a less steep increase of the attachment rate with E/N resulting in a weak negative differential conductivity (solid lines in Figure 2). A second possibility is to tailor the time dependence of the source function [6]. An electron beam with an increased current density in the beginning of the e-beam pulse will shift the J-E/N characteristic towards higher J-values for a short time to allow the system to reach the low E/N value c (I), before it approaches its steady state condition. Other solutions are to use additional external control mechanisms which alter the attachment properties of the gas mixture in a specific switch period.

## Optical Control Mechanisms

Optical control of diffuse discharges for switching applications, especially for opening switches, is a very recent research field. Besides papers on concepts [7,8], model calculations on certain proposed systems [6], and numerous papers on basic processes suitable for switching applications, there are no results on operational switching devices available. Especially laser are attractive light sources allowing the generation of high power densities, precise illumination of the discharge volume, and precise timing. Due to the high costs of laser photons, however, especially if high photon energies are required, it seems to be inefficient at this time to use lasers for sustainment. Optical discharge control for switching application is therefore considered only as an additional control for a specific phase of the switch cycle, where other means do not allow the optimization of the discharge properties.

As discussed it is possible to optimize the operation conditions of an electron beam sustained diffuse discharge switch with respect to the steady state phases and the opening phase through tailoring the E/N dependance of the attachment rate coefficients, but this optimization causes problems with respect to the closing phase. Concepts on additional optical control, therefore, concentrate on attachment and its control in one of the transition phases. In principle, there are two different methods of optical control of attachment: to use photodetachment to overcome attachment, or to use optically induced attachment in gases which otherwise do not have a strong attachment rate in the E/N range of interest.

Photodetachment can be used as a method to overcome attachment in a well defined discharge period. A negative ion considered for photodetachment as a control mechanisms is $O^-$ [7]. Several molecules, such as $O_2$, NO, $N_2O$, $NO_2$, $CO_2$, and $SO_2$, undergo dissociative attachment producing $O^-$. In all gases or gas mixtures with these gases, however, competitive attachment processes exist or subsequent reactions of $O^-$ will occur, producing molecular negative ions, which in general have lower cross sections for photodetachment.

Photodetachment experiments in low pressure $O_2$ discharges and flowing afterglows showed that, for example, a fraction of 50% of the negative ions could be detached with laser pulses with a energy flux of 35 mJ/cm$^2$ at 565 nm [7]. For attachers with a high attachment rate at high values of E/N and low or zero attachment rate at low values of E/N (s. Figure 2) photodetachment may be a suitable process to support a transition from a highly attaching state into a non-attaching state of an externally sustained discharge [6].

Optically enhanced attachment means to use a gas mixture with an additive of molecules, which in their initial state are very weak attachers, and to transfer these molecules through optical excitation and may be some subsequent spontaneous transitions into species which act as strong attachers. Optically enhanced attachment is a control mechanism considered for controlling the opening phase of diffuse discharge opening switches. Some attachers show a drastically increased attachment cross section if excited into vibrational states. For HCl [9] and $I_2$ [10] for example the attachment enhancement factor through excitation can be larger than $10^3$. There are many ways to create attachers excited into vibrational states. Only two optical method are mentioned here, which have been used before for the pumping lasers operating between vibrational states:

(1) Optical vibrational excitation of higher lying states can be accomplished through overtone excitation or excitation of combination states, and

through multi-photon excitation. Such mechanisms can be found in numerous excitation mechanisms of optically pumped IR lasers. Some examples are lasers operating in gases such as $CF_4$, NOCl, $CF_3I$, and $NH_3$, pumped by a $CO_2$ laser [11].

(2) Photodissociation of large molecules has shown to produce molecules in vibrationally excited states and is also used as excitation mechanism for molecular gas lasers. Examples are HF lasers pumped by photoelimination of HF from $CH_2CF_2$ and $CH_2CHF$, using a UV-flashlamp [12]. Some of these processes have significant cross sections at the wavelength of the ArF-laser at 193 nm. Rossi et al. [8], performend a drift tube experiment to demonstrate the feasibility of these processes for controlling the electron balance in a discharge. In 100 torr Helium with 100 mtorr $C_2H F_3$ at low values of E/N (< 3 Td), they obtained an increase of the attachment rate of up to $10^3$ with an ArF laser. Similiar experiments were performed in $C_2H_3Cl$. Schaefer et al. [13], performed measurements in a dc glow discharge at low values of E/N (0.5-5 Td), which was externally sustained by a Helium plasma injection. In a gas mixture of 60 Torr Helium and 3% $C_2H_3$ Cl, pulsed resistance changes of a factor of 3.5 were measured after irradiating the discharge with a UV spark source.

## Summary

Externally sustained diffuse discharges are promising candidates for fast, repetitive, opening switches. Low losses in the conduction phase, fast opening, and high hold-off voltages can be accomplished by using attachers with a high attachment rate at high values of E/N and a low attachment rate at low values of E/N. The optimization of the closing phase requires additional control mechanisms. Possible processes are photodetachment and optically enhanced attacnment.

## Acknowledgement

This work was supported jointly by AFOSR and ARO and in part by NSF.

## References

[1] K. H. Schoenbach, G. Schaefer, M. Kristiansen, L. L. Hatfield and A. H. Guenther, "Concepts for Optical Control of Diffuse Discharge Opening Switches," IEEE Trans. Plasma Sci., vol. PS-10, pp. 246-251, Dec. 1982.

[2] L. G. Christophorou, S. R. Hunter, J. G. Carter, and R. A. Mathis, "Gases for Possible Use in Diffuse Discharge Switches," Appl. Phys. Lett., vol. 41, pp. 147-149, July 1982.

[3] A. E. S. Green nd T. Sawada, "Ionization Cross Sections and Secondary Electron Distribution," J. Atmosph. Terr. Phys., vol. 34, pp. 1719-1728, 1972.

[4] G. Reinking, G. Schaefer, K. H. Schoenbach and G. Hutcheson, "Attachment of Initial Secondary Electrons in an Electron Beam Sustained Discharge," IEEE Int. Conf. Plasma Sci., 1985.

[5] K. H. Schoenbach, G. Schaefer, M. Kristiansen, H. Krompholz, D. Skaggs and E. Strickland, "An E-Beam Controlled Diffuse Discharge Switch," Proc. 5th IEEE Pulsed Power Conf., 1985.

[6] G. Schaefer, K. H. Schoenbach, H. Krompholz, M. Kristiansen, and A. H. Guenther, "The Use of Attachers in Electron Beam Sustained Discharge Switches - Theoretical Considerations," Laser and Particle Beams, vol. 2, pp. 273 - 291, 1984.

[7] G. Schaefer, P. F. Williams, K. H. Schoenbach, and J. T. Mosley, "Photodetachment as a Control Mechanism for Diffuse Discharge Switches," IEEE Trans. Plasma Sci., vol. PS-11, pp. 263-265, Dec. 1983.

[8] M. J. Rossi, H. Helm, and D. C. Lorents, "Photoenhanced Electron Attachment of Vinylchloride and Trifluoroethylene at 193 nm," Appl. Phys. Lett., submitted 1985.

[9] J. N. Bardsley and J. M. Wadehra, private communication, 1982.

[10] I. M. Beterov and N. V. Fatayev, "Optogalvanic Demonstration of State-to-State Dissociative Electron Capture Rate in $I_2$," Opt. Comm., vol. 40, pp. 425-429, Feb. 1982.

[11] J. J. Tiee and C. Wittig, "Optically Pumped Molecular Lasers in the 11-17 micron Region," J. Appl. Phys., vol. 49, pp. 61-64, Jan. 1978.

[12] E. R. Sirkin, and G. C. Pimentel, "HF Rotational Laser Emission Through Photoelimination from Vinyl Floride and 1, 1-Difluoroethene," J. Chem. Phys., vol. 75, pp. 604-612, July 1981.

[13] G. Schaefer, K. H. Schoenbach, and P. F. Williams, to be published.

# AN ELECTRON-BEAM CONTROLLED DIFFUSE DISCHARGE SWITCH

G. Schaefer, K. H. Schoenbach, M. Kristiansen, and H. Krompholz

Department of Electrical Engineering
Texas Tech University
Lubbock, Texas 79409

Inductive energy storage is attractive in pulsed power applications because of its intrinsic high energy density compared to capacitive storage systems. The key technological problem in developing inductive energy discharge systems, especially for repetitive operation is the development of opening switches. Promising candidates for repetitive opening switches are e-beam or laser controlled diffuse discharges [1]. The schematic diagram of an electron-beam controlled opening switch as part of an inductive storage system is shown in Fig. 1 [2]. The switch chamber is filled with a gas of pressures of 1 atm and above. The gas between the electrodes conducts and allows charging of the inductor only when an ionizing e-beam is injected into the gas. When the e-beam is turned off, electron attachment and recombination processes in the gas cause the conductivity to decrease and the switch opens.

The switch opening time, after e-beam turn-off, is determined by the electron loss processes in the diffuse discharge: recombination and attachment. In order to achieve opening times of less than a microsecond at initial electron densities $<10^{14}cm^{-3}$, the dominant loss process must be attachment, which means that the switch gas mixture must contain an electronegative gas. On the other hand, additives of attachers increase the power losses during conduction. Both low forward voltage drop and fast opening can only be obtained by choosing gases or gas mixtures which satisfy the following conditions [1,3,4,]:

(1) For low values of the reduced field strength E/N (conduction phase) the gas mixture should have a high drift velocity $v_d$ and low attachment rate coefficient $k_a$.

(2) For high E/N values (opening phase) the gas mixture should have lower drift velocities and high attachment rate coefficients.

Along with these considerations, several gas mixtures have been proposed for diffuse discharge opening switches. For our theoretical investigations $N_2$ was chosen as a buffer

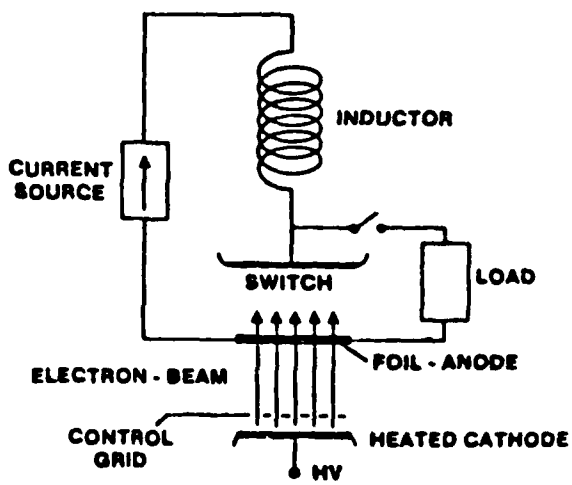


Fig. 1. Schematic of an e-beam controlled diffuse discharge opening switch.

gas with $N_2O$, $SO_2$, and $CO_2$ as the added attachers which satisfy the above mentioned conditions. Experiments were performed in the same gas mixtures and in mixtures of Argon and $C_2F_6$ [3].

Calculations of the steady-state discharge characteristics were performed with the relative attacher concentration in the buffer gas as the parameter. Figure 2 shows the current density j versus reduced field strength E/N characteristics for different $N_2O$ concentrations in an $N_2$ buffer gas. The total pressure is 1 atm. At small E/N, below 4 Td, the electron loss is due to recombination only. At about 4 Td the attachment rate coefficient rises steeply. This means that, for reasonably high attacher concentrations in the buffer gas, the losses increase drastically, causing a negative slope in the current-voltage characteristics. At 30 Td, where the attachment rate coefficient is assumed to level off, recombination becomes more important again, as demonstrated by the change in the slope of j vs E/N, at this value. In experiments the strongest negative slope in the current-voltage characteristics was found in Argon with admixtures of $C_2F_6$, while in $N_2$ with admixtures of $N_2O$ this effect was not well pronounced.

Figure 3 shows the influence of attacher concentration ($N_2O$) on the switch current. For high $N_2O$ concentrations (3%) the switch current pulse replicates the e-beam current pulse, except for the tail. The tail may be caused by the current carried by positive and negative ions. The current gain (switch current/electron beam current) is about 2 for this high attachment concentration.

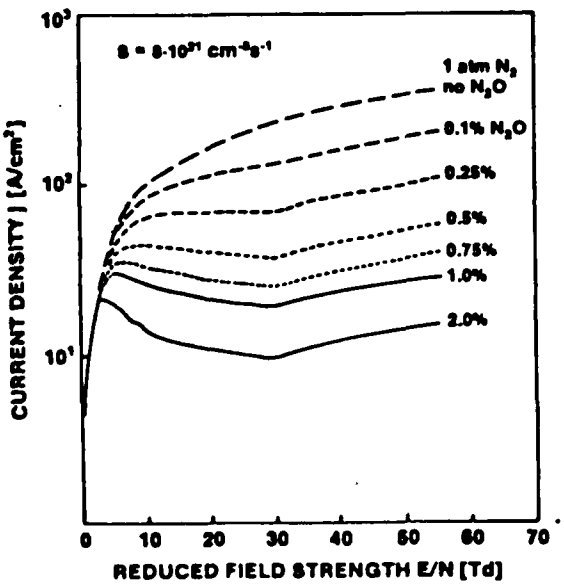


Fig. 2. Calculated steady-state j vs E/N characteristics for an e-beam sustained discharge in $N_2$ with admixtures of $N_2O$. The electron generation rate is $8 \times 10^{21} cm^{-3} s^{-1}$. The parameter is the $N_2O$ fraction in percent (see Ref. 4).

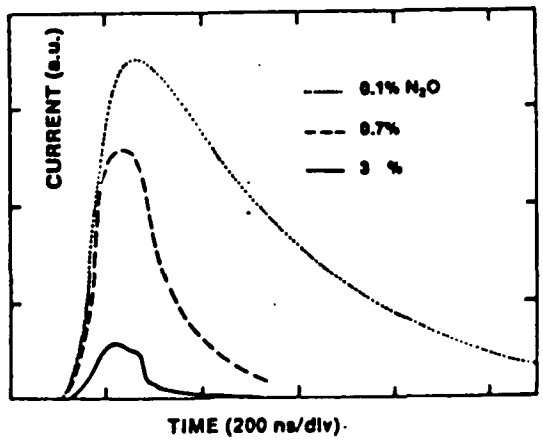


Fig. 3. Time dependence of switch current with $N_2O$ concentration as the variable parameter.

For concentrations of 0.7%, the fall time (1/e-time) increases to approximately 100 ns. For 0.1% it is on the order of 500 ns. The gain increases to values of 9 and 12 for 0.7% and 0.1% $N_2O$, respectively.

Further calculations were performed to investigate the influence of the attacher on the electron generation mechanism. For an electron beam sustained discharge operated at low values of E/N the energy of the initial secondary electrons may be well above the energy range of the steady state electron energy distribution, and also above the energy range in which the attacher used has a significant attachment cross section. These initial secondary electrons will subsequently during their relaxation move through the energy range where attachment may occur even if the steady state distribution function does not overlap with the attachment cross section.

Monte Carlo calculations for a gas mixture of $N_2$ and attachers such as $N_2O$ and $SO_2$ showed that at 3 Td the average time for an 8eV electron to reduce its energy to 2eV is $\sim 2.5 \times 10^{-10}$s. This time is almost exclusively spent in the energy range above 4eV where $N_2$ does not have significant inelastic cross sections. This causes a significant difference of the influence of the two attachers mentioned. $SO_2$ has its maximum attachment cross section at $\sim 4.5$eV. In a mixture of 90% $N_2$ and 10% $SO_2$ more than 20% of the initial secondary electrons are attached if they are generated at energies above 5eV. In a mixture of 90% $N_2$ with 10% $N_2O$ attachment of the initial secondary electrons can nearly be neglected (< 5%), since the attachment cross section of $N_2O$ has its maximum at $\sim 2.3$eV in the range where $N_2$ has its large inelastic cross sections.

## References


1. K. H. Schoenbach, G. Schaefer, M. Kristiansen, L. L. Hatfield, and A. H. Guenther, IEEE Trans. Plasma Sci. PS-10, 246 (1982).
2. C. H. Harjes, K. H. Schoenbach, G. Schaefer, M. Kristiansen, H. Krompholz, and D. Skaggs, Rev. Sci. Instrum. 55, 1684 (1984).
3. L. L. Christophourou, S. R. Hunter, J. A. Carter, and R. A. Mathis, Appl. Phys. Lettr. 41, 147 (1982).
4. G. Schaefer, K. H. Schoenbach, H. Krompholz, M. Kristiansen, and A. H. Guenther, Laser Part. Beams 2, 273 (1984).

International Conference on Plasma Science and Technology (ICPST), Beijing, China 57
June 1986

Appendix D

# NEGATIVE DIFFERENTIAL CONDUCTIVITY IN AN ELECTRON-BEAM CONTROLLED DIFFUSE DISCHARGE FOR SWITCHING APPLICATIONS*

G. Schaefer,** K. H. Schoenbach,*** M. Kristiansen,
B. E. Strickland and R. A. Korzekwa
Department of Electrical Engineering
Texas Tech University
Lubbock, Texas 79403-4439, USA

## INTRODUCTION

Inductive energy storage is attractive in pulsed power applications because of its intrinsic high energy density compared to capacitive storage systems. The key technological problem in developing inductive energy discharge systems, especially for repetitive operation, is the development of opening switches. Promising candidates for repetitive opening switches are e-beam or laser controlled diffuse discharges [1].

An e-beam controlled diffuse discharge switch opens when the e-beam is turned off. The switch opening time is determined by the electron loss processes: recombination and attachment. In order to achieve opening times of less than a microsecond at initial electron densities $n_e < 10^{14}$ cm$^{-3}$, the dominant loss process must be attachment, which means that the switch gas mixture must contain an electro-negative gas. On the other hand, additives of attachers increase the power losses during conduction. Both low forward voltage drop and fast opening can only be obtained by choosing gases or gas mixtures which satisfy the following conditions [1-3]:

* Supported by AFOSR/ARO
** Polytechnic Institute of New York, New York, USA
*** Old Dominion University, Norfolk, Virginia, USA

(1) For low values of the reduced field strength E/N (conduction phase) the gas mixture should have a high drift velocity $v_d$ and low attachment rate coefficient $k_a$.

(2) For high E/N values (opening phase) the gas mixture should have low drift velocities and high attachment rate coefficients.

It has been discussed before that such gas properties cause a discharge characteristic (current density J versus reduced electric field strength E/N) with a strong negative differential conductivity [2,4]. Such a characteristic is equivalent to a strong increase of the discharge resistivity with increasing E/N. Gas mixtures, for example, recommended for these applications are mixtures of Argon or $CH_4$ and $C_2F_6$ or $C_3F_8$ [2]. All experiments presented here were performed with mixtures of Argon and $C_2F_6$.

## EXPERIMENTS

The experimental setup used for the presented investigations is an electron-beam controlled diffuse discharge switch with an electron-beam tetrode for multiple, submicrosecond pulse operation [5,6]. The discharge itself was driven by a 2 Ohm pulse forming network, and series resistors were used to simulate high impedance systems. The discharge characteristics were investigated with a 2 Ohm system. Figures 1 and 2 show the discharge characteristics and the resistivities for different mixing ratios of Argon and $C_2F_6$. The current density reaches a maximum in the E/N range of 2-3 Td, depending on the $C_2F_6$ concentration and the source function, S. With further increasing E/N up to approximately 5 Td the current density decreases. The discharge resistivity increases in this E/N range by a factor of approximately 20. The increase of resistivity is more pronounced with increasing $C_2F_6$ concentration. It is mainly caused by the attachment properties of $C_2F_6$ and not by the E/N dependence of the drift velocity. Also mixtures of Argon and Nitrogen have a drift velocity with a maximum at low values of E/N,

however, these mixtures did not show a negative differential conductivity. The drift velocity, however, seems to influence the magnitude of the current maximum at low $C_2F_6$ concentrations since the characteristic for 0.5% $C_2F_6$ shows a lower maximum current than for 2% $C_2F_6$. Since the maximum of the current density indicates the optimum operation range for the steady state conducting phase one can conclude that the optimum Ar-$C_2F_6$ mixture contains approximately 2% $C_2F_6$.

## INTERACTION OF DISCHARGE AND CIRCUIT

If the specific switch application requires a burst of short pulses with a high repetition rate then the inductor is charged only once and the total length of the burst of pulses is in the order of the discharge time of the inductor. For this operating mode the inductor can be treated as a high impedance line and the closing and opening process have to follow the same high impedance load line [3]. Figure 3 shows the different load lines used and the experimental discharge results achieved with these load lines. It becomes obvious that the current maximum can not be utilized with a high impedance system in the repetitive mode.

The closing process is obstructed even for operating conditions for which the discharge can reach a low, loss low E/N state, since the closing process starts at high values of E/N where attachment is strong. This behavior is demonstrated in Figure 4. The characteristics measured with a 2 Ohm system and a 100 ohm system are shown. For the 2 Ohm system the steady state values are obtained in less than 100 ns. For the 100 Ohm system the j(E/N) values are plotted for 75 ns and for 350 ns after e-beam initiation. Figure 4 demonstrates that those low loss, low E/N operation conditions which can be achieved with this high impedance system are reached only after a long closing period. This behavior was already predicted for $N_2$:$N_2O$ mixtures [3].

## CONCLUSION

Gas mixtures which cause a negative differential conductivity in an intermediate E/N range are most suitable for diffuse discharge opening switches if the system is operated in a single shot mode (recharging of the inductor after every shot). For a burst mode (several shots from a single inductor charging), however, the closing process is obstructed and the maximum possible current can not be utilized. As a solution, ternary gas mixtures can be used with two attachers with attachment cross sections at different electron energies to produce a flat characterisitic over a wide E/N range and to achieve the same increase of resistivity. Another approach is to control the attachment externally [1,3].

## REFERENCES

[1] K. H. Schoenbach, G. Schaefer, M. Kristiansen, L. L. Hatfield, and A. H. Guenther, "Concepts for Optical Control of Diffuse Discharge Opening Switches," IEEE Trans. Plasma Sci., Vol. PS-10, pp. 246-251, 1982.

[2] L. L. Christophorou, S. R. Hunter, J. A. Carter, and R. A. Mathis, "Gases for Possible use in Diffuse Discharge Switches," Appl. Phys. Lett., Vol. 41, pp. 147-149, 1982.

[3] G. Schaefer, K.H. Schoenbach, H. Krompholz, M. Kristiansen, and A. H. Guenther, "The Use of Attachers in Electron Beam Sustained Discharge Switches - Theoretical Consideration," Laser and Particle Beams, Vol. 2 pp. 273-291, 1984.

[4] A. D. Barkalov and G. G. Gladush, "Domain Instability of a Non-Self-Sustaining Discharge in Electronegative Gases," Translated From Teplofizika Vysokikh Temperatur, Vol. 20, pp. 19-24, 1982.

[5] H. C. Harjes, K. H. Schoenbach, G. Schaefer, M. Kristiansen, H. Krompholz, and D. Skaggs, "An Electron Beam Tetrode for Multiple, Submicrosecond Pulse Operation," Rev. Sci. Instr., Vol. 55, pp. 1684-1686, 1984.

[6] K. H. Schoenbach, G. Schaefer, M. Kristiansen, H. Krompholz, H. C. Harjes, and D. Skaggs, "An Electron-Beam Controlled Diffuse Discharge Switch," J. Appl. Phys., Vol. 57, pp. 1618-1622, 1985.

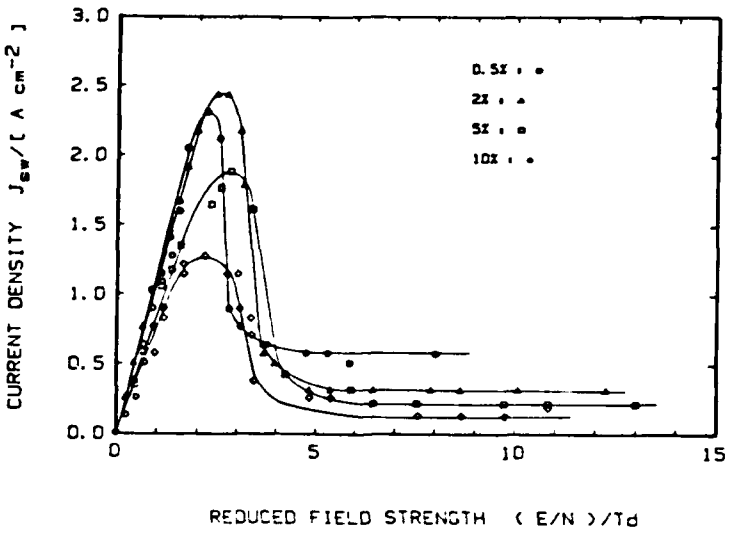


Fig. 1 Current density J versus reduced field strength E/N for different $C_2F_6$ concentrations.

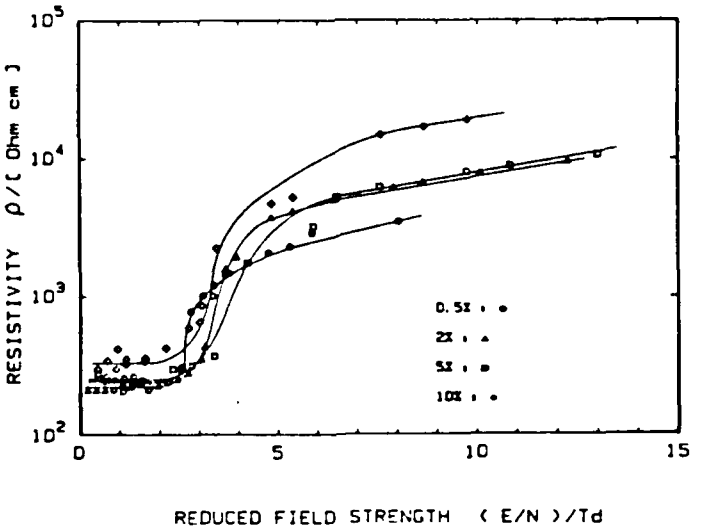


Fig. 2 Resistivity $\rho$ versus reduced field strength E/N for different $C_2F_6$ concentrations.

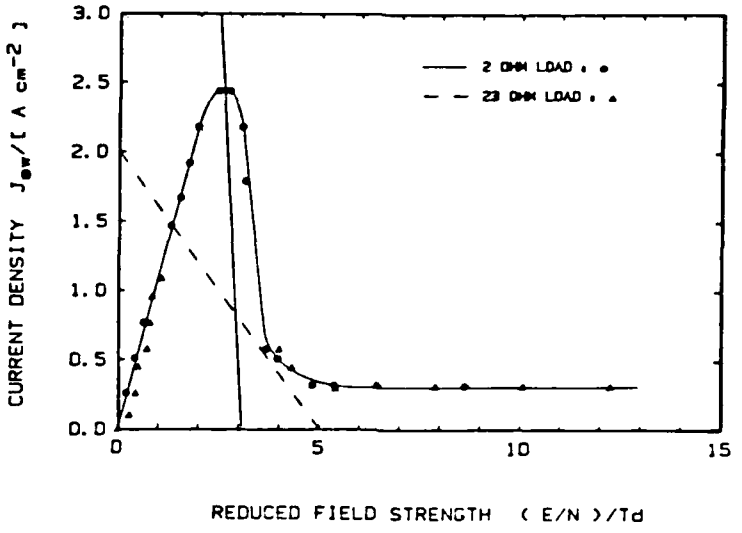


Fig. 3 Loadlines and current density J versus reduced electric field strength E/N obtained with different loadlines.

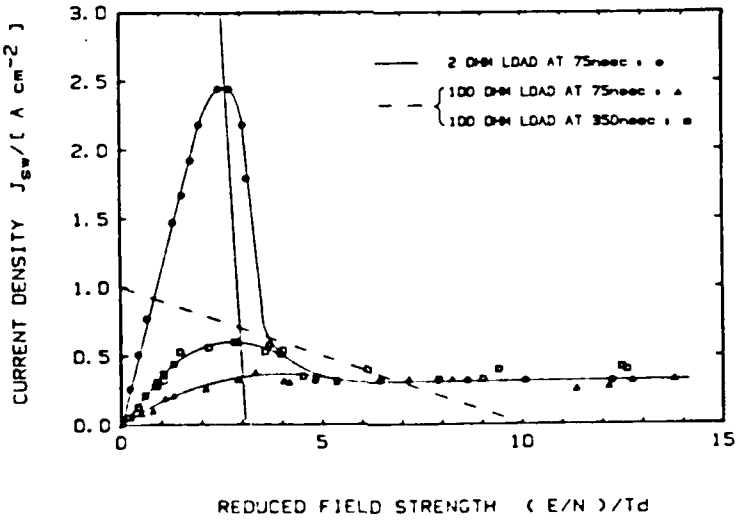


Fig. 4 Current density J versus reduced electric field strength E/N obtained at different times after e-beam initiation and different loadlines.

5th IEEE Pulsed Power Conference - Appendix E

# AN E-BEAM CONTROLLED DIFFUSE DISCHARGE SWITCH

K. H. Schoenbach, G. Schaefer, M. Kristiansen,
H. Krompholz, D. Skaggs and E. Strickland
Texas Tech University, Department of Electrical Engineering/Computer Science
Lubbock, Texas 79409

Abstract: The control efficiency and the response time of electron-beam controlled diffuse discharges is to a large extent determined by atomic and molecular properties of the switch gas composition. An e-beam tetrode was used to study switch gas properties for submicrosecond opening switches. Electrical measurements were performed with various switch gas mixtures containing small amounts of electronegative gases. Of particular interest were mixtures of $N_2O$:$N_2$ and $C_2F_6$:Ar. In both gas mixtures the resistivity increases with electric field strength. This effect is particularly strong in a mixture of 2% $C_2F_6$ in 1 atm Ar, where an increase of 25 was obtained in a reduced field strength range of 1 Td < E/N < 20 Td. The current decay times or opening times with this mixture were below 100 ns. Optical time resolved investigations of discharges in $C_2F_6$:Ar showed the occurence of striations which were perpendicular to the discharge axis. These luminous layers in the discharge can be explained as domain formations similar to those observed in direct semiconductors as e.g. the Gunn-effect in GaAs.

## Introduction

Electron-beam controlled diffuse discharges can be used as fast, repetetively operated closing and opening switches. The concept is as follows: The gas between the electrodes conducts when the ionizing e-beam is injected and the switch closes. The switch voltage remains below the self-breakdown voltage, so that avalanche ionization is negligible. Thus the discharge is completely sustained by the e-beam. When the e-beam is turned off, electron attachment and recombination processes in the gas cause the conductivity to decrease and the switch opens.

In order to achieve opening times of less than a microsecond at initial electron densities of $n_e < 10^{14}$ cm$^{-3}$, the dominant loss must be attachment. That means that the switch gas mixture must contain an electronegative gas which, however, lowers the efficiency of the switch. It causes a reduction of the current gain (switch current/e-beam current) proportional to the opening time. If the switch is part of an inductive energy circuit, both high current gain and fast opening can be obtained by choosing gas mixtures which satisfies the conditions [1,2,3]:
a) For low values of the reduced field strength E/N (conduction phase) the gas mixture should have a high drift velocity $v_d$ and low attachment rate $k_a$.
b) For high E/N values (opening phase) the gas mixture should have lower drift velocities and high attachment rate coefficients.

## Experimental Setup

For the investigation of e-beam controlled conductivity in a high pressure gas mixture with properties as discussed above, a discharge system was constructed with an e-beam tetrode as control element [4]. A schematic cross-section of the tetrode and the discharge chamber is shown in Fig. 1. The e-beam cathode is located in the Pyrex cylinder between the two plates of a stripline and consists of an electrically heated array of thoriated tungsten filaments. At a filament temperature of 2100 K, the e-beam current density is about 4 A/cm$^2$ over the 100 cm$^2$ cross-sectional area of the beam. The temporal structure of the e-beam is controlled by means of a control grid which allows the generation of a pulse train with pulse duration and pulse separation in the 100 ns time range. For some investigations the e-beam was operated as a cold cathode system, which provided e-beam current pulses of 15 A with a pulse duration of~400 ns.

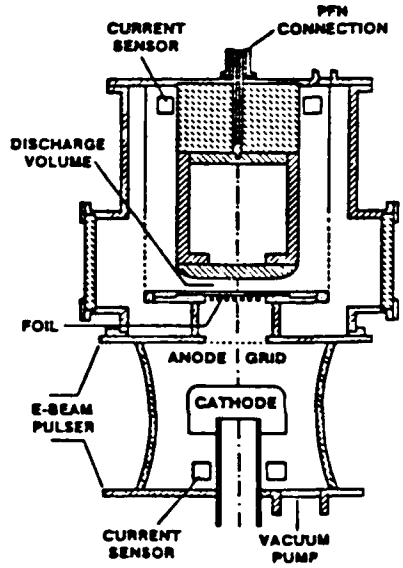


Fig. 1. Cross Section of E-Beam Tetrode and Switch Chamber.

The e-beam voltage is applied to the anode by a two-stage Marx generator, which delivers a maximum voltage of 250 kV with a 5 ns risetime and with an exponential decay time constant of about 2.5 microseconds into a 300 Ohm load. After passing through a 25 μm titanium foil and a 12.5 μm aluminum foil, which serves as an electrode in the diffuse discharge switch, the e-beam generates a diffuse plasma between the electrodes in the stainless steel discharge chamber. The current through the plasma is provided by a 2 Ohm pulse forming network.

Measurements of the e-beam current and the switch current were performed by means of transmission line current transformers [5]. Voltages were measured with fast resistive voltage dividers. In order to get information on the spatial structure of the discharge an image converter camera was built [6] using an ITT image converter diode type F4109. The camera has a high sensitivity of 225 μA/lm and a high spatial resolution of 45 lp/mm. The shutter time was about 10 ns.

## Experimental Results

Diffuse discharge experiments were performed in $N_2O$, $SO_2$, and $CO_2$ with $N_2$ as buffer gas, and $C_2F_6$ in Ar. The source term, the number of electrons produced per $cm^3$ second, was in the range of $10^{20}$ $cm^{-3}s^{-1}$ to $10^{21}$ $cm^{-3}s^{-1}$. The voltage applied at the PFN was varied between 100 Volts and 20 kV. The switch electrode gap was kept constant at 3.5 cm. Most of the measurements were performed with the $N_2O$:$N_2$ gas mixture. This gas combination was for one expected to satisfy the conditions for switch gases nicely (see introduction) and secondly it allowed modeling of the diffuse discharge [7], since a complete set of cross sections is available for $N_2$ [8] and the plasma chemistry in a mixture of $N_2$ and $N_2O$ appeared to be relatively simple.

Figure 2 shows the influence of the attacher c concentration ($N_2O$) on the opening time. For high $N_2O$ concentrations (3 %) the switch current replicates the e-beam current, except for the tail. The tail is caused by the current carried by positive and negative ions. The current gain is about 2 for this attacher concentration. For concentrations of .7 % the fall time (1/e -time) increases to approximately 100 ns. For .1 % it is in the order of 500 ns. The gain increases to values of 9 and 12, respectively.

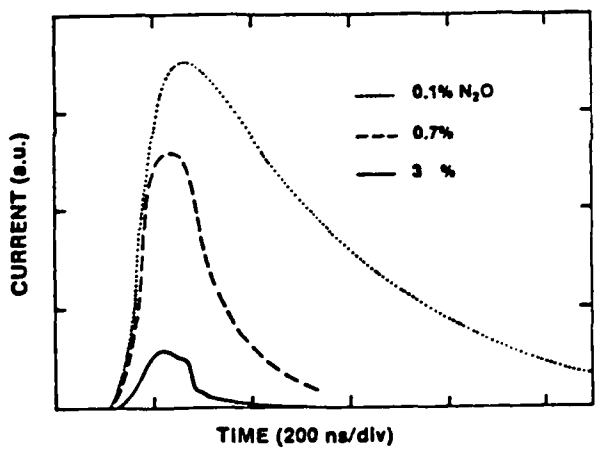


Fig. 2. Normalized Switch Current for Different Attacher Concentrations. Demonstrating the Strong Effect of the Attacher on the Current Decay (Opening Time).

Figure 3 shows the experimentally obtained current density (j) values (dots) versus reduced field strength E/N for the e-beam sustained discharge under steady state conditions in 1 atm $N_2$ with .7% $N_2O$. The curve represents calculated values [9] which were critically depending on available attachment rate coefficients or cross sections [10,11,12]. The good coincidence between model and experiment was obtained with attachment cross sections measured by Chantry [12].

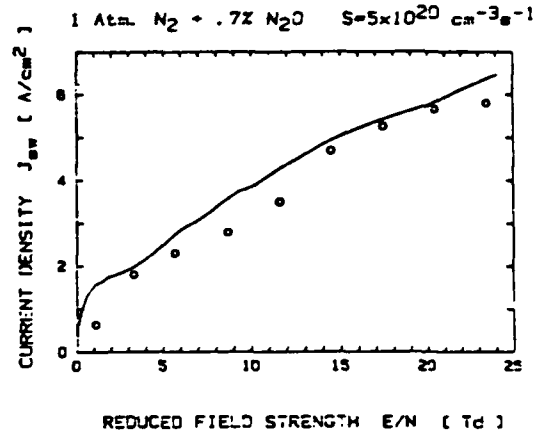


Fig. 3. Current Density j versus Reduced Field Strength E/N for a Discharge in $N_2O$:$N_2$ (Calculated Curve and Experimental Data Points).

In Fig. 4 the experimental and theoretical data are plotted in a resistivity $\rho_0$ versus E/N diagram. The desired opening switch effect, an increase in resistivity with increasing electric field, is obtained with the $N_2O$:$N_2$ gas mixture. However, the increase is moderate: about 2.5 over a field strength

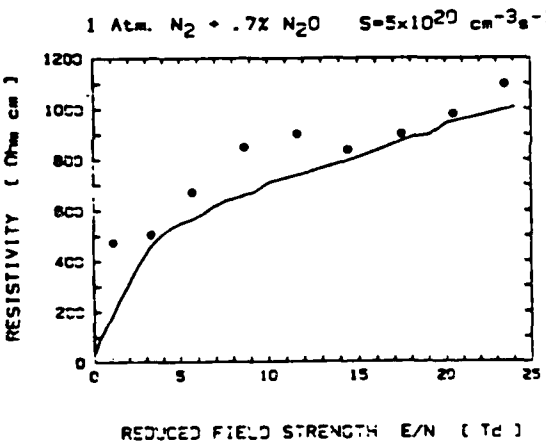


Fig. 4. Discharge Resistivity $\rho_0$ versus E/N for a Discharge in $N_2O$:$N_2$ (Calculated Curve and Experimental Data Points.)

range of 25 Td. The strong deviation of the lowest experimental value from the computed curve is probably due to the fact that the cathode fall was not included in our model. Gas combinations of $SO_2$ and $CO_2$ with $N_2$ as buffer gas showed even smaller changes in resistivity at comparable opening times.

A group of very promising gases, what the opening switch conditions concerns (see introduction), were proposed by Christophourou et. al., [3]. The total attachment rate constant $k_a$ is plotted versus mean electron energy $\epsilon$ in Fig.5. Measurements performed with the gas mixture of 2 % $C_2F_6$ in 1 atm Ar as buffer gas gave as a result a very strong increase in resistivity with field strength (Fig.6). Decay (opening) times for this mixture were below 100 ns. The mixture seems to be relatively stable.

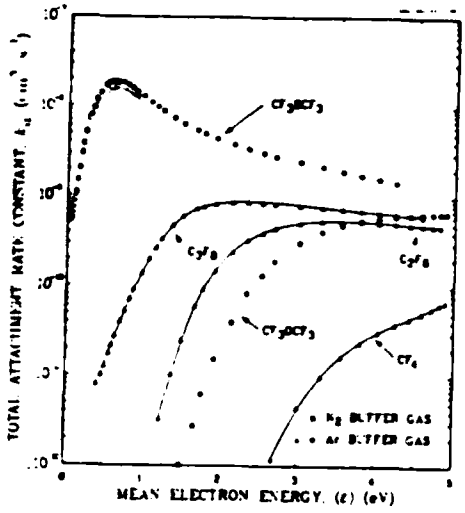


Fig. 5. Gases with Strong Increase of Attachment Rate Coefficient with Electron Energy [13].

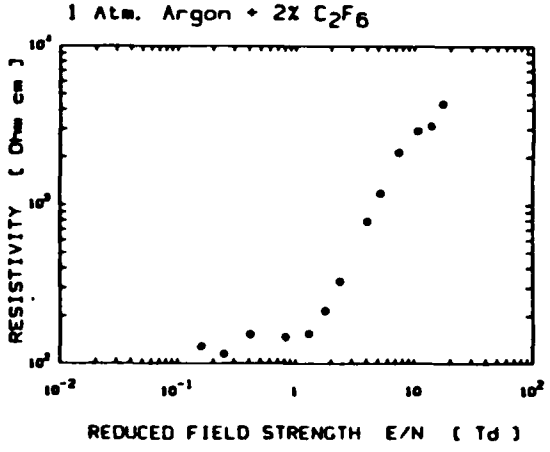


Fig. 6. Discharge Resistivity $\rho_0$ versus E/N for a Discharge in $C_2F_6$:Ar.

Reproducable results at an e-beam voltage of 150 kV were obtained for 150 shots without changing the gas.

The current density (j) versus reduced field strength (E/N) curve for this gas mixture is shown in Fig. 7. It contains a region with very pronounce negative differential conductivity (NDC). The effect which causes NDC in externally sustained diffuse discharges containing attachers is due to the increased generation of negative ions, that means

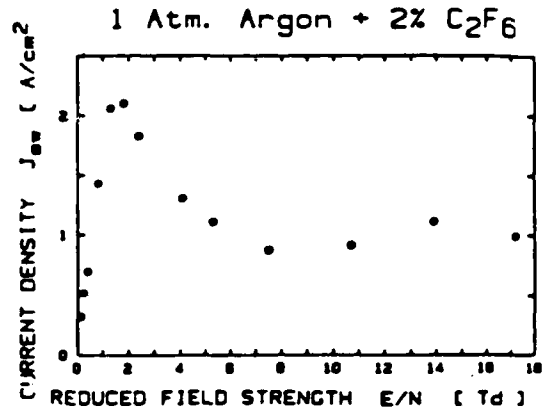


Fig. 7. Current Density j versus Reduced Field Strength E/N for a Discharge in $C_2F_6$:Ar.

negative charges with increased mass, above a certain electron energy. A similar effect is known and widely applied for high frequency generation and amplification in semiconductors, as e.g. GaAs [14]. The negative differential conductivity in semiconductors is caused similarly as in diffuse discharges by an increase in the effective mass of the electrons at higher electron energies [15]. The presence of NDC in semiconductors causes homogeneous material to become electrically heterogeneous thus causing high field dipole domains to form and propagate through the semiconductor (Gunn-effect).

The same effect, formation of high field domains, can be expected in externally sustained discharges with gas mixtures such as $C_2F_6$ in Ar. In order to prove this, the discharge was optically recorded by means of an image converter camera with a shutter time of 10 ns. Figure 8a shows side-on photographs of the discharge at different times after e-beam turn-on, Fig. 8b the corresponding photometer curves along the discharge axis. The discharge was biased so that the point of operation was in the NDC-region of the j-E/N characteristic (Fig. 7). The pictures show clearly the development of a highly luminous layer in the cathode region of the discharge. Its profile is dependent on the bias voltage; for bias points on the left hand side of the current density maximum the discharge appears homogeneous.

We consider the region of high luminosity as a high field domain, a region of enhanced energy dissipation, similar to the ones observed in semiconductors. The reduction in the width of these structures can be explained by the more than linear increase in the attachment rate coefficient in the NDC-region. A propagation of the high field domains in anode direction could not be observed. The reasons are the shot-to-shot variations in the structure which did not allow exact timing and the expected relatively slow motion of the layer ($v \approx 10^5 - 10^6$ cm/s).

The development of high field domains has probably little effect on the opening switch behavior of an e-beam controlled discharge; however, it may lead to more applications for these type of discharges. The analogy to the Gunn effect in GaAs points to the initiation of e-beam sustained discharges as high power, high frequency oscillators and amplifiers. Preliminary calculations indicate power levels of > 100 kW at frequencies < 1 GHz.

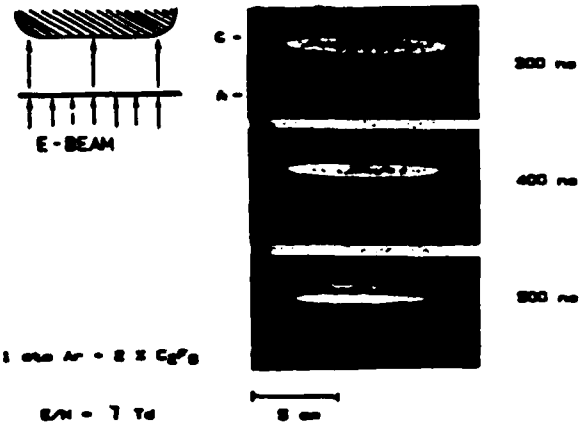


Fig. 8a Temporal Development of Striations in the E/N Range with Negative Differential Conductivity.

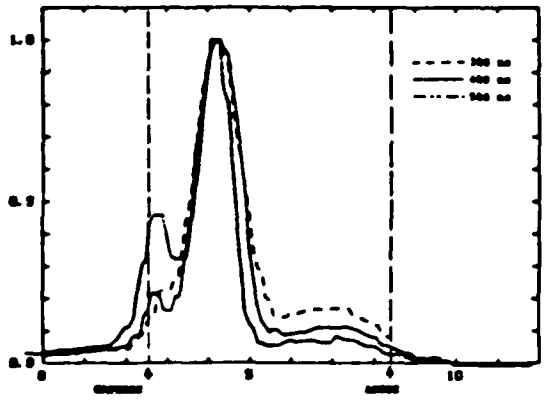

Fig. 8b. Photometer Curves of the Discharge Along the Discharge Axis.

## Summary

Different gas mixtures were tested for their use as switch gases in diffuse discharge opening switches. Best results were obtained with a mixture of $C_2F_6$ and Ar as buffer gas. For a mixture of 2% $C_2F_6$ in 1 atm Ar opening times of less than 100 ns were measured. The increase in resistivity was almost two orders of magnitude in a field strength range up to 25 Td. The current gain for this gas combination at a pressure of 6 atm and e-beam energies of 165 keV would be about 100. The current density-reduced field strength characteristic of the e-beam controlled discharge in $C_2F_6$:Ar has a distinct region with negative differential conductivity. This effect causes the formation of luminous striations in the discharge. The analogy between this type of discharge and semiconductors, which exhibit NDC, might lead to applications for externally sustained diffuse discharges as high power oscillators and amplifiers.

## Acknowledgement

This work was supported by Army Research Office and Air Force Office of Scientific Research.

## REFERENCES

[1] K.H. Schoenbach, G. Schaefer, E.E. Kunhardt, L.L. Hatfield, and A.H. Guenther, "An Optically Controlled Diffuse Discharge Switch", in Proc. 3rd IEEE Int. Pulsed Power Conf. (Albuquerque, NM, 1981), p. 142 (IEEE Catalog 81CH1662-6).

[2] K.H. Schoenbach, G. Schaefer, M. Kristiansen, L.L. Hatfield, and A.H. Guenther, "Concepts for Optical Control of Diffuse Discharge Opening Switches", IEEE Trans. Plasma Sci., vol. PS-10, p. 246, 1982.

[3] L.G. Christophourou, S.R. Hunter, J.G. Carter, and R.A. Mathis, "Gases for Possible Use in Diffuse Discharge Switches", Appl. Phys. Lett., vol. 41, p. 147, 1982.

[4] C.H. Harjes, K.H. Schoenbach, G. Schaefer, M. Kristiansen, H. Krompholz, and D. Skaggs, "Electron-Beam Tetrode for Multiple, Submicrosecond Pulse Operation", Rev. Sci. Instrum., vol. 55, p. 1684, 1984.

[5] H. Krompholz, J. Doggett, K.H. Schoenbach , J. Gahl, C. Harjes, G. Schaefer, and M. Kristiansen, "Nanosecond Current Probe for High-Voltage Experiments", Rev. Sci. Instrum., vol. 55, p. 127, 1984.

[6] The image converter camera was designed and built by M. Michel, Technische Hochschule Darmstadt, Germany.

[7] G. Schaefer, K.H. Schoenbach, H. Krompholz, M. Kristiansen, and A.H. Guenther, "The Use of Attachers in Electron-Beam Sustained Discharge Switches - Theoretical Considerations", Laser and Particle Beams, vol. 2, p. 237, 1984.

[8] A.V. Phelps, private communication.

[9] G. Schaefer et al, to be published.

[10] L.C. Lee, C.C. Chiang, K.Y. Tang, D.L. Huestis, and D.C. Lorents, "Gaseous Electronic Kinetics for E-beam Excitation of $Cl_2$, NO, and $N_2O$ in $N_2$", Second Annual Report on Coord. Res. Program in Pulsed Power Physics, Dept. Electrical Engineering, Texas Tech University, Lubbock, TX (1981).

[11] L.C. Lee and F. Li, "Shortening of Electron Conduction Pulses by Electron Attachers O2, N2O, and CF4", J. Appl. Phys., vol. 56, p. 3169, 1984.

[12] P.J. Chantry, "Temperature Dependence of Dissociative Attachment in $N_2O$", J. Chem. Phys., vol. 51, p. 3369, 1969.

[13] L.G. Christophourou, S.R. Hunter, J.G. Carter, S.M. Spyrou, V.K. Lakdawla, "Basic Studies of Gases for Diffuse-Discharge Switching Applications," Proceedings IEEE Pulsed Power Conf., p. 702, 1983.

[14] J.B. Gunn, "Microwave Oscillations of Current in III-V Semiconductors," Solid State Communications vol. 1, p. 88, 1963.

[15] B.K. Ridley, and T. B. Watkins, "The Possibility of Negative Resistance Effects in Semiconductors," Proc. Phys. Soc., vol. 78, p. 293 1961 and
C., Hilsum, "Transferred Electron Amplifiers and Oscillators," Proc. IEEE, vol. 50, p. 185, 1962.

# Influence of the circuit impedance on an electron beam controlled diffuse discharge with a negative differential conductivity

G. Schaefer,[a] K. H. Schoenbach,[b] M. Kristiansen, B. E. Strickland,[c]
R. A. Korzekwa, and G. Z. Hutcheson
*Department of Electrical Engineering/Computer Science, Texas Tech University, Lubbock, Texas 79409-4439*

(Received 17 March 1986; accepted for publication 5 May 1986)

The use of attaching gases in an externally sustained diffuse discharge opening switch with a low attachment rate at low values of $E/N$ and a high attachment rate at high values of $E/N$ allows the discharge to operate with low losses in the closed switch phase and to achieve fast opening after the sustainment source is turned off. Such an attacher generates a $J$-$E/N$ characteristic with a negative differential conductivity in an intermediate $E/N$ range. Such a characteristic obstructs the closing process of the discharge if it is operated in a high impedance system. Experiments demonstrating these effects are presented for electron beam sustained discharges in mixtures of argon and $C_2F_6$.

Inductive energy storage is attractive in pulsed power applications because of its intrinsic high-energy density compared to capacitive storage systems. The key technological problem in developing inductive energy discharge systems, especially for repetitive operation, is the development of opening switches. Promising candidates for repetitive opening switches are electron beam ($e$-beam) or laser controlled diffuse discharges.

An $e$-beam controlled diffuse discharge switch utilizes an externally sustained discharge as the switch medium in which ionization is solely maintained by the $e$-beam. The switch opens when the $e$-beam is turned off. The switch opening time is determined by the electron loss processes: recombination and attachment. In order to achieve opening times of less than a microsecond at initial electron densities $n_i < 10^{14}\ \mathrm{cm}^{-3}$, the dominant loss process must be attachment, which means that the switch gas mixture must contain an electronegative gas. On the other hand, additives of attachers increase the power losses during conduction. Both low forward voltage drop and fast opening can only be obtained by choosing gases or gas mixtures which satisfy the following conditions[1-3]:

(1) For low values of the reduced field strength, $E/N$ (conduction phase), the gas mixture should have a high drift velocity $v_d$ and low attachment rate coefficients $k_a$.

(2) For high $E/N$ values (opening phase) the gas mixture should have low drift velocities and high attachment rate coefficients.

It has been discussed before that such gas properties cause a discharge characteristic (current density $J$ versus reduced electric field strength $E/N$) with a strong negative differential conductivity.[2,4] Such a characteristic is equivalent to a strong increase of the discharge resistivity with increasing $E/N$. Gas mixtures which show the above-mentioned properties and were recommended for these applications include mixtures of argon or $CH_4$ and $C_2F_6$ or $C_3F_8$ (Ref. 2). Some of these gas mixtures have been used for switching experiments in $e$-beam sustained discharges.[5,6] The experiments presented here were performed with mixtures of argon and $C_2F_6$.

The experimental setup used for our investigations is an $e$-beam controlled diffuse discharge switch with an $e$-beam tetrode for multiple, submicrosecond pulse operation.[7,8] The discharge itself is driven by a 2-Ω pulse-forming network and series resistors are used to simulate high impedance systems.

The discharge characteristics were investigated with a 2-Ω system. Figures 1 and 2 show the discharge characteristics and the resistivities for different mixing ratios of argon and $C_2F_6$. The source function was kept constant at a value of $S = 1.3\times10^{20}\ \mathrm{cm}^{-3}\,\mathrm{s}^{-1}$. The current density reaches a maximum in the $E/N$ range of 2–3 Td, depending on the

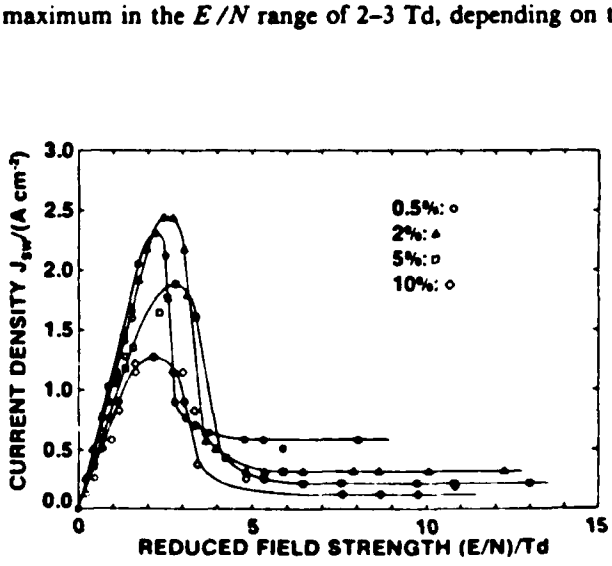


FIG. 1. Current density $J$ vs reduced field strength $E/N$, for an $e$-beam sustained discharge in argon with admixtures of $C_2F_6$. The source function is $S = 1.3\times10^{20}\ \mathrm{cm}^{-3}\,\mathrm{s}^{-1}$. The variable parameter is the $C_2F_6$ fraction.

[a] Present address: Department of Electrical Engineering, Polytechnic University, Farmingdale, NY 11735
[b] Present address: Department of Electrical Engineering, Old Dominion University, Norfolk, VA 23508
[c] Present address: Maxwell Laboratories, San Diego, CA 92123

 0003-6951/86/261776-03$01.00 

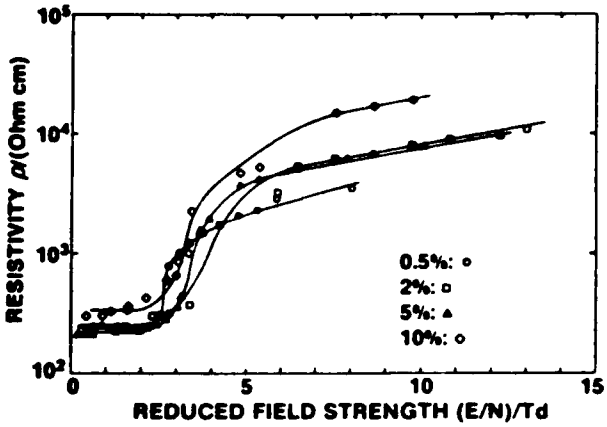


FIG. 2. Resistivity $\rho$ vs reduced field strength $E/N$ for an $e$-beam sustained discharge in argon with admixtures of $C_2F_6$. The source function is $S = 1.3\times10^{20}$ cm$^{-3}$ s$^{-1}$. The variable parameter is the $C_2F_6$ fraction.

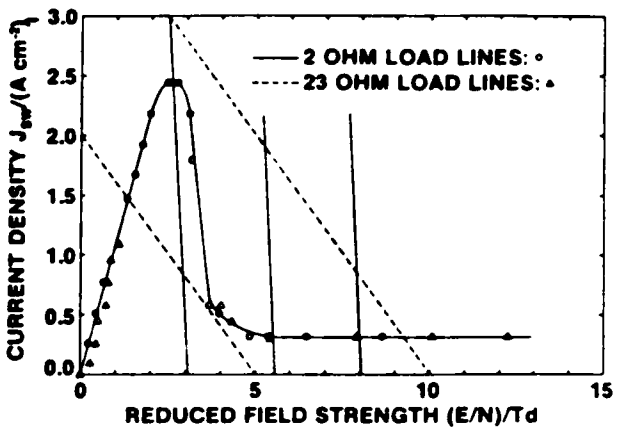


FIG. 3. Load lines and current density $J$ vs reduced electric field strength $E/N$, for an $e$-beam sustained discharge in argon with an admixture of 2% $C_2F_6$, obtained with different load lines.

$C_2F_6$ concentration and the source function $S$. With further increasing $E/N$ up to approximately 5 Td the current density decreases. The discharge resistivity increases in this $E/N$ range by a factor of approximately 20. The increase of resistivity is more pronounced with increasing $C_2F_6$ concentration. It is mainly caused by the attachment properties of $C_2F_6$ and not by the $E/N$ dependence of the drift velocity. Also mixtures of argon and nitrogen have a drift velocity with a maximum at low values of $E/N$; however, these mixtures did not show a negative differential conductivity. The drift velocity, however, seems to influence the magnitude of the current maximum at low $C_2F_6$ concentrations since the characteristic for 0.5% $C_2F_6$ shows a lower maximum current than for 2% $C_2F_6$. Since the maximum of the current density indicates the optimum operation range for the steady-state conducting phase one can conclude that the optimum Ar-$C_2F_6$ mixture contains approximately 2% $C_2F_6$.

It should also be mentioned that the self-breakdown voltage and the glow-to-arc transition voltage increase with increasing $C_2F_6$ concentration. The $E/N$ values for the glow-to-arc transition were 8, 12, and 15 Td, and > 20 Td for $C_2F_6$ concentrations of 0.5%, 2%, 5%, and 10%, respectively.

If the specific switch application requires a burst of short pulses with a high repetition rate, then the inductor is charged only once and the total length of the burst of pulses is shorter or in the order of the discharge time of the inductor. For this operating mode the inductor can be treated as a high impedance transmission line and the closing and opening processes have to follow the same high impedance load line.[3] This load line, therefore, also determines the maximum voltage $V_m$, which can be obtained with an open circuit. The next closing process, starting with $V_m$, will then follow the load line until it reaches the steady-state condition of the discharge, given by the $J$-$E/N$ characteristic of the discharge.

These operating conditions were simulated in our experiment by using resistors in series with the pulse forming network. Figure 3 shows the different load lines used and the experimental discharge results achieved with these load lines. It becomes obvious that the current maximum cannot be utilized with a high impedance system in the repetitive mode.

The closing process is obstructed (the closing time increases significantly) even for operating conditions for which the discharge *can* reach a low loss, low $E/N$ state, since the closing process starts at high values of $E/N$ where attachment is strong. This behavior is demonstrated in Fig. 4. The characteristics measured with a 2-Ω system and a 100-Ω system are shown. For the 2-Ω system the steady-state values are obtained in less than 100 ns. For the 100-Ω system the $E/N$ values are plotted for 75 ns and for 350 ns after $e$-beam initiation. The ionizing $e$-beam had a rise time of approximately 10 ns and a nearly flat maximum over a pulse length of 400 ns.[7] The source function for these measurements again was $S = 1.3\times10^{20}$ cm$^{-3}$ s$^{-1}$. Figure 4 demonstrates that those low loss, low $E/N$ operating conditions which can be achieved with this high impedance system are reached only after a long closing period. This behavior was already predicted for $N_2$:$N_2O$ mixtures.[3]

We therefore have to conclude that gas mixtures which

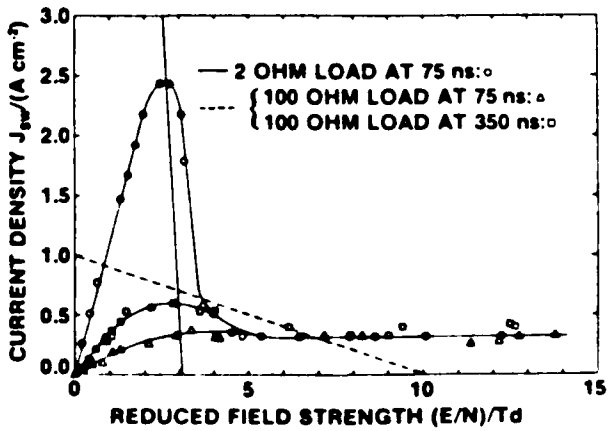


FIG. 4. Current density $J$ vs reduced electric field strength $E/N$ for an $e$-beam sustained discharge in argon with an admixture of 2% $C_2F_6$, obtained at different times after $e$-beam initiation and with different load lines.

cause a negative differential conductivity in an intermediate $E/N$ range are most suitable for diffuse discharge opening switches only if the system is operated in a single shot mode (recharging of the inductor after every shot). For a burst mode (several shots from a single inductor charging), however, the closing process is obstructed and the maximum possible current cannot be utilized. For such an application a discharge characteristic is required where the current rises strongly with $E/N$ up to the operating point of the discharge in the closed phase. Above this $E/N$ value the current should stay constant or decrease slowly with $E/N$ over a wide $E/N$ range to assure a high self-breakdown voltage. Ternary gas mixtures can be used with two attachers with attachment cross sections at different electron energies to produce such a flat characteristic over a wide $E/N$ range and to achieve the same increase of resistivity. Another approach to solve this problem is to control the attachment externally.[1,3]

This work was jointly supported by Air Force Office of Scientific Research and Army Research Office under contract AFOSR 84-0032.

[1]K. H. Schoenbach, G. Schaefer, M. Kristiansen, L. L. Hatfield, and A. H. Guenther, IEEE Trans. Plasma Sci. PS-10, 246 (1982).
[2]L. L. Christophorou, S. R. Hunter, J. A. Carter, and R. A. Mathis, Appl. Phys. Lett. 41, 147 (1982).
[3]G. Schaefer, K. H. Schoenbach, H. Krompholz, M. Kristiansen, and A. H. Guenther, Laser Part. Beams 2, 273 (1984).
[4]A. D. Barkalov and G. G. Gladush, translated from Teplofiz. Vys. Temp. 20, 19 (1982).
[5]P. Bletzinger, Proceedings of 4th IEEE Pulsed Power Conference, IEEE Catalog No. 83CH1908-3, 37, Albuquerque, NM, 1983.
[6]R. J. Commisso, R. F. Fernsler, V. E. Scherrer, and I. M. Vitkovitsky, Proceedings of 4th IEEE Pulsed Power Conference, IEEE Catalog No. 83CH1908-3, 87, Albuquerque, NM, 1983.
[7]H. C. Harjes, K. H. Schoenbach, G. Schaefer, M. Kristiansen, H. Krompholz, and D. Skaggs, Rev. Sci. Instrum. 55, 1684 (1984).
[8]K. H. Schoenbach, G. Schaefer, M. Kristiansen, H. Krompholz, H. C. Harjes, and D. Skaggs, J. Appl. Phys. 57, 1618 (1985).

# INTERACTION OF DISCHARGE AND CIRCUIT IN AN ELECTRON-BEAM CONTROLLED DIFFUSE DISCHARGE OPENING SWITCH

G. Schaefer,[a] K. H. Schoenbach,[b] M. Kristiansen, B. E. Strickland,[c]
R. A. Korzekwa, G. Z. Hutcheson,[d] and K. R. Rathbun
Department of Electrical Engineering/Computer Science
Texas Tech University, Lubbock, Texas 79409-4439, USA

## Abstract

The use of attaching gases in an externally sustained diffuse discharge opening switch with a low attachment rate at low values of E/N allows the discharge to operate with low losses in the closed switch phase and to achieve fast opening after the sustainment source is turned off. Such an attacher generates a J-E/N characteristic with a negative differential conductivity in an intermediate E/N range, as demonstrated in electron beam sustained discharges. Such a characteristic obstructs the closing process of the discharge if it is operated in a high impedance system. Experiments demonstrating these effects are presented for electron beam sustained discharges in mixtures of Argon and $C_2F_6$.

Another approach discussed is to control the attachment externally by generating vibrationally excited molecules, which are known to have higher attachment cross sections. Experiments are presented, demonstrating increased resistivity in self sustained and externally sustained dc discharges in gas mixtures containing attachers such as $NH_3$ and $C_2HF_3$, after vibrational exctitation with a low power $CO_2$ laser.

## Introduction

For many pulsed power applications weight and volume have become the major limiting factors for scaling these systems to higher energies. Inductive energy storage is, therefore, attractive for these applications because of its intrinsic high energy density compared to present capacitive storage systems. The key technological problem in developing inductive energy discharge systems, especially for repetitive operation, is the development of opening switches. Promising candidates for repetitive opening switches are electron beam or laser controlled diffuse discharges.

An electron beam controlled diffuse discharge switch utilizes an electron beam sustained discharge as the switch medium. The voltage across the switch is always kept below the voltage of the self sustained discharge, which means that ionization is solely maintained by the electron beam. The switch opens when the electron beam is turned off. The switch opening time is determined by the electron loss processes: recombination and attachment. In order to achieve opening times of less than a microsecond at initial electron densities $n_e < 10^{14}$ cm$^{-3}$, the dominant loss process must be attachment, which means that the switch gas mixture must contain an electro-negative gas. On the other hand, additives of attachers increase the power losses during conduction. Both low forward voltage drop and fast opening can only be obtained by choosing gases or gas mixtures which satisfy the following conditions [1-3]:

(1) For low values of the reduced field strength, E/N, (conduction phase) the gas mixture should have a high drift velocity, $v_d$, and low attachment rate coefficients, $k_a$.
(2) For high E/N values (opening phase) the gas mixture should have low drift velocities and high attachment rate coefficients.

## Discharge Characteristics

It has been discussed before that such gas properties cause a discharge charateristic (current density, J, versus reduced electric field strength, E/N) with a strong negative differential conductivity [2-4]. Such a characteristic is equivalent to a strong increase of the discharge

---

a) Permanent Address: Polytechnic University, Farmingdale, New York, USA

b) Permanent Address: Old Dominion University, Norfolk, Virginia, USA

c) Permanent Address: Maxwell Laboratories, Inc., San Diego, California, USA

d) Permanent Address: Mission Research Corporation, Albuquerque, New Mexico, USA

resistivity with increasing E/N. Gas mixtures which show the above mentioned properties and were recommended for these applications include mixtures of Argon or $CH_4$ and $C_2F_6$ or $C_3F_8$ [2]. Some of these gas mixtures have been used for switching experiments in electron beam sustained discharges [5,6]. The experiments presented here were performed with mixtures of Argon and $C_2F_6$.

The experimental setup used for our investigations is an electron beam controlled diffuse discharge switch with an electron beam tetrode for multiple, submicrosecond pulse operation [7,8]. The discharge itself is driven by a 2 Ω pulse forming network and series resistors are used to simulate high impedance systems.

The discharge characteristics were investigated with a 2 Ω system. Figure 1 shows the discharge charateristics for different mixing ratios of Argon and $C_2F_6$. The source function was

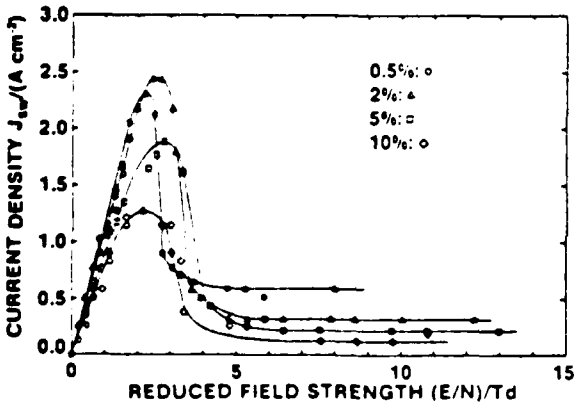


Fig. 1 Current density, J, versus reduced electric field strength, E/N, for an e-beam sustained discharge in Argon with admixtures of $C_2F_6$. The source function is $S = 1.3 \cdot 10^{20}$ cm$^{-3}$s$^{-1}$. The variable parameter is the $C_2F_6$ fraction.

kept constant at a value of $S = 1.3 \cdot 10^{20}$ cm$^{-3}$ s$^{-1}$. The current density reaches a maximum in the E/N range of 2-3 Td, depending on the $C_2F_6$ concentration and the source function, S. With further increasing E/N up to approximately 5 Td the current density decreases. This decrease of current density, corresponding to an increase of resistivity is more pronounced with increasing $C_2F_6$ concentration, caused by the attachment properties of $C_2F_6$

## Interaction of Discharge and Circuit

Fast, repetitive transfer of power from an inductive energy storage device to a load requires detailed considerations of the circuit elements as transmission lines, implying a high characteristic impedance and a fixed transit time [9]. If the specific switch application requires a burst of short pulses with a high repetition rate then the inductor is charged only once and the total length of the burst of pulses is in the order of the discharge time of the inductor. For this operating mode the inductor can be treated as a high impedance line and the closing and opening processes have to follow the same high impedance load line [3]. Figure 2 shows the different load lines used and the experimental discharge results achieved with these load lines. The closing

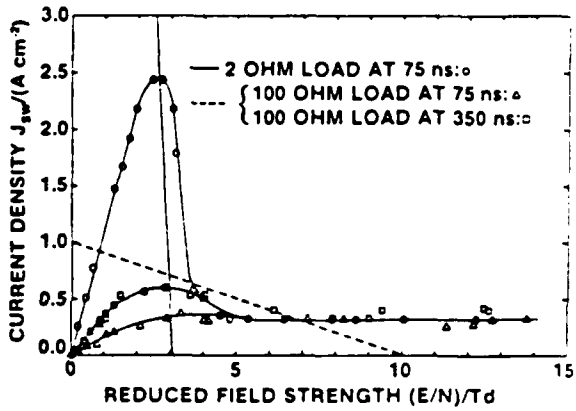


Fig. 2 Current density, J, versus reduced electric field strength, E/N, for an e-beam sustained discharge in Argon with an admixture of 2% $C_2F_6$, obtained at different times after e-beam initation and with different loadlines.

process is obstructed even for operating conditions for which the discharge can reach a low loss, low E/N state, since the closing process starts at high values of E/N where attachment is strong. For the 2 Ω system the steady state values are obtained in less than 100 ns. For the 100 Ω system the E/N values are plotted for 75 ns and for 350 ns after electron beam initiation. The ionizing electron beam had a risetime of approximately 10 ns and a nearly flat maximum over a pulse length of 400 ns [7]. The source function for these measurements again was $S = 1.3 \cdot 10^{20}$ cm$^{-3}$s$^{-1}$. Figure 2 demonstrates that

those low loss, low E/N operation conditions which can be achieved with this high impedance system are reached only after a long closing period. This behavior was already predicted for $N_2$:$N_2O$ mixtures [3].

We, therefore, have to conclude that gas mixtures which cause a negative differential conductivity in an intermediate E/N range are most suitable for diffuse discharge opening switches only if the system is operated in a single shot mode (recharging of the inductor after every shot). For a burst mode (several shots from a single inductor charging), however, the closing process is obstructed and the maximum possible current can not be utilized.

## IR Induced Attachment

Another approach considered to achieve a low forward voltage drop and a fast opening time is to control the attachment externally. Certain attachers are known to have a drastically increased attachment cross section if excited into higher lying rotational and vibrational states. One way to excite molecules into such states is to use lasers to optically excite molecules like $CF_4$ or $NH_3$, similar to techniques used in optically pumped IR lasers [10]. We, therefore, performed experiments in self sustained and externally sustained dc discharges, irradiated with a chopped CW $CO_2$ laser.

The self sustained discharge was operated in a discharge tube ($\phi$ = 4 mm) with the two electrodes in side arms and with two probe electrodes to measure the voltage drop only across the positive column. With this arrangement, only the positive column was irradiated. A large series resistor ensured operation at constant current. Experiments were performed in mixtures of Argon and $NH_3$. During irradiation with a $CO_2$ laser (P20 at 10.591 μm) the voltage across the column showed a small increase, indicating an increased resistivity.

Figure 3 shows the relative change of the discharge resistance under the influence of the $CO_2$ laser. The measurements were performed with the current density as the variable parameter since the discharge voltage was nearly constant. The value of E/N at the stability limit with low currents was approximately 50 Td and decreased with increasing current by less than 10% in the current range investigated.

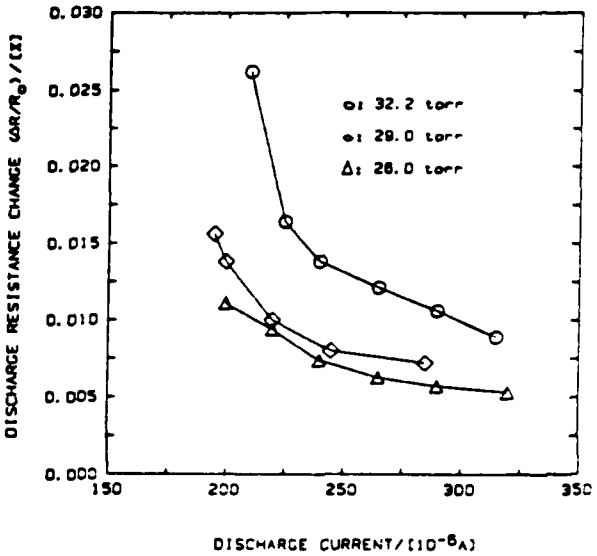


Fig. 3 $CO_2$-laser induced relative discharge resistance change, $\Delta R/R_o$, versus discharge current, J, in a self sustained glow discharge in a mixture of 57% $NH_3$ and 43% Argon. The variable parameter is the gas pressure, P.

Since the self sustained discharge does not allow independent control of E/N, we also performed experiments in an externally sustained discharge, sustained by injecting the plasma from a flowing hollow cathode discharge. First, experiments were performed at constant E/N in a buffer gas of Argon with 5% Helium (the Helium was used in the hollow cathode) and $NH_3$. The discharge resistance decreased during laser irradiation with the $CO_2$ laser (P20 at 10.591 μm). The results for different $NH_3$ concentrations are shown in Fig. 4.

The increase of resistivity is small and mainly occurs at high values of E/N. This behavior is expected since $NH_3$ has a low attachment cross section with its maximum at approximately 5.6 eV. If vibrational excitation causes an enhancement of attachment, then the cross section will increase and its maximum will shift to lower energies.

In recent experiments with admixtures of halogenated hydrocarbons ($C_2HF_3$, $C_2H_3F$, and $C_2H_3Cl$), significantly higher resistance changes were achieved. The selection of the attacher and the attacher concentration also allowed the adjustment of the E/N range where the relative increase of the resistance had its maximum. With $C_2H_3F$, for example, a resistance change of 1% was

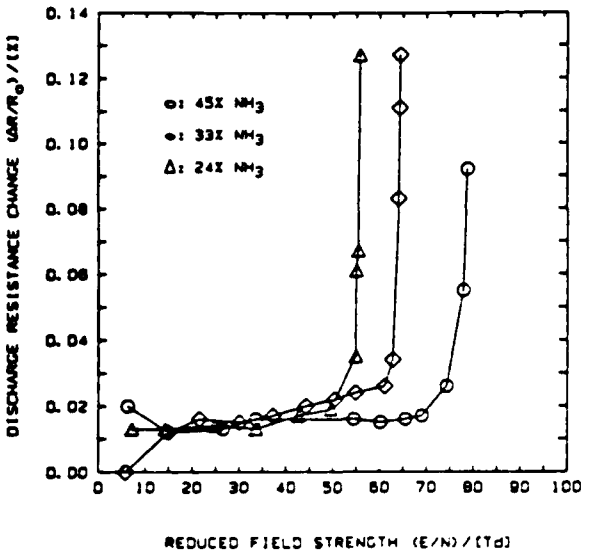


Fig. 4 $CO_2$-laser induced relative resistance change, $\Delta R/R_o$, versus E/N in an externally sustained dc discharge in a mixture of $NH_3$ and a buffer gas of Argon and 6% Helium at 32 torr total gas pressure. The variable parameter is the % $NH_3$ concentration.

observed with a laser power of less than 1 W $cm^{-2}$. It should, however, be mentioned that experiments with electron beam sustained discharges containing other attachers have to date failed to show a significant increase of the attachment rate after irradiation with a pulsed $CO_2$ laser [11]. It was suggested that electron vibrational excitation and quenching collisions negate the selective excitation with the laser. A careful analysis of all processes involved seems, therefore, to be necessary to select suitable attachers, buffer gases, and laser wavelengths. Vibrational excitation into higher lying states with larger photon energies may have a better chance to generate states which are not produced in the discharge.

## Acknowledgments

This work was jointly supported by the Air Force Office of Scientific Research and the Army Research Office under contract AFOSR 84-0032.

## References

[1] K. H. Schoenbach, G. Schaefer, M. Kristiansen, L. L. Hatfield, and A. H. Guenther, "Concepts for Optical Control of Diffuse Discharge Opening Switches," IEEE Trans. Plasma Sci., Vol. PS-10, pp. 246-251, 1982.

[2] L. L. Christophorou, S. R. Hunter, J. A. Carter, and R. A. Mathis, "Gases for Possible Use in Diffuse Discharge Switches," Appl. Phys. Lett., Vol. 41, pp. 147-149, 1982.

[3] G. Schaefer, K. H. Schoenbach, H. Krompholz, M. Kristiansen, and A. H. Guenther, "The Use of Attachers in Electron Beam Sustained Discharge Switches - Theoretical Consideration," Laser and Particle Beams, Vol. 2, pp. 273-291, 1984.

[4] A. D. Barkalov and G. G. Gladush, "Domain Instability of a Non-Self-Sustaining Discharge in Electronegative Gases," Translated From Teplofizika Vysokikh Temperatur, Vol. 20, pp. 19-24, 1982.

[5] P. Bletzinger, "Scaling of Electron Beam Switches," Proc. 4th IEEE Pulsed Power Conf., pp. 37-40, Albuquerque, NM 1983.

[6] R. J. Commisso, R. F. Fernsler, V. E. Scherrer, and I. M. Vitkovitsky, "Application of Electron Beam Controlled Diffuse Discharges to Fast Switching," Proc. 4th IEEE Pulsed Power Conf., pp. 87-90, Albuquerque, NM 1983.

[7] H. C. Harjes, K. H. Schoenbach, G. Schaefer, M. Kristiansen, H. Krompholz, and D. Skaggs, "An Electron Beam Tetrode for Multiple, Submicrosecond Pulse Operation, " Rev. Sci. Instr., Vol. 55, pp. 1684-1686, 1984.

[8] K. H. Schoenbach, G. Schaefer, M. Kristiansen, H. Krompholz, H. C. Harjes, and D. Skaggs, "An Electron-Beam Controlled Diffuse Discharge Switch," J. Appl. Phys., Vol. 57, pp. 1618-1622, 1985.

[9] M. Kristiansen, "Fundamentals of Inductive Energy Storage," Proc. ARO Workshop on Repetitive Opening Switches,edited by M. Kristiansen and K. H. Schoenbach, Tamarron, CO 1981. (DTIC No. AD-A110770)

[10] J. J. Tiee and C. Wittig, "Optically Pumped Molecular Lasers in the 11-17 Micron Region," J. Appl. Phys., Vol. 49, pp. 61, 1978.

[11] F. L. Eisele, "Photon Induced Electron Attachment, " Final Report, AFWAL-TR-85-2015, 1984.

# OPTIMIZATION OF GAS MIXTURES FOR ELECTRON-BEAM CONTROLLED DIFFUSE DISCHARGE OPENING SWITCHES

G. Schaefer,[a] K. H. Schoenbach,[b] M. Kristiansen,
R. A. Korzekwa, and G. Z. Hutcheson[c]
Department of Electrical Engineering/Computer Science
Texas Tech University, Lubbock, Texas 79409-4439

## Abstract

Electron beam controlled diffuse discharges are promising candidates for high power opening switches. In order to achieve short opening times when the electron beam is turned off, the switch gas mixture must contain an attacher. Both low forward voltage drop and fast opening can be obtained by choosing gas mixtures with a low attachment rate coefficient, $k_a$, at low E/N and a high attachment rate coefficient at high E/N. Such gas properties cause a discharge characteristic (current density, J, versus reduced electric field strength, E/N) with a strong negative differential conductivity. For switch applications requiring a burst of short pulses, the inductor has to be treated as a high impedance line. Here the closing process is obstructed since it starts at high values of E/N where attachment is strong, and the maximum possible current can not be utilized. Experiments with varying system impedances were performed with mixtures of argon and $C_2F_6$ demonstrating this effect. As an alternative, ternary gas mixtures can be used with two attachers with attachment cross sections at different electron energies to produce a flat characteristic over a wide E/N range. A further approach for improving switch efficiency is presented using Penning additives such as $C_2H_2$ to increase the ionization efficiency of the electron beam.

## Introduction

For many pulsed power applications weight and volume have become the major limiting factors for scaling these systems to higher energies. Inductive energy storage is, therefore, attractive for these applications because of its intrinsic high energy density compared to present capacitive storage systems. The key technological problem in developing inductive energy discharge systems, especially for repetitive operation, is the development of opening switches. Promising candidates for repetitive opening switches are electron beam or laser controlled diffuse discharges.

An electron beam controlled diffuse discharge switch utilizes an electron beam sustained discharge as the switch medium. The voltage across the switch is always kept below the voltage of the self sustained discharge, which means that ionization is maintained by the electron beam. The switch opens when the electron beam is turned off. The switch opening time is determined by the electron loss processes: recombination and attachment. In order to achieve opening times of less than a microsecond at initial electron densities $n_e < 10^{14}$ cm$^{-3}$, the dominant loss process must be attachment, which means that the switch gas mixture must contain an electro-negative gas. On the other hand, additives of attachers increase the power losses during conduction. Both low forward voltage drop and fast opening can only be obtained by choosing gases or gas mixtures which satisfy the following conditions [1-3]:

(1) For low values of the reduced field strength, E/N, (conduction phase) the gas mixture should have a high drift velocity, $v_d$, and a low attachment rate coefficient, $k_a$.

(2) For high E/N values (opening phase) the gas mixture should have a low drift velocity and a high attachment rate coefficient.

## Discharge Characteristics

It has been discussed before that such gas properties cause a discharge charateristic (current density, J, versus reduced electric field strength, E/N) with a strong negative differential conductivity [2,4]. Such a characteristic is equivalent to a strong increase of the discharge resistivity with increasing E/N. Gas mixtures which show the above mentioned properties and were recommended for these applications include mixtures of argon or $CH_4$ and $C_2F_6$ or $C_3F_8$ [2]. Some of these gas mixtures have been used for switching experiments in electron beam sustained discharges [5,6]. The experiments presented here were performed with mixtures of argon and $C_2F_6$.

The experimental setup used for our investigations is an electron beam controlled diffuse discharge switch with an electron beam tetrode for multiple, submicrosecond pulse operation [7,8]. The discharge itself is driven by a 2 Ω pulse forming network and series resistors are used to simulate high impedance systems.

The discharge characteristics were investigated with a 2 Ω system. Figure 1 shows the discharge charateristics for different mixing ratios of argon and $C_2F_6$. The source function was kept constant at a value of $S = 1.3 \times 10^{20}$ cm$^{-3}$ s$^{-1}$. The current density reaches a

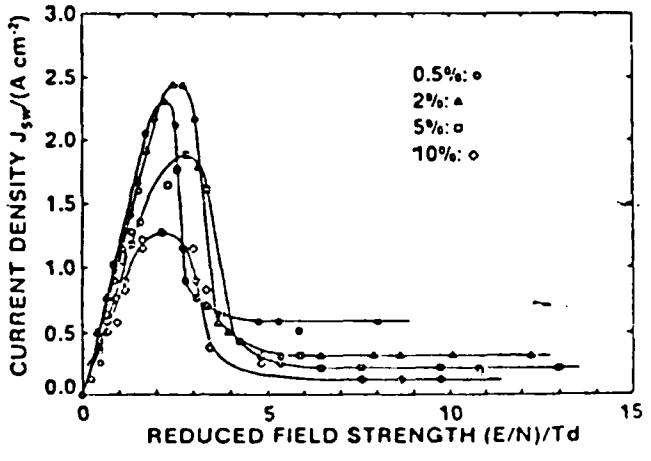


Fig. 1 Current density, J, versus reduced electric field strength, E/N, for an e-beam sustained discharge in argon with admixtures of $C_2F_6$. The source function is $S = 1.3 \times 10^{20}$ cm$^{-3}$s$^{-1}$. The variable parameter is the $C_2F_6$ fraction.

---

a) Permanent Address: Polytechnic University, Farmingdale, New York

b) Permanent Address: Old Dominion University, Norfolk, Virginia

c) Permanent Address: Mission Research Corporation, Albuquerque, New Mexico

maximum in the E/N range of 2-3 Td, depending on the $C_2F_6$ concentration and the source function, S. With further increasing E/N up to approximately 5 Td the current density decreases. This decrease of current density, corresponding to an increase of resistivity as shown in Fig. 2, is more pronounced with increasing $C_2F_6$

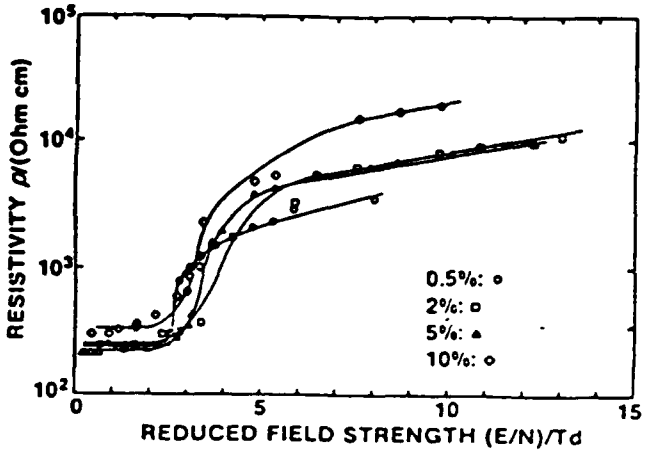


Fig. 2 Resistivity, ρ, versus reduced electric field strength, E/N, for an e-beam sustained discharge in argon with admixtures of $C_2F_6$. The source function is $S = 1.3 \cdot 10^{20}$ cm$^{-3}$ s$^{-1}$. The variable parameter is the $C_2F_6$ fraction.

concentration. It is mainly caused by the attachment properties of $C_2F_6$ and not by the E/N dependence of the drift velocity. Also, mixtures of argon and nitrogen have a drift velocity with a maximum at low values of E/N, however, these mixtures did not show a negative differential conductivity, as shown in Fig. 3. The

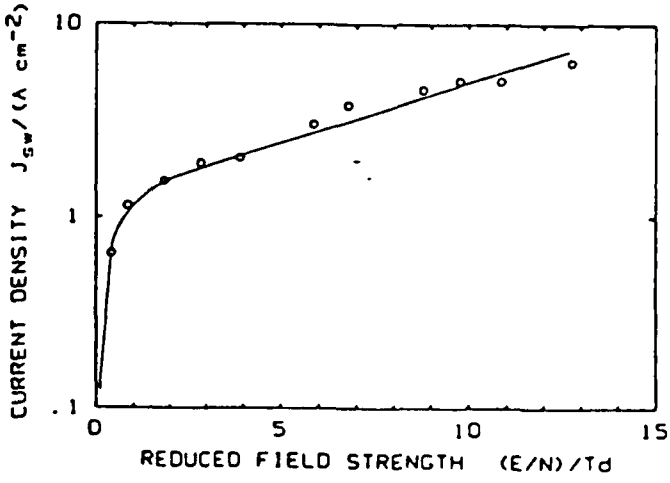


Fig. 3 Current density, J, versus reduced electric field strength, E/N, for an e-beam sustained discharge in argon with an admixture of 5% $N_2$. The source function is $S = 1.3 \cdot 10^{20}$ cm$^{-3}$ s$^{-1}$.

drift velocity, however, seems to influence the magnitude of the current maximum at low $C_2F_6$ concentrations since the characteristic for 0.5% $C_2F_6$ shows a lower maximum current than for 2% $C_2F_6$. Since the maximum of the current density indicates the optimum operation range for the steady state conduction phase one can conclude that the optimum Ar-$C_2F_6$ -mixture contains approximately 2% $C_2F_6$.

It should also be mentioned that the self breakdown voltage and the glow-to-arc transition voltage increase with increasing $C_2F_6$ concentration. The E/N values for the glow-to-arc transition were 8 Td, 12 Td, 15 Td, and > 20 Td for $C_2F_6$ concentrations of 0.5%, 2%, 5%, and 10%, respectively.

## UV SUSTAINED DISCHARGE

It is interesting to notice that a similar discharge characteristic has been found in optically sustained discharges using the same gas mixtures. Figure 4 shows the characteristics for 10% $C_2F_6$ in argon in an electron beam sustained discharge with a source function of $S = 1.3 \cdot 10^{20}$ cm$^{-3}$ s$^{-1}$ and for an optically sustained discharge with a source function of $S = 1.6 \cdot 10^{19}$ cm$^{-3}$ s$^{-1}$. In the case of the optically

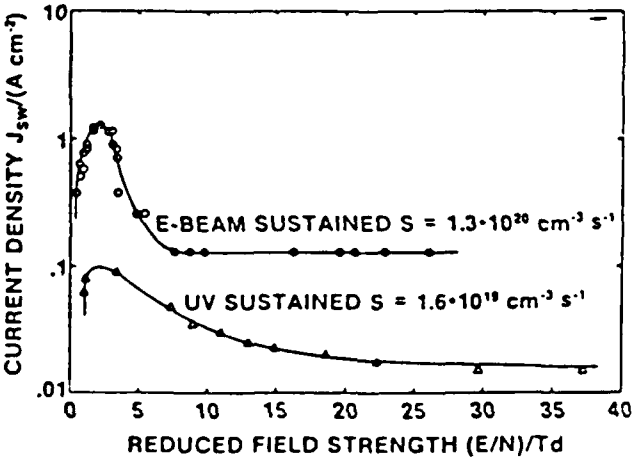


Fig. 4 Current density, J, versus reduced electric field strength, E/N, for an e-beam sustained discharge and for a UV sustained discharge in argon with an admixture of 10% $C_2F_6$.

sustained discharge approximately 350 ppm dimethylaniline was used as an additive with a low ionization potential. One would expect the onset of the negative differential conductivity to be more pronounced if the source function decreases since the influence of recombination is reduced [3]. According to Fig. 4 the opposite is found. A significant difference between the two ionization sources is that the average energy of the electrons produced by the UV source is very low (<< 1 eV) while the electrons produced by the electron beam have an average energy in the order of several eV. This effect, in combination with attaching gases, may have a significant effect on the electron energy distribution function and consequently on the onset of attachment with increasing E/N [9]. Also, the additive of dimethylaniline may contribute to a change of the electron energy distribution.

## Interaction of Discharge and Circuit

Fast, repetitive transfer of power from an inductive energy storage device to a load requires detailed considerations of the circuit elements as transmission lines, implying a high characteristic impedance and a fixed transit time[10].

If the specific switch application requires a burst of short pulses with a high repetition rate then the inductor is charged only once and the total length of the burst of pulses is in the order of the discharge time of the inductor. For this operating mode the inductor can be treated as a high impedance line and the closing and opening processes have to follow the same high impedance load line [3]. Figure 5 shows the different load lines used and the experimental discharge results achieved with these load lines. It becomes obvious that the current maximum can not be utilized with a high impedance system in the repetitive mode.

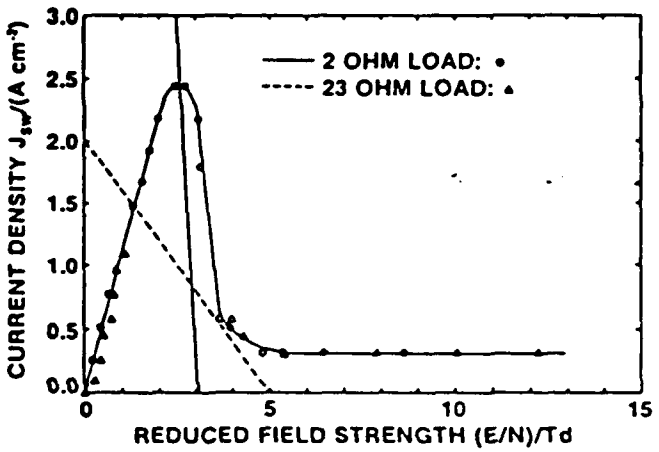


Fig. 5 Loadlines and current density, J, versus reduced electric field strength, E/N, for an e-beam sustained discharge in argon with an admixture of 2% $C_2F_6$, obtained with different loadlines.

The closing process is obstructed even for operating conditions for which the discharge can reach a low loss, low E/N state, since the closing process starts at high values of E/N where attachment is strong. This behavior is demonstrated in Fig. 6. The

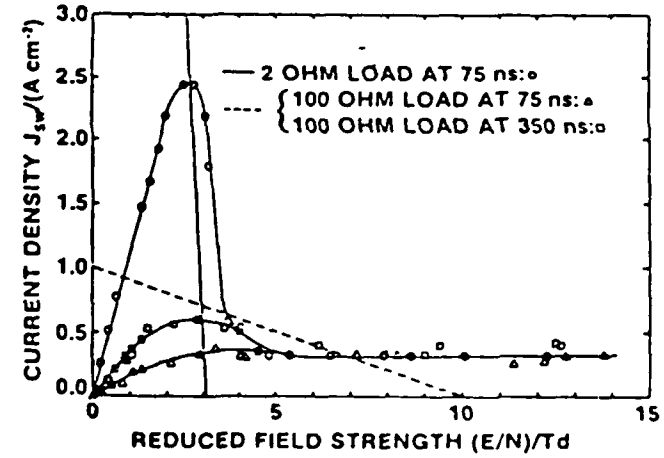


Fig. 6 Current density, J, versus reduced electric field strength, E/N, for an e-beam sustained discharge in argon with an admixture of 2% $C_2F_6$, obtained at different times after e-beam initation and with different loadlines.

characteristics measured with a 2 Ω system and a 100 Ω system are shown. For the 2 Ω system the steady state values are obtained in less than 100 ns. For the 100-Ω system the E/N values are plotted for 75 ns and for 350 ns after electron beam initiation. The ionizing electron beam had a risetime of approximately 10 ns and a nearly flat maximum over a pulse length of 400 ns [7]. The source function for these measurements again was $S = 1.3 \cdot 10^{20}$ cm$^{-3}$s$^{-1}$. Figure 6 demonstrates that those low loss, low E/N operating conditions which can be achieved with this high impedance system are reached only after a long closing period. This behavior was already predicted for $N_2$:$N_2O$ mixtures [3].

We, therefore, have to conclude that gas mixtures which cause a negative differential conductivity in an intermediate E/N range are most suitable for diffuse discharge opening switches only if the system is operated in a single shot mode (recharging of the inductor after every shot). For a burst mode (several shots from a single inductor charging), however, the closing process is obstructed and the maximum possible current can not be utilized.

## Gas Mixtures With Two Attachers

For fast repetitive operation a discharge characteristic is required where the current rises strongly with E/N up to the operating point of the discharge in the closed phase. Above this E/N value the current should stay constant or decrease slowly with E/N over a wide E/N range to assure a high self breakdown voltage. Ternary gas mixtures can be used with two attachers, with attachment cross sections at different electron energies, to produce such a flat characterisitic over a wide E/N range and to achieve the same increase of resistivity. The differences in the magnitudes of the cross sections have to be compensated by using appropriate concentrations of the different gas components. The results with a mixture of 49% argon, 49% $CF_4$, and 2% $C_2F_6$, as an example, are shown in Fig. 7. The discharge characteristic demonstrates that

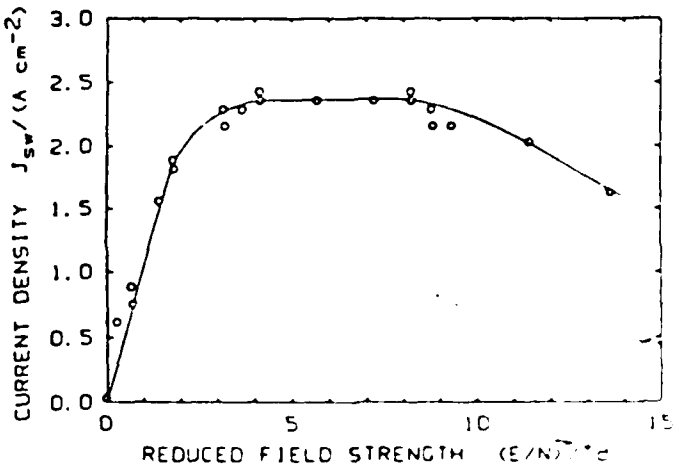


Fig. 7 Current density, J, versus reduced electric field strength, E/N, for an e-beam sustained discharge in a mixture of 49% argon, 49% $CF_4$ and 2% $C_2F_6$. The source function is $S = 5.3 \cdot 10^{20}$ cm$^{-3}$ s$^{-1}$.

a flat portion over a wide E/N range is possible (2.5 -10 Td). Above 10 Td the current density decreases again, ensuring high electron losses during switch opening. The maximum current density achieved is approximately the same as for Ar and $C_2F_6$ mixtures in

experiments with the same electron beam current (see Fig. 1). It should however be mentioned that due to the different values of stopping powers, the source function was four times higher in Ar-$CF_4$ mixtures than in Ar.

## Penning Ionization Ternary Gas Mixtures

The source function, S, of an electron beam as the external ionization source is inversely proportional to the so called W-value, $W_i$, which is the average energy required to produce one electron-ion pair:

$$S = (dW/dx)J_{eb}(eW_i)^{-1} \qquad (1)$$

where dW/dx is the spatial rate of electron beam energy loss in the gas and $J_{eb}$ is the electron beam current density. This W-value is usually in the order of twice the ionization energy of the gas, which means that approximately half of the energy, transferred from the electron beam into the gas is converted into excitation. This excitation energy has to be considered as a loss for devices which only utilize free electrons, such as diffuse discharges, for switches. It has been suggested that a fraction of this excitation energy can be recovered for ionization by using Penning additives [11]. Measurements in gas mixtures of argon and $C_2F_6$, for example, showed a significant decrease of the W-value if small admixtures (0% to ≃ 10%) of, for example, $C_2H_2$ were used. These experiments were performed in an ionization chamber with an alpha source at a very low source function.

To investigate the applicability of these measurements for opening switches we performed electron beam sustained discharge experiments using the same gas mixtures. In Fig. 8, curves a and b show a comparison of the steady state discharge characteristics for argon + 2% $C_2F_6$ and for (argon + 2% $C_2F_6$) + 5% $C_2H_2$. The two characteristics, measured with the same energy deposition of the electron beam into the gas, demonstrate a significant increase of the current density if the Penning additive was used.

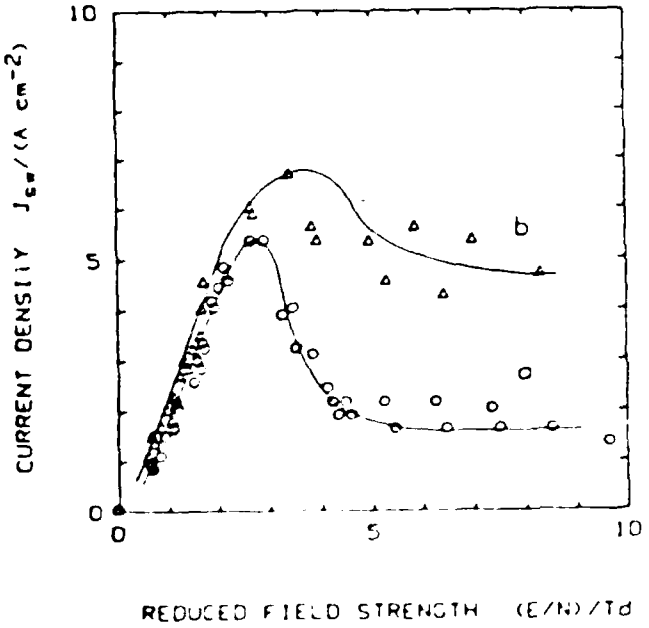


Fig 8 Current density J versus reduced electric field strength E/N, for an e-beam sustained discharge in argon with 2% $C_2F_6$. The source function is $S = 1.3 \cdot 10^{20}\ cm^{-3}\ s^{-1}$. Where (a) has no Penning additive and (b) has 5% $C_2H_2$ added

For the evaluation of the W-value we concentrated on the recombination dominated regime between 1 Td and 3 Td. Here the rate equation for the electron density, $n_e$, becomes:

$$dn_e/dt = S - k_r n_e^2 = 0 \qquad (2)$$

with $k_r$ being the recombination rate coefficient. With the additional equation for the discharge current density, $J_d$:

$$J_d = n_e e \mu_e E \qquad (3)$$

with $\mu_e$ being the electron mobility and E the electric field intensity, using Eq (1) we get a relation for J(E/N) with the W-value as a parameter:

$$J = ((e(dW/dx)J_{eb})/k_r)^{1/2} \mu_e N (W_i)^{-1/2} (E/N) \qquad (4)$$

In the E/N range considered, 1-3 Td, the electron mobility, $\mu_e$, of argon with 2% $C_2F_6$ can be considered to be constant [12]. Neglecting the E/N dependence of the recombination rate coefficient, $k_r$, we get from Eq. (4):

$$dJ_d/d(E/N) \propto (W_i)^{-1/2} \qquad (5)$$

Comparison of two measurements, one without the Penning additive and one with n% $C_2H_2$ allows the evaluation of the value, $W_n$, of the mixture with n% $C_2H_2$:

$$W_n = W_o \frac{(dJ_d/d(E/N))_o^2}{(dJ_d/d(E/N))_n^2} \qquad (6)$$

$W_o$ is the W-value without the Penning additive. The results of this evalution using the known value $W_o$ = 27 eV for argon plus 2% $C_2F_6$ [11] are plotted in Fig. 9 and compared with the previous measurements. Figure 9 demonstrates that in both experiments a dependence of the W-value on the percentage of $C_2H_2$ was observed in the range from 0% to 5% $C_2H_2$. It should be mentioned, however, that the error in our measurement is in the order of 5% due to the reproducibility of the discharge experiments.

A comparison of curves a and b in Fig. 8 also shows a significant increase of the discharge current density in the attachment dominated regime above 5 Td when the Penning additive was used. A similar analysis in this E/N regime to evaluate the W-value has failed to give any reasonable results. We therefore conclude that the Penning additive interferes with the attachment related processes. Further investigations are necessary to explain this behavior.

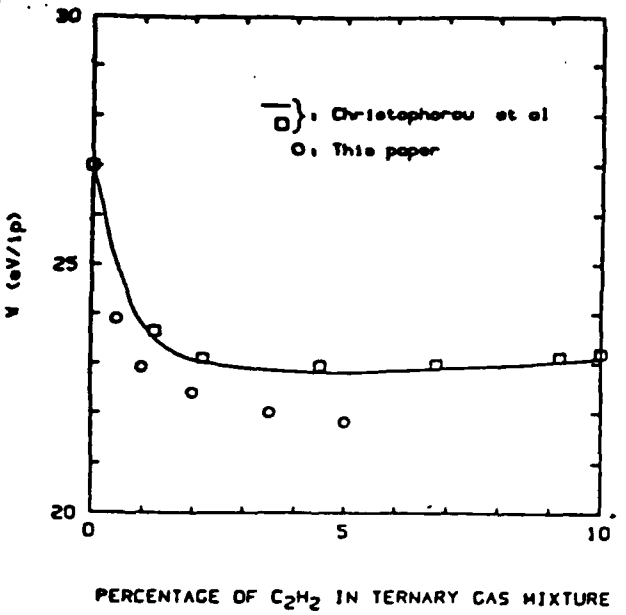


Fig. 9 W-values in argon + 2% $C_2F_6$ + $C_2H_2$ versus the concentration of the admixture of the Penning additive, $C_2H_2$.


## Acknowledgments

This work was jointly supported by the Air Force Office of Scientific Research under contract AFOSR 84-0032, the Army Research Office, and the National Science Foundation.


## References


[1] K. H. Schoenbach, G. Schaefer, M. Kristiansen, L. L. Hatfield, and A. H. Guenther, "Concepts for Optical Control of Diffuse Discharge Opening Switches.," *IEEE Trans. Plasma Sci.*, Vol. PS-10, 1962, pp. 246-251.

[2] L. L. Christophorou, S. R. Hunter, J. A. Carter, and R. A. Mathis, "Cases for Possible Use in Diffuse Discharge Switches," *Appl. Phys. Lett.*, Vol. 41, 1982, pp. 147-149.

[3] G. Schaefer, K. H. Schoenbach, H. Krompholz, M. Kristiansen, and A. H. Guenther, "The Use of Attachers in Electron Beam Sustained Discharge Switches - Theoretical Consideration," *Laser and Particle Beams*, Vol. 2, 1984, pp. 273-291.

[4] A. D. Barkalov and G. G. Gladush, "Domain Instability of a Non-Self-Sustaining Discharge in Electronegative Cases," *Translated From Teploftzika Vysokikh Temperatur*, Vol. 20, 1982, pp. 19-24.

[5] P. Bletzinger, "Scaling of Electron Beam Switches," *Proc. 4th IEEE Pulsed Power Conf.*, Albuquerque, NM 1983, pp. 37-40.

[6] R. J. Commisso, R. F. Fernsler, V. E. Scherrer, and I. M. Vitkovitsky, "Application of Electron Beam Controlled Diffuse Discharges to Fast Switching," *Proc. 4th IEEE Pulsed Power Conf.*, Albuquerque, NM 1983, pp.87-90.

[7] H. C. Harjes, K. H. Schoenbach, G. Schaefer, M. Kristiansen, H. Krompholz, and D. Skaggs, "An Electron Beam Tetrode for Multiple, Submicrosecond Pulse Operation," *Rev. Sci. Instr.*, Vol. 55, 1984, pp. 1684-1686.

[8] K. H. Schoenbach, G. Schaefer, M. Kristiansen, H. Krompholz, H. C. Harjes, and D. Skaggs, "An Electron-Beam Controlled Diffuse Discharge Switch," *J. Appl. Phys.*, Vol. 57, 1985, pp. 1618-1622.

[9] G. Schaefer and K. H. Shoenbach, "External Control of Diffuse Discharge Switches," *Proc. 5th IEEE Pulsed Power Conf.*, Arlington, VA 1985, pp. 644-647.

[10] M. Kristiansen, "Fundamentals of Inductive Energy Storage," *Proc. ARO Workshop on Repetitive Opening Switches*, edited by M. Kristiansen and K. H. Schoenbach, Tamarron, CO 1981.(DTIC NO. AD-A11070)

[11] K. Nakanishi, L. G. Christophorou, J. G. Carter, and S. R. Hunter, "Penning Ionization Ternary Gas Mixtures for Diffuse Discharge Switching Applications," *J. Appl. Phys.*, Vol. 58, 1985, pp. 633-641.

[12] S. R. Hunter, J. G. Carter, L. G. Christophorou, and V. K. Lakdawala, "Transport Properties and Dielectric Strengths of Gas Mixtures for use in Diffuse Discharge Opening Switches", Gaseous Dielectrics IV, edited by L. G. Christoophorou and M. O. Pace, Pergamon Press, 1984, pp. 224-237.

To be presented at the 6th Pulsed Power Conf., Arlington VA, June '86

# METHANE-ATTACHER MIXTURES IN AN ELECTRON BEAM CONTROLLED DIFFUSE DISCHARGE OPENING SWITCH

G. Schaefer*, R. A. Korzekwa**, and M. Kristiansen**

* Weber Research Institute, Polytechnic University
Farmingdale, NY 11735-3996
** Dept. of Electrical Engineering, Texas Tech Univ.
Lubbock, TX 79409-4439

For a diffuse discharge opening switch a gas mixture containing an attaching gas has to be used in order to reduce the electron number density rapidly when the switch opens at an increasing value of E/N. During the low E/N conduction state the attachment rate should be low. Gas mixtures containing argon or methane ($CH_4$) and the attachers Freon 116 ($C_2F_6$) and Freon 14 ($CF_4$) have been suggested [1]. Previous experiments show that gas mixtures of argon with the above mentioned attachers have the inherent problem of a low dc E/N breakdown limit and an even lower glow-to-arc transition E/N limit [2]. Methane based mixtures were investigated in an attempt to eliminate these problems.

The steady state current density, J, versus reduced electric field strength, E/N, characteristics for combinations of gas mixtures containing methane and <u>one</u> attaching gas are shown in Fig. 1 and Fig. 2. Figure 1 shows the curve for 100% methane which has a high current density maximum but at a rather high value of E/N which significantly increases the power losses. The other curve shown in Fig. 1 is for 98% methane + 2% Freon 116. The addition of Freon 116 greatly decreases the maximum current density, but the maximum is also shifted to a lower value of E/N which helps to reduce power losses in the switch.

In Fig. 2, the J-E/N characteristics of mixtures of methane and Freon 14 are compared. Again the addition of Freon 14 greatly reduces the current density maximum. In the low E/N range both 50% methane + 50% Freon 14 and 100% Freon 14 are essentially the same. Again the current density maximum is shifted to a lower E/N region through the addition of the attacher.

Gas mixtures using two attachers allow the J-E/N characteristics to be shaped over a wide E/N range. Figure 3 shows the J-E/N characteristics for mixtures of equal fractions of methane and Freon 14 with varying Freon 116 fractions. The best mixture for opening switch operation is the mixture with 2% Freon 116 since the current density maximum is the highest and at the lowest value of E/N.

In conclusion we find that the J-E/N characteristics of methane based mixtures containing attachers can be shaped to fulfill the requirements for a good switch gas. The methane based mixtures also have a much greater dc E/N breakdown limit than argon based mixtures which increases the voltage operation range.

This work was jointly supported by AFOSR/ARO.

[1] S. R. Hunter, J. G. Carter, I. G. Christophorou, and V. K. Lakdawala, "Transport Properties and Dielectric Strengths of Gas Mixtures for use in Discharge Opening Switches," Proc. 4th Int. Symp. on Gaseous Dielectrics, Knoxville, TN, 1984, pp. 224-237.

[2] G. Schaefer, K. H. Schoenbach, M. Kristiansen, B. E. Strickland, R. A. Korzekwa, and G. Z. Hutcheson, "Influence of the Circuit Impedance on an Electron Beam Controlled Diffuse Discharge with a Negative Differential Conductivity," Appl. Phys. Lett., Vol. 48, No. 26, 1986, pp. 1776-1778.

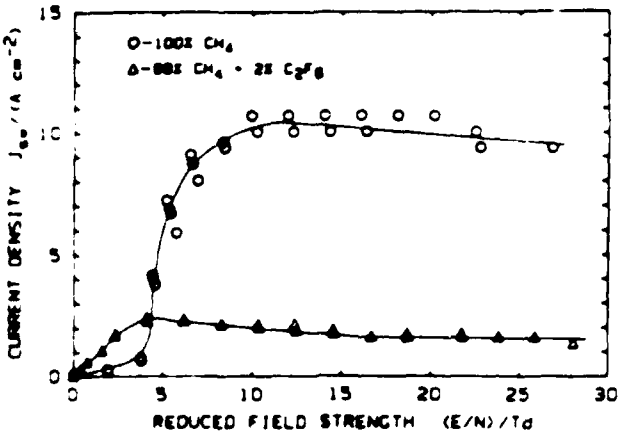


Fig 1 Current density, J, versus reduced electric field strength, E/N, for an e-beam sustained discharge in $CH_4$ with admixtures of $C_2F_6$.

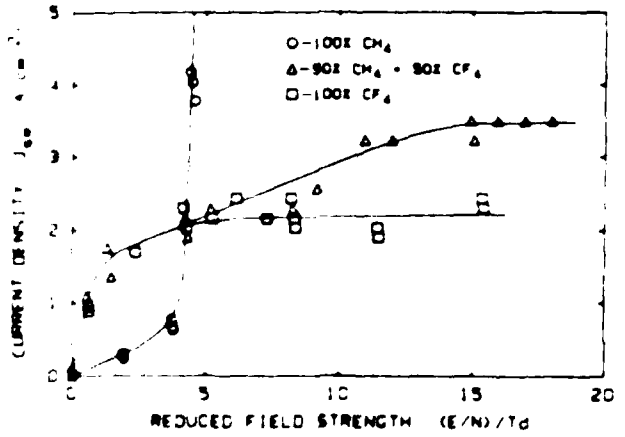


Fig 2 Current density, J, versus reduced electric field strength, E/N, for an e-beam sustained discharge in $CH_4$-$CF_4$ mixtures.

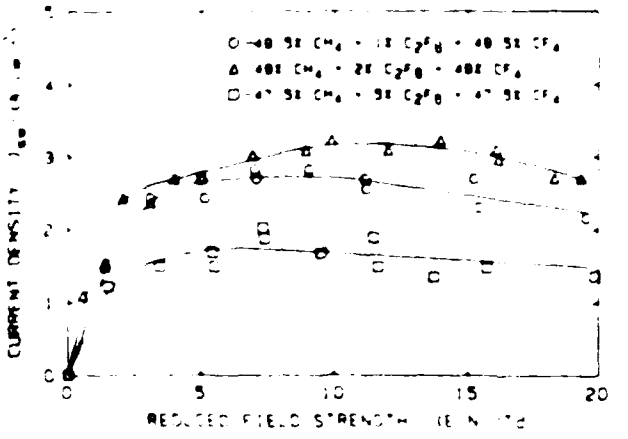


Fig 3 Current density, J, versus reduced electric field strength, E/N, for an e-beam sustained discharge in mixtures with equal percentages of $CH_4$ and $CF_4$, and $C_2F_6$.

# THE INFLUENCE OF $N_2$ ON ARGON BASED GAS MIXTURES FOR AN ELECTRON BEAM CONTROLLED DIFFUSE DISCHARGE

R. A. Korzekwa*, G. Schaefer**, M. Kristiansen* and K. H. Schoenbach***

* Department of Electrical Engineering, Texas Tech University, Lubbock, TX 79409-4439

** Weber Research Institute, Polytechnic University, Farmingdale, NY 11735-3995

*** Department of Electrical Engineering, Old Dominion University, Norfolk, VA 23508

## Introduction

The key technological problem in developing inductive energy discharge systems is the development of opening switches [1]. Promising candidates are electron beam sustained diffuse discharges [2]. The switch opens when the electron beam is turned off. In order to achieve short opening times, the dominant loss process must be attachment. Both low forward voltage drop and fast opening can only be obtained by choosing gases or gas mixtures which satisfy the following conditions:

(1) For low values of the reduced field strength, E/N (conduction phase), the gas mixture should have a high drift velocity, $v_d$, and low attachment rate coefficients, $k_a$.

(2) For high E/N values (opening phase) the gas mixture should have a low drift velocity and high attachment rate coefficients.

Such gas properties cause a discharge characteristic (current density J versus reduced electric field strength E/N) with a strong negative differential conductivity (NDC).

Argon based gas mixtures containing attachers such as $C_2F_6$ and $CF_4$ have been suggested as switch gases which fulfill the above mentioned requirements [3-5]. An inductive energy storage system has a high characteristic impedance and requires a J-E/N characteristic with a small (NDC) region in order to avoid the obstruction of the closing process in a repetitive opening switch [5]. Such a J-E/N characteristic would have a high current density at a low E/N and a slowly decreasing current density with increasing E/N thereafter. Gas mixtures of argon and two attaching gases with attachment cross sections at different electron energies have been used to produce such J-E/N characteristics.

It has also been shown that the addition of a small percentage of $N_2$ to argon increases the drift velocity at low values of E/N [6]. This effect is based on the fact that at low E/N, vibrational excitation of $N_2$ keeps the electron energy distribution within the Ramsauer minimum of the elastic scattering cross section of argon. It was therefore suggested to use mixtures of argon with both admixtures of attachers and $N_2$ to improve the performance of the switch [7]. The following results demonstrate the influence of these admixtures on the discharge characteristics.

## Results

The first set of experiments utilized $C_2F_6$ as the attacher. A gas mixture of Ar + 2% $C_2F_6$, as seen in Fig. 1, generates a J-E/N characteristic that fulfills the requirements for an opening switch. The NDC region is

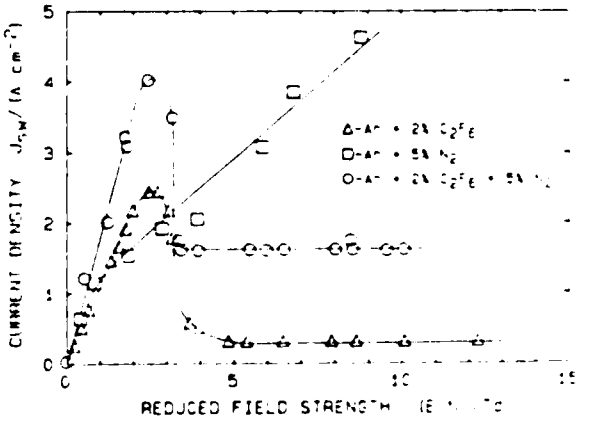


Fig. 1 Current density, J, versus reduced electric field strength, E/N, for an electron beam sustained discharge in mixtures of Ar, $C_2F_6$, and $N_2$.

produced by the onset of attachment at approximately 2-3 Td. Figure 1 also shows the J-E/N characteristic for Ar + 5% $N_2$ which confirms that the NDC in the Ar + 2% $C_2F_6$

mixture is indeed due to the onset of attachment. The decrease of the slope of this curve above 1 Td indicates that the electron mobility has a higher value below 1 Td. Next, experiments were performed with a gas mixture of Ar + 2% $C_2F_6$ + 5% $N_2$. The J-E/N characteristic has essentially the same shape as the characteristic of Ar + 2% $C_2F_6$: however, the current density, J, is significantly higher for all values of E/N. These results demonstrate that both properties, attachment rate coefficient and drift velocity, can be optimized through different gas additives.

Argon based mixtures with two attachers, which are useful in a high impedance inductive energy storage system, and the influence of $N_2$ in these mixtures were also investigated. The discharge characteristic for a mixture containing Ar + 2% $C_2F_6$ + 20% $CF_4$ with and without 5% $N_2$ are shown in Fig. 2.

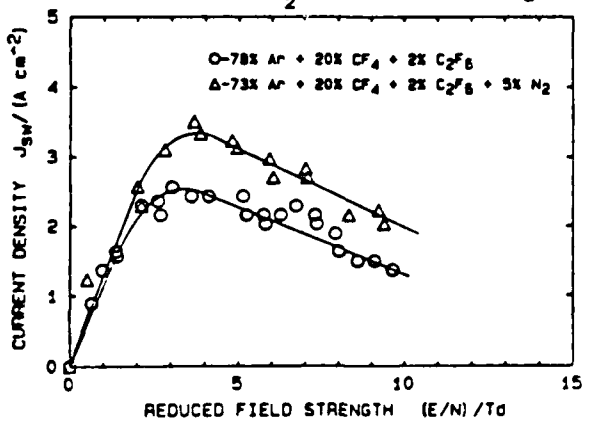


Fig. 2 Current density, J, versus reduced electric field strength, E/N, for an electron beam sustained discharge in mixtures of Ar, $CF_4$, $C_2F_6$, and $N_2$.

Again we see that the shape of the curve is essentially unchanged but the current density increases when $N_2$ is added. The relative current density increase however, is smaller than in the case of the mixture of Ar + 2% $C_2F_6$, as shown in Fig. 1. The discharge characteristic for a mixture containing argon and $CF_4$ at equal concentrations, 2% $C_2F_6$, and 0% or 5% $N_2$ was also investigated, as shown in Fig. 3. The discharge characteristics show that the addition of $N_2$ increases the current density only in the E/N range below 1 Td. The maximum current density remains nearly the same.

The effect of $N_2$ decreases with decreasing argon concentration in the buffer gas. This result indicates that the influence of $N_2$ is in fact due to the increase of

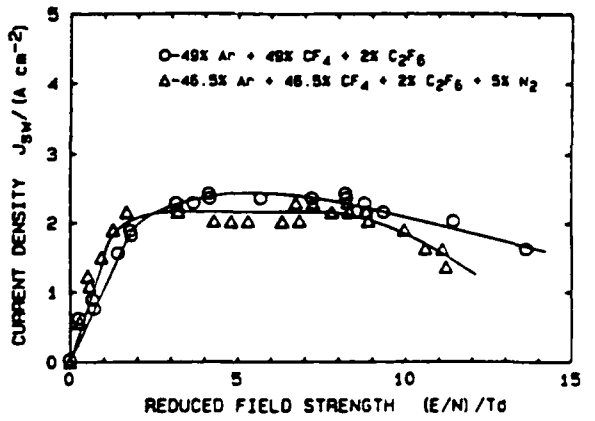


Fig. 3 Current density, J, versus reduced electric field strength, E/N, for an electron beam sustained discharge in mixtures of the same fraction of Ar and $CF_4$, with $C_2F_6$ and $N_2$.

the drift velocity as known in mixtures of just argon and $N_2$.

## Conclusions

Gas mixtures containing argon as a buffer gas and an attacher, such as $C_2F_6$ and/or $CF_4$, are useful in diffuse discharge opening switches. An addition of a small percentage of $N_2$ increases the current density in mixtures with high percentages of argon. This effect is considered to be the consequence of increased electron drift velocity. The increase in current density at the operating point of the switch, high J at low E/N, reduces power losses in the switch which is an important factor in a practical opening switch.

## Acknowledgement

This work was supported by NSF under contract ECS-8316122 and by AFOSR/ARO under contract 84-0032.

[1] K. H. Schoenbach, M. Kristiansen, and G. Schaefer, 1984, Proc IEEE, 72, 1019-1040.
[2] G. Schaefer, and K. H. Schoenbach, 1986, IEEE Trans. on Plasma Sci., PS-14, 561-574.
[3] G. Schaefer, K. H. Schoenbach, M. Kristiansen, B. E. Strickland, R. A. Korzekwa, and G. Z. Hutcheson, 1986, Appl. Phys. Lett., 48, 1776-1778.
[4] S. R. Hunter, J. G. Carter, L. G. Christophorou, and V. K. Lakdawala, 1984, Proc. 4th Int. Symp. on Gaseous Dielectrics, 224-237.
[5] G. Schaefer, K. H. Schoenbach, M. Kristiansen, R. A. Korzekwa, and G. Z. Hutcheson, 1986, Proc. of 17th Power Modulator Symp, 66-90.
[6] P. Burrow, 1986, Private communication.
[7] C. N. Haddad, 1983, Aust. J. Phys., 36, 297-303.

To be published in 1987
Gaseous Dielectrics V
L.G. Christophorou 9ed.)
Pergamon Press

Appendix K

# PENNING IONIZATION TERNARY GAS MIXTURES FOR DIFFUSE DISCHARGE OPENING SWITCHES

G. Schaefer*, K. H. Schoenbach**, R. A. Korzekwa***, and M. Kristiansen***

* Weber Research Institute, Polytechnic University,
Farmingdale, NY 11735-3995
**Department of Electrical Engineering,Old Dominion University,
Norfolk, VA 23508
*** Department of Electrical Engineering, Texas Tech University,
Lubbock, TX 79409-4439

## ABSTRACT

Electron beam controlled diffuse discharges are promising candidates for high power opening switches in inductive energy storage circuits. In order to achieve short opening times when the electron beam is turned off, the switch gas mixture must contain an attacher. Ternary gas mixtures using a Penning additive in a mixture consisting of a buffer gas and an electron attacher can increase the switch efficiency through optimization of the ionization efficiency of the electron beam. The Penning additive, however, also decreases the breakdown voltage of the gas mixture. This paper presents experiments demonstrating these effects.

## KEYWORDS

Opening switch; high pressure diffuse discharge, electron beam control, gas properties; Penning ionization.

## INTRODUCTION

Electron beam controlled diffuse discharges are promising candidates for high power opening switches. In order to achieve short opening times when the electron beam is turned off, the gas mixture must contain an attacher. Both low forward voltage drop and fast opening can be obtained by choosing gas mixtures with a low attachment rate coefficient and a high electron drift velocity at low E/N, and a high attachment rate coefficient and a low drift velocity at high E/N. The optimization of gas mixtures with respect to these properties has been described in many previous papers. A review is given by Schaefer and Schoenbach, 1986. A further improvement of the switch efficiency by using Penning additives was first propsed by Nakanishi and others in 1965. The ionization efficiency of an electron beam is determined by the W-value of the switch gas. W is the average energy required to produce one electron-ion pair. During the energy deposition of the electron beam in the gas, approximately half of the energy absorbed is converted into excitation. The W-value is, therefore, usually in the order of twice the ionization energy of the gas. The excitation energy has to be considered a loss

for devices which utilize only free electrons for conduction Penning ionization can be used to recover part of this energy by introducing a small amount of gas with a low ionization energy, which is lower than the energy of the dominant excited states present in the discharge

Recent papers (Nakanishi and others, 1965, Reinking and others, 1986) demonstrates that a decrease in the W-value of the gas occurs in mixtures of argon and an electron attacher such as freon 14 ($CF_4$) and freon 116 ($C_2F_6$), with acetylene ($C_2H_2$) as the Penning additive Gas mixtures of just argon and freon 116 have already proven to be suitable switch gases for specific modes of operation (Schaefer and others,1986). We therefore performed experiments with Penning ionization ternary gas mixtures using the electron beam sustained diffuse discharge experiment described previously (Schoenbach and others, 1985) These experiments provide information as to whether the behavior of the gas discharge is influenced by the additive of acetylene only through the change of the W-value or also by other properties of the additive

## DISCHARGE CHARACTERISTICS

A first insight into the specific properties of a gas mixture used in a diffuse discharge switch is given by investigating the steady state discharge characteristic. All experiments were performed with a mixture of 98% argon and 2% freon 116 and acetylene as the Penning admixture with varying concentrations Figure 1 shows as an example two J-E/N curves, one without acetylene and one with 5% acetylene The general shape of the curve without acetylene is mainly a result

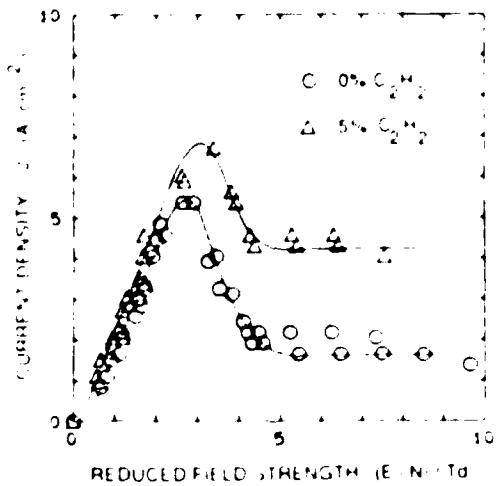


Fig 1 Current density, J, versus reduced electric field strength, E/N, for an e-beam sustained discharge in 98% argon, 2% freon 116, and a varying admixture of acetylene. The variable parameter is the acetylene fraction.

of the attachment properties of this gas mixture. The attachment coefficient has a threshold at approximately 2 5 Td and increases with E/N (Hunter and others, 1984). Below 2.0 Td the discharge is recombination dominated and J increases with E/N. The onset of attachment generates a negative differential conductivity above

2 5 Td and the discharge becomes attachment dominated. The addition of acetylene clearly increases the current density, and this effect seems to be larger in the attachment dominated regime

## DISCHARGE ANALYSIS

To evaluate the influence of the Penning additive on the discharge characteristics, we have to evaluate the conduction properties of the discharge. The current density of the electron beam sustained discharge, J, depends on the electron number density, $n_e$, and the mobility, $\mu_e$, according to

$$J = en_e\mu_e E \ . \tag{1}$$

where both $n_e$ and $\mu_e$ are functions of E/N, and -e is the charge of an electron. The rate equation for the electron number density, $n_e$, is

$$dn_e/dt = S + k_i n_e N - k_r n_e n_+ - k_a n_e N_a \ . \tag{2}$$

where S is the electron beam source function, $k_i$ is the ionization rate coefficient, $k_r$ is the recombination rate coefficient, $k_a$ is the attachment rate coefficient, $n_+$ is the positive ion density, N is the total number density, and $N_a$ is the attacher number density. For externally sustained discharges, ionization through the discharge electrons can be neglected ($k_i$=0). The source function, S, for the electron beam is given by

$$S = J_{eb}\langle d\varepsilon/dx\rangle/eW \ . \tag{3}$$

where $J_{eb}$ is the electron beam current density, $\langle d\varepsilon/dx\rangle$ is the average electron beam energy absorbed per unit length, and W is the average energy needed to create one electron-ion pair in the gas.

It is convenient to analyze those regions of the steady state discharge characteristic separately in which only one electron depletion mechanism dominates, recombination or attachment. In the closed phase (low E/N) of the switch the discharge is recombination dominated ($k_a$= 0 and $n_+ = n_e$) so that Eq. (2) becomes

$$S - k_r(n_e)^2 = 0 \quad \text{or} \quad n_e = (S/k_r)^{1/2} \ . \tag{4}$$

The current density then becomes

$$J = \mu_e e(S/k_r)^{1/2} E \ . \tag{5}$$

In the open phase, the discharge is attachment dominated, and Eq. (2) becomes

$$S - k_a n_e N_a = 0 \quad \text{or} \quad n_e = S/(k_a N_a) \ . \tag{6}$$

The current density then becomes

$$J = e\mu_e S/k_a N_a \ E \ . \tag{7}$$

## THE INFLUENCE OF THE W-VALUE

The two regions of the J-E/N characteristics, the recombination dominated and the attachment dominated region, can also be used to evaluate the influence of a Penning additive. The method chosen here is to assume that the W-value changes

with the percent of the Penning admixture and that the other properties such as mobility, recombination coefficient, and attachment coefficient remain unchanged, at least in a certain range of E/N, as long as the fraction of the Penning additive is low. With this assumption we can find an expression for the W-value for a given gas mixture. Comparison with the correct values measured previously (Nakanishi and others, 1985; Reinking and others, 1986) will then show whether other properties of the discharge are changed at the same time. In the recombination dominated region we use Eq.s (3) and (5) to gain an expression for the switch current with the W-value as the variable parameter.

$$J = ((e\langle d\alpha/dx\rangle J_{eb})/k_r)^{1/2}\mu_e N(W)^{-1/2}(E/N) \quad . \tag{8}$$

Since the discharge characteristic is linear from 0.5 to 2.0 Td, we can use the slope of J(E/N) to determine the variation in the W-value of the gas mixtures.

$$dJ/d(E/N) \; \alpha \; (W)^{-1/2} \quad . \tag{9}$$

This relationship holds if the E/N dependence of $\mu_e$ and $k_r$ are assumed negligible in this region of E/N. The W-value for argon + 2% freon 116 is known to be 27 eV (Nakanishi and others, 1985), and the ratio of the W-value for n% and 0% acetylene can be obtained from Eq. (9)

$$W_n = W_o \; [(dJ/d(E/N))_o^{\,2}/(dJ/d(E/N))_n^{\,2}] \quad . \tag{10}$$

In the attachment dominated region we can use Eq.s (3) and (7) to get again an expression for the switch current with the W-value as a variable parameter.

$$J = [J_{eb}\langle d\alpha/dx\rangle \mu_e N/k_a N_a](W)^{-1}(E/N) \quad . \tag{11}$$

where $k_a$ and $\mu_e$ are both functions of E/N. Choosing a suitable constant value for E/N we again get an equation for the ratio of the W-values for n% and 0% acetylene

$$W_n = W_o(J_n/J_o) \quad . \tag{12}$$

where $W_o$ is again the known W-value for Ar + 2% freon 116 + 0% acetylene.

Figure 2 shows the evaluation of Eq. (10) in the recombination dominated regime. Although the values for W for low acetylene concentrations seem to show a trend similar to the directly measured values by Nakanishi and others in 1985, there is a clear discrepancy which becomes especially severe for higher acetylene concentrations. The deviation is considered to be mainly the consequence of the influence of the admixture of acetylene on the drift velocity. Both, freon 116 and acetylene, as low concentration additives to argon, generate drift velocities with a maximum at low values of E/N. A maximum at, for example, 1.5 Td is achieved with approximately 2-5% freon 116 (Hunter and others, 1984) or approximately 5-10% acetylene (Cristophorou and others 1979). A further increase of the admixture concentration will again decrease the drift velocity. We therefore conclude that the admixture of acetylene to the mixture of 98% argon and 2% freon 116 increases the drift velocity up to a concentration of approximately 5% and then decreases it at a higher concentration. The important result for switching applications is that the current maximum at low values of E/N can be increased by up to 25% using a few percent of acetylene as an additive.

In the attachment dominated regime, there is an increase of the current density of at least a factor of 3 in the E/N range between 5 to 10 Td which is too large to be associated with a change of the W-value. Here the increase of the current density is dominated by the change of drift velocity.

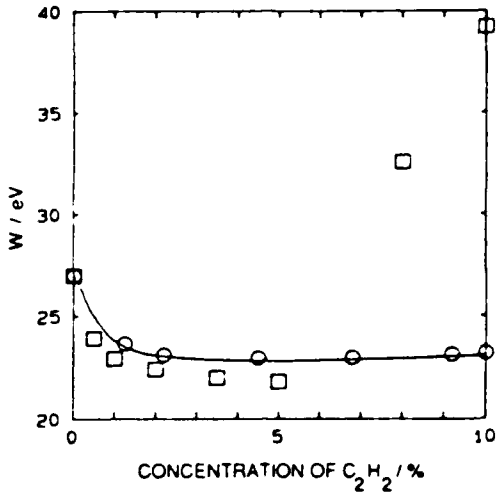


Fig. 2 W-values for a mixture of 98% argon, 2% freon 116, and an admixture of acetylene versus the concentration of acetylene (—, □ from Nakanishi and others, 1985; ○ evaluated from discharge characteristics using Eq. (10)).

## SELF BREAKDOWN LIMIT OF E/N

The voltage accross an opening switch in an inductive energy storage system increases significantly when the switch opens. The efficiency of such a circuit depends of the ratio of the maximum voltage drop after switch opening and the voltage drop during condution. The self breakdown value of E/N should, therefore, be as high as possible since the operating voltage always has to be kept well below self breakdown to avoid arcing.

We, therefore, performed measurements of the breakdown characteristic of the same ternary gas mixture using the same experimental setup. The E/N value at breakdown, depending on the fraction of the acetylene admixture in percent, is shown in Fig. 3. We can see that an admixture of only 0.5% acetylene significantly decreases the breakdown value of E/N from 42 Td to 24 Td. A further increase of the acetylene concentration will again increase the breakdown limit but not enough to compensate for the initial decrease.

## CONCLUSION

Penning ionization gas mixtures can be used to increase the ionization efficiency of electron beams and consequently to increase the current density of electron beam sustained discharges for opening switches during the conduction phase at low E/N. Experiments were performed in gas mixtures of 98% argon and 2% freon 116 with admixtures of the Penning additive acetylene. The current density maximum could be increased significantly. This effect is considered to be a combination of the reduction of the W-value and an increase of the drift velocity.

The admixture of the Penning additive also reduces the breakdown voltage of the diffuse discharge switch significantly. This decrease of the breakdown limit very possibly outweighs the advantage of the decreased W-value for applications in opening switches.

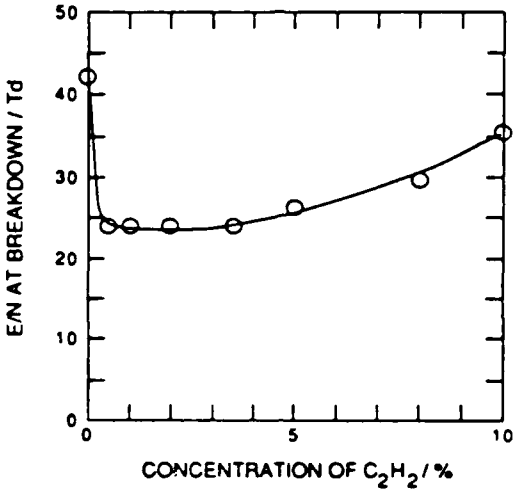


Fig. 3 E/N at breakdown for a mixture of 98% argon, 2% freon 116, and an admixture of actylene versus the concentration of acetylene.

ACKNOWLEDGEMENT

This work was supported by NSF under contract ECS-8318122 and by AFOSR/ARO under contract 84-0032. The authors wish to thank Dr.'s L. G. Christophorou and S. R. Hunter, and G. Reinking for many valuable discussions.

REFERENCES

Christophorou, L. G., D. L. McCorkle, D. V. Maxey, and J. G. Carter (1979). Nucl. Instrum. Methods, 163, 141-149.

Harjes, H. C., K. H. Schoenbach, G. Schaefer, M. Kristiansen, H. Krompholz, and D. Skaggs (1984). An electron beam tetrode for multiple, submicrosecond pulse operation. Rev. Sci. Instr., 55, 1684-1686.

Hunter, S. R., J. G. Carter, J. L. Christophorou, and V. K. Lakdawala (1984). Transport properties and dielectric strengths of gas mixtures for use in diffuse discharge opening switches. In L. G. Christophorou and M. O. Pace (Eds.), Gaseous Dielectrics IV. Pergamon, New York.

Nakanishi, K., L. G. Christophorou, J. G. Carter, and S. R. Hunter (1985). Penning ionization ternary gas mixtures for diffuse discharge switching applications. J. Appl. Phys., 58, 633-641.

Reinking, G. F., L. G. Christophorou, and S. R. Hunter (1986). Studies of total ionization in gases/mixtures of interest to pulsed power applications. J. Appl. Phys., 60, 499-508.

Schaefer, G., K. H. Schoenbach, M. Kirstiansen, B. E. Strickland, R. A. Korzekwa, and G. Z. Hutcheson (1986). The influence of the circuit impedance on an electron beam controlled diffuse discharge with a negative differential conductivity. Appl. Phys. Lett., 48, 1776-1778.

Schaefer, G., and K. H. Schoenbach (1986). A review of diffuse discharge opening swithces. IEEE Trans. Plasma Sci., PS-14, 561-574.

Schoenbach, K. H., G. Schaefer, M. Kristiansen, H. Krompholz, H. C. Harjes, and D. Skaggs (1985). An electron beam controlled discharge switch. J. Appl. Phys., 57, 1618-1622.

Appendix L

DRAFT

To be submitted to the J. Appl. Phys.

# OPTIMIZATION OF GAS MIXTURES FOR ELECTRON BEAM CONTROLLED DIFFUSE DISCHARGE OPENING SWITCHES

R. A. Korzekwa*, G. Schaefer**, and M. Kristiansen*

* Department of Electrical Engineering, Texas Tech University, Lubbock, TX 79409-4439

** Weber Research Institute, Polytechnic University, Farmingdale, NY 11735-3995

## ABSTRACT

The electrical characteristics of gas mixtures for an electron beam controlled diffuse discharge opening switch are presented. In an opening switch an attaching gas must be used to obtain a fast opening time in a diffuse discharge. Two different types of gas mixtures are considered in the process of optimizing the gas mixtures used in the switch. The first type of gas mixture utilizes one attaching gas, $C_2F_6$ or $CF_4$. The other type of mixtures, ternary gas mixtures, utilizing two attaching gases, both $C_2F_6$ and $CF_4$, and are used in the optimization process for repetitive switching in an inductive energy storage system. Recommendations are made for the gas mixtures to be used in single shot and repetitive opening switches for inductive energy storage.

# INTRODUCTION

Pulsed power systems utilizing inductive energy storage systems require the developement of repetitive opening switches in order to make this type of energy storage a realistic alternative to capacitive energy storage [1] An electron beam controlled diffuse discharge is a candidate for the opening switch The results presented here were obtained using different gas mixtures in an electron beam controlled opening switch

In order to optimize the gas mixture used in an electron beam controlled opening switch, several processes that take place in the discharge must be taken into consideration, such as ionization, excitation, recombination, attachment, and elastic collisions All these processes contribute to the charge carrier balance and the transport properties of the carriers, and therefore can be utilized in the optimization process For the repetitive operation of such a switch ,both the opening and closing phases have to be considered when optimizing the switch gas

In order to produce short opening times in an electron beam controlled discharge, an attaching gas must be used. Using previous research [2] to determine how the attachment rate coefficient, $k_a$, and the drift velocity, $v_d$, vary with the reduced electric field strength, E/N, for a variety of gases leads to a list of candidate gas mixtures to be tested in the switch. The optimum attachment rate coefficient, $k_a$,

for the gas would be low during the closing phase of the switch (at low E/N) and high during the opening phase (at high E/N), as demonstrated in Fig. 1. Also, the drift velocity, $v_d$, would conversely be high during the closing phase and low during the opening phase.

Using the processes mentioned above to optimize the discharge and also taking into account the external energy storage circuit, the optimum switch current density, $J_{sw}$, versus reduced electric field strength, E/N, characteristics can be obtained for the switch discharge. The gas mixtures that were investigated had one or two attachers.

## EXPERIMENTAL SETUP

The experimental setup consists of an electron beam pulser, a discharge chamber, a pulse forming network (PFN) used to drive the discharge, and various diagnostics used to monitor the system. As shown in Fig. 2, the electron beam chamber is below the discharge chamber. The electron beam must penetrate two foils in order to reach the gas in the discharge volume and produce the necessary ionization for the diffuse discharge which is used as the switching medium. The electron beam is generated by a high vacuum 100 $cm^2$ cold cathode (actually an unheated dispenser cathode) [3].

AD-A178 625 COORDINATED RESEARCH PROGRAM IN PULSED POWER PHYSICS (U) TEXAS TECH UNIV LUBBOCK DEPT OF ELECTRICAL ENGINEERING 16 FEB 87 ARO-21856.34-PH AFOSR-84-0032 2/2

UNCLASSIFIED F/G 10/2 NL

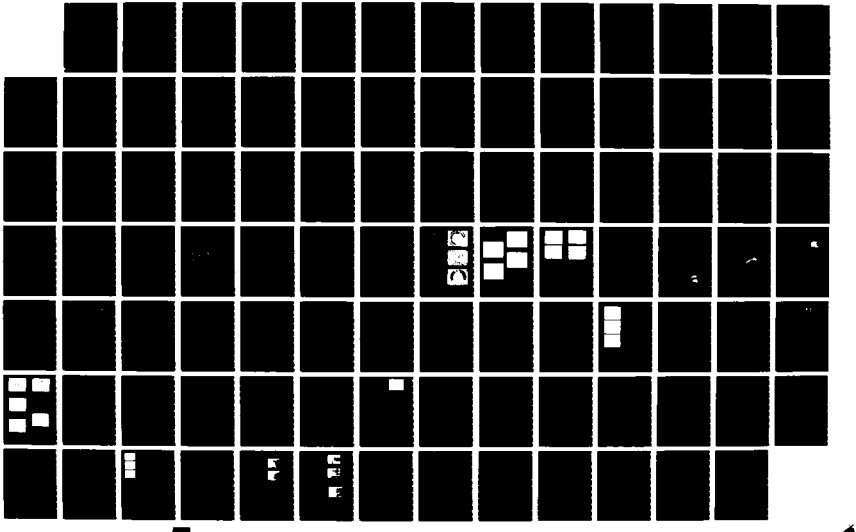

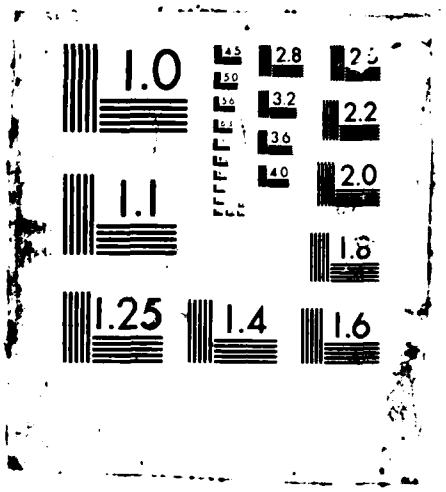
1.0
1.1
1.25
1.4
1.6
1.8
2.0
2.2
2.8
3.2
3.6
4.0
4.5
5.0
5.6

## INFLUENCE OF ATTACHERS ON THE DISCHARGE CHARACTERISTICS

In order to obtain fast switch opening times, an attaching (electronegative) gas should be added to the buffer gas in the switch [4]. A high attachment rate coefficient at the high E/N range implies that the electron attachment cross setion should be large at high electron energies (a few eV). The electron attachment coefficient is a function of the electron energy distribution, $f(\epsilon,E/N)$, expressed as :

$$k_a(E/N) = (2/m)^{1/2}\int_o^\infty f(\epsilon,E/N)\epsilon^{1/2}\sigma_a(\epsilon)d\epsilon \ , \qquad (1)$$

where $\sigma_a(\epsilon)$ is the attachment cross section as a function of electron energy and m is the electron mass [5]. Since $f(\epsilon,E/N)$ shifts to higher electron energies for an increasing E/N, the attachment rate increases with E/N (shaded area), as shown in Fig. 3. It has been suggested that $C_3F_8$, $C_2F_6$, $CF_3OCF_3$, and $CF_4$ are candidates for attachers to be used in the gas mixtures, since they have significant attachment cross sections at higher electron energies (> 1 eV) [2]. Of these attachers, only $C_2F_6$ and $CF_4$ were used, since only with these gases is attachment produced in the energy range of interest.

The $J_{sw}$-E/N characteristics of the electron beam sustained discharge is dependent on the electron number density, $n_e$, and the drift velocity, $v_d$, as seen by the expression

$$J_{sw} = -q(n_e v_d) \ . \qquad (2)$$

where both $n_e$ and $v_d$ are functions of E/N, and q is the charge on an electron. The electron number density rate equation is

$$\frac{dn_e}{dt} = S - k_r(n_e)^2 - k_a n_e N_a \ . \tag{3}$$

where S is the electron beam source function, $k_r$ is the recombination rate coefficient, $k_a$ is the attachment rate coefficient, and $N_a$ is the attacher number density. The steady state equation is

$$S_f - k_r(n_e)^2 - k_a n_e N_a = 0 \ . \tag{4}$$

During the closed phase (low E/N) of the switch the discharge should be recombination dominated so that Eq. (4) becomes

$$S = k_r(n_e)^2 \quad \text{or} \quad n_e = (S/k_r)^{1/2} \ . \tag{5}$$

From Eq's. (2) and (5) it is seen that $v_d$ should be large and $k_r$ should be small in this region of the discharge in order to achieve a high current density at a low E/N.

When the switch is in the open phase, the discharge should be attachment dominated, such that Eq. (4) becomes

$$S = k_a n_e N_a \quad \text{or} \quad n_e = S/(k_a N_a) \ . \tag{6}$$

Equations (2) and (6) imply that during the opening phase of the switch

$v_d$ should be low and $k_a$ should be large in order to obtain a fast opening time and high voltage hold-off in the gap.

During switch conduction a high gain is necessary to achieve a high efficiency. Unfortunately, as the source function increases (an increase in $n_e$) the recombination rate increases by $n_e^2$, thus reducing the current gain. Because of this, there is a trade off between the gain and the maximum achievable switch current density for a certain gas mixture.

## GAS MIXTURES WITH ONE ATTACHER

Gas mixtures containing Ar (or $CH_4$) and a small percentage of $C_2F_6$ satisfy the requirements for $v_d$ and $k_a$ versus E/N. Therefore, experiments were performed under steady state conditions of the electron beam sustained discharge to determine the $J_{sw}$-E/N characteristics for these gas mixtures.

### Experimental Results

The first experiments were performed using pure and binary gas mixtures in the switch and the steady state electrical characteristics of these mixtures were measured. Other important parameters that were measured are the glow-to-arc transition (if any), the dc breakdown limit, the source function, and the switch gain of the gases. The system used in these experiments had a low series impedance of 2 Ω.

The experimental $\rho$-E/N characteristics for mixtures of Ar and different percentages of $C_2F_6$ are displayed in Fig. 4. These results show that at the low E/N range the resistivity is low (low power losses) and at the high E/N range the resistivity is high (faster turn off times). These are exactly the types of characteristics needed for the opening and the closing phases discussed previously. Figure 4 also shows a region of strong negative differential conductivity (NDC) from 3-5 Td. This region is demonstrated more clearly in Fig. 5, showing a reduction in current density for an increase in the E/N. Figure 5 also shows a current maximum for each of the characteristic curves in the E/N range of 2-3 Td. From this it is seen that Ar + 2% $C_2F_6$ has the highest current maximum. Since this mixture has the lowest power losses during switch operation it is considered the optimum mixture among the Ar-$C_2F_6$ mixtures. The Ar + 0.5% $C_2F_6$ mixture has a lower current density maximum due to a decrease in the drift velocity in this mixture as compared to the drift velocity in the Ar + 2% $C_2F_6$ mixture at this E/N [2].

In order to determine whether the NDC region of the Ar-$C_2F_6$ mixtures is caused by the onset of attachment or the Ramsauer-Townsend minimum in the electron scattering cross section of Ar [6], an experiment was performed in Ar + 5% $N_2$ with the results shown in Fig. 6. Although Fig. 6 clearly shows the change of the differential discharge resistivity at $\approx$ 1 Td there is no NDC region in this mixture and, therefore, the conclusion is that the onset of attachment is the primary cause for the NDC region in the Ar-$C_2F_6$ mixtures.

It is known that the addition of a small percentage of nitrogen to argon increases the drift velocity significantly in the E/N range of interest [7], [8]. Therefore, the $J_{sw}$-E/N characteristics for the mixture 93% Ar + 2% $C_2F_6$ + 5% $N_2$ were also measured. Figure 6 shows a increase of the current density maximum due to the addition of nitrogen, but there is also an increase of the current density in the attachment dominated region of the discharge (high E/N) which is larger than the increase in the recombination dominated region (low E/N). Therefore the change in resistivity from the low E/N conduction state to the high E/N open state is not as large with the addition of $N_2$ to Ar + 2% $C_2F_6$.

Gas mixtures using $CH_4$ (methane) instead of Ar as the buffer gas were also used in the discharge. Figure 7 shows the results using these mixtures. Pure $CH_4$ has the highest current maximum obtained thus far, but unfortunately this maximum occurs at a high E/N and would, therefore, produce significant power losses. The $CH_4$ + 2% $C_2F_6$ mixture has a current maximum at a lower E/N but due to the attaching gas the maximum is much lower than for 100% $CH_4$. The $CH_4$ + 2% $C_2F_6$ characteristics also have a slight NDC from 5 Td and up, which can be an advantage when used in an inductive energy storage system.

Figure 8 shows the $J_{sw}$-E/N characteristics of mixtures containing $CH_4$ and $CF_4$. The first part of the 100% $CH_4$ characteristics are again plotted for a comparision with mixtures containing $CF_4$. The 50% $CH_4$ + 50% $CF_4$ mixture does not reach a current maximum until at least 15 Td. The operating point, however, would be at approximately 3-4 Td, the first change in the slope, where the power losses are low. Also shown in Fig. 8 are the $J_{sw}$-E/N characteristics for 100% $CF_4$. The operating

point is idential with 50% $CH_4$ + 50% $CF_4$, and since 100% $CF_4$ has a higher resistivity at high E/N range it would be the better gas of the two to use in an opening switch

The glow-to-arc transition E/N limits and the dc E/N breakdown limits were measured for all gases. The Ar-$C_2F_6$ mixtures have an upper E/N limit at which a glow-to-arc transition instability occurs. This E/N limit increases for an increasing concentration of $C_2F_6$ in Ar. No such instability was observed in the $CH_4$-based mixtures. The $CH_4$ based mixtures have a much higher dc E/N breakdown limit than the Ar based mixtures. The Ar-based mixtures have, by far, the lowest limit, due to the small amount of attaching gas in the mixtures. For all of the mixtures, an increase in the amount of attaching gas always increases the breakdown limit.

## EFFECTS OF THE CIRCUIT ON THE DISCHARGE CHARACTERISTICS

When treated as a transmission line, an inductive energy storage system would have a high characteristic impedance [4]. Therefore, the ideal $J_{sw}$-E/N characteristics of a switch needed in such a system can be constructed, using the appropriate criteria. It will be shown that the proposed $J_{sw}$-E/N characteristic is important, especially for repetitive operation in a burst (several pulses, $\approx$ 100 ns long each, after one charging process), where both the opening and closing processes of the switch must be taken into consideration.

Since a high impedance system is of interest, it is helpful to look at a plot of the $J_{sw}$-E/N characteristics with high and low impedance loadlines, as in Fig. 9. These loadlines are derived from the current and voltage of the switch gap, and in this particular switch, the E/N (in Td) is approximately the same as the voltage (in kV) across the switch. A low impedance system is used to measure the full characteristics of the gas mixture in the system, while the high impedance loadline is a more practical representation of the system. Referring to Fig. 9, the mixture of Ar + 2% $C_2F_6$, the high impedance system would produce an obstruction of the closing process since the current maximum could never be reached at the low E/N state. Also it is expected that, since there is a high attachement rate at high E/N, at the beginning of the closing process it would take longer to reach the steady state maximum in this high impedance system. From this we conclude that, as seen in Fig. 10, the ideal $J_{sw}$-E/N characteristics would have a high current maximum at a low E/N and a gradually decreasing current density as the E/N increases until breakdown occurs at a value of E/N as high as possible. This would help eliminate the obstruction processes due to both a large NDC (negative differential conductivity) and high attachment at high E/N.

The experimental results for $CH_4$ + 2% $C_2F_6$, Fig. 7, showed a $J_{sw}$-E/N characteristic very much like the ideal characteristic just described. Since the addition of $N_2$ increases $v_d$, it would also be advantageous to find a gas mixture containing Ar as a buffer that has similar results but with a maximum at lower values of E/N. One method of accomplishing this is to use Ar with admixtures of two attaching

gases with significant attachment cross sections that have different threshold electron energies. Referring to Fig. 2, it is seen that $C_2F_6$ has a strong onset of attachment at approximately 5 Td. By adding an attaching gas with an attachment cross section at higher electron energies than $C_2F_6$ and also a drift velocity maximum at higher E/N than $C_2F_6$, a discharge characteristic as shown in Fig. 3 should result. Since $C_2F_6$ has an onset of attachment at approximately 3 eV [5], $CF_4$ was chosen as the second attacher with an onset of attachment at approximately 6 eV [5]. Also since $CF_4$ has a smaller cross section than $C_2F_6$, a larger percentage of $CF_4$ is added to the gas mixture. The gas mixtures proposed for this are mixtures of Ar + 2% $C_2F_6$ + varying percentages of $CF_4$. Also mixtures of $CH_4$ + $C_2F_6$ + $CF_4$ were investigated to determine the effects of two attachers in $CH_4$, since $CH_4$ based mixtures have higher dc E/N breakdown limits than argon.

## GAS MIXTURES WITH TWO ATTACHERS

In order to investigate the expected effects of the inductive energy storage circuit on the discharge characteristics of the gas mixtures, high impedance systems were simulated using different series resistances and the resulting characteristics were measured. After these processes were verified, the steady state characteristics of new gas mixtures were measured. These new gas mixtures were chosen to try to alleviate the problem of an inherent high characteristic impedance in

an inductive storage system. Also the different E/N limits for the breakdown of the gas mixtures were measured.

The first task was to measure the characteristics of an Ar-$C_2F_6$ mixture in a high impedance circuit. In Fig. 11, the $J_{sw}$-E/N characteristics for Ar + 2% $C_2F_6$ were measured using a 23 Ω series resistor. The effective loadline for this system is plotted and results show that the current maximum is unattainable in this system, as expected.

## Experimental Results

The first gas mixtures to be investigated were mixtures of Ar + 2% $C_2F_6$ + varying percentages of $CF_4$. In Fig. 12, the characteristics of these gas mixtures are shown, which confirm that an addition of $CF_4$ can produce the necessary characteristic for a high impedance system. Of the two gas mixtures, the optimal mixture contains 49% $CF_4$ for a high impedance system, since the gas with 20% $CF_4$ still has a negative differential conductivety which is too strong. The mixture with 49% $CF_4$ has a more gradual negative differential conductivity, which fulfills the requirement for high impedance systems. However, in an attempt to increase the breakdown limit of the gas mixture, $CH_4$-based mixtures were also investigated.

The J-E/N characteristics for mixtures containing $CH_4$ + $C_2F_6$ + $CF_4$ are shown in Fig. 13. As seen in these curves, all of the mixtures produced the desired high impedance characteristic curve shape. For a high impedance system the optimal gas mixture, of the three mixtures, is 49.5% $CH_4$ + 2% $C_2F_6$ + 49.5% $CF_4$, since it has a higher current maximum

at the low E/N operating point during the conduction phase of the switch.

The Ar based ternary gas mixtures also exhibited an E/N limit for the occurrence of a glow-to-arc transition, just as in the binary Ar mixtures. It is seen that the $CH_4$-based mixtures have the highest dc breakdown limits, the mixture with 5% $C_2F_6$ having the largest value. Again, as in the single attacher mixtures, the Ar based mixtures have the lowest breakdown limits. Even so, the high concentration of $CF_4$ in the Ar mixtures has dramatically increased the breakdown limit compared to the low percentage $C_2F_6$-Ar mixtures.

## CONCLUSIONS AND RECOMMENDATIONS

With the experimental results presented previously, a discussion of the advantages and disadvantages of the mixtures along with recommendations for certain systems will be given. The two different types of switching considered are outlined below:

1) A repetitive switch for inductive energy storage is considered, which must take into account the characteristic high impedance of this system during a burst of pulses.
2) An opening switch is also considered, where a high holdoff voltage, low power dissipation and a large NDC are most important.

The important parameters for these gas mixtures are tabulated and presented in Table 1. In Table 1, the subscript, OP, indicates the

parameters at the operating point of the discharge. In column 4, $E/N_{NDC}$ represents the E/N range in which the NDC occurs. In column 8, $RHO_{15\ Td}$ is the resistivity at 15 Td. Referring to the values in the last two columns, $E/N_{BR}$ is the dc breakdown limit and $E/N_{GtoA}$ is the glow-to-arc transition limit.

A discussion of the types of breakdown is appropriate at this point. In general an opening switch used in an inductive energy storage system should have a very high breakdown limit. As seen in Table 1, two different breakdown limits are listed, the dc E/N breakdown limit and a glow-to-arc transition breakdown which is found in argon-$C_2F_6$ mixtures only and occurs only during the operation of the switch as opposed to dc breakdown which occurs independently from switch operation. Some general observations made from Table 1 are discussed below. The $CH_4$-based mixtures have a higher dc breakdown limit than argon-based mixtures and no glow-to-arc transition limit. Because of this and the fact that the glow-to-arc transition limits of the argon-based mixtures are very low, the argon-based mixtures are less promising than the $CH_4$-based mixtures. Also, the addition of the attachers $C_2F_6$ and $CF_4$ increases the dc breakdown limit.

The resistivity at different E/Ns is also an important factor when discussing switch operation, therefore a few observations will be made at critical points. As shown in Table 1, comparing the values of $\rho$ at 15 Td with the values of $\rho$ at the operating point and at low E/N (minimum $\rho$), it is seen that in all cases $\rho$ incrreases when the E/N is increased. This result is due to either the onset of attachment or the reduction of the drift velocity or a combination of both effects, as the

E/N increases. This is an important effect, since an opening switch requires a high $\rho$ at a high E/N.

## A Repetitive Switch for Inductive Energy Storage

When considering an electron beam controlled diffuse discharge for use as a fast (100 ns pulses) repetitive opening switch, certain criteria are used to choose the best gas mixture. The three most important criteria for this type of repetitive switching are a high current density at low E/N , a high E/N breakdown limit, and only a slight negative differential conductivity (slowly decreasing current density with increasing E/N) after the current density maximum. The optimization process will be divided into two parts, the optimum argon based and $CH_4$ based mixtures.

For the $CH_4$ based mixtures the optimum gas mixture is 49% $CH_4$ + 2% $C_2F_6$ + 49% $CF_4$, since, as seen in Table 1, it has the highest current density at a comparatively low E/N, an appropriate negative differential conductivity, the highest current gain, and, most importantly, the highest dc E/N breakdown limit. With the small negative differential conductivity, the closing process will not be obstructed when used in a high impedance inductive energy storage system.

For the ternary argon based mixtures, again referring to Table 1, the best mixture for a repetitive opening switch can be obtained. When considering the high impedance system, the 78% Ar + 2% $C_2F_6$ + 20% $CF_4$ mixture still has an NDC which is too large. Since 49% Ar + 2% $C_2F_6$ + 49% $CF_4$ has a more gradual NDC, it would better accomodate higher impedance systems. Also the 49% Ar + 2% $C_2F_6$ + 49% $CF_4$ mixture has a

higher dc E/N breakdown limit which is important in an opening switch. Unfortunately the argon based mixtures have a glow-to-arc transition E/N limit which is much lower than the dc breakdown E/N limit. Because of this the $CH_4$-based ternary mixtures appear to be much better for use in an opening switch.

## A Single Shot Opening Switch

When considering a single shot or repetitive opening switch, both a high current density at a low E/N and a large negative differential conductivity are important factors in the optimization process. Since, in a single shot opening switch, the system impedance during the initial charging of an inductive storage system is low (no transmission line effects), the operating point will always initially be reached in either high or low impedance systems. Of the ternary two attacher gas mixtures, 78% Ar + 2% $C_2F_6$ + 20% $CF_4$ has the largest negative differential conductivity and therefore the fastest opening time which is one of the most important factors in a single shot opening switch. However, the glow-to-arc transition limit in Ar based mixtures is very low, as seen in Table 1. Therefore it may be necessary to use a $CH_4$-based mixture for a higher breakdown limit at the expense of the faster opening time.

## SUMMARY

When considering a high impedance system the shape of the J-E/N characteristic curve it is important that the obstruction of the closing process, in a repetitive opening switch, is to be avoided. Using two attachers ($C_2F_6$ and $CF_4$) in argon and $CH_4$ based mixtures can produce the necessary J-E/N characteristic curve for such a system.

The $CH_4$-based mixtures are considered to be better than the argon-based mixtures since the E/N breakdown limit is much higher and there is no glow-to-arc transition which is inherent in the argon-based mixtures. Also, the choice of the mixture depends on the type of switching involved, where different criteria are of importance.

## ACKNOWLEDGEMENT

This work was jointly supported by Air Force Office of Scientific Research and Army Research Office under contract 84-0032.

# REFERENCES

[1] K. H. Schoenbach, M. Kristiansen, and G. Schaefer, "A Review of Opening Switch Technology for Inductive Energy Storage," Proc. IEEE, Vol. 72, No. 8, 1984, pp. 1019-1040.

[2] S. R. Hunter, J. G. Carter, L. G. Christophorou, and V. K. Lakdawala, "Transport Properties and Dielectric Strengths of Gas Mixtures for use in Discharge Opening Switches," Proc. 4th Int. Symp. of Gaseous Dielectrics, Knoxville, TN 1984, pp. 224-237.

[3] G. Schaefer and K. H. Schoenbach, "A Review of Diffuse Discharge Opening Switches," IEEE Trans. on Plasma Sci., Vol. PS-14, No. 5, 1986, pp. 561-574.

[4] G. Schaefer, K. H. Schoenbach, H. Krompholz, M. Kristiansen, and A. H. Guenther, "The Use of Attachers in Electron Beam Sustained Discharge Switches - Theoretical Considerations," Laser and Particle Beams, Vol. 2, No. 3, 1984, pp. 273-291.

[5] L. G. Christophorou, S. R. Hunter, J. G. Carter, S. M. Spyrou, and V. K. Lakdawala, "Basic Studies of Gases for Diffuse-Discharge Switching Applications," U.S.-F.R.G. Joint Seminar on Externally Controlled Diffuse Discharges, Texas Tech University, Lubbock, Tx, February 1983, pp. 104-133.

[6] Z. Lj. Petrovic', R. W. Crompton, and G. N. Haddad, "Model Calculations of Negative Differential Conductivity in Gases," Aust. J. Phys., Vol. 37, 1984, pp. 23-34.

[7] G. N. Haddad, "Drift Velocity of Electrons in Nitrogen-Argon Mixtures," Aust. J. Phys., Vol. 36, 1983, pp. 297-303.

[8] P. Burrow, Private communication, 1986.

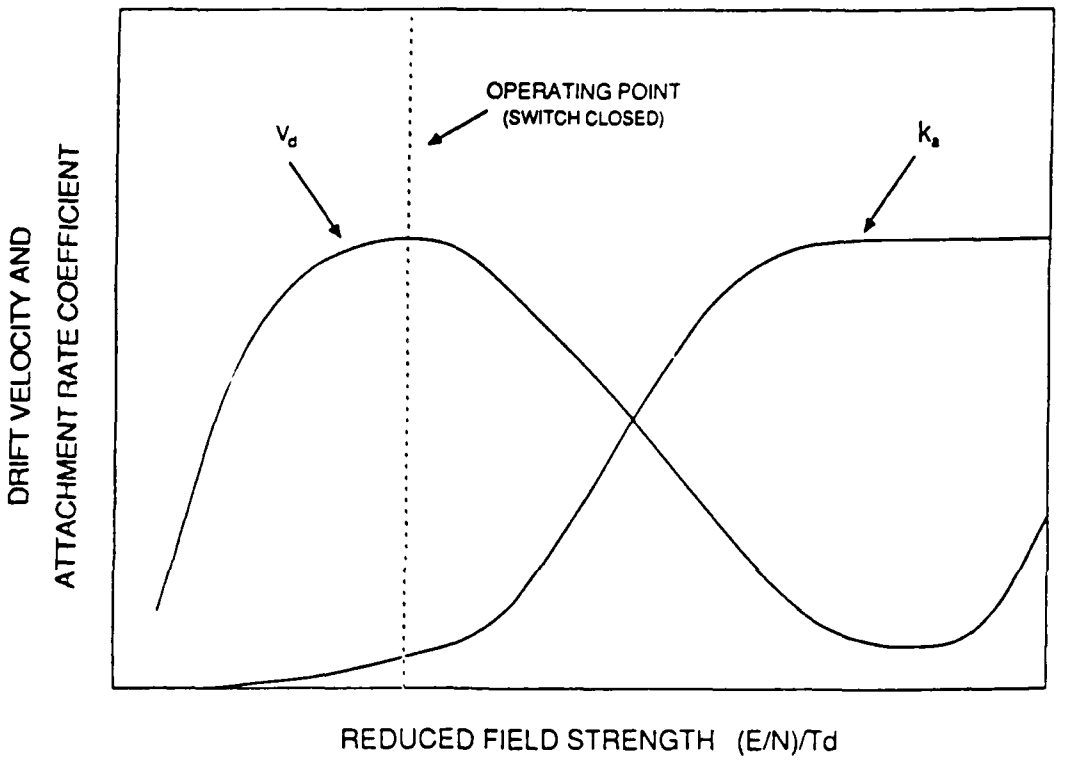


Fig. 1 The optimum realistic characteristics of the attachment rate coefficient, $k_a$, and the drift velocity, $v_d$, versus the reduced field strength, E/N.

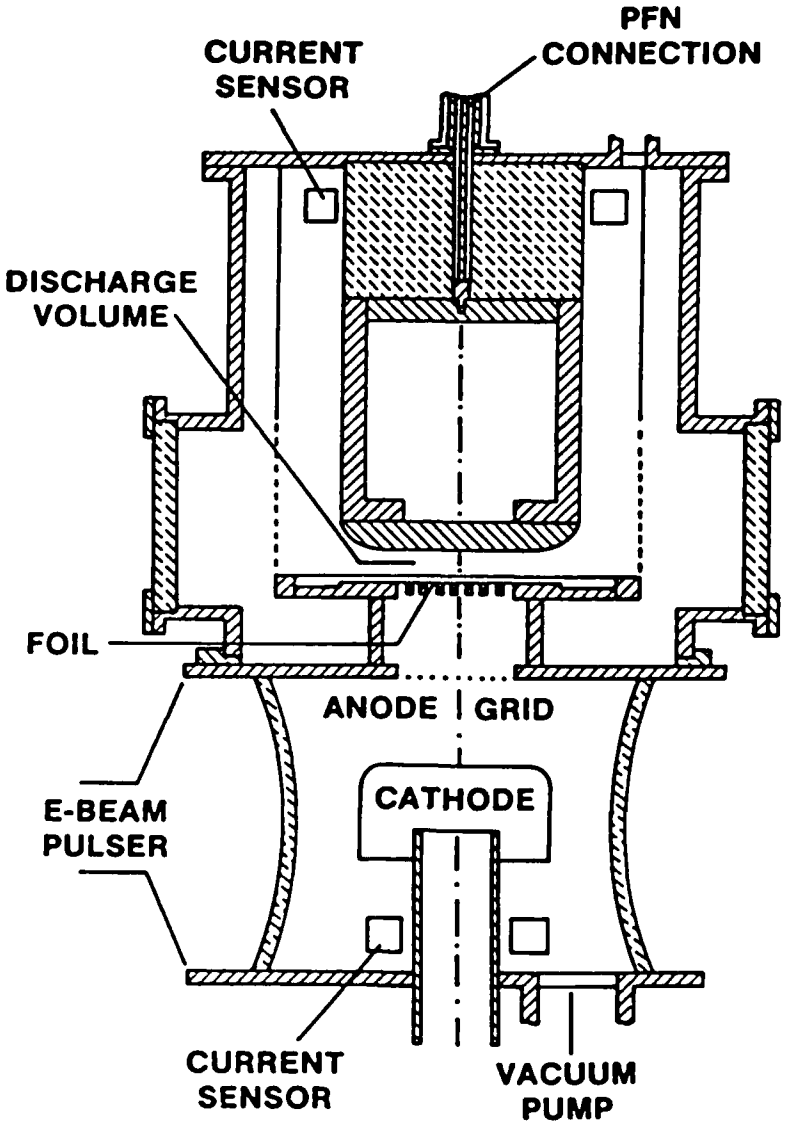


Fig. 2 A cross sectional view of the electron beam sustained diffuse discharge apparatus.

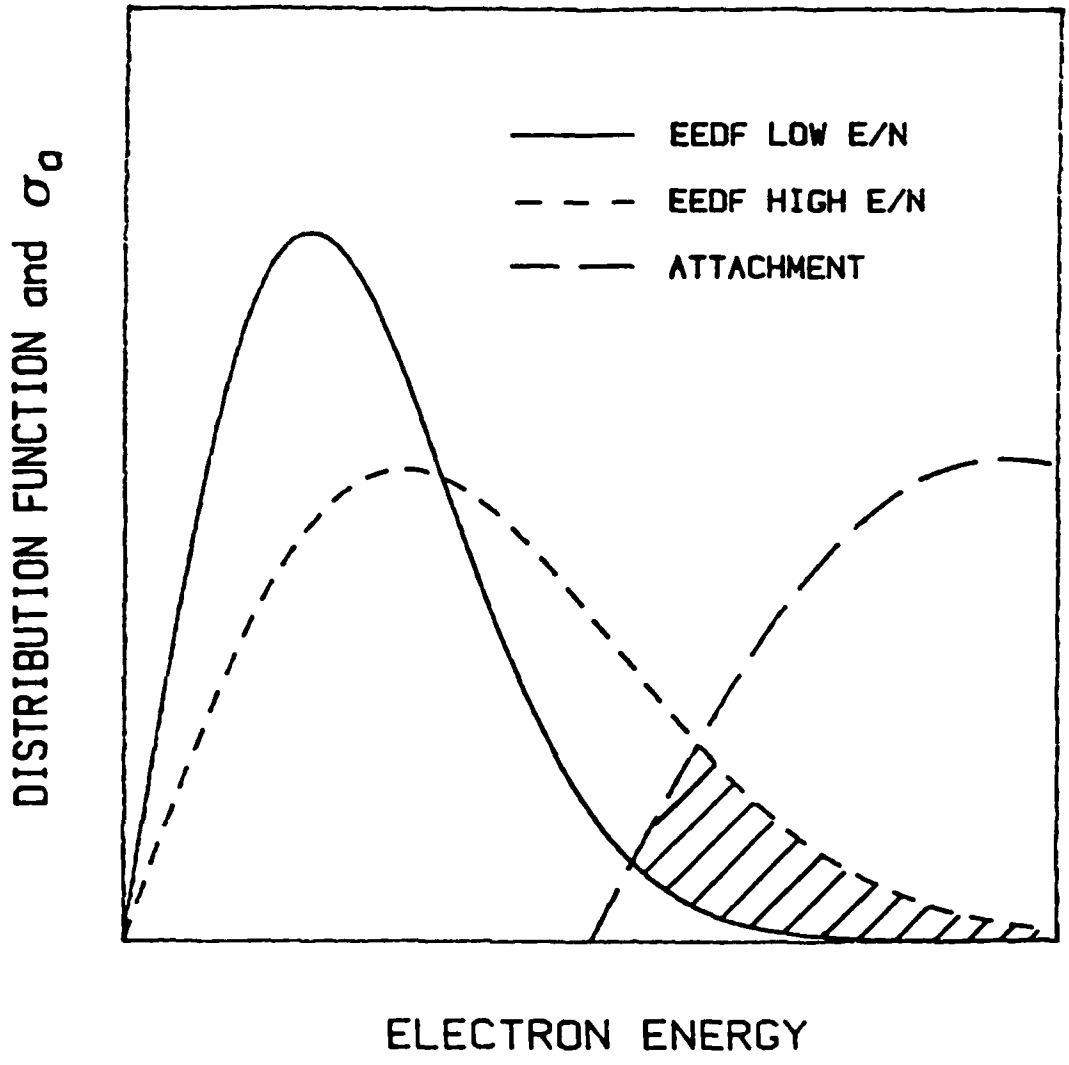


Fig. 3 The electron energy distribution function, at high and low E/N, and attatchment cross section, $\sigma_a$, versus electron energy.

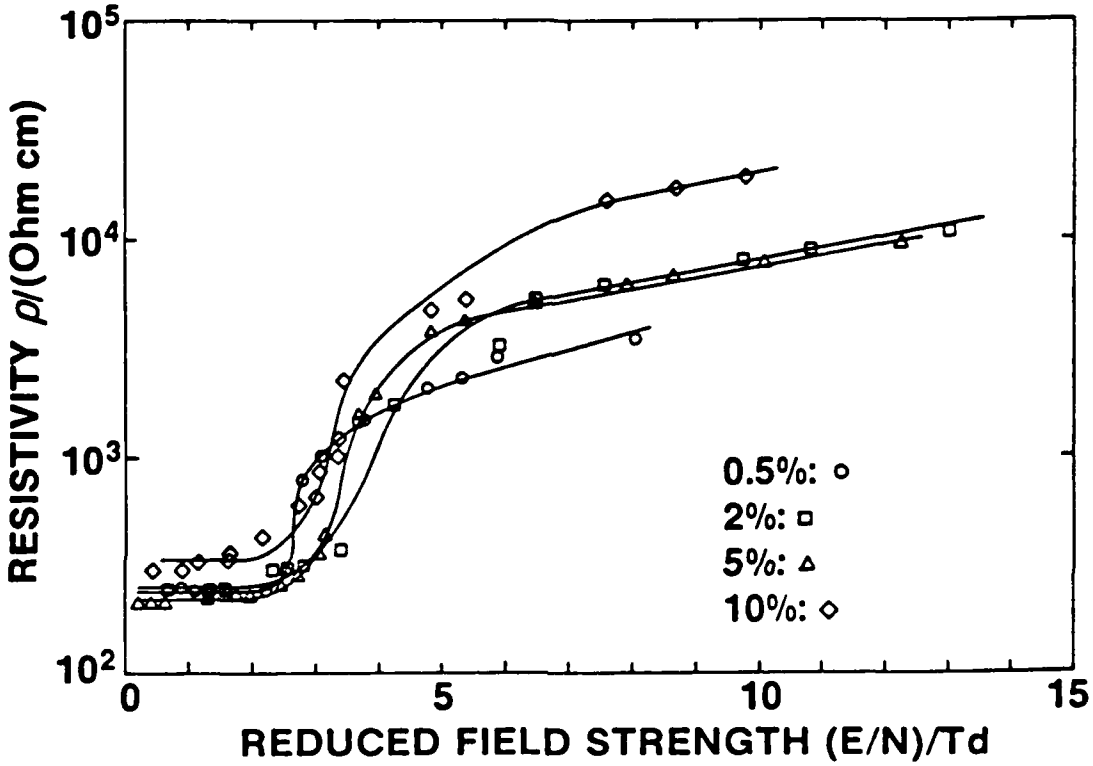


Fig. 4 Resistivity, $\rho$, versus reduced electric field strength, E/N, for an e-beam sustained discharge in Ar with admixtures of $C_2F_6$.

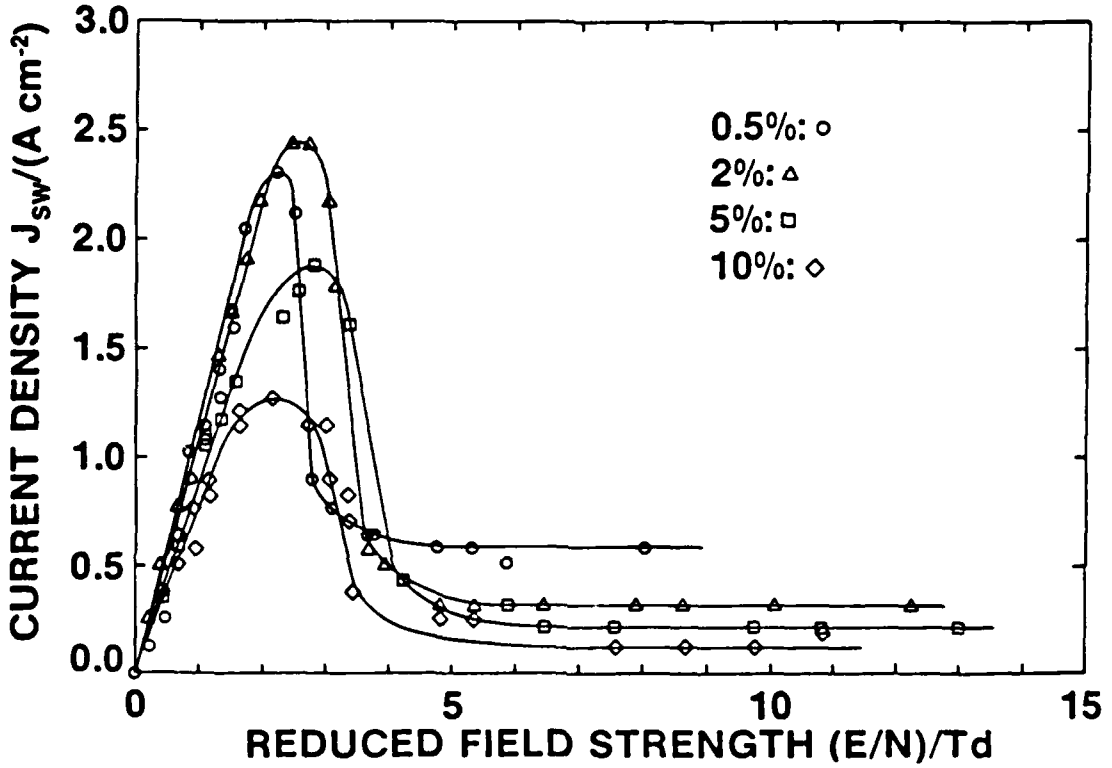


Fig. 5 Current density, J, versus reduced electric field strength, E/N, for an e-beam sustained discharge in Ar with admixtures of $C_2F_6$.

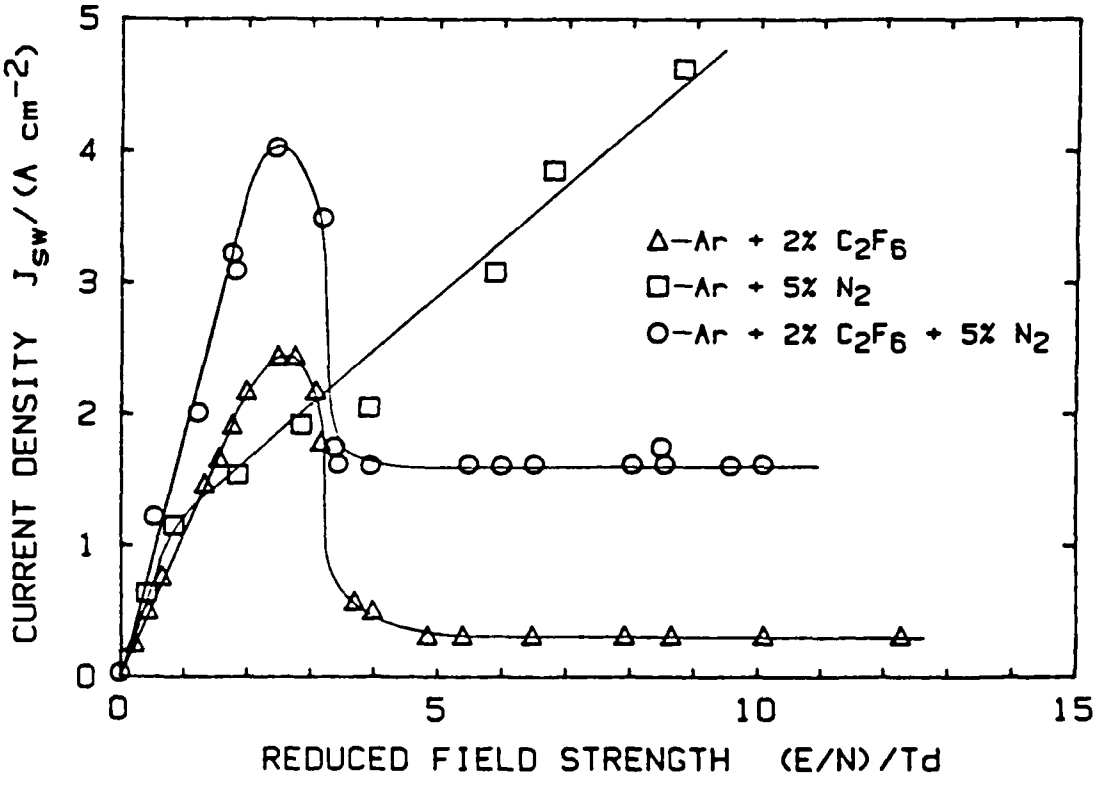


Fig. 6 Current density, J, versus reduced electric field strength, E/N, for an e-beam sustained discharge in mixtures of Ar, $C_2F_6$, and $N_2$.

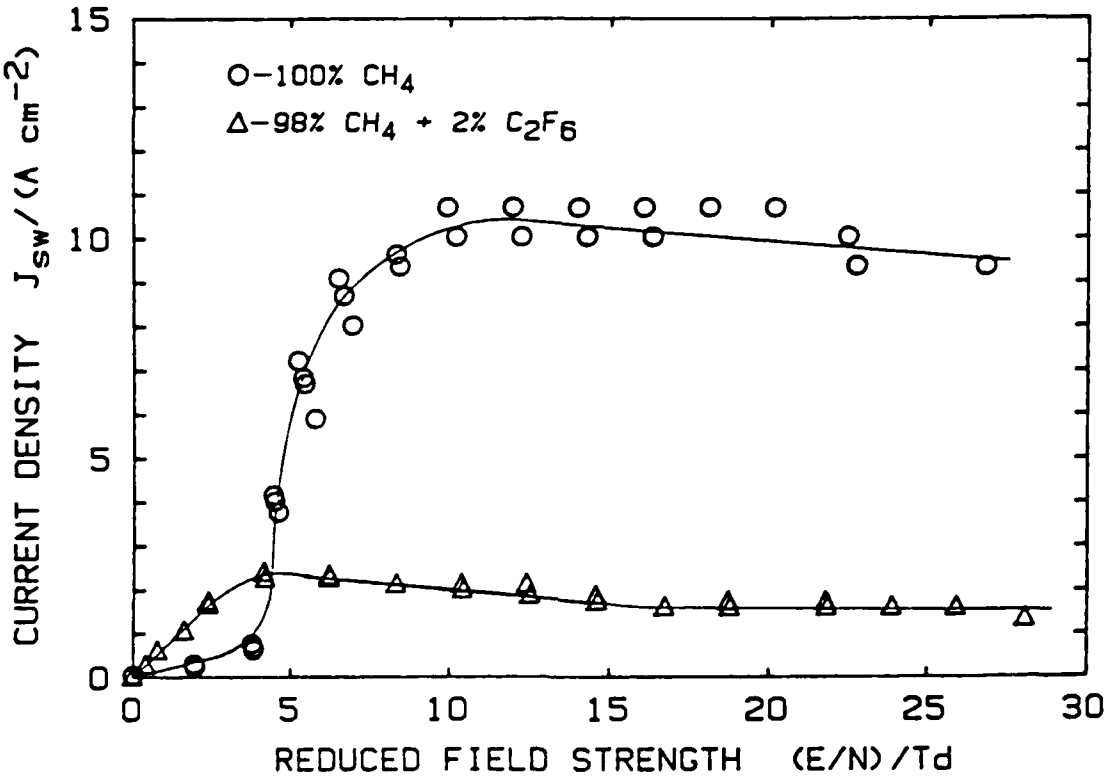


Fig. 7 Current density, J, versus reduced electric field strength, E/N, for an e-beam sustained discharge in $CH_4$ with admixtures of $C_2F_6$.

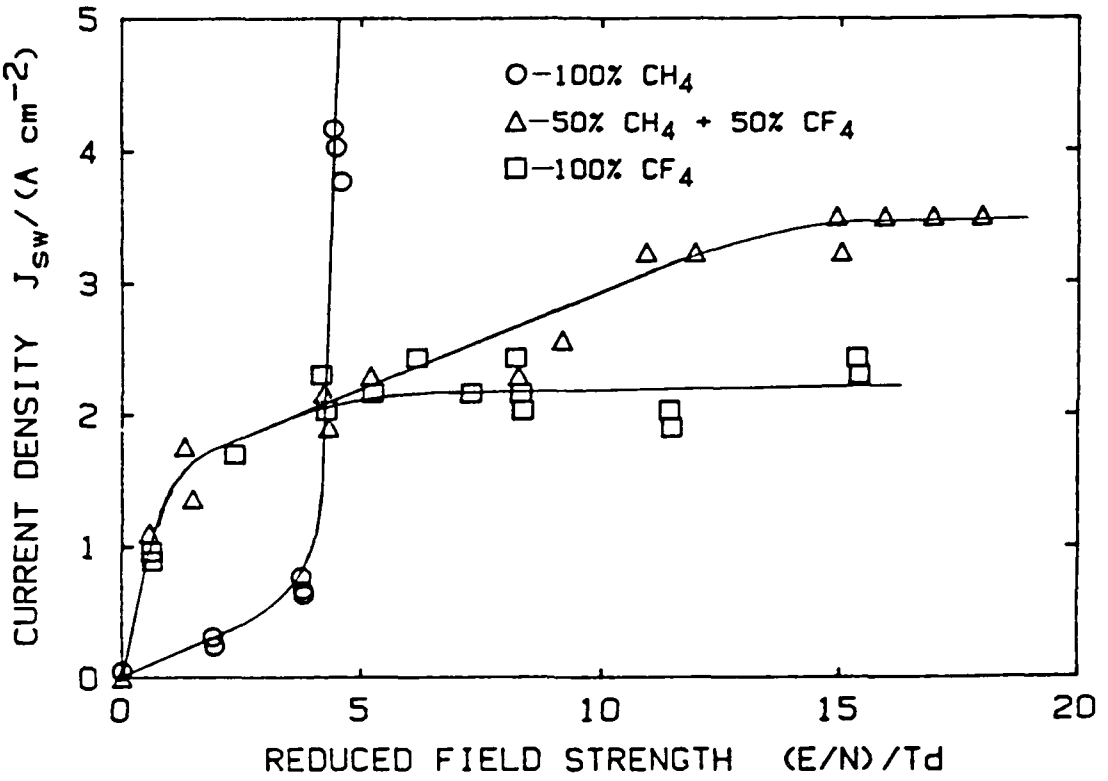


Fig. 8 Current density, J, versus reduced electric field strength, E/N, for an e-beam sustained discharge in $CH_4$-$CF_4$ mixtures.

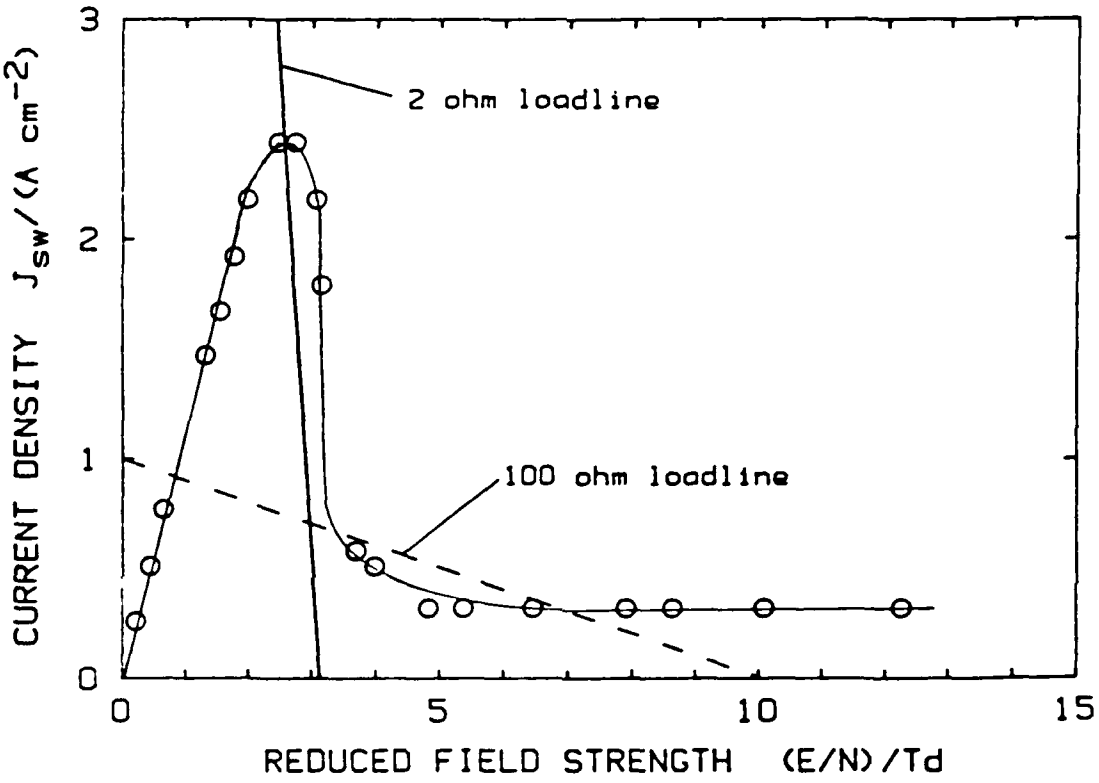


Fig. 9 Current density, J, versus reduced electric field strength, E/N, for an e-beam sustained discharge showing the different impedance loadlines in a mixture of Ar + 2% $C_2F_6$.

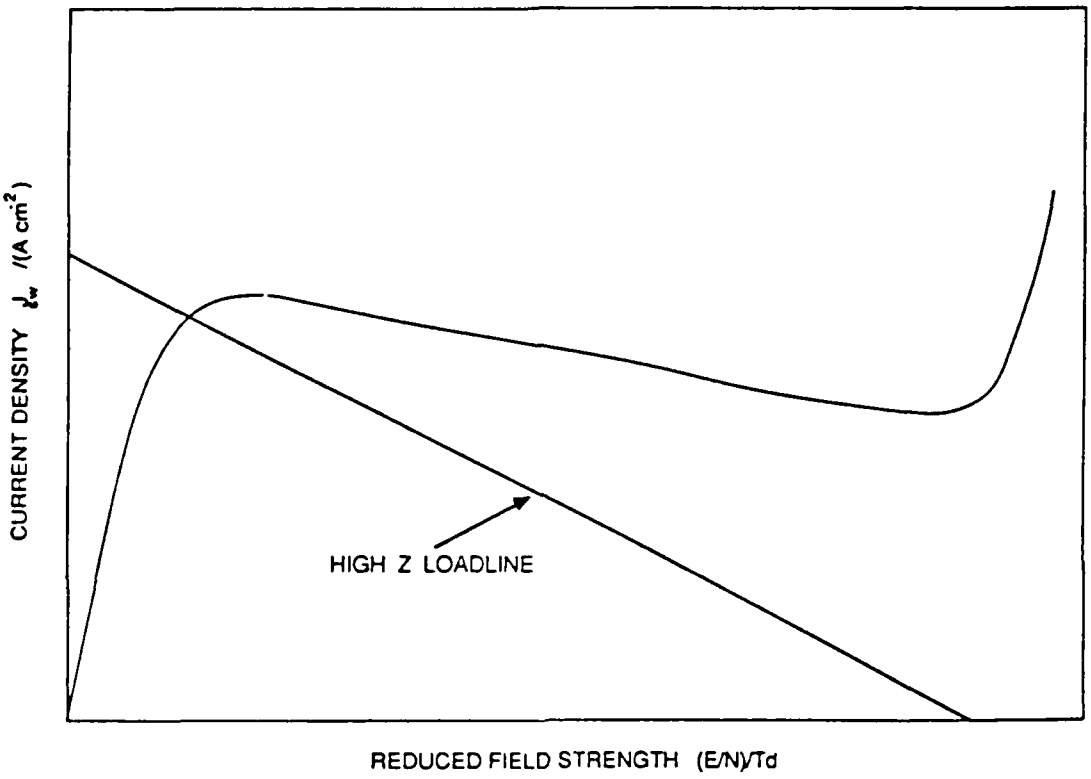


Fig. 10 The ideal current density, J, versus reduced electric field strength, E/N, for an e-beam sustained discharge for a high impedance repetitive switching system.

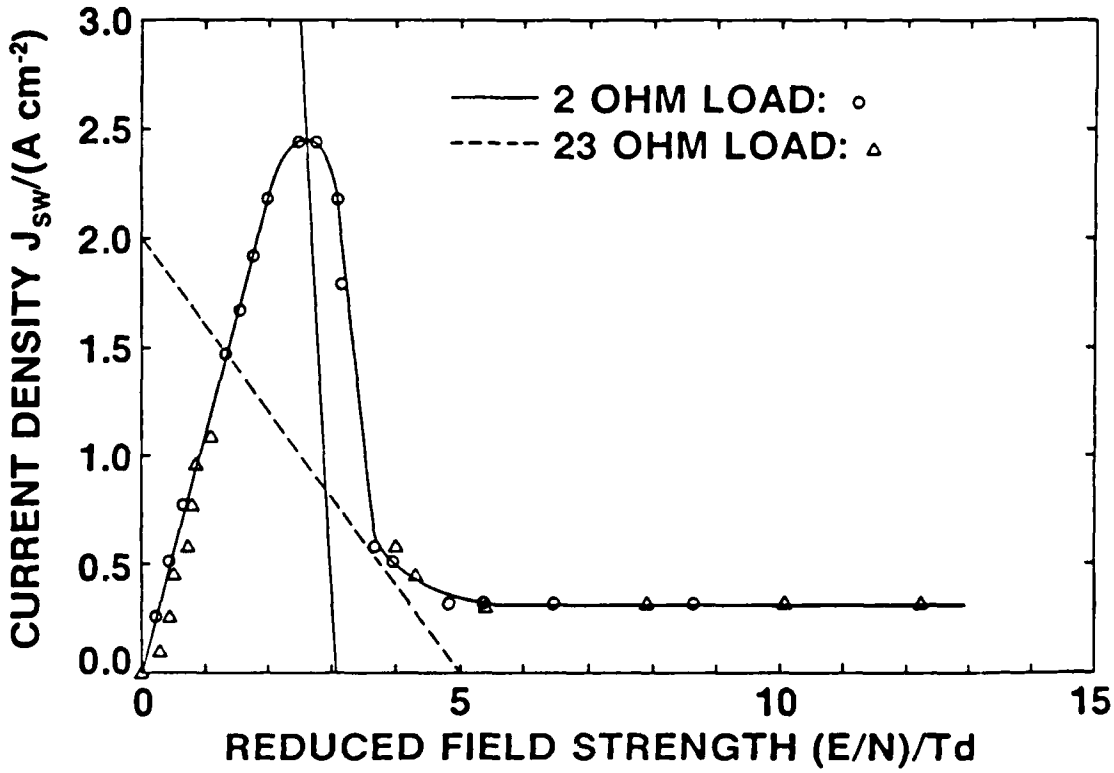


Fig. 11 Loadlines and current density, J, versus reduced electric field strength, E/N, for an e-beam sustained discharge, obtained with different loadlines in Ar + 2% $C_2F_6$.

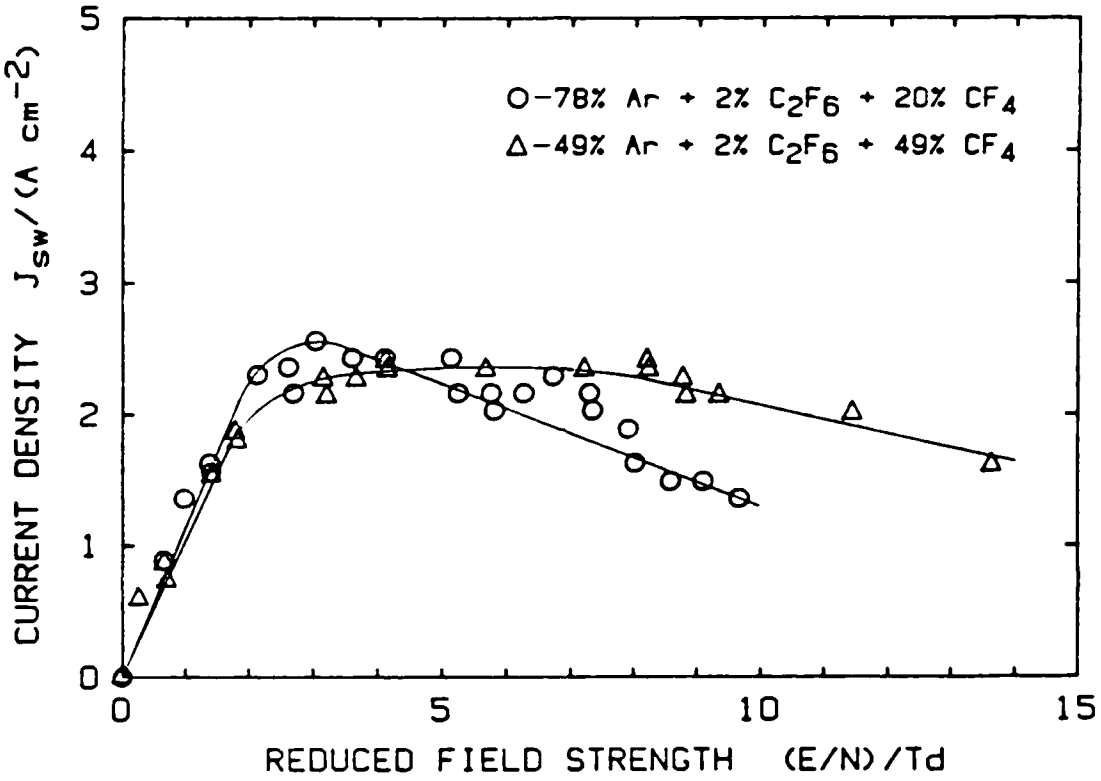


Fig. 12 Current density, J, versus reduced electric field strength, E/N, for an e-beam sustained discharge in mixtures of Ar, 2% $C_2F_6$, and $CF_4$.

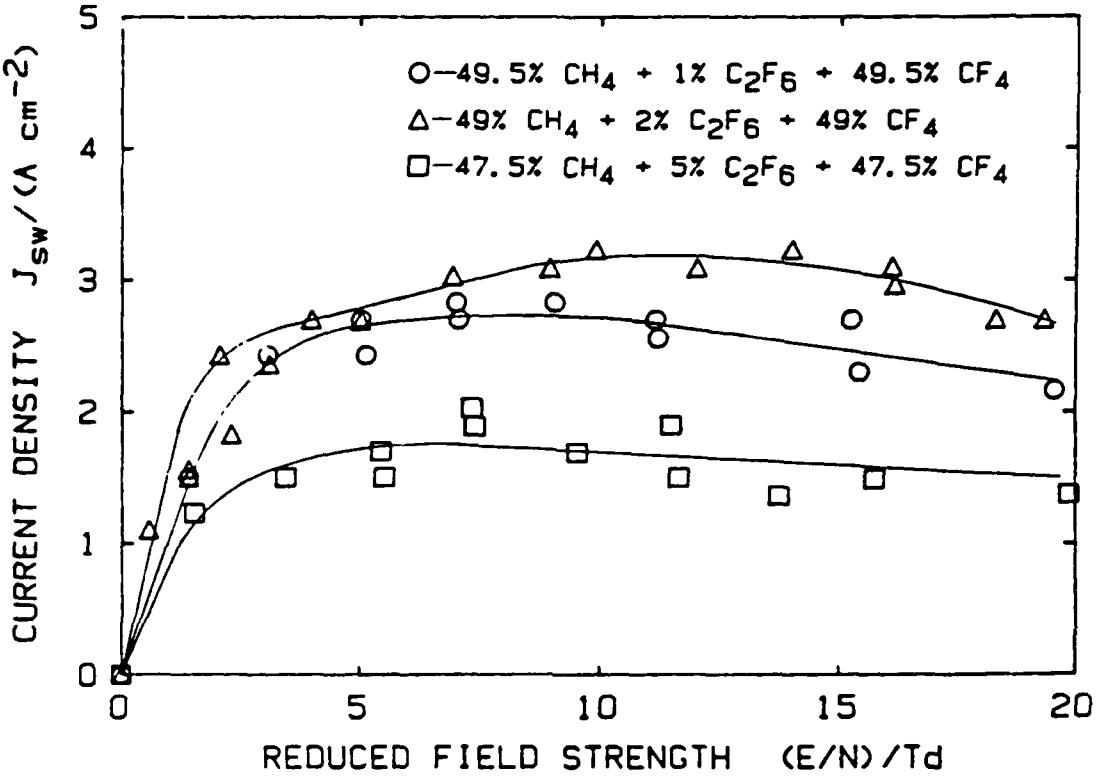


Fig. 13 Current density, J, versus reduced electric field strength, E/N, for an e-beam sustained discharge in mixtures of $CH_4$+$CF_4$+$C_2F_6$.

TABLE 1
GAS PARAMETER

| GAS MIXTURE | $J_{swOP}$ ($A\ cm^{-2}$) | $E/N_{OP}$ (Td) | $[NDC_{max}]^{-3}$ (1/ohm-cm) | $E/N_{NDC}$ (Td) | $GAIN_{OP}$ | $RHO_{OP}$ (ohm-cm) | $RHO_{min}$ (ohm-cm) | $RHO_{max}$ (ohm-cm) | $E/N_{BR}$ (Td) | $E/N_{GtoA}$ (Td) |
|---|---|---|---|---|---|---|---|---|---|---|
| 99.5% Ar + 0.5% $C_2F_6$ | 2.3 | 2.2 | -18.8 | 2 - 3 | 20 | 240 | 230 | 6,600 | 33.5 | 8 |
| 98% Ar + 2% $C_2F_6$ | 2.4 | 2.5 | -12.7 | 2.5 - 3.5 | 20 | 250 | 210 | 12,000 | 42 | 12 |
| 95% Ar + 5% $C_2F_6$ | 1.8 | 2.3 | -7.3 | 3 - 4 | 17 | 320 | 220 | 14,700 | 53 | 15 |
| 90% Ar + 10% $C_2F_6$ | 1.3 | 2.2 | -5.49 | 3 - 3.5 | 12 | 420 | 300 | 20,200 | 55 | >20 |
| 95% Ar + 5% $N_2$ | 1.5 | 1.8 | --- | --- | 12 | 300 | 160 | 400 | 28.8 | --- |
| 93% Ar + 2% $C_2F_6$ + 5% $N_2$ | 4.0 | 2.4 | -10.0 | 2.5 - 3.5 | 42 | 152 | 120 | 2,400 | 55.8 | 11 |
| 78% Ar + 2% $C_2F_6$ + 20% $CF_4$ | 2.6 | 3.0 | -0.86 | 5 - 10 | 14 | 300 | 180 | 3,800 | 68.8 | 15 |
| 49% Ar + 2% $C_2F_6$ + 49% $CF_4$ | 2.4 | 4.1 | -0.14 | 5 - 10 | 14 | 420 | 230 | 2,500 | 89.3 | 15 |
| 100% $CH_4$ | 10.7 | 10 | 0 | 10 - 15 | 60 | 250 | 200 | 360 | 85.5 | --- |
| 98% $CH_4$ + 2% $C_2F_6$ | 2.4 | 4.1 | -0.25 | 5 - 15 | 13 | 420 | 330 | 1,400 | 94.7 | --- |
| 50% $CH_4$ + 50% $CF_4$ | 3.5 | 15 | 0 | 15 - 20 | 20 | 1070 | 240 | 1,100 | 104 | --- |
| 49.5% $CH_4$ + 1% $C_2F_6$ + 49.5% $CF_4$ | 2.7 | 5 | -0.21 | 10 - 20 | 15 | 470 | 240 | 1,600 | 104 | --- |
| 49% $CH_4$ + 2% $C_2F_6$ + 49% $CF_4$ | 3.0 | 7 | 0 | 10 - 15 | 17 | 570 | 230 | 1,300 | 106 | --- |
| 47.5% $CH_4$ + 5% $C_2F_6$ + 47.5% $CF_4$ | 2.0 | 7.3 | 0 | 5 - 15 | 11 | 900 | 310 | 2,600 | 110 | --- |
| 100% $CF_4$ | 2.3 | 4.2 | 0 | 5 - 15 | 13 | 450 | 180 | 1,700 | 111.6 | --- |

J. Applied Physics
Submitted January 1987

Appendix M

# THE INFLUENCE OF PHOTODETACHMENT ON THE J-E/N CHARACTERISTICS OF DIFFUSE DISCHARGES CONTAINING OXYGEN

G. Schaefer[a], G. Z. Hutcheson[b], K. H. Schoenbach[c], and P. F. Williams[d]

Department of Electrical Engineering/Computer Science
Texas Tech University, Lubbock, TX 79409-4439

(Received

Externally sustained discharges can be used as opening and closing switches in pulsed power systems. Admixtures of attachers with a low attachment rate at low values of E/N and a high attachment rate at nigh values of E/N will allow a low loss operation in the conduction phase as well as rapid opening when the external sustaining source is terminated. Losses, however, will increase in the closing transition when the external sustaining source is turned on. Photodetachment has been proposed as an additional control mechanism to overcome these losses in the closing transition. This paper presents measurements on photoionization sustained discharges in argon and nitrogen containing admixtures of $O_2$ under the influence of laser radiation. Strong changes of the voltage-current characteristics have been observed. The influence of parameters such as percentage of $O_2$, laser power, laser pulse width, and circuit impedance is presented. Additionally, it is shown that photodetachment can enhance the stability of diffuse discharges.

Inductive energy storage is attractive in pulsed power applications because of its intrinsic high energy density and its ability to operate at low prime voltage. The key technological problem in developing inductive energy storage systems, especially for repetitive operation, is the development of a fast opening switch. Diffuse discharges have advantages for switching because of their low inductance, small electrode erosion and heating rates and moderate energy density which offer the possibility of external control of the opening and closing process by means of electron beams and/or lasers.

To achieve short opening times in an externally sustained discharge with electron densities in the range $n_e \leq 10^{14}$ $cm^{-3}$ electron attachers have to be used. Attachers with high attachment rates at high values of reduced field strength, E/N, and low attachment rates at low values of E/N will allow fast opening when the electron beam is turned off and low losses in the conduction phase.[1,2] Such attachers, however, increase the closing time and increase the loss during switch closure, especially if closure has to be performed in a high impedance system. This effect has been demonstrated in calculations on discharges[3] in $N_2$ containing $N_2O$ and in experiments on discharges[4] in Argon containing $C_2F_6$.

It has been proposed that photodetachment can be used to overcome these losses during closure.[3,5] The influence of photodetachment will mainly influence the discharge characteristics in an intermediate E/N range. At low values of E/N attachment will not dominate the discharge if the attacher used has the properties as mentioned above. At high values of E/N - above self breakdown - ionization through the discharge electrons

will dominate.[6] For applications as a repetitive closing and opening switch the discharge therefore has to be operated at low values of E/N not influenced by attachment in the conduction phase, and at intermediate values of E/N well below self-breakdown and subsequently dominated by attachment in the nonconducting phase, and the transitions between these two phases. The influence of photodetachment can subsequently be demonstrated by measuring the current density (J) versus reduced field strength (E/N) characteristics under the influence of photodetachment.

The experimental setup used for our experiments is shown in Fig. 1. The major component is the discharge chamber with a TEA-laser electrode configuration (variable gap distance, d = 3.5-10 mm, active electrode width, w = 20 mm, electrode length, l = 200 mm). The electrodes of this chamber are connected to a 125Ω line which is charged to a voltage below self-breakdown of the discharge gap. A resistor in series is used to vary the system impedance. A spark array UV source is located behind a screen in one of the main electrodes. This UV source can produce light pulses with 5 ns risetime and nearly constant emission over several 100 ns. When the UV source is fired an externally sustained discharge will be initiated in the discharge chamber. Current and voltage probes in the main line allow the evaluation of the time dependence of current, voltage, and impedance of the discharge. Side windows at the discharge chamber allow the illumination of the discharge volume with a flashlamp pumped dye laser. This laser produces pulses of approximately 1000 ns length and nearly constant power

of ~ 1 MW over the central 400 ns at 590 nm. With a pockel cell chopper, short pulses of 50 ns length and ~ 500 kW power can be obtained. The time dependent measurements of current and voltage across the discharge, with and without laser, allow the evaluation of the influence of photodetachment on the J-E/N characteristics and on the transient behavior of the discharge.

The measurements reported here were performed in mixtures of argon and nitrogen with admixture of oxygen as the attacher. Attachers producing $O^-$ as the dominant negative ion are good candidates for photodetachment experiments, since $O^-$ has a relatively high photodetachment cross section[8] for photons of approximately 2 eV which can be produced efficiently with flashlamp pumped dye lasers.

The mixture of argon and nitrogen optimizes the ionization efficiency of the UV source. Nitrogen is known to increase the UV yield of the spark sources[9] while the admixture of argon increases the penetration depth of the ionizing radiation. The ionization efficiency was further enhanced by using N,N dimethylaniline as an additive with a low ionization potential.[10]

The first set of experiments was performed to evaluate the influence of attachment on the steady state J-E/N characteristic of the discharge. For these experiments the system impedance was kept small compared to the impedance of the discharge (with nearly constant discharge voltage). One set of data was taken without the laser. Figure 2 shows the J-E/N characteristics for gases with varying concentrations of $O_2$. The mixtures used with higher $O_2$ concentrations generated regions of negative differential conductivity in intermediate E/N ranges of the characteristics. This

effect is the consequence of an attachment coefficient that strongly increases with E/N. At high values of E/N the currents increased drastically. In this E/N range internal ionization through discharge electrons becomes significant and, therefore, represents the transition to self-sustained discharges.

Figure 3 shows the influence of photodetachment for varying concentrations of $O_2$. For these experiments, the UV source was triggered at the peak power of the 1000 ns laser pulse. The laser power density in the discharge chamber was $8 \times 10^5$ W/cm$^2$. Discharges that did not contain oxygen showed no change in resistance when illuminated by the laser. No influence of the laser on the discharge characteristics was observed in the low E/N range where no dissociative attachment occurs. The influence of the laser starts in the range where the current density reaches a minimum. In this E/N range attachment is strong and the density of negative ions is high. The strongest changes of the resistance at constant values of E/N were observed in the transition regime to the self-sustained discharges. Increased electron density, due to internal ionization, along with the high E/N caused a high density of negative ions which, in turn, gave a strong photodetachment effect. The higher oxygen concentrations produced a more pronounced change in resistance, as a result of the higher negative ion densities.

The dependence of the resistance change on the laser intensity was also measured and was found to be linear up to the maximum intensity of our laser, $8 \times 10^5$ W/cm$^2$. This result indicated that only a fraction of the negative ions were being photodetached, and, that with higher laser powers, stronger resistance changes could have been attained.[5]

Further experiments involved determining the effect of photodetachment on a high impedance circuit. A 13 kΩ resistor was placed in series with the transmission line of the diffuse discharge circuit. In such a circuit the increase of current is associated with a decrease of E/N and, consequently, a reduction of the attachment rate. The effect of the laser is therefore expected to be smaller. The laser was operated again in the long pulse mode, and the UV source was triggered at the time of peak laser power. The results, plotted as changes in discharge resistance, are shown in Fig. 4. As in the low impedance measurements, the strongest changes in resistances occurred in the transition regime from externally to self-sustained discharges.

Schaefer, et al.[3] have demonstrated through simulations that short laser pulses occurring soon after discharge initiation can strongly alter the J-E/N characteristics of the discharge for the remainder of the discharge pulse. Figure 5 shows similar results in our experiment in which the laser pulse was only on for ~50 ns soon after discharge initiation. Current density changes caused by short laser pulses occurring later in the discharge were smaller and more closely followed the laser in time.

As a final demonstration of the influence of photodetachment, laser enhanced stability experiments were performed in the 125Ω system in a mixture of Ar with 5.3% $O_2$ and 350 ppm dimethylaniline at 1 atm. Sudden voltage collapse and current changes in the discharges indicated formation of arcs. As in the previous experiments, the laser was used with a peak intensity of approximately $8 \times 10^5$ W/cm$^2$. In five out of five cases where the discharges were not illuminated by the dye laser, arc development

occurred anywhere from 350 ns to 1 μs after discharge initiation as previously demonstrated by Norris and Smith.[11] However, for five out of five cases where the discharges were illuminated, no arcs were observed. By increasing the electron density[12] and lowering the effective attachment rate, photodetachment enhances discharge stability.

The experiments presented demonstrate that externally sustained discharges in mixtures of argon and nitrogen, containing admixtures of oxygen exhibit a negative differential conductivity in an intermediate E/N range. This effect is believed to be the consequence of the attachment coefficient for the dissociative process ($e+O_2 \rightarrow O^- + O$), increasing strongly with E/N.

Photodetachment with a visible laser can be used to significantly change the discharge characteristics. Resistance changes at moderate laser powers (800 kW/cm$^2$) were strongest (factor of 8) at the E/N range where the ratio of the negative ion density to the electron density is highest. This E/N range corresponds to the regime just below the transition from externally sustained to self-sustained, which is the E/N range close to the initial E/N values that would be used for a diffuse discharge switch in a high impedance system. Short laser pulses during discharge initiation are sufficient to change the behavior of the entire discharge pulse.

From these experiments, we believe that discharges can be operated as opening switches with low loss in high impedance, burst mode systems, if photodetachment is utilized during discharge initiation. For both switches and lasers, photodetachment can be used as a mechanism to improve the

stability of diffuse discharges and, thereby, one may be able to increase repetition rates or conduction times.

The authors would like to thank R. A. Korzekwa for his assistance in the preparation of this letter. This work was jointly supported by the Air Force Office of Scientific Research and the Army Research Office under contract AFOSR 84-0032 and by the National Science Foundation under grant No. ECS-8318122.

# AUTHOR'S INDEX

a) Present address: Department of Electrical Engineering
Polytechnic University
Farmingdale, NY 11735

b) Present address: Mission Research Corporation
1720 Randolph Road, SE
Albuquerque, NM 87106

c) Present address: Department of Electrical Engineering
Old Dominion University
Norfolk, VA 23508

d) Present address: Department of Electrical Engineering
University of Nebraska - Lincoln
Lincoln, NE 68588-0511

# REFERENCES

[1]K. H. Schoenbach, G. Schaefer, M. Kristiansen, L. L. Hatfield and A. H. Guenther, IEEE Trans. on Plasma Science, PS-10, 246, (1982).

[2]L. L. Christophourou, S. R. Hunter, J. A. Carter, and R. A. Mathis, Appl. Phys. Lett., 41, 147, (1982).

[3]G. Schaefer, K. H. Schoenbach, H. Krompholz, M. Kristiansen, and A. H. Guenther, Laser and Particle Beams, 2, 273, (1984).

[4]G. Schaefer, K. H. Schoenbach, M. Kristiansen, B. E. Strickland, R. A. Korzekwa, and G. Z. Hutcheson, Appl. Phys. Lett., 48, 1776, (1986).

[5]G. Schaefer, P. F. Williams, K. H. Schoenbach, and J. Moseley, IEEE Trans. on Plasma Sci., PS-11, 263, (1983).

[6]R. T. VanBrunt and M. Misakian, J. Appl. Phys., 54, 3074, (1983).

[7]R. Cooper, G. Hutcheson, M. Kristiansen, G. Schaefer, K. H. Schoenbach, and A. H. Guenther, Proc. 4th IEEE Int. Pulsed Power Conf., Albuquerque, NM, (1983).

[8]L. M. Branscomb, S. J. Smith, and G. Tisone, J. Chem. Phys., 43, 2906, (1965).

[9]H. J. J. Seguin, D. McKen, and J. Tulip, J. Appl. Phys., 28, 487, (1976).

[10]D. F. Grosjean and P. Bletzinger, IEEE J. Quantum Electron, QE-13, 898, (1977).

[11]B. Norris and A. L. S. Smith, J. Phys. D: Appl. Phys., 10, L237,(1977).

[12]R. A. Haas, in Applied Atomic Collision Physics, Volume 3 - Gas Lasers, edited by E. W. McDaniel and W. L. Nighan (Academic Press, New York, 1982).

# FIGURE CAPTIONS

Figure 1. Experimental setup for UV sustained, photodetachment controlled discharge.

Figure 2. J-E/N characteristics of UV sustained and UV initiated discharges for several concentrations of $O_2$ with 2.6% $N_2$, 350 ppm dimenthlaniline, and balance of Ar at 1 atm.

Figure 3. The influence of the laser on the discharge resistance $R_L/R_o$, where $R_L$ is the resistance with laser illumination and $R_o$ is the resistance without laser illumination versus E/N for 125Ω system impedance. Gas mixtures contained various concentrations of $O_2$, 2.6% $N_2$, 350 ppm dimethylaniline, and balance of Ar at 1 atm.

Figure 4. The influence of the laser on the discharge resistances $R_L/R_o$, where $R_L$ is the discharge resistance with laser illumination and $R_o$ is the discharge resistance without laser illumination versus initial E/N for 13 kΩ system impedance. Gas mixture contained varying concentrations of $O_2$, 2.6% $N_2$, 350 ppm dimethylaniline, and balance of Ar at 1 atm.

Figure 5. Current versus time with and without short laser pulse for a gas composition of 13.2% $O_2$, 2.6% $N_2$, 84.2% Ar, and 350 ppm dimethylaniline at 1 atm, initial E/N = 50.2 Td, and a laser power density = 400 $kW/cm^2$.

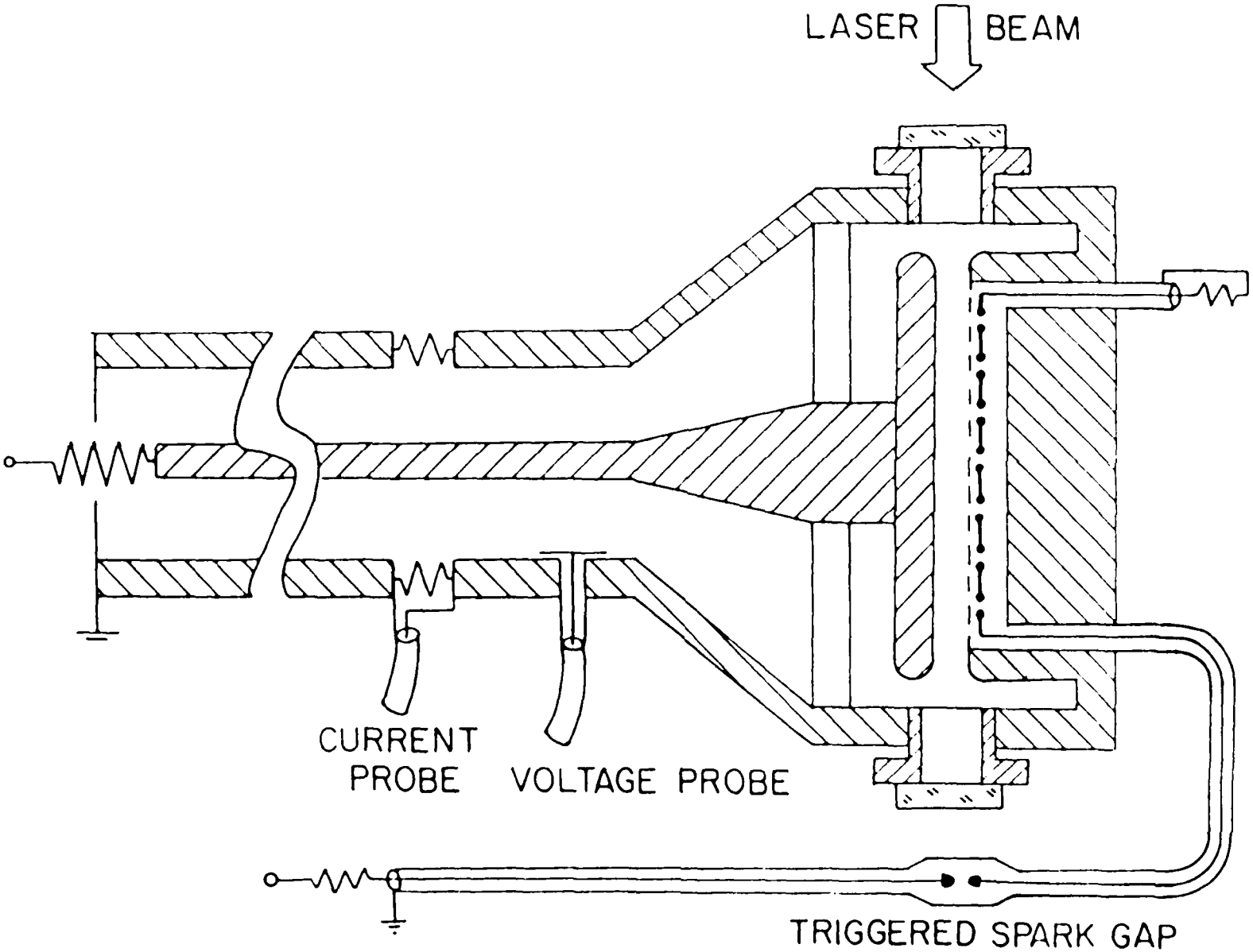


Fig. 1 of S, G. Schaefer, Appl. Phys. Lett.

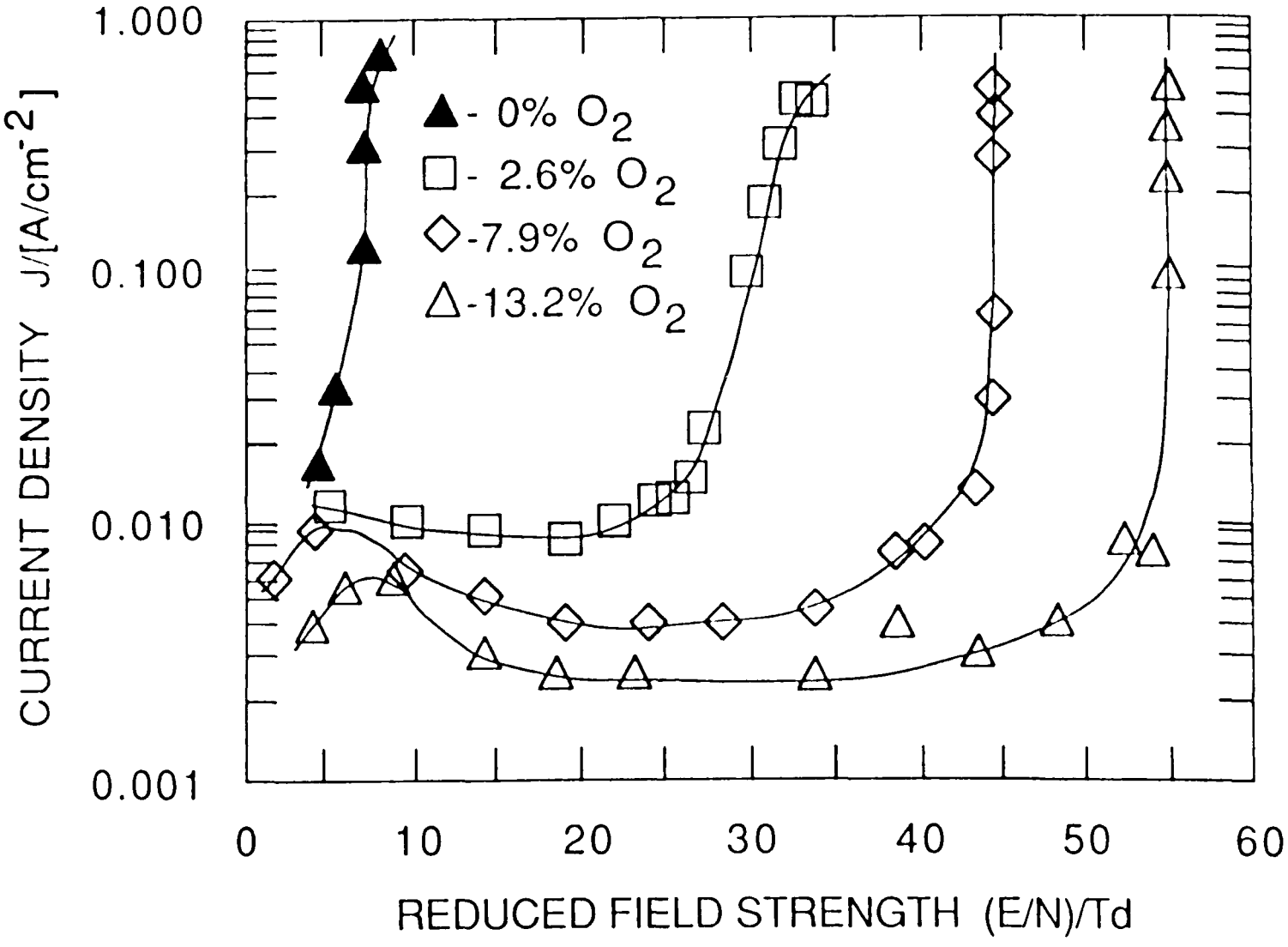


Fig. 2 of 5, G.Schaefer, Appl. Phys. Lett.

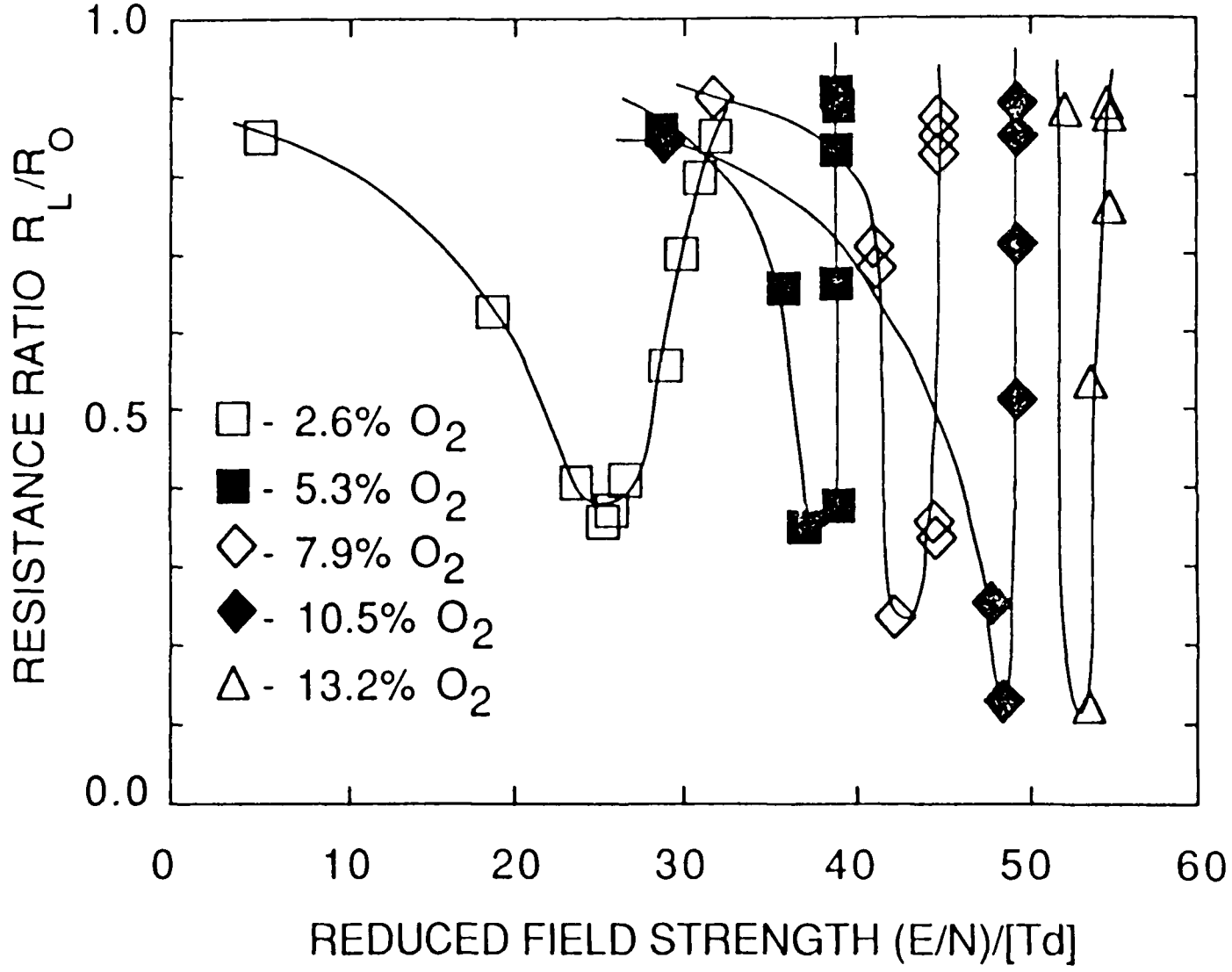


Fig. 3 of 5, G. Schaefer, Appl. Phys. Lett.

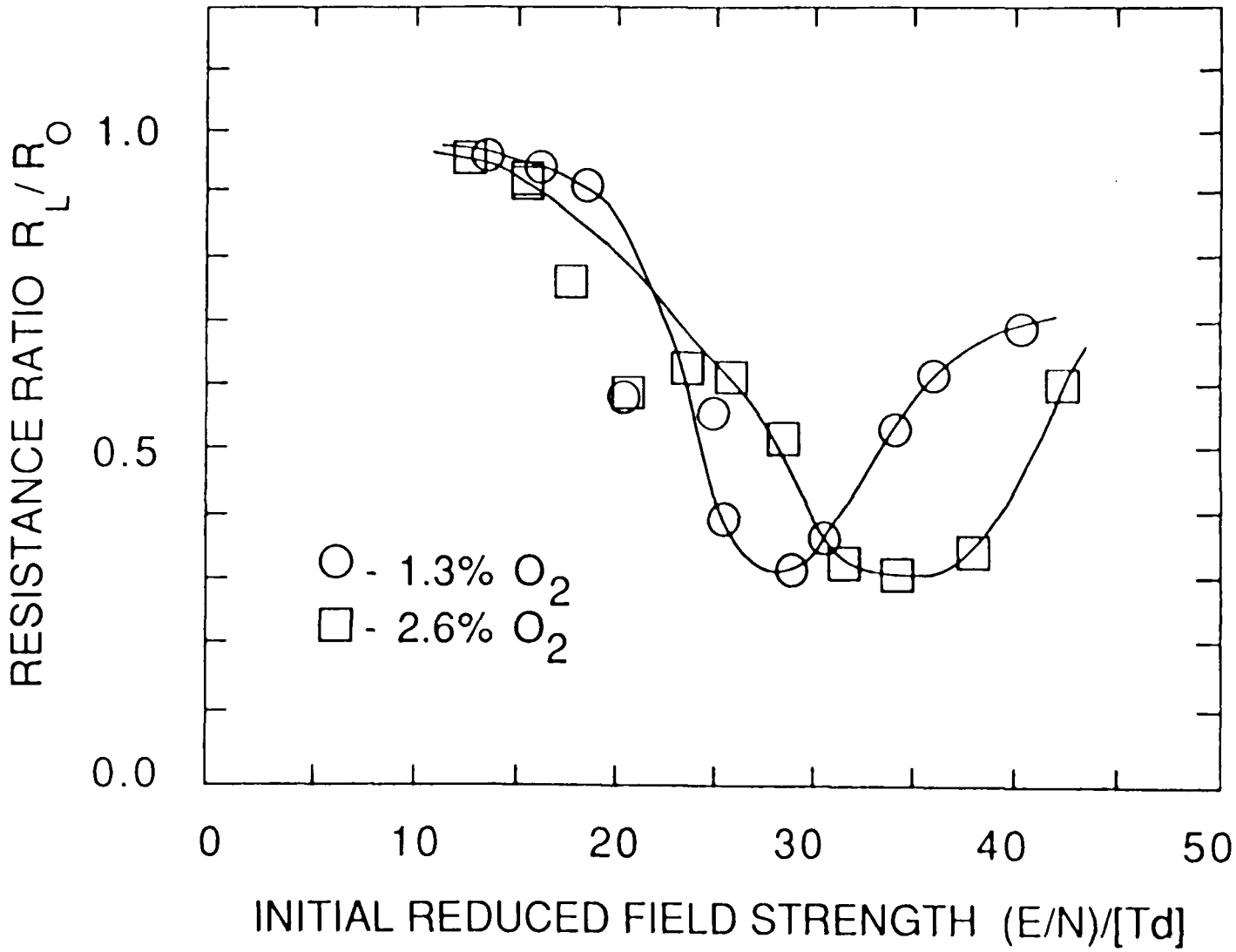


Fig. 4 of 5, G. Schaefer, Appl. Phys. Lett.

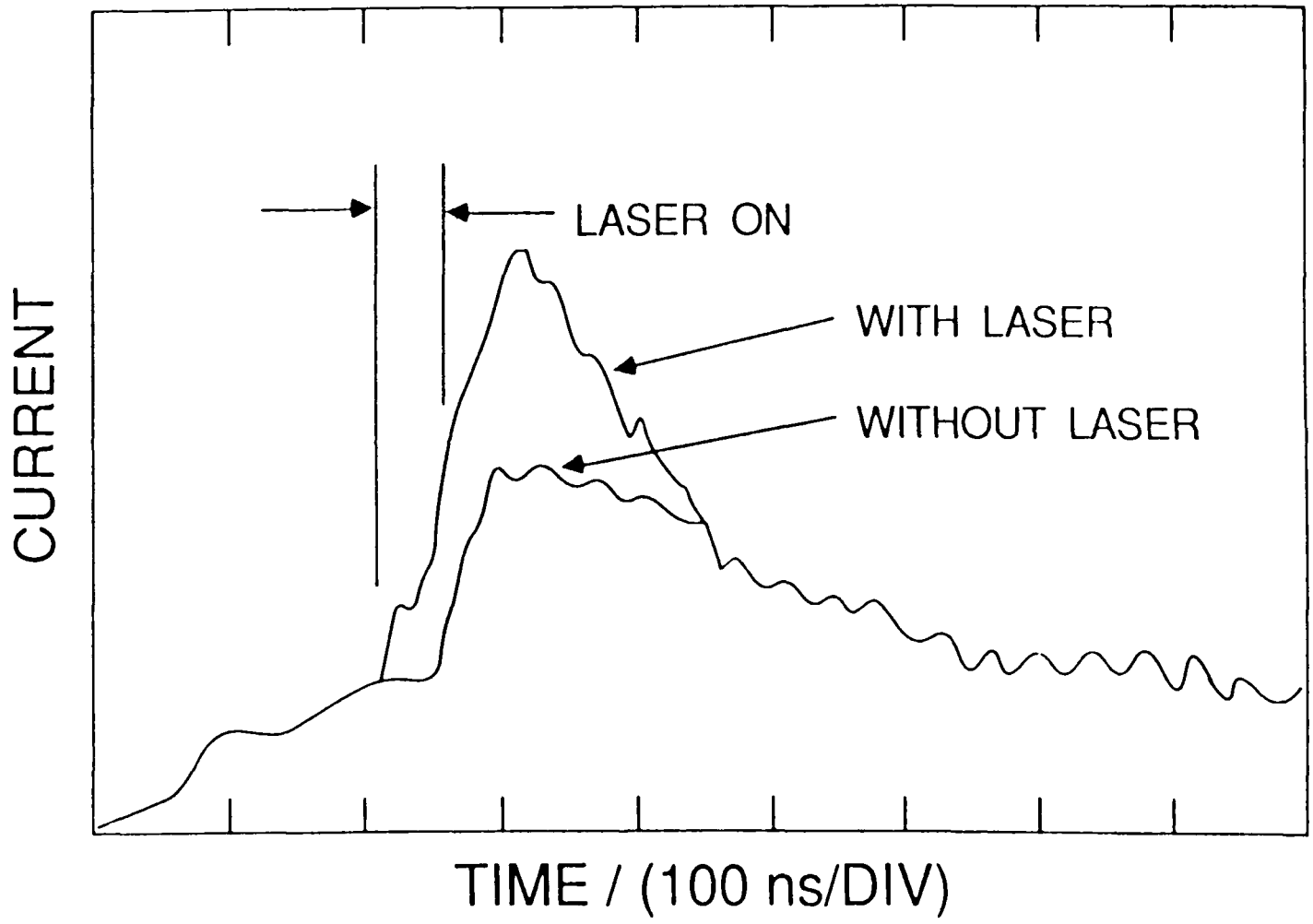


Fig. 5 of 5, G. Schaefer. Appl. Phys. Lett.

5th IEEE Pulsed Power Conf.
Arlington, VA, June 1985

Appendix N

# Analysis of Electrode Surface Damage in High Energy Spark Gaps*

A. L. Donaldson, M. Kristiansen, H. Krompholz, and M. O. Hagler
Department of Electrical Engineering/Computer Science
L. L. Hatfield and G. R. Leiker
Department of Physics
Texas Tech University
Lubbock, Texas 79409 USA
P. K. Predecki
University of Denver
Denver, Colorado 80208 USA
G. L. Jackson
The BDM Corporation
Huntsville, Alabama 35805 USA

## Abstract

The surfaces of stainless steel electrodes used in a high energy, gas-filled spark gap have been analyzed using Auger Electron Spectroscopy (AES) and Scanning Electron Microscopy (SEM). The analysis of electrode cross-sections revealed areas of enhanced erosion and crack formation as a result of temperature cycling of the arc and enhanced chemical attack along manganese "stringers" which were present in the stainless steels. The depth of the cracks was considerably less in nitrogen (20 μm) than in air (80 μm) and except at the cracks the damage was generally less than 10 μm. The use of low sulphur steels and cutting the electrodes so that the stringers ran parallel to the surface both proved to be effective means of eliminating crack formation, thus reducing the chance of electrode failure.

## Introduction

The surface damage and subsequent electrode erosion resulting from high energy arcs has been of interest for a considerable time as a major factor limiting the lifetime of spark gaps used as switching components in a variety of pulsed power systems. Recent work on electromagnetic launchers ("rail guns") has renewed the interest in understanding electrode erosion, especially for very high currents (> 100 kA). The work reported here contains results on material effects likely to play a role in electrode reliability in the high current regime.

In order to thoroughly study the processes and effects resulting in electrode surface damage, the following questions should be addressed:

- What effect was observed?
- What is its importance to spark gap performance (via electrode erosion for example)?
- What is (are) the cause(s)?
- How can it be corrected/altered/designed around?

A listing of some of the surface alterations which have occurred are given in Table I along with a brief summary of their significance.

Table I
Listing of Surface Damage/Alteration Effects

| Effect | Significance |
|---|---|
| Material Removal (Erosion)* | Increase in Breakdown Voltage |
| Micro Cracks (Hexagonal "Riverbed")* | Possible Fracturing of Electrode, Bulk Material Removal; Subsequent Failure to Operate |
| Material Transfer Electrode to Electrode* | Surface Stability & Erosion Rate; A Function of Opposite Electrode |
| Macro Cracks* | Fracturing of Electrode Subsequent Failure to Operate |
| Macro Protrusions | Reduction in Breakdown Voltage |
| Micro Protrusions | Alteration of Breakdown Voltage Stability |
| Chemical Compound Formation on Surface | Alteration of Breakdown Voltage Stability |
| Micro Craters | None, Except the Sum Leads to Net Material Removal |

*Likely to be of increasing importance at very high currents.

Specifically, the work reported here will concentrate primarily on one of these effects, namely, surface cracking and the resulting hexagonal structure in stainless steel.

## Experimental Setup

The electrode erosion experiments described below were performed on the Mark II energy storage and spark gap system. The spark gap was coaxial in design and was essentially like the one shown in Figure 1. (Some modifications have been made to allow for water cooling of the electrodes and inner gap housing in order to remove the bulk heat at high rep-rates and high Coulomb transfer.) The spark gap was designed for frequent electrode and insulator replacement and to allow for accurate control of the electrode alignment and gap spacing.

*Supported by AFOSR

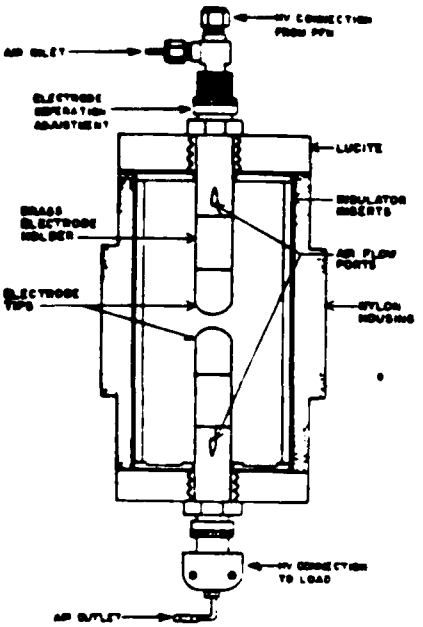


Figure 1. Mark II spark gap (original).

The hemispherically shaped electrodes are all 2.5 cm in diameter and were attached to a stainless steel (304) electrode holder. The insulator inserts provide protection for the main gap housing and studies of the surfaces of these inserts have given information about the insulator damage resulting from the discharge byproducts [1]. A detailed description of the spark gap assembly and diagnostic systems are given elsewhere [2]; however, the operating parameters for the gap are summarized in Table II.

Table II
Mark II Operating Conditions

| | |
|---|---|
| Gap Spacing | < 0.75 cm |
| Voltage | < 30 kV |
| Current | < 25 kA |
| Capacitance | 21 μF |
| Charge/Shot | 0.6 Coul |
| Energy/Shot | < 9 kJ |
| Pulse Width | 25 μs |
| Rep-Rate | 5 pps |
| Pressure | 1 atm (absolute) |

The analysis of the electrodes was performed using several pieces of equipment including a PHI model 595 Auger Electron Spectrometer, a JEOL JSM-2 Scanning Electron Microscope and an Olympus BHM Optical Microscope.

## Results

Previous experiments performed by the authors [3] have shown that stainless steel (304) electrodes subjected to 50,000 shots showed a significant reduction in electrode erosion (1.5 to 0.7 $\mu cm^3/coul$) when the switching gas was changed from air to nitrogen. The surfaces of these electrodes, shown in Figure 2a,b,c indicate a regular surface pattern with cracks similar in appearance to a dried up river bed.

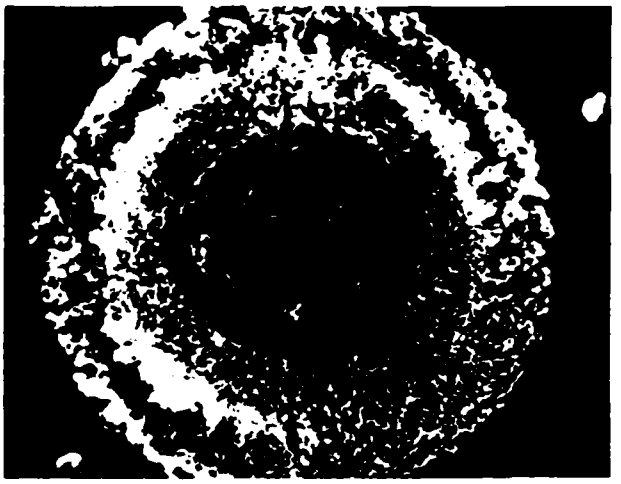

(a) 2 mm

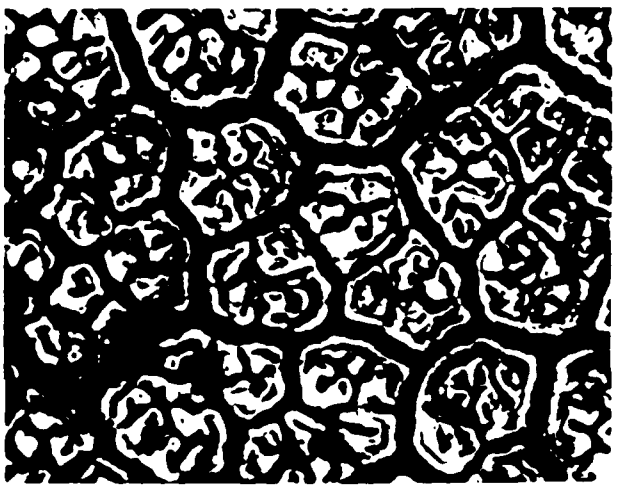

(b) 200 μm

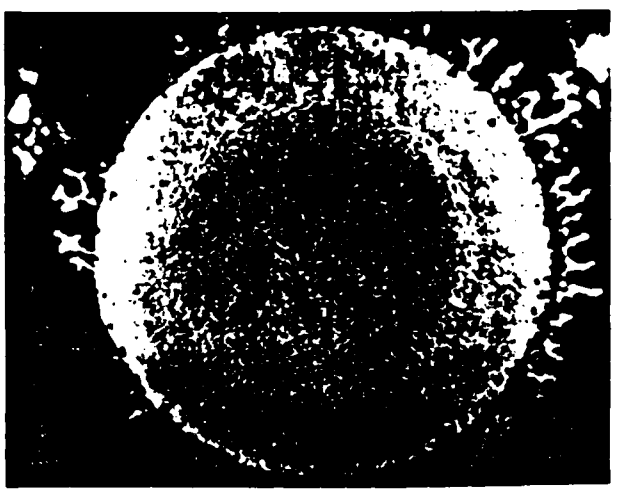

(c) 2 mm

Figure 2. Surfaces of stainless steel (304) cathode: (a) in air, low magnification; (b) in air, high magnification; (c) in nitrogen, low magnification.

The cross sections of these electrodes, shown in Figure 3a,b reveal cracks with depths of approximately 80 μm for electrodes run in air and 20 μm for electrodes run in nitrogen. At first it was thought that the cracks were due solely to temperature cycling in the material with the "hexagonal" pattern resulting from the biaxial tensile forces present during resolidification of the molten surface. (A simple calculation showed that a temperature change of 200°C could lead to crack formation.)

(a) 50 μm

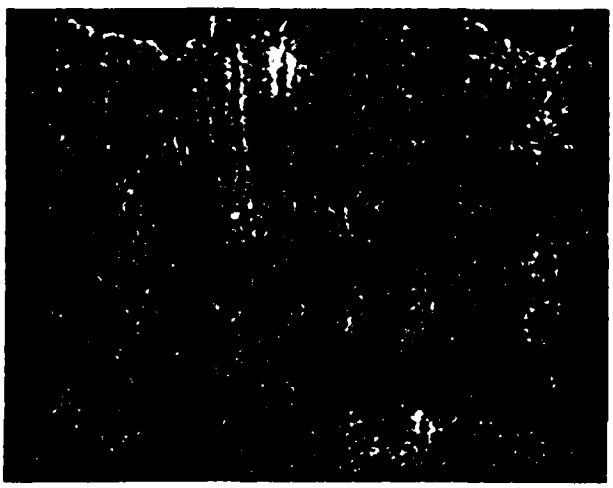

(b) 50 μm

Figure 3. Cross sections of stainless steel (304) cathode: (a) in air; (b) in nitrogen.

However, further examination of the cracks shown in Figure 4a,b revealed that the crack orientation was coincident with manganese "stringers" present in the steel, which are perpendicular to the surface (parallel to the length of the rod from which the electrode tip was cut).

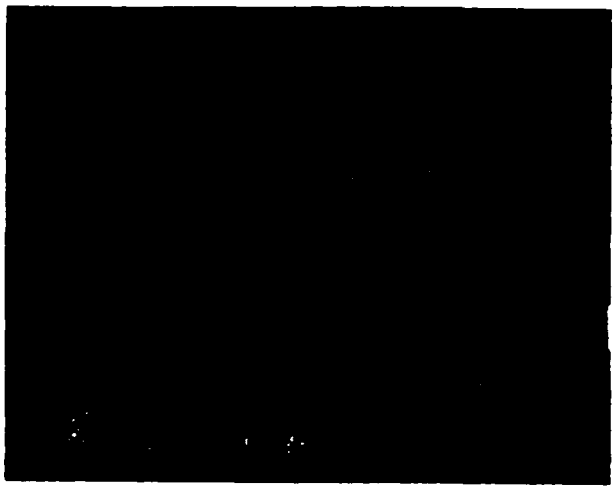

(a) 50 μm

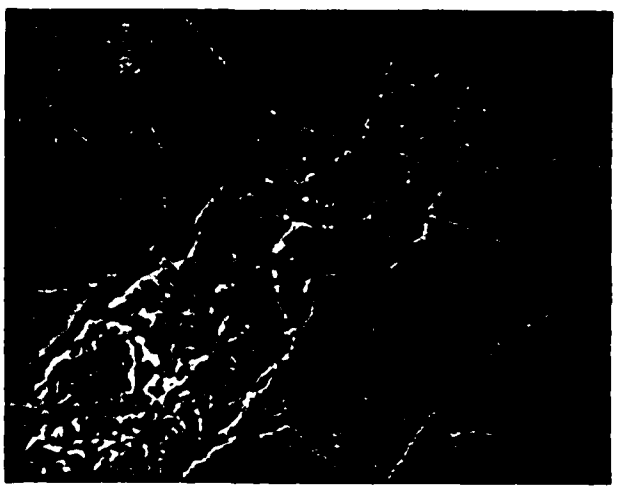

(b) 5 μm

Figure 4. Cross sections of stainless steel (304) cathode in air: (a) on the outer edge; (b) SEM photograph at region examined by Auger analysis.

Auger analysis of the cracks indicated that the manganese acted as a "getter" for the sulphur present in the steel which at high temperatures resulted in a chemical reaction leading to material removal at the manganese sites. However, since many more manganese sites exist than those occurring just at the cracks, it was concluded that the resulting surface formation was a combination of both temperature cycling and chemical attack.

To validate the importance of the stringers, an experiment was performed using a cathode (304) which was cut so that the stringers ran parallel to the surface of the steel and an anode which had the original orientation to serve as a control. The resulting surfaces shown in Figure 5ab indicated that no surface cracking occurred in the cathode (as expected), whereas the anode remained the same.

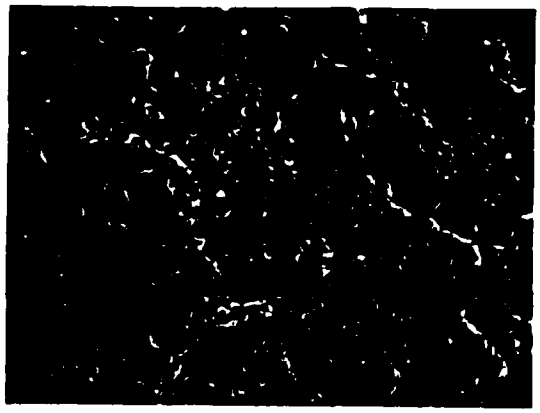

(a) 20 μm

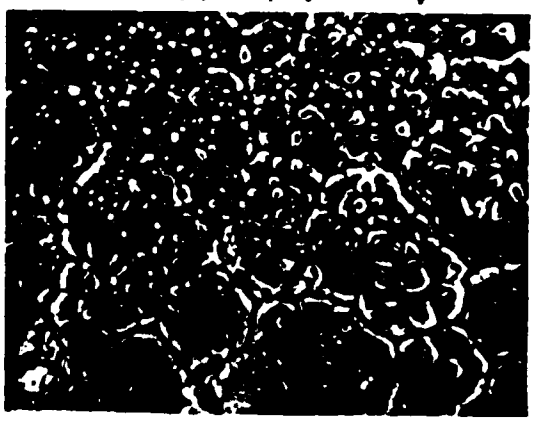

(b) 200 μm

Figure 5. Surfaces of stainless steel (304) in air: (a) cathode--cut so that stringers ran parallel to the surface; (b) anode--the same as previous runs.

In addition, at the suggestion of the steel manufacturer, a second steel was tried (316) which might have lower sulphur content. The results, shown in Figure 6a,b, also indicate an absence of cracks, although no significant reduction in bulk erosion occurred.

One should not conclude from these experiments that surface cracking requires the presence of manganese stringers or even chemical attack--any mechanism which leads to a weakening of the material surface during temperature cycling can prove sufficient to produce the observed structure. Indeed, crack formation has been observed by the authors and others in electrodes made of copper in a tungsten matrix [3-5] and tantalum [6], although the processes leading to the surface cracking are unclear.

Examination of electrodes run for 2,000, 10,000 and 50,000 shots indicated that the depth of the cracks increases with shot number and, although the damage at 50,000 shots (80 μm cracks) was not enough to produce catastrophic failure of the electrode, it is quite plausible that for normal switching use ($10^6$ to $10^8$ shots) crack formation could present a significant materials problem.

## Acknowledgments

The authors would like to thank M. McNeil for her work on the manuscript and M. Chandran, L. Heck, G. Jorden, L. Stephenson, H. Tanumihardja, and B. Tucker for their work on the data acquisition system and experimental facility.

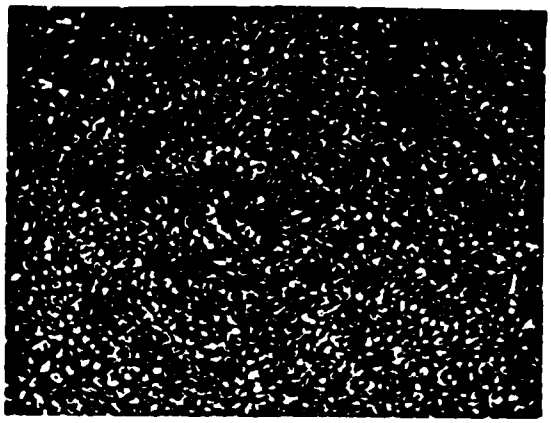

(a) 100 μm

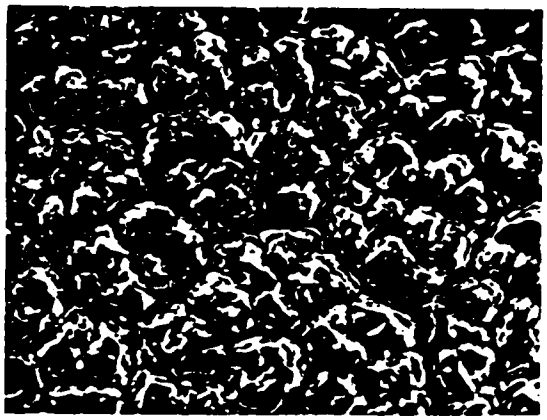

(b) 200 μm

Figure 6. Comparison of cathode surfaces of two different stainless steels: (a) 316; (b) 304.

## References

[1] G. L. Jackson, L. Hatfield, M. Kristiansen, M. Hagler, A. L. Donaldson, G. Leiker, R. Curry, R. Ness, L. Gordon and D. Johnson, "Surface Studies of Dielectric Materials Used in Spark Gaps," J. Appl. Phys. 55 (1) (1984).

[2] A. L. Donaldson, "Electrode Erosion in a High Energy Spark Gap," Master's Thesis, Texas Tech University (August 1982).

[3] A. L. Donaldson, M. O. Hagler, M. Kristiansen, L. L. Hatfield and G. L. Jackson, "Electrode Erosion Phenomena in a High Energy Pulsed Discharge," IEEE Trans. on Plasma Science, PS-12 (1), pp. 28-38 (March 1984).

[4] Y. Suzuki, Y. Kawakita, M. Kume and M. Kawai, "A 150 kV, 100 kA Spark Gap Switch for Marx Generators," in Proc. 3rd IEEE Int. Pulsed Power Conf. (Albuquerque, NM), pp. 444-447 (June 1981).

[5] M. T. Magnusson, "Erosion and formation of cracks in W/Cu Impregnated Materials of Different Tungsten Grain Size," ETZ (A), 98, pp. 239-240 (1977).

[6] E. I. Zolotarev, V. Mukhin, L. E. Polyanskii and V. N. Trapeznikov, Sov. Phys. Tech. Phys. 21, pp. 340-344 (1978).

# HIGH CURRENT SURFACE DISCHARGE SWITCH

P.M. Ranon, H. Krompholz, M. Kristiansen
Department of Electrical Engineering/Computer Science
L.L. Hatfield
Department of Physics and Engineering Physics
Texas Tech University
Lubbock, Texas 79409

## Abstract

The erosion of several dielectrics has been investigated in a single channel surface discharge switch (SDS). The switch was operated in an oscillating circuit in a self break mode (capacitance 1.85 μF, charged to 40 kV, peak current 130 kA, charge transfer .74 C/shot, frequency 300 kHz). Delrin, Teflon, and the epoxy-fiberglass laminate G-10 were used as dielectric surfaces with Copper-Tungsten (K33) electrodes. Repetition rates on the order of 1/3 pulse per second (pps), which increased during operation as the surface eroded and the breakdown voltage decreased, were used. Delrin withstood 100 shots before the 1.6 mm thick sample melted through. Teflon eroded at a lesser rate. G-10 samples quickly shattered or developed a carbonized track which lowered the breakdown voltage to 5 kV.

## Introduction

Very little information can be found on insulators which have been tested to repetitive high level currents in excess of MA's, but various dielectric materials are considered as insulators in pulsed power applications due to their availability and cost. G-10, for example, has been used in rail guns, primarily due to its ease of machining and mechanical strength. In such an application, the G-10 is subjected to MA current levels at a very low rep-rate. The present experiment uses field enhanced electrodes which confine currents in excess of 100 kA to a highly localized region on the insulator surface.

The purpose of this paper is to describe the erosion of Delrin, Teflon, and G-10 as they were subjected to high current levels. Hold-off voltage characteristics of the three dielectric materials were measured and are reported. It is interesting to note the drastic difference of 130 kA switching effects on the dielectrics as compared to previous 5 kA switching studies. G-10 for example, exhibited the best characteristics for 5 kA switching [1], but was the poorest for 130 kA switching. Despite the gross erosion pattern left on the its samples, Delrin exhibited far superior performance compared to G-10. Finally, Teflon exhibited the best overall characteristics of the three materials tested.

## Experimental Arrangement

As shown in Fig. 1, the dielectric samples were inserted into a 6 Ohm, 1 m long strip line. The electrodes, made of K 33, can be continuously adjusted to accommodate gap separations from 0 to 30 cm. The strip line shown is 20.3 cm wide and the separation is provided by a Blue Nylon dielectric, 30.5 cm wide and .65 cm thick. The energy storing, 1.85 μF, Scyllac capacitor, shown in Fig. 2, is integrated into the strip line and can store 1.48 kJ of energy when charged to 40 kV. The DC charged SDS, operated in air, is allowed to self break at about 40 kV initially, and allowed to free run, at about 1/3 pps, as determined by the self break voltage which decreased as the dielectric surface eroded away. Both the voltage and current waveforms are damped RLC in nature, with their amplitudes determined by the charging voltage. The best results of 130 kA peak current and 0.74 Coulombs/shot charge transfer were obtained across a 3.5 cm gap.

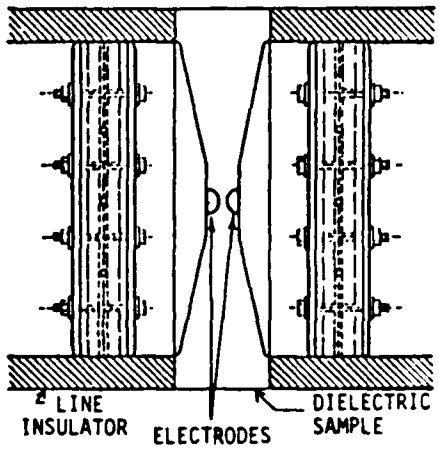


(a) Top View

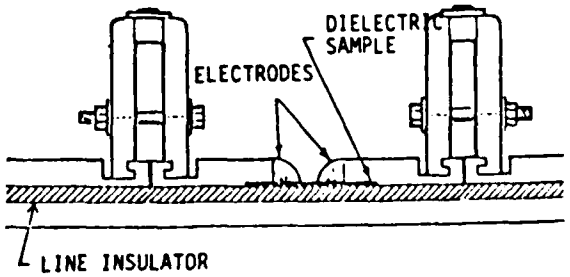


(b) Side View

Fig. 1 Surface Discharge Switch

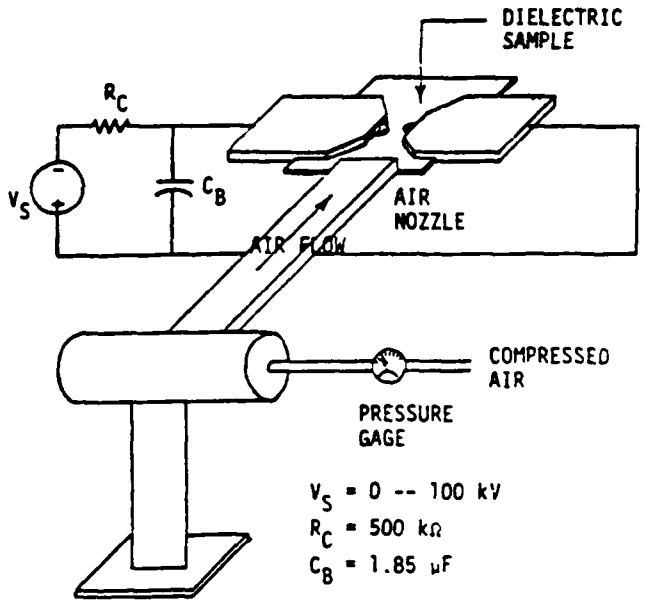


Fig. 2 Experimental Setup

## Results

### G-10

1) Hold-off voltage, 2) total charge transferred, and 3) total energy transferred are plotted against the number of shots for a typical G-10 sample in Fig. 3. After the first few preconditioning shots, the hold-off voltage dropped quite drastically. As shown in Fig. 4, two different levels of forced air cooling is compared to no cooling with no significant improvement. Fig. 5 shows the cold recovery after the surface has been allowed to cool, but not long enough for the surface charge to be discharged (surface resistance of sample times the capacitance >> cooling time). Visual inspection by the naked eye of the G-10 samples with a severely reduced hold-off voltage (approximately 1/10 of initial hold-off voltage), showed signs of a carbonized track approximately 0.5 mm wide burned between the two electrodes, as shown in Fig. 6.

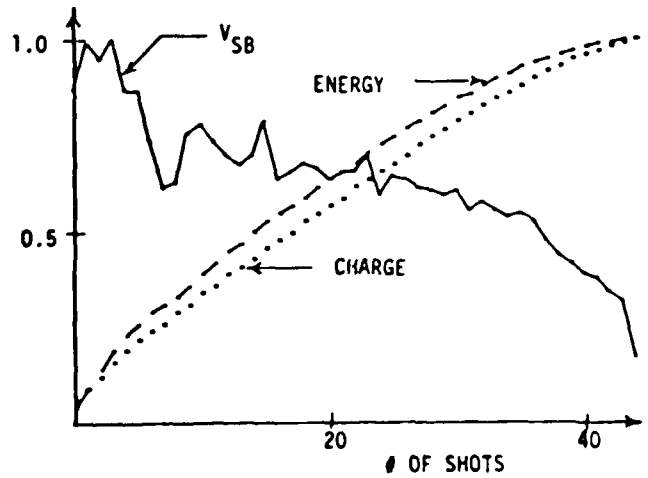


Fig. 3 Typical G-10 Hold-Off Voltage Plot

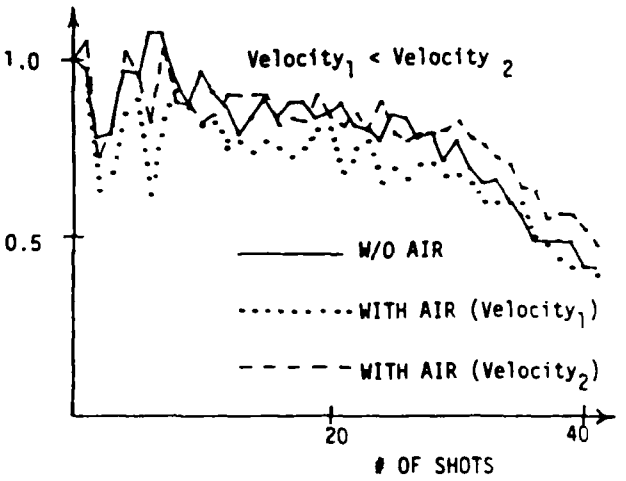


Fig. 4 Effect of Forced Air Cooling on G-10

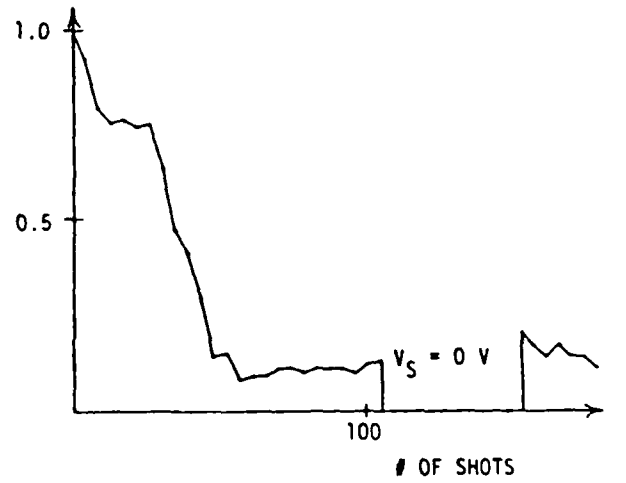


Fig. 5. Cold Recovery of G-10.

Fig. 6 Erosion Pattern on G-10

Delrin

1) Hold-off voltage, 2) total charge transferred, and 3) total energy transferred are plotted against the number of shots for a non air cooled Delrin sample in Fig. 7. In the case of air cooled samples, there is quite an impressive improvement over the non air cooled sample, as can be seen in Fig. 8. Cold recovery of Delrin using the same method as in the G-10 sample, shows that the material can recover, unlike the G-10 sample. A non air cooled sample is plotted to show the cold recovery of Delrin in Fig. 9. A typical erosion pattern on Delrin is shown in Fig. 10 and it can be seen that the erosion pattern is rather uniform. It is interesting to note that Nylon 66 samples were also tested and showed almost identical patterns overall to those of Delrin and thus not reported separately here.

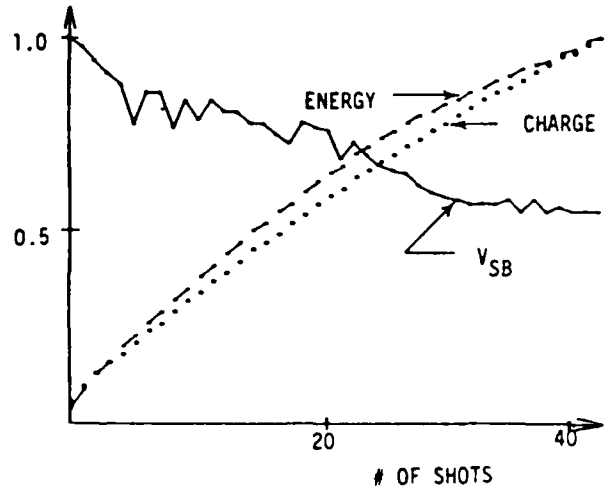


Fig. 7 Non Air Cooled Delrin Hold-Off Voltage Plot

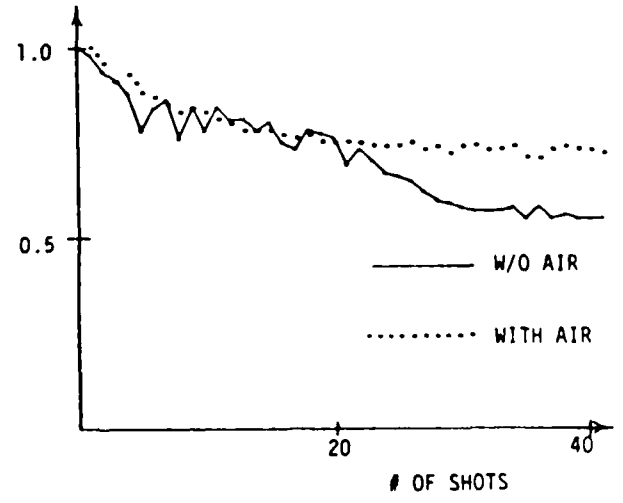


Fig. 8 Effect of Forced Air Cooling on Delrin

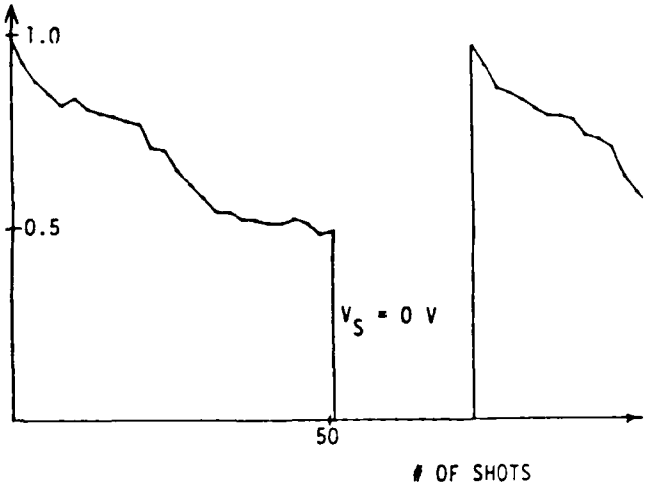


Fig. 9 Cold Recovery of Delrin

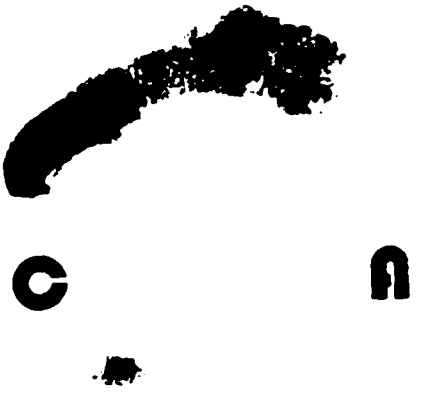

Fig. 10 Erosion Pattern on Delrin

Teflon

In Fig. 11, 1) Hold-off voltage, 2) total charge transferred, and 3) total energy transferred are plotted against the number of shots for a non air cooled Teflon sample. As can be seen from the figure, the hold-off voltage remained consistently high throughout the run. Forced air cooling on Teflon samples seemed to have an effect as it did for the Delrin, but the results did not seem as significant due to the consistently high hold-off voltage. Due to this high hold-off voltage characteristics, it is difficult to determine whether the Teflon has actually recovered for the test shown in Fig. 13. Figure 14 shows the erosion pattern left on a Teflon sample.

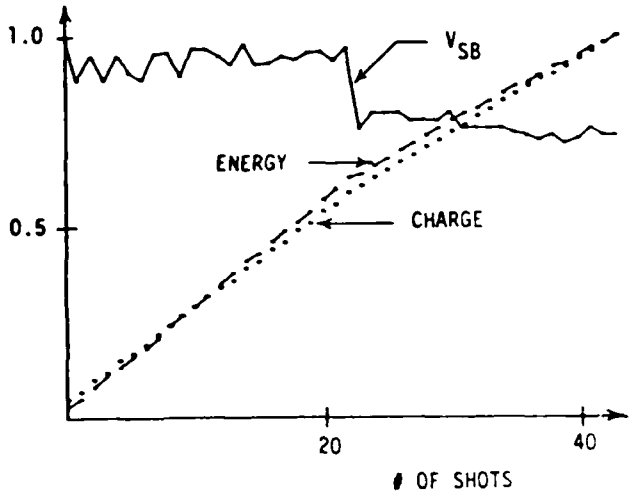


Fig. 11 Non Air Cooled Teflon Hold-Off Voltage Plot

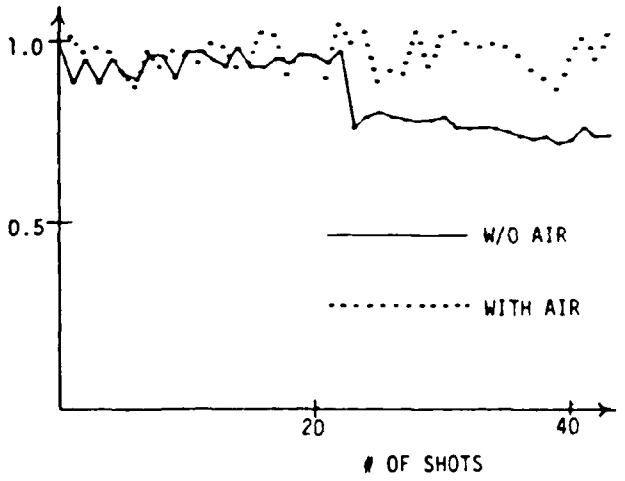


Fig. 12 Effect of Forced Air Cooling on Teflon

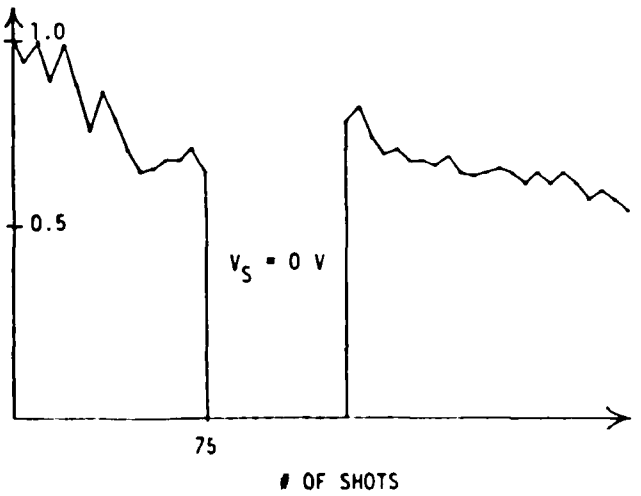


Fig. 13 Cold Recovery of Teflon


Fig. 14 Erosion Pattern on Teflon

## Discussion of Results

Johnson [2], measured no significant reduction of the hold-off voltage of G-10 and Delrin at relatively low current levels even after exposing them to several thousand shots at current levels of a few thousand Amperes. It is clearly evident that the erosion of dielectric materials depend very heavily on the maximum current as is especially evident for G-10. For Delrin, the hold-off voltage depends very heavily on the surface temperature and not the physical volumetric erosion. With no prior reports on Teflon it is impossible to make any type of contrasting comparison but Teflon seems very promising as a high current insulator for these types of applications.

## Acknowledgment

This work was supported by the Air Force Office of Scientific Research and the Army Research Office. The authors would like to extend their appreciation to Stephen Whiteside, Mike Ingram, Marie Byrd, and Tom Morris for their technical support.

## References

1. R.D. Curry, Master's Thesis, Texas Tech University, (May, 1984).

2. D. Johnson, Master's Thesis, Texas Tech University, (1982).

# A new design concept for field distortion trigger spark gaps

G. Schaefer, B. Pashaie, P. F. Williams[a], K. H. Schoenbach, and H. Krompholz
*Department of Electrical Engineering/Computer Science, Texas Tech University, Lubbock, Texas 79409*

(Received 16 August 1984; accepted for publication 30 October 1984)

**A common field distortion triggered spark gap utilizing geometric field enhancement at sharp edges usually operates in a cascade mode via the trigger electrode. A new trigger concept is proposed allowing strong field enhancement and direct breakdown between the two main electrodes. A test setup was designed to prove the feasibility of this concept. Experimental results on delay and jitter depending on percent breakdown voltage are presented. Best results achieved are a delay of 9 ns and a jitter of 2 ns at a self-breakdown voltage of 15 kV.**

## I. INTRODUCTION AND TRIGGER CONCEPT

Spark gaps using field distortion triggering are initially designed to provide hold-off voltage without trigger, and a trigger electrode shaped and located on an equipotential surface in the gap is then added. Triggering is accomplished by abruptly changing the potential of this electrode, thereby increasing the field between the trigger electrode and one of the gap electrodes. A typical example is the three electrode gap with a blade as a midplane trigger electrode located approximately half way between the main electrodes.[1] In the hold-off state the blade is in the plane of an equipotential and no field enhancement is generated at the edge of the blade. By changing the potential of the trigger electrode a very strong field enhancement at the edge can be produced. Since the maximum field enhancement occurs at the trigger electrode, however, the switch operates usually in a cascade mode in which the gap between one electrode and the trigger electrode is first closed (initiated by the trigger pulse) and then the second half of the gap is closed by the voltage across the switch.

To allow for geometrically enhanced field distortion and still to avoid cascade breakdown, field enhancement at an edge of one of the main electrodes can be used. This edge, however, must also be shielded in the hold-off state of the gap.[2] A schematic diagram of a spark gap based on this concept is shown in Fig. 1. In this device the trigger electrode is used to shape the electric field intensity in the gap in both the hold-off state and the triggering state. In the hold-off state the trigger electrode is kept at the same potential as electrode (1) and its surface towards the gap is shaped to minimize the geometric field enhancement effects at the main gap electrode, thereby maximizing the hold-off voltage. In the triggering state the potential of the trigger electrode is moved towards the potential of electrode (2). The trigger electrode subsequently serves to enhance the field, providing improved triggering, in two ways: moving the equipotential toward one gap electrode, and simultaneously turning on the geometric field enhancement. Such a trigger concept combines several advantages:

(1) Geometrically enhanced field distortion can be utilized.

(2) The strongest field enhancement occurs at one of the main electrodes, and breakdown, without cascading via the trigger electrode, is possible.

(3) Since the electrode can be shape without changing the hold-off performance, the field enhancement at a main electrode can be much larger than in common field distortion triggering.

(4) Shape and surface conditions of this main electrode do not determine the hold-off performance of the gap, making the gap more independent of erosion.

This concept would have to be applied to both main electrodes for protection of both.

## II. TEST SETUP

The experimental setup used to test this trigger concept is shown in Fig. 2. A parallel plane line was used as charging and transmission line (total impedance $\sim 12.5\ \Omega$). The switch consisted of eight individual gaps. The upper conductor of the lines was divided into eight individual stripes to provide for transit time insulation of the individual gaps (im-

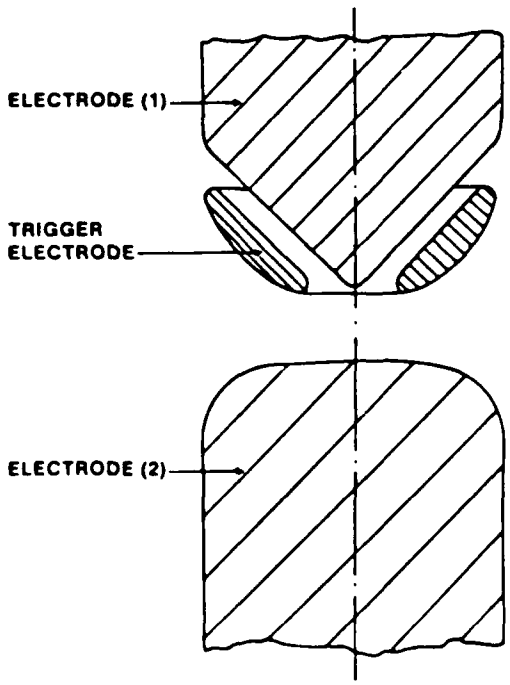


FIG. 1. Schematic diagram of a spark gap with geometrically enhanced field distortion at the main electrode

[a]P. F. Williams is now with the University of Nebraska, Department of Electrical Engineering, Lincoln, Nebraska 68508.

 0021-8979/85/072507-05$02.40 

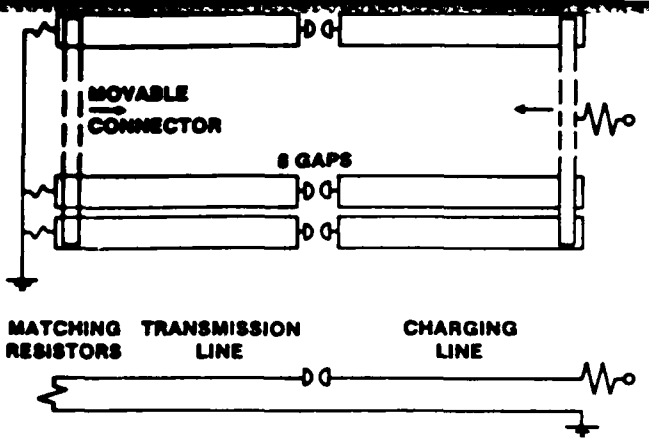


FIG. 2. Experimental setup.

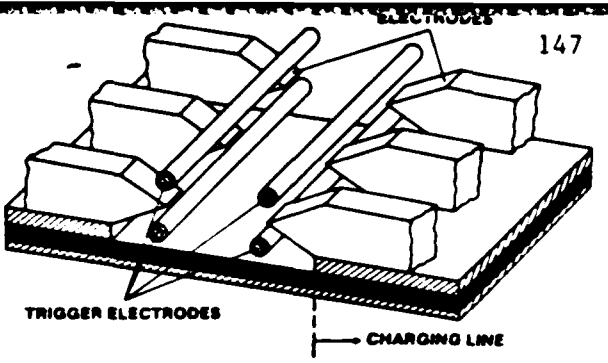


FIG. 4. Trigger electrode arrangement.

pedance/stripe ~ 100 Ω). The time constant for the transit time insulation could be varied in the range of 0–5 ns by moving metal bars connecting the individual transmission and charging lines.

Two different electrode configurations were used as shown in Fig. 3. The configuration (A) uses one triangular shaped main electrode (1) with a pair of two rods as trigger electrodes and one rounded main electrode (2), while the configuration (B) uses a symmetric configuration with two triangular main electrodes. The trigger electrodes in any case were pairs of rods triggering all eight individual gaps at the same time as demonstrated for the configuration (B) in Fig. 4. Bare stainless steel bars as well as bars covered with a dielectric material (glass tubes or epoxy) or with a resistive material (graphite-filled epoxy) have been used.

The trigger circuits are shown in Fig. 5. The trigger pulse was provided by a secondary gap which was operated in the self-breakdown mode and the breakdown voltage was adjusted through changing the secondary gap electrode separation. In the hold-off state the trigger electrodes are at the potential of the adjacent main electrode. When the secondary gap fires the potential of the trigger electrode is driven towards the potential of the opposite electrode.

For the circuits (A), (B), and (C) the full charging voltage of the line can be applied to the trigger electrode, while for the circuit (D) both trigger electrodes potentials move towards the midplane potential of the gap.

## III. EXPERIMENTAL RESULTS

The experiments performed concentrated on the spark gap performance with respect to delay and jitter depending on the applied voltage in percent of the breakdown voltage. The first experiments to determine the optimum type of trigger electrode and polarity were performed with an electrode geometry as shown in Fig. 3(a) and a circuit as shown in Fig. 5(a). Although the system could be triggered with either polarity, clearly better trigger results were obtained with the electrode (1) being at positive potential and the trigger electrode being driven towards a negative potential. Triggering

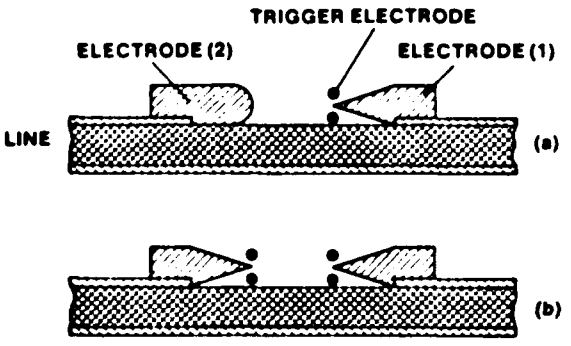


FIG. 3. Electrode geometries.

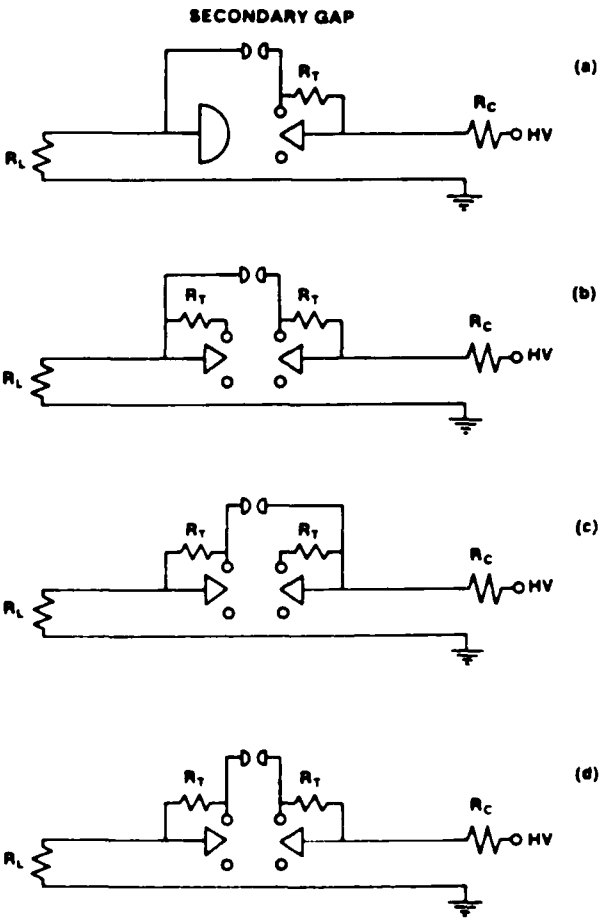


FIG. 5. Trigger circuits.

was possible with all types of trigger electrodes used. Bare metal rods as trigger electrodes had the disadvantage that a very precise symmetric alignment was necessary to avoid arcs between the trigger electrode and the main electrode. The best results were obtained with electrodes covered with a dielectric layer (glass or epoxy). Since the system performance did not depend on repetition rate ($10^{-2}$–1 Hz) surface charges on the surface of the dielectric seemed not to affect the performance of the trigger method at these low repetition rates. Surface charges could be eliminated with resistive layers instead of a dielectric, but arcing to the trigger electrode again required precise alignments unless layers with high resistivity were used (thickness ~0.5 mm, resistivity ~$10^6$ $\Omega$ cm).

The circuits in Figure 5(b) and 5(c) are equivalent to circuit (A) since only *one* pair of trigger electrodes changes its potential. No significant differences in the performance of the spark gaps was realized for these circuits as long as the right polarity was used. The performance of the gap with the circuit shown in Figure 5(d) was significantly worse with respect to delay and jitter.

The optimum position of the trigger electrodes was determined through measurements of the self-breakdown voltage shown in Fig. 6(a). In these experiments the pair of trigger electrodes was moved in the direction of the interelectrode spacing as shown in Fig. 6(b). The results clearly show the shielding of the edged main electrode resulting in an increase of the self-breakdown voltage of more than a factor of 2 compared to the gap without trigger electrodes. For optimum shielding no significant difference was observed for the two different types of trigger electrodes. The maximum self-breakdown voltage observed is nearly the uniform field breakdown value.

The following measurements on the trigger performance were obtained with the circuit in Fig. 5(a) and 5(d) and a positive charging voltage. All experiments are performed in atmospheric air. The rise time of the trigger pulse was of the order of 12 ns. Delay and jitter were determined by measuring the time between the voltage rise at the trigger electrode and at the main electrode. Figure 7 shows the delay depending on percent self-breakdown voltage (% $V_{SB}$) for the two circuits. It should be pointed out that the maximum voltage of the trigger pulse always equals the charging voltage in the circuit used. So with a decreasing value of % $V_{SB}$ the maximum voltage of the trigger pulse automatically decreased.

As demonstrated in Fig. 7, a minimum delay time of 9 ns was achieved with circuit Fig. 5(a) for a self-breakdown voltage of 15 kV. Above 90% $V_{SB}$ self-breakdown the delay does not significantly change with % $V_{SB}$ as required for

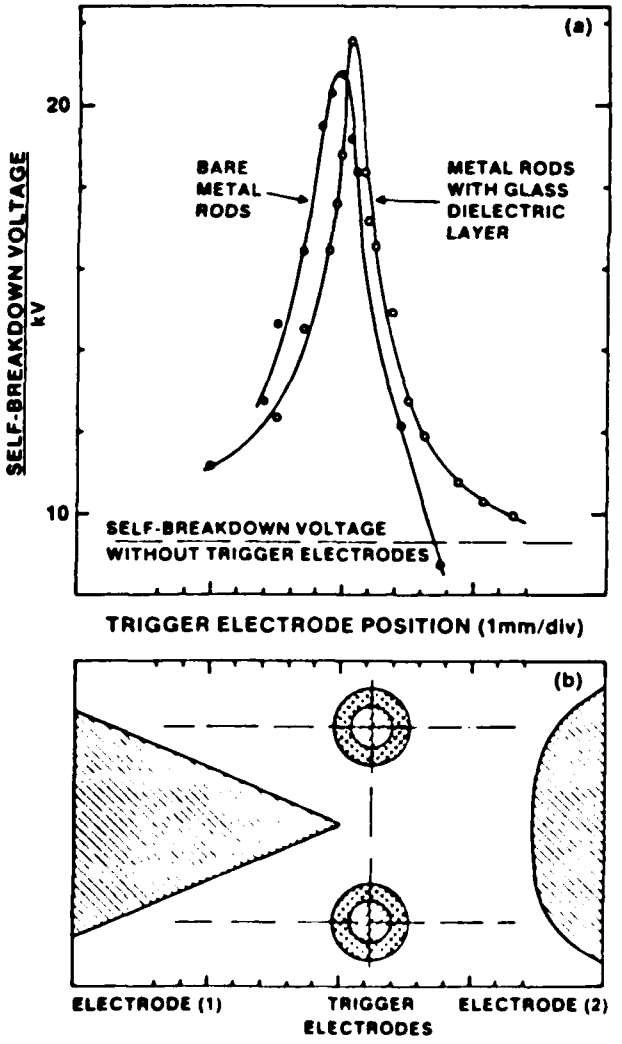


FIG 6. Self-breakdown voltage as a function of trigger electrode position (a) and electrode geometry (b)

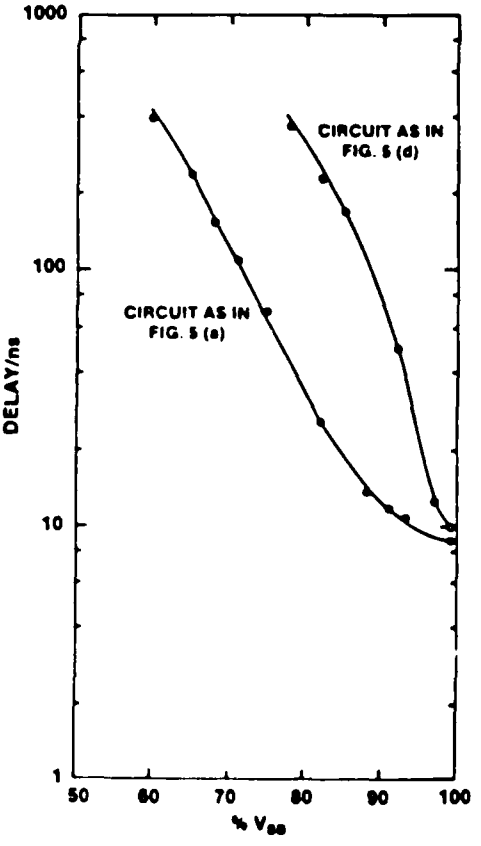


FIG 7. Delay vs % self-breakdown voltage for two trigger circuits ($V_{SB}$ = 15 kV)

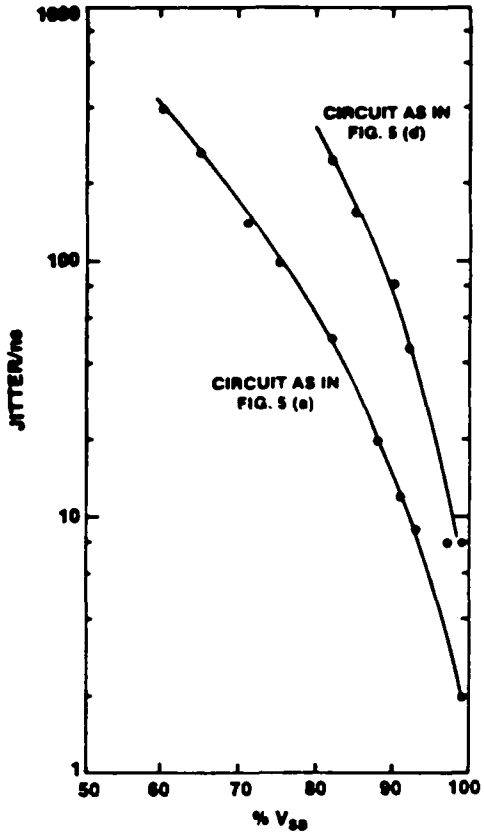


FIG. 8. Jitter vs % self-breakdown voltage for two trigger circuits ($V_{SB}$ = 15 kV).

multichanneling or parallel triggering of several gaps.

Figure 8 shows the jitter depending on % $V_{SB}$ for the same operation conditions as in Fig. 7. The jitter shown here is the *maximum* jitter in a series of 20 shots. Close to 100% $V_{SB}$ a jitter of ~2 ns could be achieved.

These results were also proven through parallel operation of the eight gaps with *one* pair of trigger electrodes for all gaps as shown in Fig. 4. With a transit time insulation of 5 ns, parallel triggering of all gaps was achieved if the charging voltage was kept above 95% $V_{SB}$. Fine adjustment of the self-breakdown voltage of each gap was difficult, however, and it is likely that some gaps were operated at significantly lower values of % $V_{SB}$.

## IV. DISCUSSION

The exploratory experiments demonstrate the feasibility of the proposed field distortion trigger concept. Results on delay time and jitter indicate that this method may be suitable for multichanneling and the parallel operation of spark gaps. Field code calculations are required to optimize the geometry for a maximum hold-off voltage in the off-state and maximum field enhancement in the on-state. Further experiments are required with a test gap allowing operation in different gases with variable pressure and a trigger circuit allowing the independent variation of % $V_{SB}$ and trigger pulse parameters.

The physical mechanisms responsible for triggering are of interest. Referring to Fig. 1, in the triggered state with the trigger electrode connected electrically to electrode (2), a very high electric field exists in the vicinity of electrode (1), while a much reduced field is produced in the main gap region between the trigger electrode and electrode (2). Two mechanisms for triggered breakdown seem possible. In the first, a streamer is launched inside the high field region, and propagates past the trigger electrode into the low applied field region. Propagation continues because the streamer body forms a weakly conducting needle connected to electrode (1), thereby producing high electric fields in the vicinity of its tip. After the streamer has traversed the gap, ohmic heating occurs and converts the weakly conducting channel left by the streamer into an arc channel.

In the second case, initial breakdown occurs through a purely Townsend mechanism. In this case, the criterion for breakdown is that sufficient electron avalanche multiplication occurs so that one electron leaving the cathode may reproduce itself at the cathode through the avalanching and other appropriate secondary processes. Here, the relevant quantity is the electron amplification due to impact ionization, $A = \int_0^d \alpha(E)dx$, where $E = E(x)$ is the applied field, assuming no space-charge distortion. $E$ is subject to the constraint $\int_0^d E(x)dx = V$, where $V$ is the gap voltage. Since the impact ionization coefficient $\alpha$ is a strongly increasing function of field for fields around the breakdown field, the amplification factor $A$ will be much larger for the highly nonuniform field produced in the triggering state than for the uniform field produced when the triggering electrode is connected to electrode (1). Thus, according to the Townsend criterion, the gap may be strongly overvolted in the triggered configuration, while remaining undervolted in the normal configuration.

The experimental data on delay suggest that both mechanisms occur. For applied voltages near the static breakdown voltage, the delay is found to be approximately 10 ns. Considering the substantially reduced field in the region between the triggering electrode and electrode (2), electrons emitted from the cathode [electrode (2)] would require ~50 ns to traverse the gap. Thus, it seems difficult to explain delay times less than about 100 ns with the Townsend mechanism. At the opposite extreme, delays approaching 1 $\mu$s are observed for low applied voltages. Even considering the dielectric relaxation time required for a streamer to produce the high field enhancements needed in this regime, a streamer transit time exceeding 100 ns seems unlikely. Additional time is required, of course, to convert this streamer channel into an arc channel but this time should not be a strong function of the applied voltage, and considering the 10 ns delay observed at 95% $V_{SB}$, should not exceed several tens of nanoseconds at 50% $V_{SB}$. Thus the low voltage data suggest that a Townsend mechanism is at work. The two mechanisms, streamer and Townsend, are not incompatible, and it is likely that there is continuous transition from one to the other as the gap voltage is reduced.

## V. PERSPECTIVES

The proposed trigger concept is well suited to combine field distortion with other trigger concepts to improve the switch performance. The important feature of this concept

here again is that the field enhancement occurs close to the surface of one main electrode and that this main electrode is partially shielded from the field in the hold-off state.

For trigatrons, it is well known that delay and jitter are drastically improved by overvolting the gap. Subsequently the combination of a trigatron trigger in the main electrode and a field enhancement generated by a field distortion in volume close to this trigatron electrode could provide for the same condition without the need to overvolt the total gap. The same considerations also hold for those laser triggered gaps where the laser spark is produced at or close to the surface of one main electrodes. The combination of the proposed field distortion concept with one of these trigger methods would therefore provide significantly improved performance in an undervolted main gap.

## ACKNOWLEDGMENTS

This work was supported jointly by the Air Force Office of Scientific Research and the Army Research Office.

[1]A. E. Bishop and G. D. Edmonds, Proc. IEE 113, 1549 (1966).
[2]J. K. Hepworth, R. C. Klewe, and B. A. Tozer, Proc. IEE 119, 1751 (1972).

# Field-enhancement calculations for a field-distortion triggered spark gap

B. Pashaie, G. Schaefer,[a] and K. H. Schoenbach[b]
*Department of Electrical Engineering, Texas Tech University, Lubbock, Texas 79409-4439*
P. F. Williams
*Department of Electrical Engineering, University of Nebraska-Lincoln, Lincoln, Nebraska 68588-0511*

(Received 5 June 1986; accepted for publication 1 October 1986)

We present the results of numerical field calculation which supplement a recent article in which we described a new design concept for field-distortion triggered spark gaps. The calculations verify the shielding and field enhancement assumptions made in the article, and they provide insight into the interaction of the design tradeoffs associated with simultaneously maximizing the holdoff voltage and the triggering capability of the gap.

Recently we described a new design concept for field-distortion triggered spark gaps.[1] Briefly, the design consisted of a pointed main gap electrode shielded in the untriggered state by the trigger electrode as shown in Fig. 1. Triggering was accomplished by changing the potential of the trigger electrode from that of the nearby pointed electrode to that of the opposite main gap electrode. In this configuration a very high field is generated at the tip of the pointed main gap electrode, causing large field enhancements and rapid breakdown of the main gap. We also reported the results of proof-of-concept experiments which demonstrated the validity of the design. With a simple switch we obtained a closing delay of $\sim 10$ ns, with a jitter of $\sim 2$ ns, for charging voltages of 90% of the static, self-breakdown voltage, $V_{SB}$.

We have extended this work by calculating numerically the electric field for a gap geometry similar to that we reported on earlier. These calculations verify the shielding of the pointed electrode by the trigger electrode and the sensitivity of this shielding to the position of the trigger electrode. The calculations also verify the presence of very high field enhancements in the triggered state. In this communication we present the results of these calculations and discuss their application to the design of field-distortion triggered spark gaps such as we described previously.

The numerical code we used for the field calculations was written by researchers associated with the Tetra Corporation, Albuquerque, NM, for analyzing the field distribution in discharges for lasers and switches.[2,3] Briefly, the code operates by determining a set of boundary-fitted coordinates which match the given boundary value surfaces. Laplace's equation for the electrostatic potential is then solved in these coordinates using a successive over-relaxation technique, and the electric field is determined by taking the gradient of this potential numerically. Although the configuration of interest here contains three electrode surfaces, the potential of two of these surfaces is the same in the two states of interest (holdoff and triggered) so that the boundary condition specification for the code consisted of two surfaces, one surface in each case containing two electrodes.

Figure 2 shows the electrode geometry used in these calculations. The gap is taken to have cylindrical symmetry, and the figure shows a cross section containing the gap axis. The experiments we reported utilized a linear rather than cylindrical geometry, but the fields in the two cases should be similar. The gap field was calculated using the code for both the holdoff and the triggered cases for a number of positions of the triggered electrode. In either case, the trigger electrode was connected to one of the main gap electrodes. A $17 \times 17$ element grid mesh was used in the calculations.

Figures 3(a) and 3(b) show the equipotential lines for the holdoff and triggered cases, respectively, for a particular positioning of the trigger electrode corresponding to the maximum field enhancement factor at the tip of the pointed electrode. The efficiency of the shielding of the pointed electrode by the trigger electrode in the untriggered state is apparent in Fig. 3(a), where the field is seen to be reasonably uniform throughout the gap region, with no field enhancement in the vicinity of the pointed electrode. In the triggered state, on the other hand, shown in Fig. 3(b), the field is highly nonuniform, with large fields appearing near the tip of the pointed electrode. In this case the maximum field is of the order of 100 times the uniform field value. Corona and other phenomena associated with high overvoltages would be expected to appear promptly at the electrode tip with triggering.

We can define a field enhancement factor $\beta$ as the ratio of the maximum field at the surface of an electrode, $E_{max}$, to the mean field in the gap, $\langle E \rangle$, $\beta = E_{max}/\langle E \rangle$. Figures 4(a)

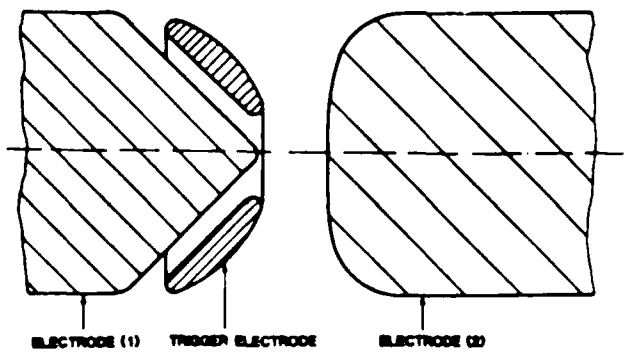


FIG. 1. Schematic drawing of the triggering concept discussed in Ref. 1

[a] Present address: Department of Electrical Engineering, Polytechnic University of New York, Farmingdale, NY 11735.
[b] Present address: Department of Electrical Engineering, Old Dominion University, Norfolk, VA 23508.

 0021-8979/87/020790-03$02.40 

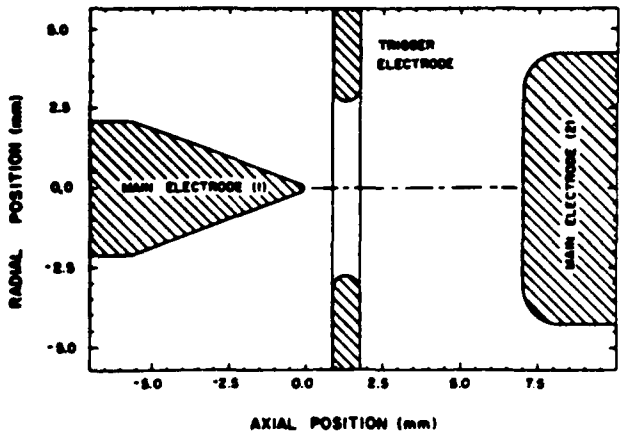


FIG. 2. Drawing showing the electrode geometry used in the calculations reported here.

and 4(b) show $\beta$ at both the pointed main gap electrode and the trigger electrode as a function of trigger electrode position in the holdoff and triggered states, respectively. In these figures the position refers to the center plane of the trigger electrode. When the trigger electrode is placed well behind the tip of the pointed electrode, we see that the field enhancement factor $\beta$ in the holdoff state [Fig. 4(a)] reaches a value of $\sim 6$, which corresponds to the field enhancement of the bare, unshielded, pointed electrode. For trigger electrode

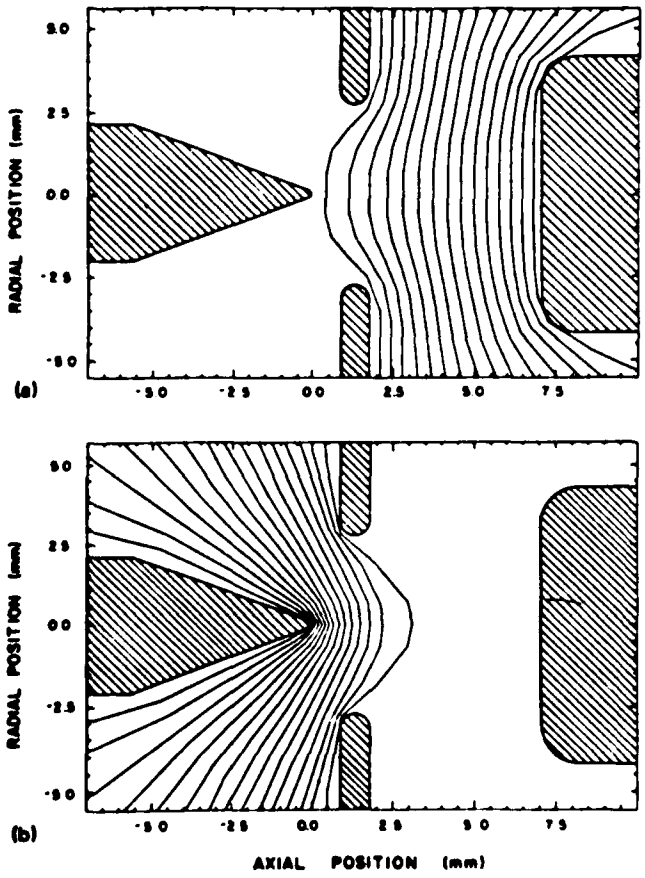


FIG. 3. Plots showing the calculated equipotentials for the spark gap. The position refers to the center plane of the trigger electrode. (a) Holdoff state. (b) Triggered state.

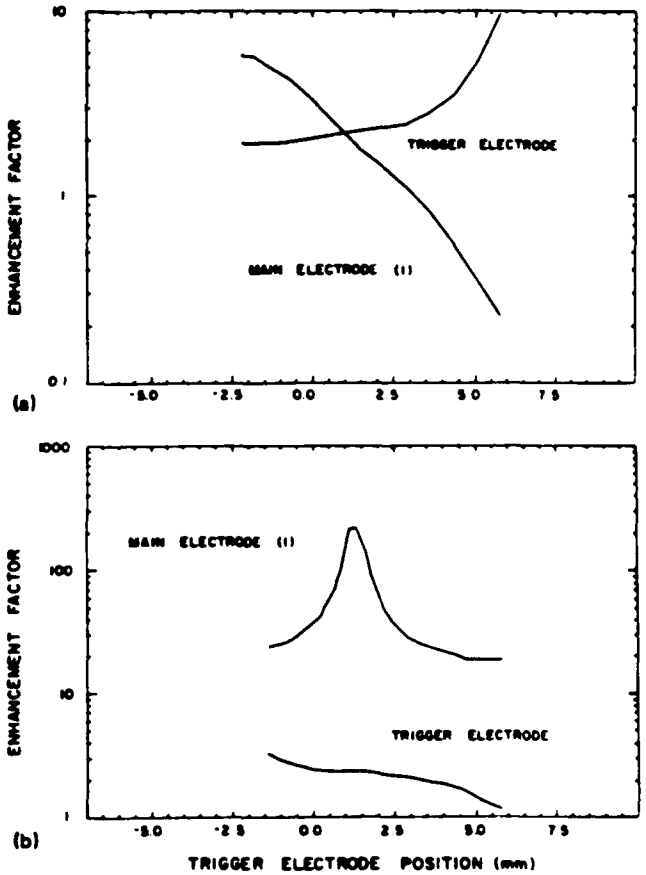


FIG. 4. Plots showing the maximum field enhancement factor at the pointed electrode and the triggered electrode as a function of the position of the center plane of the trigger electrode. (a) Holdoff state. (b) Triggered state.

positioning just in front of the adjacent main electrode point, the field enhancement factor falls to nearly unity, indicating that the holdoff voltage of the gap will be comparable to that of the uniform field gap. Figure 4(b) shows that in the triggered state the maximum field enhancement at the main gap electrode peaks sharply for a trigger electrode position about 1.2 mm in front of the main electrode tip. For this design the trigger electrode position for maximum triggered state enhancement is nearly the same as the position for minimum holdoff state enhancement, a desirable condition for achieving maximum holdoff voltage with maximum triggering capability.

In the experimental work we previously reported,[1] we found that the breakdown voltage in the untriggered state was a strong function of the position of the trigger electrode, peaking sharply at a position just in front of the main electrode point. In order to compare this empirical result with our field calculation results, we assume that the breakdown condition is determined by the maximum field found anywhere in the gap. Thus, the ratio of the actual breakdown voltage to the breakdown voltage of a comparable uniform field gap will be proportional to the inverse of the field enhancement factor, $1/\beta$. In Fig. 5 we show $1/\beta$ and the empirically determined breakdown voltage, both normalized with respect to the maximum value in the untriggered case, plotted against trigger electrode position. The results are similar in both the experimental and theoretical cases. There

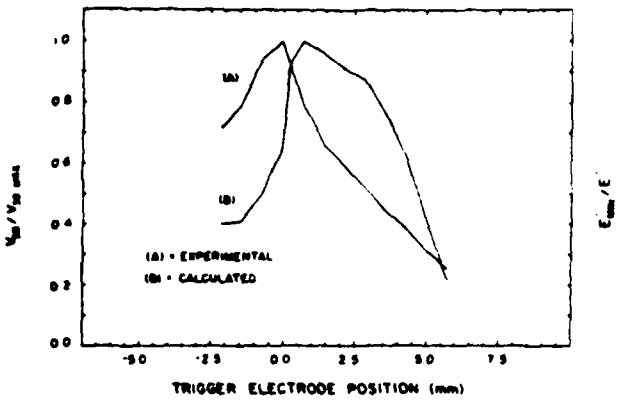


FIG. 5. Plots comparing the numerical estimates with experimental results for the maximum holdoff voltage in the untriggered state as a function of trigger electrode position. (a) Experimental results from Ref. 1 plotted normalized to the maximum holdoff voltage observed. (b) Plots of the inverse of the maximum field anywhere in the gap ($E'$) as a function of electrode position, normalized to the minimum value of $E'$ ($E'_{MIN}$). In the simple model discussed in the text, the trigger electrode position producing $E'_{MIN}$ should produce $V_{SB\,MAX}$.

is a small difference in the position of the maximum breakdown voltage and the minimum field enhancement factor, but such a difference is not surprising in light of the difference between the geometries in the experiment and calculation, and the simplicity of the assumption that the breakdown voltage is determined solely by the maximum value of the field anywhere in the gap.

We have shown that with proper understanding of the physical mechanisms involved in the triggered breakdown of spark gaps, new and potentially improved designs for these devices can be generated. Clearly, more experimental work is required to refine and determine the limits of the design concept we proposed earlier.[1] Of perhaps more importance, however, is the development of understanding of the triggered breakdown process itself in these gaps. We believe that breakdown is initiated by the creation of a streamer in the highly field-enhanced region just outside the pointed main gap electrode which then propagates across the gap. Very little quantitative information is available, however, about the propagation of streamers in such highly nonuniform fields. Even less is known about the propagation of these streamers in the substantially reduced field present in the gap between the trigger and the opposite main gap electrodes. It is quite possible that an optimum design would involve setting the trigger electrode potential at some value between the potentials of the two main gap electrodes in the triggered state, or using a selected trigger pulse length in order to provide high fields for streamer initiation, but then to provide a field near the uniform field value for propagation across the main gap.

The authors are grateful to Dr. W. Moeney and Dr. M. von Dadelszen of Tetra Corporation for making the field calculator code available to us and for helpful comments and advice on using it. This work was jointly supported by AFOSR and ARO.

[1] G. Schaefer, B. Pashaie, P. F. Williams, K. H. Schoenbach, and H. Krompholz, J. Appl. Phys. 57, 2507 (1985).
[2] P. J. Roache, W. M. Moeny, and J. A. Filcoff, in *Proceedings of the 3rd IEEE Pulsed Power Conference, Albuquerque, NM*, edited by T. H. Martin and A. H. Guenther (Texas Tech Press, Lubbock, 1981), p. 282.
[3] P. J. Roache, H. J. Happ, and W. M. Moeny, in *Proceedings of the 4th IEEE Pulsed Power Conference, Albuquerque, NM*, edited by T. H. Martin and M. F. Rose (Texas Tech Press, Lubbock, 1983), p. 426.

# Transmission Line Current Sensor

H. Krompholz, K. Schoenbach, and G. Schaefer

Department of Electrical Engineering
Texas Tech University
Lubbock, Texas 79409

**Abstract**

A matched slow wave transmission line is used as a current probe. It provides a linear response, fast risetime (< 2 ns) and high sensitivity ( ≈1 V/A) for current pulses up to microsecond duration. The duration of a distortionfree monitored current pulse is limited by dispersion in the slow wave transmission line.

## 1. Inductive Current Sensors

Rogowski coils are commonly used as current sensors in pulsed power experiments. They consist of a helical coil placed around the current to be measured with an induced voltage related to this primary current. In the usual mode of operation, the coil is terminated with a small resistance R. The output signal, i.e. the voltage measured across this resistor is

$$V(t) = \frac{R}{N}\int \frac{dI}{dt}(t')\exp\left(-\frac{R}{L}(t'-t)\right)dt' \qquad (1)$$

where N = number of turns
L = coil inductance
dI/dt = time derivative of the current to be measured.

The risetime of these devices is usually in the order of 1 ns with a sensitivity [1] R/N in the order of $10^{-3}$ V/A. For high current experiments this sensitivity is sufficient, for currents less that 100 A, however, characteristic output signals are in the millivolt range and therefore susceptible to noise.

## 2. Transmission line current sensor

A more detailed consideration of this current transformer - especially for temporal variations of the primary current in the nanosecond regime - has to take transit time effects into account [2]. In this approximation the distributed capacitance between coil and surroundings (e.g. an electrostatic shield) enters as additional parameter. The equivalent circuit of the transformer can be described as a transmission line (Fig. 1) with distributed induced voltage sources

$$V_{IND}dz = -\frac{N\mu_0}{(2\pi\rho)^2}S\frac{dI}{dt}dz \qquad (2)$$

where ρ is the major diameter, S is the cross-sectional area of the coil. The probe current i is then described by the inhomogeneous wave equation

$$\frac{\partial^2 i}{\partial t^2} - \frac{1}{L'C'}\frac{\partial^2 i}{\partial z^2} = \frac{1}{N}\frac{d^2 I}{dt^2} \qquad (3)$$

and the boundary conditions: shorted at one end, terminated with the resistor R at the other end.

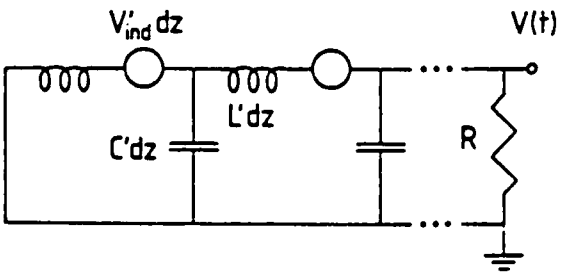


Fig. 1 Equivalent Circuit

In order to illustrate the response of such a transmission line current sensor, an input current I(t) as a unit step function is assumed producing output signals as sketched in Fig. 2. Using the lumped parameter description for $R \ll \sqrt{L/C}$, an exponentially decaying output signal is produced, whereas the transmission line properties generate a stepwise decreasing function due to reflections at both ends of the line. If the terminating resistance is large compared to the line impedance, the output is oscillatory with a periodicity of four times the transit time.

Reprinted from PROCEEDINGS OF THE IMTC — IEEE INSTRUMENTATION AND MEASUREMENT TECHNOLOGY CONFERENCE, March 20-22, 1985

For the matching terminating resistor ($R=\sqrt{L/C}$) the output voltage is exactly proportional to the primary current for times smaller than twice the transit time

$$T = \sqrt{LC} \qquad (4)$$

resulting in the response on the general input I(t)

$$V(t) = \frac{R}{2N}\,[I(t) - I(t-2T)] \qquad (5)$$

From equations (4) and (5) it is obvious, that for a transmission line transformer the sensitivity and characteristic time of the system can be adjusted independently from each other, whereas in common Rogowski coils there is always a trade-off between sensitivity and decay time.

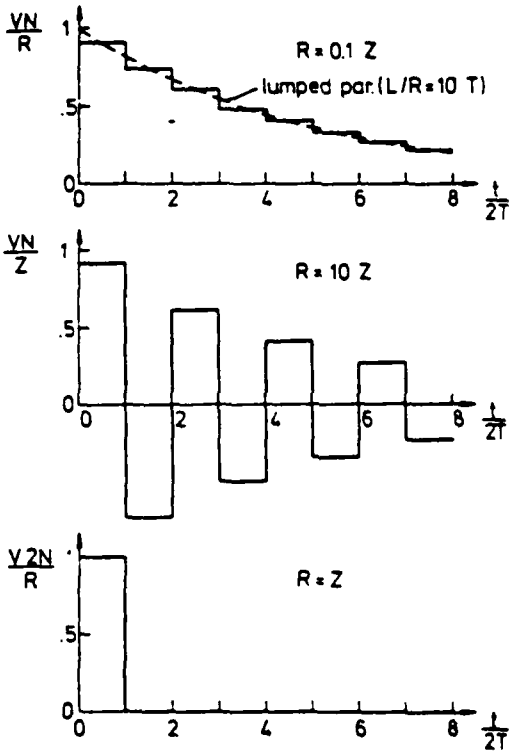


Fig. 2 Unit Step Response for Different Load Resistances

For the transmission line probe, two modes of operation and evaluation depending on the ratio of pulse duration and twice the transit time are possible. If the duration of the primary current is larger that 2T, a simple discrete time shift deconvolution (inversion of equation (5)) allows reconstruction of the primary current from the measured voltage. If, on the other hand, the transit time is increased to values larger than the duration of the primary current pulse, the probe acts as an ideal current transformer (output voltage exactly proportional to input current). High sensitivities in the order of 1 V/A are possible, and the transit time T can be increased by either high values of the distributed inductance or the distributed capacitance.

## 3. Experimental device

In order to utilize the concept of a waveguide current probe with high transit time, a matched device has been constructed which consists of a helix in a slotted metallic torus with high capacitance between helix and torus [3] (Fig. 3, Data are given in Table 1).

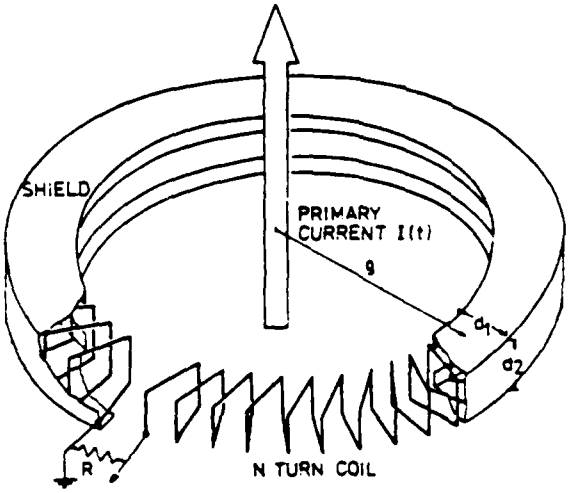


Fig. 3 Experimental Current Probe

Table 1

| | | |
|---|---|---|
| l | (number of turns) | :400 |
| ρ | (major radius) | :8.7 cm |
| $d_1=d_2$ | (sides of cross section) | :1.06 cm |
| L' | (inductance per unit length) | :1.518 H/cm |
| C' | (capacitance per unit length) | :19.2 pF/cm |
| z | (characteristic impedance) | :280 |
| v | (propagation velocity) | :$1.9\times10^8$cm/s |
| T | (transit time) | :290 ns |
| $R_w$ | (wire resistance) | :1.8 |
| $S=\frac{z}{2N}$ | (sensitivity) | :0.35 V/A |

The probe has been tested in a coaxial 50-Ohm cavity with rectangular input current pulses of variable duration. Examples for input current pulses and responses are depicted in Fig. 4. Figure 4a shows the risetime in the order of 2 ns. For input current duration < 200 ns the output is proportional to the input, for higher input current durations increasing oscillations are observed indicating deviations from the simple transmission line model (Fig. 4b, 4c).

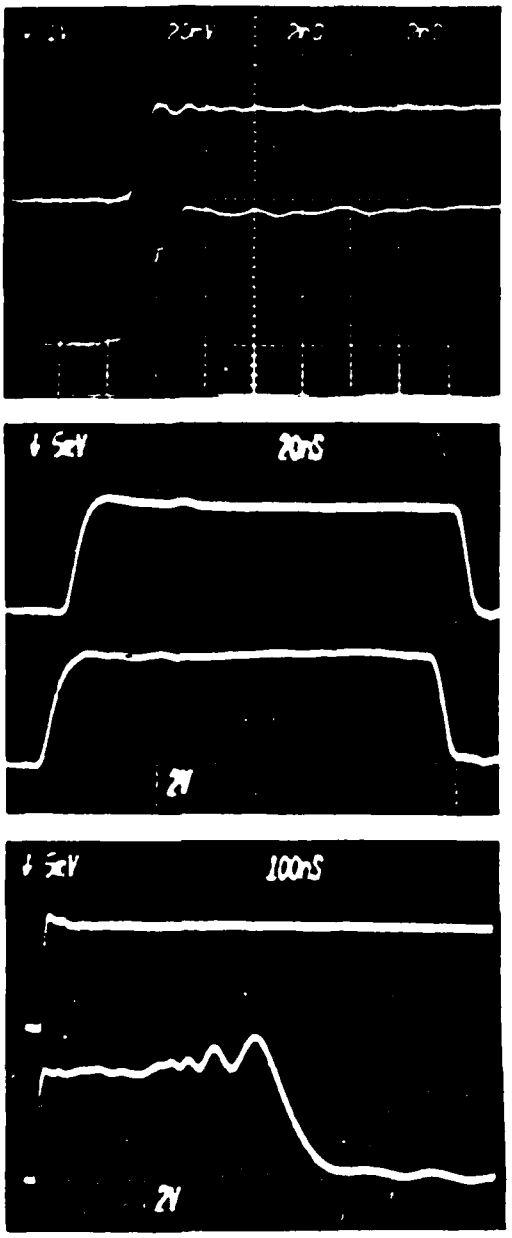


Fig. 4 Measured Probe Responses
a) risetime
b) input pulse duration 180 ns
c) step function input

4. Limitations due to dispersion

In order to describe the oscillation effects quantitatively, an analysis of the system using field theory has been performed. The helical inner conductor was modeled as "sheeth-helix", i.e. an anisotropic conductor with infinite conductivity in the direction of the helix and zero conductivity in all other directions. The slit in the outer conductor which allows the penetration of the primary current magnetic field into the probe prevents azimuthal current flow. This structure allows modelling of the outer conductor with currents only in axial direction.

Maxwell's Equations for this system have been solved resulting in the dispersion relation for waves travelling in axial direction [4]

$$\frac{\omega^2}{c^2\tau^2}\cot^2\psi = -\frac{I_0(\tau a)}{I_1(\tau a)K_1(\tau a)I_0(\tau b)} \cdot \left[I_0(\tau a)K_0(\tau b) - I_0(\tau b)K_0(\tau a)\right] \qquad (6)$$

where $\tau^2 = k^2 - \frac{\omega^2}{c^2}$

$\psi$ is the angle between helical and azimuthal direction

$I_0$, $I_1$, $K_0$, $K_1$ modified Bessel functions

a,b radii of inner and outer conductor.

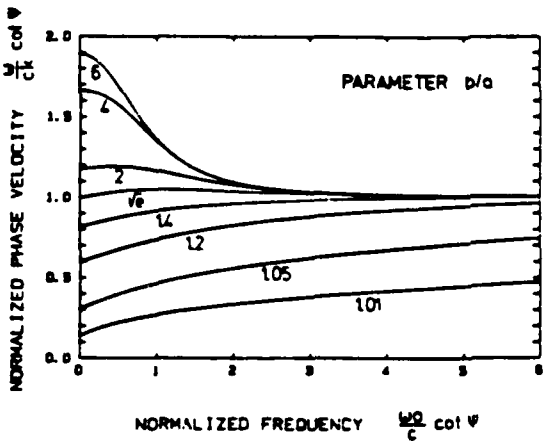


Fig. 5 Dispersion relation

The phase velocity $\omega/k$ as a function of frequency $\omega$ is plotted in normalized units in Fig. 5. The previously discussed transmission line behavior with neglected dispersion is given by the limit $\omega \to 0$. Minimum dispersion is achieved for the ratio of radii b/a of $\sqrt{e}$. Using the equivalent data of the experimental device in Table 1, Fourier transform has been used to calculate its unit step response. The result is plotted in Fig. 6, where an

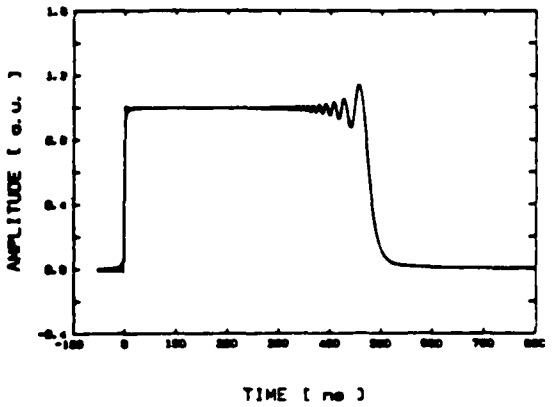


Fig. 6 Calculated unit step response

additional damping factor proportional to the frequency has been assumed. This factor describes dielectric losses in the system. The agreement between measured and calculated behavior is good considering the simplifying model assumptions.

To minimize dispersion, the concept of increasing the transit time by increasing the capacitance has to be abandoned, since the ratio of radii is fixed to the value of $\sqrt{e}$. Only the inductance (number of turns per unit length) remains as a variable determining the transit time. Results of pulse response calculations for an optimized coil are plotted in Fig. 7.

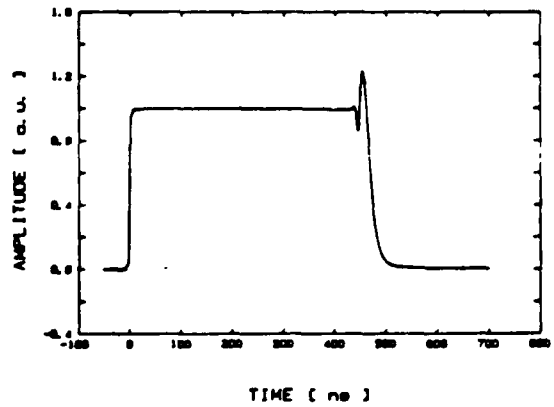


Fig. 7. Calculated unit step response of optimized probe (input pulse risetime 2 ns)

## 4. Discussion

Consideration of current sensors as transmission lines including dispersion show the feasibility for construction of distortionfree current sensors with a large transit time of up to the microsecond range and a sensitivity in the order of 1 V/A. This sensitivity is high enough to measure current amplitudes in the order of milliamperes with standard oscilloscopes.

Further applications of the discussed helical slow wave structures are in the field of compact pulse generators for rectangular pulses with a duration of several microseconds and rise and fall times in the nanosecond regime [5].

Limitations are imposed by dispersive effects, however, through careful design it is possible to minimize these effects for applications in electrical diagnostics as well as for pulse forming networks.

References

1. M. DiCapua in "Measurements of Electrical Quantities in Pulse Power Systems:, edited by R.M. McKnight and R.E. Hebner (NBS, Colorado 1982) p. 175.

2. W. Stygar and G. Gerdin, IEEE Trans. Plasma Science, PS-10, p. 40 (1982).

3. H. Krompholz, J. Doggett, K. Schoenbach, J. Gahl, C. Harjes, G. Schaefer, and M. Kristiansen, Rev. Sci. Instrum., 55, 127 (1984).

4. D.A. Watkins, "Topics in Electromagnetic Theory", Wiley, p. 62 (1958).

5. H. Krompholz, K. Schoenbach, G. Schaefer, "Pulse Forming Network Using a Helical Delay Line", to be published.

---

This work was supported by the Air Force Office of Scientific Research (AFOSR) and the Army Research Office (ARO).

Proc. 17th Power Mod. Symp.
Seattle, WA, June 1986

Appendix S

# SLOW WAVE LINE-TYPE PULSERS*

H. Krompholz, J. R. Cooper, J. Doggett[1],
K. H. Schoenbach[2], and C. Schaefer[3]
Texas Tech University
Dept. of Electrical Engineering/Computer Science
P. O. Box 4439
Lubbock, TX, 79409

## Abstract

Two different high voltage, line-type pulsers, each with a risetime of less than 10 ns and a potential pulse length greater than 1 μs, have been designed, constructed and tested. These devices produce square pulses which remain extremely flat for the majority of the pulse length. The pulsers can both be described as an intermediate step between a transmission line, with its distributed capacitance and inductance, and a pulse forming network constructed with discrete components. The devices can be designed to have impedances less than 10 Ω, can be switched by conventional spark gaps, are extremely compact in size, and can be operated repetitively. The configuration of such pulsers is similar to that of certain types of delay lines. Slow wave structures such as this are by their nature dispersive, which causes some distortion of the tail of the pulse. This distortion can be eliminated by means of a crowbar circuit.

## Introduction

In many pulsed power and laser engineering applications, there is a need for a high voltage pulser which has a risetime of the order of nanoseconds, a constant voltage amplitude throughout the pulse, a relatively long pulse duration, and a moderately low impedance. A charged piece of high voltage cable can produce a pulse with a fast risetime and a flat top, but the pulses are usually limited in length to less than 100 to 200 ns due to practical considerations. Also, the choice of impedances available for these cables is rather small. A pulse forming network can deliver a long pulse and can be designed for a specific impedance, but these devices tend to have slow risetimes (>10% of the pulse width) and pulse amplitudes which vary considerably during the duration of the pulse due to the absence of the higher harmonics of the pulse [1]. If the load impedance is well defined, an auxiliary network to the PFN can be used to decrease the risetime and to smooth the top of the pulse, but this technique is not always practical to use. This information suggests that a hybrid device combining the features of discrete component and distributed parameter pulsers may be a solution when a fast risetime, long pulse length pulser is desired.

The initial motivation for this work was the need for a pulser with a risetime of less than 10 ns and a pulse with a constant voltage amplitude to drive a discharge for use in diffuse discharge opening switch research [2]. The pulse width was desired to be longer than 400 ns, and the device was required to have an impedance of 50 Ω and to operate at voltages greater than 20 kV. In addition, the pulser was desired to be compact, light in weight, inexpensive, and simple to construct. Two different designs for "hybrid" pulsers were investigated in an effort to meet these specifications. The configuration and design considerations of each of these is described below.

## Design and Theoretical Considerations

One of the devices which was considered is shown in Fig. 1. It is a coaxial system with copper tape wound in a helix around a form for the center conductor and a solid outer conductor. The outer conductor has a slit in the axial direction which prevents current flow in the azimuthal direction. The dielectric for this pulser is water. Devices similar

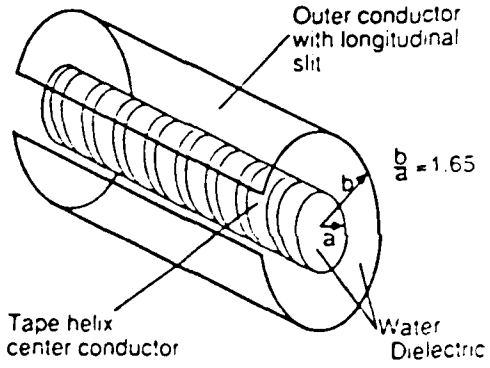


Fig. 1. Helical line pulser.

to this have been the subject of previous investigations [3]. A qualitative description of the operation of this pulser is fairly straightforward. The inductance per unit length for this device, L', is given primarily by the inductance of the helical center conductor. C', the capacitance per unit length in the pulser, is, in the first approximation, the same as if the center conductor were not a helix but a solid conductor. The characteristic impedance $Z_o$ of a transmission structure is $\sqrt{L'/C'}$ and its wave velocity is $1/\sqrt{L'C'}$. In this device, L' is much larger than that of a coaxial device of the same size with a solid center conductor. C' is also larger in this case than it would be in a polyethylene dielectric coaxial cable of the same size due to the high electric permittivity of the water which is used as the dielectric for the helical line. Since L' and C' are both much larger than their counterparts in an ordinary coaxial line, the wave velocity is much smaller and as a consequence the pulse length characteristic of this device is much longer than the pulse length produced by a coaxial cable of the same dimensions. By varying the inductance of the center conductor or the spacing between the inner and outer conductors, the characteristic impedance of the device can be varied

---

* This work supported by AFOSR Grant # 84-0032

Authors presently with:
1. Martin Marietta Denver Aerospace, P. O. Box 179, Denver, CO, 80201
2. Old Dominion University, Dept. of Electrical Engineering, Norfolk, VA, 23508
3. Polytechnic University, Dept. of Electrical Engineering, Rte. 110, Farmingdale, NY, 11735

One difficulty associated with slow wave pulsers is the fact that all such devices are dispersive, i. e., the phase velocity in the device is a function of frequency. This dispersion causes degradation of the pulse shape which tends to increase with increasing pulse length. It has been shown by Watkins [4] that for a coaxial, helical center conductor delay line, there is an optimal value for the ratio of the radii of the inner and outer conductors which minimizes the dispersion of the pulse. An illustration of this is given in Fig. 2., which is a plot of the normalized phase velocity versus the normalized frequency of the wave which is propagating in the device. In this

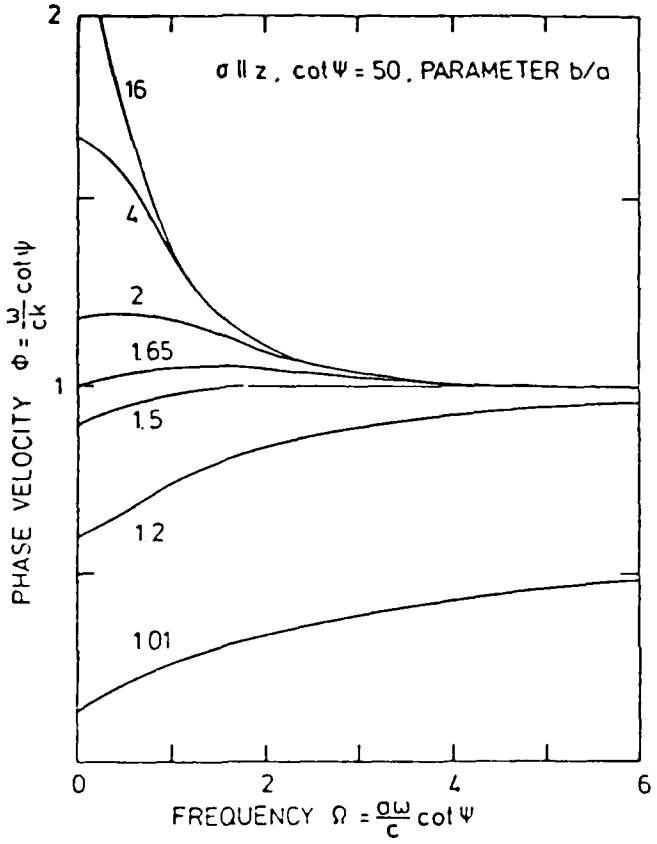


Fig. 2. Phase velocity vs. frequency in the helical delay line.

figure, a is the inner radius of the device, b is the outer radius, c is the speed of light in a vacuum, k is the wave number, ω is the frequency, and ψ is the angle between the direction of the conductor in the helix and the azimuthal direction. It can be seen from the figure that a ratio of outer conductor diameter to inner conductor diameter of 1.65 is the optimum value to minimize the dispersion in a helical coaxial line. Note that this constraint eliminates the possibility to change the device impedance by varying C', so the only way to tune the pulser to the desired impedance is to vary the inductance of the center conductor.

The second type of slow wave pulser examined in this work is shown in Fig. 3. It consists of alternating conducting and magnetic material disks. The conducting disks are electrically connected to a conductor running through their centers, and the magnetic material disks are insulated from both the conducting disks and the center conductor which connects them. This entire structure is covered by a layer of mylar, then another layer of copper sheet. The copper sheet is the outer conductor of the coaxial device, the alternating disk structure is the center conductor, and the mylar layer is the dielectric

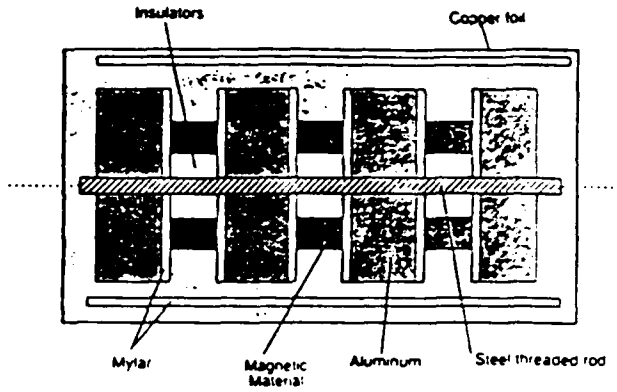


Fig. 3. Magnetic material pulser.

between the two. From the figure it can be seen that the small distance between the conducting disks and the outer conductor causes the capacitance per unit length C' of this device to be very large compared to a coaxial transmission line of the same outer diameter and an impedance in the range of typical coaxial cables (17 - 75 Ω). The magnetic material disks have a high relative magnetic permeability $\mu_r$, which causes the inductance per unit length L' to be much larger than that of a corresponding coaxial transmission line. Therefore, as in the helical line, the wave velocity $1/\sqrt{L'C'}$ is much lower than in a normal transmission line and the pulse length is much longer. The impedance (and the pulse length as well) can be varied by changing the size of the conducting disks or the magnetic material disks, by changing the dielectric thickness, by changing the relative permittivity $\epsilon_r$ of the dielectric, or by changing the $\mu_r$ of the magnetic material. Work is currently in progress to model this device in a similar manner to the modeling of the helical line pulser.

## Results and Conclusions

A 50 Ω, 1 meter long helical line of 10 cm outside diameter and 6.06 cm inside diameter was constructed to test the theory presented above. The inner conductor is a 64 turn 1.27 cm wide tape helix with approximately 0.3 cm spacings between turns. The helical line was tested at low (0 - 50 V) voltages initially as the charged line in a mercury reed switch pulser to determine its characteristics. The oscilloscope trace of the voltage output is shown in Fig. 4. The initial part of the pulse displays some overshoot and the effects of the dispersion of the pulse are evident its tail. The risetime of the pulse is less than 5 ns and is limited by the inductance of the connection with the reed pulser. The top of the pulse is flat for 400 ns, and the FWHM pulse width is approximately 550 ns, which corresponds to a transit rate of 275 ns/m. For comparison, note that the small pulse just before the beginning of the helical line pulse in Fig. 4 was the pulse produced by the cable connecting the helical pulser to the mercury reed switch. This cable is 1 meter long, as is the helical pulser, but its pulse length is significantly shorter.

The helical line has also been tested at higher voltages. The test circuit consisted of a 0.1 μF capacitor which was used to pulse charge the line through a spark gap and a 350 Ω isolation resistor. The pulse produced by the line was switched through another spark gap to a 50 Ω low inductance load resistor. A Pearson coil was used to measure the current delivered to the load by the pulser. Figs. 5a, 5b, and 5c show the output pulses produced at charging

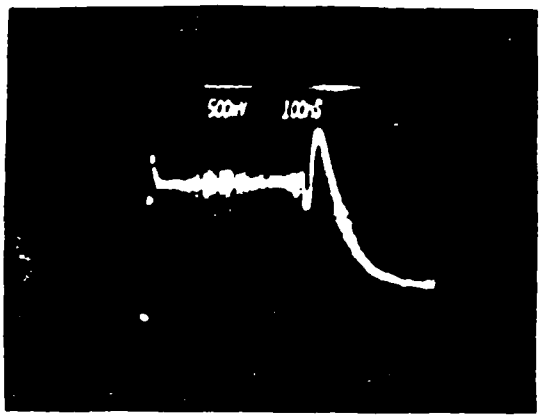

Fig. 4. Output pulse of the helical line pulser at a charging voltage of 4 V. The transit rate is 275 ns/m.

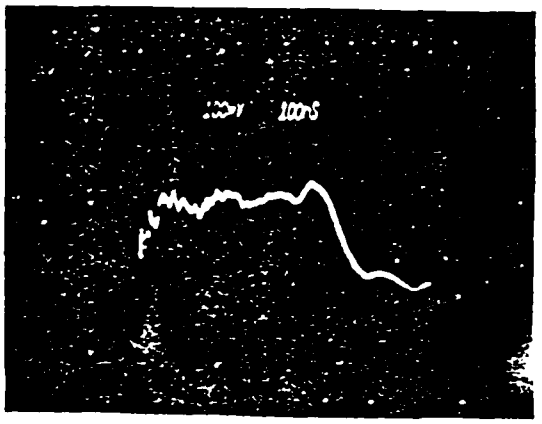

Fig. 5a). Output pulse of the helical line pulser at a charging voltage of 4.5 kV.

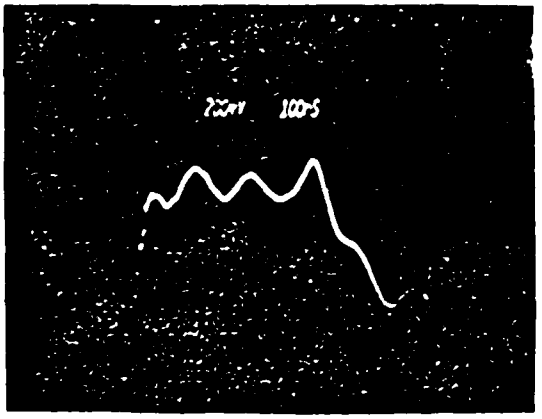

Fig. 5b). Output pulse of the helical line pulser at a charging voltage of 6 kV.

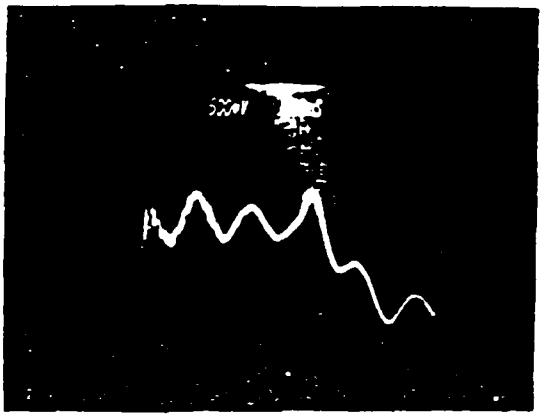

Fig. 5c). Output pulse of the helical line pulser at a charging voltage of 14 kV.

voltages of 4.5, 6, and 14 kV, respectively. In these figures it appears that the high frequency components of the pulse are being attenuated. It is believed that this is due to impurities in the water dielectric and thus could be eliminated in a cleaner system.

A device to test the magnetic pulser concept has also been constructed. The device has an outer diameter of slightly over 7.8 cm, a conducting disk diameter of 7.62 cm and thickness of 1.1 cm. The magnetic disks are a powdered nickel-iron alloy with a $\mu_r$ of 200. They are square toroids with an outer diameter of 6 cm and a thickness of 1.2 cm. The mylar dielectric is 0.0127 cm thick and the device is 23 cm long (10 stages). Fig. 6 shows the voltage output for this device obtained with the mercury reed pulser. The output pulse is 100 ns long FWHM, which corresponds to a 217 ns/m transit rate in the device. In comparison, the transit rate for RG-58 cable is 5.06 ns/m. No dispersive effects are evident in this short section of the pulser, but they should appear when more stages are added.

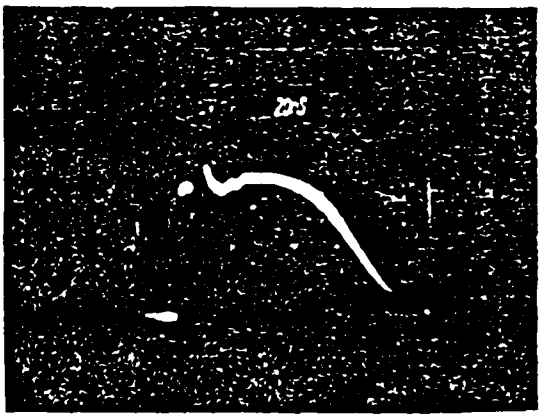

Fig. 6. Output pulse of magnetic material pulser. The transit rate is 217 ns/m.

Each of these two devices has a particular set of limitations inherent with its use. The helical line needs a water dielectric to keep its impedance as low as possible, which is generally desirable. This requirement, however, limits the charge time and pulse length possible with this device. Also, it appears that the water purity is critical to the operation of this device. The magnetic pulser, on the other hand, has a mylar dielectric, which is much easier to use from a practical standpoint. However, this device is limited in current by the saturation flux of the magnetic material. If the current in this pulser is

high enough to saturate the magnetic material, then the device begins to act as a capacitor rather than a transmission line. For the pulser we constructed, saturation of the cores occurred at a current of approximately 30 A, which is too small to be of practical interest for most pulsed power applications. However, if a physically larger device using a magnetic material with a high saturation flux such as Metglas were constructed, usable power levels could be obtained. The charging voltage of such a device is only limited by the dielectric, so the current is the principal limiting factor. Also, in order to produce pulsers with long pulse lengths, some technique to compensate for the dispersion of the pulse should be developed. A crowbar circuit is a brute force method of accomplishing this end, but several more elegant techniques are presently under investigation.

The devices described above could have a variety of applications due to their compactness, light weight, and simplicity. For example, some gas discharge lasers operate most efficiently when the impedance of the source driving the discharge is matched to the discharge impedance. One of the pulsers described above could be used to drive a few microsecond pulse length laser. The entire system would be compact and relatively light in weight and as such would have a variety of applications. These devices still require further study, but their potential as useful pulsers is very promising.

## References


[1] G. N. Glasoe and J. V. Lebacqz, eds., *Pulse Generators*, New York: McGraw-Hill Book Co., Inc., 1948.

[2] J. R. Cooper, K. H. Schoenbach, and C. Schaefer, "Magnetic control of diffuse discharges," *IEEE Trans. on Plasma Sci.*, to be published August 1986.

[3] M. T. Buttram, "Transmission lines for pulsed power applications," Sandia Natl. Labs. Report SAND83-0957, May 1984.

[4] D. A. Watkins, *Topics in Electromagnetic Theory*, New York: John Wiley and Sons, Inc., 1958.

JAPANESE JOURNAL OF APPLIED PHYSICS
VOL. 25, NO. 3, MARCH, 1986, pp. L198-L199

# Conical Liner Implosion as a Projectile Injector for Mass Drivers*

Kazunari IKUTA** and Magne KRISTIANSEN

*Department of Electrical Engineering and Computer Science, Texas Tech University, Lubbock, Texas 79409, USA*

(Received December 12, 1985; accepted for publication February 22, 1986)

An electro-magnetic method for injecting a projectile into a mass driver using a conical liner in proposed.

Most of the serious problems for electro-magnetic accelerators of projectiles, such as rail guns[1] and ablation mass drivers[2-4] occur at the low velocity section of the accelerator, since most of the electrode erosion occurs in this low velocity section of the accelerators. Here the low velocity means the velocity lower than about 1 km s$^{-1}$. This is because of the fact that the heat load on the surface of the electrode in the low velocity section becomes extremely high since it is approximately inversely proportional to the projectile velocity.

In order to minimize this problem, the projectile should have a high injection speed into the accelerator. Using light gas guns as injectors to give an initial speed to the projectile, however, induces other complicated problems since these guns also inject large amounts of gas into the discharge chamber where the armature propels the projectile. This can, for instance, cause restrike at the breech of the gun. The initial projectile speed should, therefore, be caused by other means than using gas pressure.

Another serious problem is the stiffness of the accelerator. The operating stress for accelerator rails and insulators must be low enough to avoid unacceptable mechanical distortions. This latter problem must be solved by the careful choices and the development of the materials. We do not discuss this problem in this work.

The purpose of the present letter is to propose a new method of injecting projectile into elelctromagnetic accelerators. At the exist of the injectors, the projectile should have the velocities of the order of a few km s$^{-1}$ in order to avoid the electrode erosion of the main accelerator.

A potential alternative method for impacting the necessary injection speed to the projectile is to use an imploding conical liner which squeezes an insulating working fluid (*e.g.*, oil) into the accelerator instead of the gas. The driven fluid can then give the forward thrust to the projectile. This principle of conical liner injector is shown in Fig. 1.

The dynamic behavior of the metallic cone is as follows. Once the switch is turned on, the current flows along the conical surface (conical $z$-pinch). As long as the current is sufficiently high, the cone is compressed by the magnetic pressure, as shown in Fig. 2. The eventual change of the shape of the cone squeezes the fluid into the barrel and the projectile, together with the ablator, is propelled by the fluid.

An estimate of the attainable velocity is as follows. The equation of motion of the conical shell together with the fluid, the ablator, and the projectile is approximately described by

$$M\frac{d^2z}{dt^2}=\frac{\mu_0 I^2}{2\rho}g, \tag{1}$$

where $M$ is the total mass including the fluid, the ablator and the projectile, $I$ is the total current along the conical shell, $\mu_0$ is the magnetic permeability of vacuum, $z$ is the distance along the cone, and $g$ is a constant of order unity. Here, the mass of the moving shell is neglected. If the length of the cone is $h$ and the current is supplied by a constant current source, the final velocity, $v_0$, obtained is

$$v_0=\left(\frac{\mu_0 g h}{\rho M}\right)^{1/2}. \tag{2}$$

If the required speed for the injection is $v_0 = 10^3$ m s, eq.

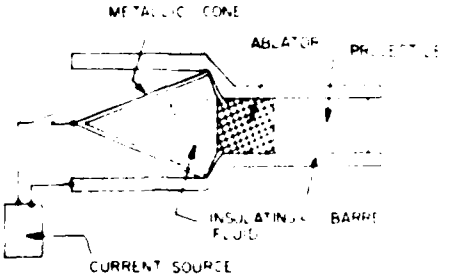


Fig. 1. Structure of injector using a metallic conical liner.

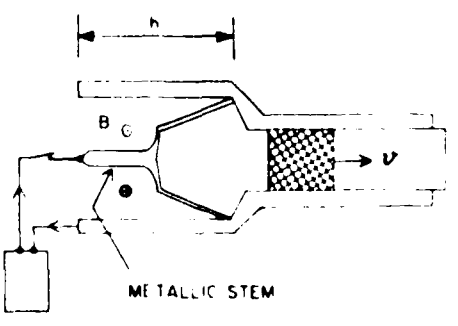


Fig. 2. Change of the shape of the metallic cone when current is driven along it. Note the formation of the stem.

*This work was supported by the AFOSR and ARO.
**Institute of Plasma Physics, Nagoya University, Nagoya, 464 Japan.

*K. Ikuta, M. Kristiansen and M. F. Rose: Submitted to J. Appl. Phys.

(2) is reduced to

$$\frac{I^2 h}{M} \simeq 0.25 \times 10^{13} \tag{3}$$

in MKS unit. Specifically, when the current $I$, is $10^6$ amperes and the mass, $M$, is 0.1 kg, the length of the cone becomes

$$h \simeq 0.25 \text{ (meter)}. \tag{4}$$

In conclusion, we have suggested a possible method for injecting the projectile into an electromagnetic mass driver without using gas pressure. The necessary cone for the acceleration of the projectile is acceptably short, provided that the driven current along the conical shell is of the order of $10^6$ amperes. The quasi-steady current of order $10^6$ amperes should be obtained by the method employed in the work.[1]

In addition, it is possible to compress the liner by induced current azimuthally on the surface of the liner (conical $\theta$-pinch), although only the case of conical $z$-pinch compression of the liner is discussed in this work. In spite of less efficient acceleration with a conical $\theta$-pinch than with a conical $z$-pinch, the non-destructible conical $\theta$-pinch accelerator is possible.

## References

1) S. C. Rashleigh and R. A. Marshall, J. Appl. Phys. **49** (1978) 2540.
2) K. Ikuta, Jpn. J. Apl. Phys. **24** (1985) 862.

DEPARTMENT OF THE AIR FORCE
AIR FORCE WRIGHT AERONAUTICAL LABORATORIES (AFSC)
WRIGHT-PATTERSON AIR FORCE BASE, OHIO 45433

REPLY TO ATTN OF: FI

5 JUN 1985

SUBJECT: Appreciation

TO: Dr Marion O. Hagler
Chairman, Dept of Electrical Engineering
Texas Tech University
Lubbock, Texas 79409

1. The Flight Dynamics Laboratory of the Air Force Wright Aeronautical Laboratories wishes to express its appreciation to Dr M. Kristiansen, Head of the Plasma and Switching Laboratory, for his outstanding contributions to technical discussions held at Maxwell Laboratories, Inc., San Diego, CA, on 1 May 1985.

2. These discussions were conducted to solve problems with a pulsed power KrF laser triggered crowbar switch which is a critical component of a full threat lightning simulation generator. This generator is being built under contract for the Air Force's Atmospheric Electricity Hazards Protection Advanced Development Program (AFWAL/FIEA). These problems had plagued the contractor for over a month and had delayed the delivery of the generator. This delay was costing the Air Force money as it further delayed other Air Force contracted efforts.

3. Dr Kristiansen contributed significantly to the technical discussions at Maxwell Laboratories which resulted in a concise detailed plan of approach to solve the problems with this pulsed power switch. Prior to the discussions, Dr Kristiansen identified to the Air Force those individuals in the United States who could contribute most significantly to these discussions. He solicited and arranged the participation of Dr A. H. Guenther, Chief Scientist, Air Force Weapons Laboratory. Unable to attend the Thursday meetings due to prior commitments, he arrived two days early and set the stage for all discussions which followed. He determined concisely the problems, made significant recommendations and pre-briefed the other participants. As a result of his efforts, the technical discussions held on Thursday were a monumental success. Dr Kristiansen's superb technical abilities in the area of pulsed power and his extreme interest in solving this significant U.S. Air Force problem bring credit upon himself and Texas Tech University.

4. For providing his superb technical abilities, arranging his schedule to participate in the technical discussions and his outstanding contributions to the solution of this Air Force problem, the Flight Dynamics Laboratory is extremely grateful and wishes to express its appreciation to Dr Kristiansen, Head of the Texas Tech University Plasma and Switching Laboratory.

JAMES J. MATTICE
Acting Director
Flight Dynamics Laboratory

# Electron-beam tetrode for multiple, submicrosecond pulse operation[a)]

C. H. Harjes, K. H. Schoenbach, G. Schaefer, M. Kristiansen, H. Krompholz, and D. Skaggs

*Department of Electrical Engineering, Texas Tech University, Lubbock, Texas 79409*

(Received 9 April 1984; accepted for publication 4 June 1984)

The design and the operation of a 250-kV, 400-A, *e*-beam tetrode is described. A simple trigger circuit allows the generation of a burst of *e*-beam pulses with variable pulse duration and pulse separation.

## INTRODUCTION

There is an increasing interest in fast, repetitive opening switches for inductive energy storage systems.[1] An opening switch concept that shows promise for fast, repetitive operations is the electron-beam-controlled diffuse discharge switch.[2-4] It contains a gas mixture which becomes conductive when an ionizing *e*-beam is injected. When the *e*-beam is turned off, electron attachment and recombination processes cause the reduction of the electron density in the gas and the switch opens. For the investigation of *e*-beam-controlled conductivity in switch gases, an *e*-beam tetrode was designed. The operating characteristics are: (a) burst mode operation in the Mpps (Megapulses/second) range; (b) variable pulse duration and pulse separation; (c) turn-on and turn-off times in the range of 10 ns; (d) variation of *e*-beam energy ($E_B < 250$ keV); and (e) variation of *e*-beam current density ($J_B < 4$ A/cm$^2$).

## I. ELECTRON-BEAM GUN

A cross section of the tetrode is shown in Fig. 1(a). The cathode is located in an evacuated ($p = 2 \times 10^{-7}$ Torr) Pyrex cylinder, between the two plates of a stripline. The anode consists of a grid of 250-$\mu$m molybdenum wires at a distance of 7 cm to the cathode. The anode grid covers the entrance of a 12.9-cm-long drift tube which is terminated by a 25-$\mu$m titanium foil. The foil is supported by an array of titanium bars. The bottom plate of the stripline is grounded and the *e*-beam voltage is applied to the top plate by a two-stage Marx generator. The generator (Physics International Co. FRP-250) can deliver a maximum voltage of 250 kV with a 10-ns rise time and with an exponential decay time constant of about 2.5 $\mu$s into a 300-$\Omega$ load.

A more detailed cross section of the cathode is shown in Fig. 1(b). The electron source is an electrically heated array of 375-$\mu$m-diam thoriated tungsten filaments. A negatively biased spreader plate ($V_s = -500$ V) prevents electron current flow from the filaments back to the grounded cathode base when no plate voltage is applied. At a filament temperature of about 2100 K, the *e*-beam current density is about 4 A/cm$^2$ over the 100-cm$^2$ cross sectional area of the beam. The current density can be varied independently of the accelerating voltage by adjusting the filament temperature.

The control grid is located 0.4 cm above the filament array. It is formed by an array of 250-$\mu$m-diam molybdenum wires stretched across a 17.5-cm-diam circular hole in the outer shell of the cathode assembly. A negative bias voltage, $V_B = 4$ kV, is applied to the grid to hold the *e*-beam off, even

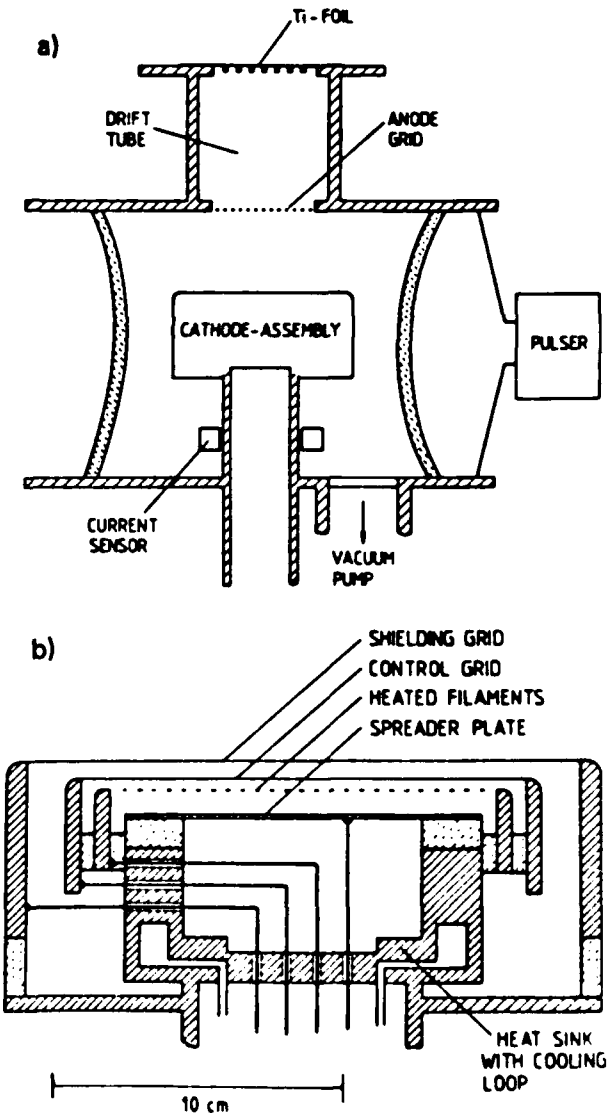


FIG. 1. (a) Cross section of *e*-beam tetrode. (b) Cross section of cathode assembly.

 0034-6748/84/101684-03$01.30  

when the accelerating voltage is applied to the plate. The *e*-beam is turned on by applying a positive voltage pulse of typically $V_2 = +4$ kV to the grid. A second grid, which is biased to $+4$ kV, shields the control system electrostatically. It is positioned 0.6 cm above the control grid. The grids and cathode are connected to external power supplies through high-vacuum electrical feedthroughs located in the aluminum base of the cathode. The base is water cooled and serves as a heat sink for the cathode.

## II. CONTROL SYSTEM

The pulser driving the grid is depicted in Fig. 2(a). It consists of two, 75-$\Omega$ cables (lengths $d_1$ and $d_2$) separated by a triggerable spark gap. Cable 1 is connected to the grid, as shown, and is charged to the negative bias voltage $-V_B$. Cable 2 is charged through a 10-M$\Omega$ resistor to the voltage $+V_2$. After triggering the spark, the positive voltage from cable 2 propagates towards the grid, is reflected with the same polarity, travels back to the charging resistor, and is reflected again. The negative bias voltage from cable 1 is reflected at the open end, etc. Hence, the cable pulser with two open ends generates a periodic rectangular grid voltage $V_g$, with alternating polarity as shown in Fig. 2(b), and the electron beam is repetitively turned on and off.

The primary advantage of this pulser is its simplicity and versatility. The pulse magnitudes are variable by changing the cable charging voltages, and the pulse width and pulse separation can be adjusted by changing the lengths of the cables. However, due to the effect of the capacitive termination in the tetrode and cable dispersion, subsequent pulses are degraded. This degradation limits the useful length of the pulse train to three or four pulses. The output of the grid pulser, when fired into a 100-k$\Omega$ dummy load, is shown in Fig. 3. The rise and fall time of the first pulse is about 10 ns

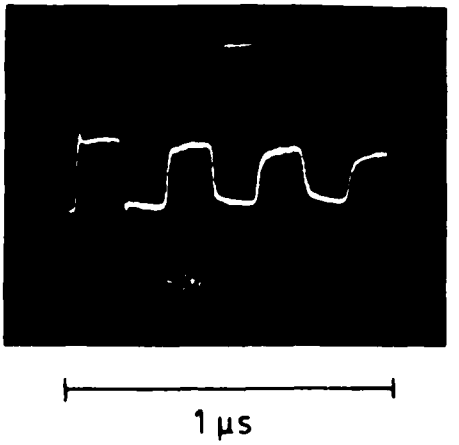


FIG. 3. Grid pulser signal output into 100-k$\Omega$ load

and of the second and third pulses 20 and 30 ns, respectively. The reduction of the pulse amplitude is not important as long as the pulse voltage is above the threshold voltage for *e*-beam turnon.

## III. ELECTRON-BEAM CURRENT MEASUREMENT

Measurements of the electron-beam current at the cathode and at the anode—after passing the titanium foil—were performed with transmission line current transformers.[5] Figure 4(a) shows current signals, $i_{out}(t)$, recorded at the cathode. The *e*-beam current pulses shown in Fig. 4(b) are evaluated from these signals by using the relation $i_{out} = 1/(2N)[I(t) - I(t-T)]$, where $I(t)$ is the current to be measured, $T$ denotes the coil transit time, and $N$ is the number of turns.[5] The decay in amplitude is caused by the exponential plate voltage decay. Because of the reduced transmission of electrons through the foil at lower electron energies, the effective time of operation is limited to approximately 1$\mu$s for the voltage generator used in this experiment.

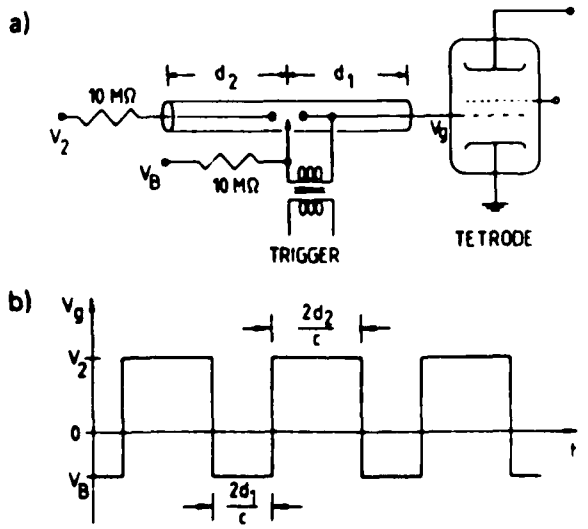


FIG. 2. (a) Schematic diagram of grid pulser. (b) Ideal output signal of the grid pulser

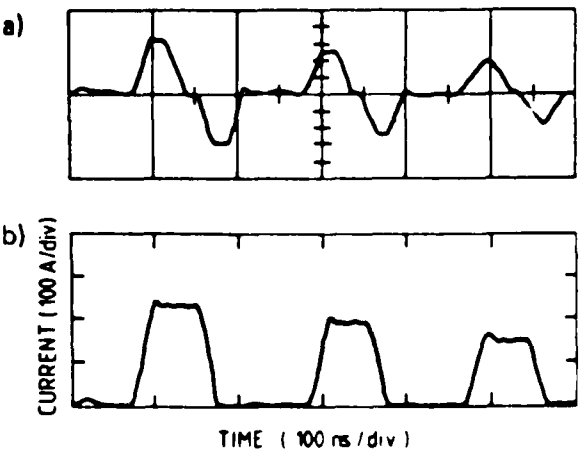


FIG. 4. (a) Current signals obtained with transmission line current transformer at the cathode. (b) Corresponding *e*-beam pulses

[a]Supported by ARO and AFOSR.

[1]K. H. Schoenbach, M. Kristiansen, and G. Schaefer, Proc. IEEE 72, 1019 (1984).
[2]M. R. Hallada, P. Bletzinger, and W. F. Bailey, IEEE Trans. Plasma Sci. PS-10, 218 (1982).
[3]R. J. Commisso, R. F. Fernsler, V. E. Scherrer, and I. M. Vitkovitsky, IEEE Trans. Plasma Sci. PS-10, 241 (1982).
[4]K. H. Schoenbach, G. Schaefer, M. Kristiansen, L. L. Hatfield, and A. H. Guenther, IEEE Trans. Plasma Sci. PS-10, 246 (1982).
[5]H. Krompholz, J. Doggett, K. H. Schoenbach, J. Gahl, C. Harjes, G. Schaefer, and M. Kristiansen, Rev. Sci. Instrum. 55, 127 (1984).

IEEE TRANSACTIONS ON PLASMA SCIENCE, VOL. PS-12, NO. 4, DECEMBER 1984

# Pulsed Hollow Cathode Discharge with Nanosecond Risetime

GERHARD SCHAEFER, SENIOR MEMBER, IEEE, PER O. HUSOY, KARL H. SCHOENBACH, SENIOR MEMBER, IEEE, AND HERMANN KROMPHOLE, SENIOR MEMBER, IEEE

*Abstract*—This paper reports the operation of a cylindrical hollow cathode discharge with current risetimes of a few nanoseconds at current densities at the entrance of the cathode in the range of 50–560 A · cm$^{-2}$ and at voltages of 280–850 V. Time-dependent measurements of the impedance of the discharge are presented. They allow for the evaluation of discharge quantities such as risetime, delay time, discharge voltage, and current, depending on the operation parameters as applied voltage, pressure, and preionization. The power density in the active region of the hollow cathode exceeded 200 kW · cm$^{-3}$.

## I. Introduction

THE ENERGY LOADING of discharges for TEA lasers and Diffuse Discharge Switches is mainly limited due to instabilities caused by the use of admixtures of attachers [1]–[3]. In most cases, streamer development and subsequent arcing starts at the electrodes, preferably at the cathode [1]. Reduction of the electric field intensity in the cathode region could delay or even prevent the onset of instabilities. Hollow cathode discharges (HCD) are known to operate at lower potential differences then plane electrodes [4]. Therefore TEA laser electrodes with a large number of small holes may allow operation of discharges with a lower cathode fall voltage. Hollow cathode discharge operation, however, is restricted to a certain range of $pD$ (1 torr cm $\leq pD \leq$ 10 torr cm, for rare gases), where $p$ is the gas pressure and $D$ the diameter of the hollow cathode [4]. This range is shifted to smaller values of $pD$ if molecular gases are used. For atmospheric pressure the holes should have diameters of the order of a few microns depending on the filling gas. In addition, such an electrode structure may allow one to flush the hollow cathodes from the back side with a very slight flow of an atomic gas (preferably a rare gas) and, subsequently further reduce the potential difference across the cathode fall.

At this time an important application of dc hollow cathode discharges is its use as the active medium of a gas laser [5]. In a recent paper it was also demonstrated that pulsed hollow cathode discharges allow one to produce high densities of excited states with energies of several tens of electronvolts above the ground state [6]. The efficient use of the excitation of high-lying levels to produce a population inversion for a laser is, in general, supported by a fast risetime of the excitation process.

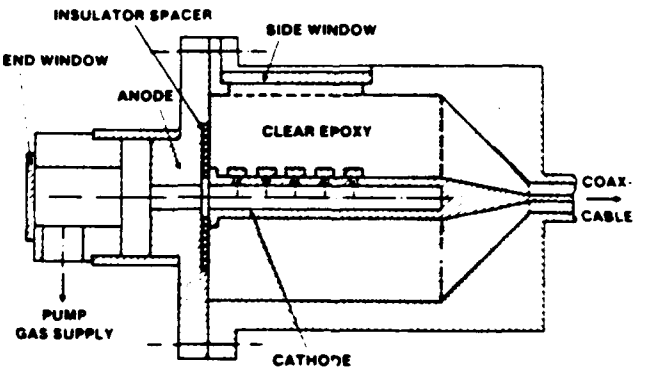


Fig. 1. Design of hollow cathode.

The feasibility of these HCD applications strongly depends on the risetime that can be achieved with hollow cathode discharges. It is known that in the steady-state operation the hollow cathode makes more efficient use of the UV light emitted from the negative glow and collisions of ions and excited particles (in rare gases preferably mestables) with the cathode surface. The build-up mechanism of the HCD and the dynamic of the densities of these species in the hollow cathode, however, has not yet been investigated. The aim of this work, therefore, was to investigate the initiation characteristics of the hollow cathode discharge and to operate a hollow cathode with fast risetime and at high current densities.

## II. Experimental Procedure

The design of the hollow cathode discharge device is shown in Fig. 1. Similar designs have been used for dc discharges [7]. The cathode is a 3.86-mm inner diameter stainless steel tube. Anodes were made of aluminum and stainless steel. The spacer between cathode and anode is a 10-$\mu$m thick mylar foil. End-on and side-on windows allow optical diagnostics of the hollow cathode discharge. Except for the discharge itself the HCD device is totally matched to the impedance of the cable $Z_0$ = 75 Ω (Belden 8870). The dielectric in the cathode regime is a clear epoxy.

The experimental setup is shown in Fig. 2. A charging cable with the length $l_c$ is charged by a power supply and discharged by a spark gap into a transmission cable. The voltage is adjusted through pressure controlled self breakdown. The transmission

Manuscript received April 18, 1984. This work was supported by the Center for Energy Research, Texas Tech University, Lubbock, TX, and by AFOSR.

G. Schaefer, K. H. Schoenbach, and H. Kromphole are with the Department of Electrical Engineering, Texas Tech University, Lubbock, TX 79409.

P. O. Husoy was with the Department of Electrical Engineering, Texas Tech University, Lubbock, TX 79409. He is now with the Technical University of Norway, Trondheim, Norway.

0093-3813/84/1200-0271$01.00 

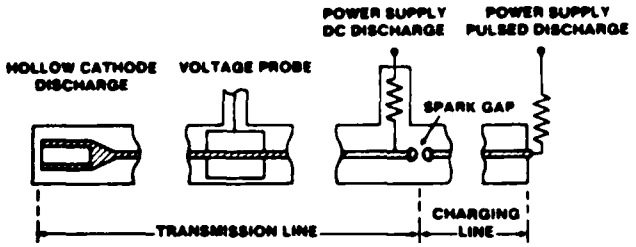


Fig. 2. Experimental setup.

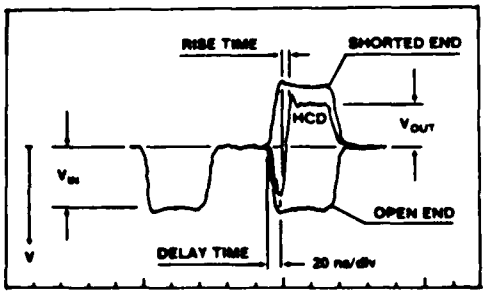


Fig. 3. Three typical ostillograms measured with the voltage probe, for an open end, for a shorted end, and for a hollow cathode discharge.

line is terminated by the HCD. An additional power supply in series with a large resistor is connected to the transmission line and allows the HCD to operate at a low dc level providing for preionization of the pulsed discharge. A capacitive voltage divider is located in the center of the transmission line. Since the length of the transmission cable $l_t$ is more than twice the length of the charging cable ($l_t < 2 \cdot l_c$), the voltage probe will record the incoming pulse and the reflected pulse from the HCD without overlapping. This setup allows measurement of the time dependence of voltage, current, and impedance.

Typical oscillograms of the voltage measured with the voltage probe are shown in Fig. 3. For clarification of the evaluation method three voltage traces are superimposed: one for a typical hollow cathode discharge, one for an open end (infinite impedance) and one for a shorted end (zero impedance). The system with the hollow cathode acts for a time as an high-impedance system. Then the impedance drops to some value which is considered to be the impedance of the pulsed hollow cathode discharge $Z_{HCD}$:

$$Z_{HCD} = Z_0 \frac{1 + V_{out}/V_{in}}{1 - V_{out}/V_{in}}.$$

The time interval between the voltage increase of the reflected pulse and the onset of the decay of the reflected voltage is considered the *delay time* for the initiation of the pulsed hollow cathode discharge. The time interval in which the reflected voltage changes from its maximum to its minimum (90 percent-10 percent) is considered the *risetime* of the hollow cathode discharge (see Fig. 3).

## III. Results

The operation parameters of the pulsed hollow cathode system were varied in the following ranges allowing for stable arc-free operation:

gas: He with pressures: $1 \text{ torr} \leq p \leq 6 \text{ torr}$

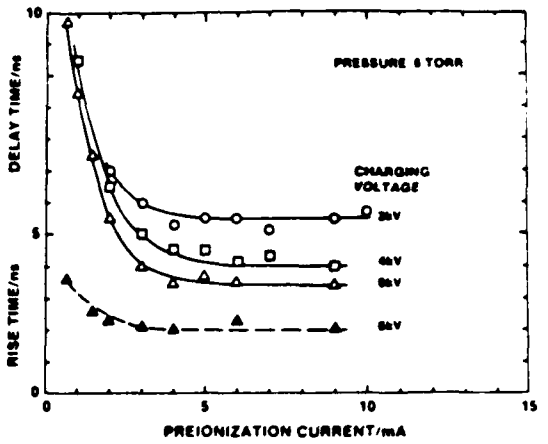


Fig. 4. Delay time (○, □, △) and risetime (▲) for the initiation of the pulsed hollow cathode discharge in helium versus dc-preionization current with the charging voltage as variable parameter.

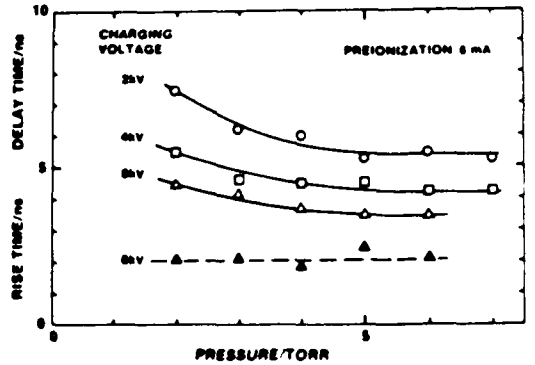


Fig. 5. Delay time (○, □, △) and risetime (▲) for the initiation of the pulsed hollow cathode discharge versus He-pressure with the charging voltage as variable parameter.

charging voltage: $2 \text{ kV} \leq V_0 \leq 13 \text{ kV}$
preionization current: $0 \text{ mA} \leq I_{PI} \leq 10 \text{ mA}$.

With the stainless steel anode, operation at pressures above approximately 8 torr and charging voltages above approximately 13 kV caused small arcs to bridge the gap between cathode and anode, but without damaging the system. With the aluminum anode the stable operation regime was further reduced. In addition, arcing caused permanent damage requiring repolishing of the electrodes.

The first important result was that without preionization the system acted like an open end, indicating that the delay time was at least longer than the pulse length of 50 ns. The dependance of the delay time on the preionization current with the charging voltage as a variable parameter is plotted in Fig. 4. The pressure is constant at 6 torr. At low preionization currents (below 3 mA) the delay time strongly decreases with increasing preionization current but approaches a nearly constant value above approximately 6 mA. The dependance of the delay time on the pressure with the charging voltage as the variable parameter at a preionization current of 6 mA is plotted in Fig. 5, indicating that the pressure does not significantly effect the delay time, especially for the higher values of the charging voltage. At pressures $\geq 5$ torr the delay time seems to be constant. Fig. 6 shows the charging voltage dependance of the de-

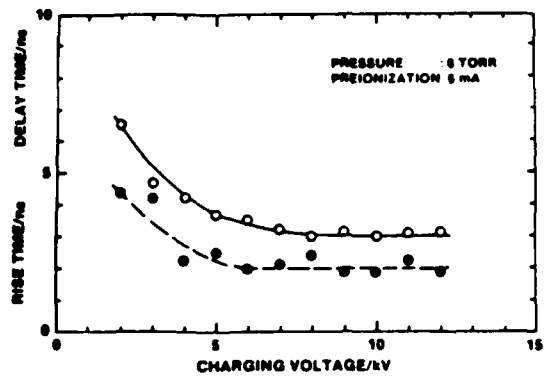


Fig. 6. Delay time (o) and risetime (•) for the initiation of the pulsed hollow cathode discharge in helium versus charging voltage.

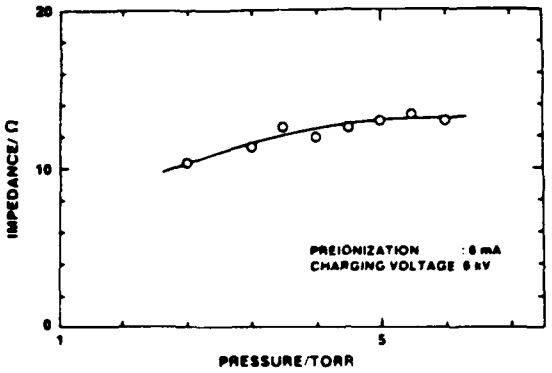


Fig. 7. Impedance of the pulsed hollow cathode discharge versus He-pressure.

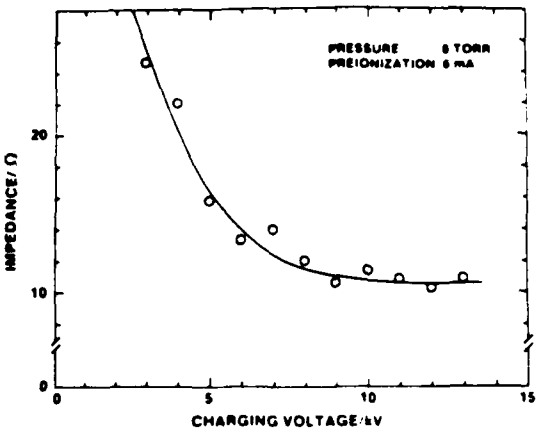


Fig. 8. Impedance of the pulsed hollow cathode discharge in helium versus charging voltage.

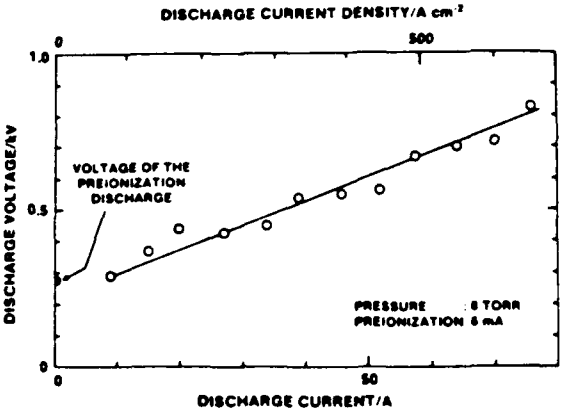


Fig. 9. Discharge voltage versus discharge current and current density, respectively, for the pulsed hollow cathode discharge.

lay time for a pressure of 6 torr and a preionization current of 6 mA. At low charging voltages the delay time strongly decreases with increasing charging voltage but approaches a constant value of approximately 3 ns. From Figs. 4–6 it can be concluded that the minimum delay time which can be obtained with this device is approximately 3 ns.

Figs. 4–6 also show the dependance of the risetime on the same operation parameters. The general behavior of the risetime is similar to that of the delay time although much less pronounced. The minimum risetime was $T_R = 2$ ns. This makes the total initiation time for the pulsed HCD (delay time plus risetime) $T_D + T_R = 5$ ns nearly independent of the operation parameters, if the pulsed HCD is operated in the following range:

$$\left.\begin{array}{l} T_D \text{ 3-ns delay} \\ \text{and} \\ T_R \text{ 2-ns risetime} \end{array}\right\} \text{ if } \left\{\begin{array}{l} I_{PI} \geq 6 \text{ mA (preionization current)} \\ p \geq 5 \text{ torr (He pressure)} \\ V_c \geq 6 \text{ kV (charging voltage).} \end{array}\right.$$

In this operation range the jitter of the total initiation time was in the order of 1 ns. It should be noted that the uncertainty of the time measurement is in the order of ∓0.5 ns.

For the evaluation of the impedance of the discharge only the flat part of the measured voltage pulse was used (see Fig. 3). The voltage peak directly after the initiation of the pulsed HCD is due to the capacitance between cathode and anode and, therefore, not taken into consideration. Once the discharge is initiated, its impedance does not depend on the preionization current. The influence of the pressure on the pulsed HCD (Fig. 7) seems not to be significant, while there is a strong dependance of the impedance on the charging voltage for values below 5 kV. For large values (8 kV and above) the impedance tends to approach a nearly constant value. The dependance of the impedance on the operation parameters is of special importance in designing matched systems for high efficiency.

The data used in Fig. 8 also allow the evaluation of the discharge characteristic (Fig. 9) and the power dissipated in the discharge (Fig. 10). The characteristic presented in Fig. 9 indicates a nearly constant dynamic impedance with voltages in the range of 300–800 V and with currents in the range of 10–65 A. This results in a maximum current density at the entrance of the hollow cathode of 560 A · cm$^{-2}$. The maximum power dissipated in the discharge was 52 kW. From the side-on observation of the light emitted from the discharge it can be concluded that the penetration depth of the pulsed discharge into the cathode is approximately 20 mm. Thus with the inner cathode radius of 3.86 mm, the maximum power density becomes approximately 220 kW · cm$^{-3}$.

The limitations of the current regime in the experiments presented are determined by two properties of the experimental setup limiting the charging voltage.

1) The spark gap design did not allow triggering below 2 kV; therefore the characteristic of the discharge in the low current density range of 10–100 A · cm$^{-2}$, which may be of interest

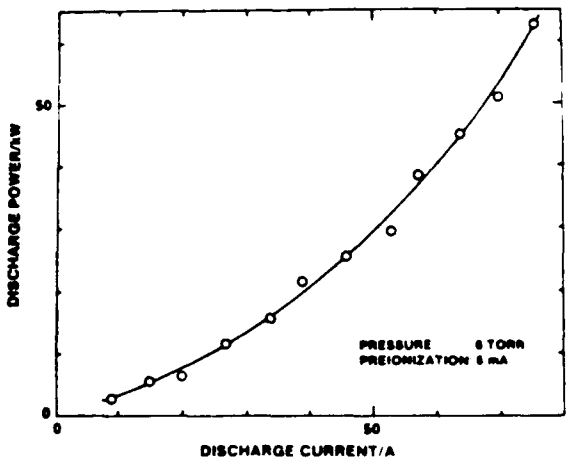


Fig. 10. Discharge power versus discharge current for the pulsed hollow cathode discharge.

for applications in large area diffuse discharges, was not investigated in detail.

2) At charging voltages above 13 kV, frequent arcing occurred across the gap between the electrodes. In this case the oscilloscope traces showed an initial reflection just as for the HCD (see Fig. 3) and then a transition to an unmeasurable small impedance (arcing). Arcing never occurred after the hollow cathode discharge was initiated. At charging voltages of approximately 10 kV, arcing never occurred, even if no preionization was used, resulting in a total reflection of the pulse (open end). Considering a maximum allowed charging voltage for operation without arcing, the maximum current is only limited by the line impedance $Z_0$. For a 10-$\Omega$ line which, according to our impedance measurements, would be matched to the given HCD in the high-current regime and, for a charging voltage of 10 kV, one would expect arc-free operation at currents of up to 500 A.

Further information on the initiation mechanism of a fast-pulsed HCD can be obtained by recording the time-dependent spatial emission of radiation from the HCD. The existing device will allow side-on and end-on observations (see Fig. 1). A streak camera analysis is planned.

## IV. Summary

In conclusion, we report the successful operation of a pulsed high-power density hollow cathode discharge. The delay time between applied voltage and initiation of the discharge strongly depends on a preionization source (dc discharge). Delay times of 3 ns and discharge risetimes of 2 ns were obtained at a jitter of 1 ns or less. The short initiation time combined with low jitter will allow synchronized operation of parallel hollow cathode discharges. In the given device, the maximum power density was in the range of 200 kW $\cdot$ cm$^{-3}$. With an impedance matched line (approximately 10 $\Omega$ for the given HCD), power densities up to $10^3$ kW $\cdot$ cm$^{-3}$ should be expected. These features indicate that such a device may be useful for the fast production of high energy levels with short decay times as required in discharges for pulsed UV gas lasers. The feasibility of using multiple hollow cathodes for the production of diffuse discharges will depend on the scaling behavior when smaller diameter hollow cathodes are used.

## References

[1] D. H. Douglas-Hamilton and S. A. Mani, "Attachment instability in an externally ionized discharge," *J. Appl. Phys.*, vol. 45, pp. 4406-4415, Oct. 1974.

[2] R. A. Haas, "Stability of excimer laser discharges," in *Applied Atomic Collision Physics*, vol. 3, *Gas Lasers*. New York: Academic, 1982, pp. 423-452.

[3] W. H. Long, Jr., "Discharge stability in e-beam-sustained rare-gas halide lasers," *J. Appl. Phys.*, vol. 50, pp. 168-172, Jan. 1979.

[4] J. W. Gewartowski and H. A. Watson, *Principles of Electron Tubes*. Princeton, NJ: Van Nostrand, 1965, p. 56.

[5] L. Csillag, M. Janossy, K. Rozsa, and T. Salamon, "Near infrared CW laser oscillation in CuII," *Phys. Lett. A*, vol. 50, pp. 13-14, 1974.

[6] R. W. Falcone and K. D. Pedrotti, "Pulsed hollow-cathode discharge for extreme-ultraviolet lasers and radiation sources," *Opt. Lett.*, vol. 7, pp. 74-76, Feb. 1982.

[7] H. J. Eichler, H. J. Koch, J. Salk, and G. Schaefer, "Performance of CuII lasers with cylindrical hollow cathodes," *IEEE J. Quantum Electron.*, vol. QE-15, pp. 908-912, Sept. 1979.

# An electron-beam controlled diffuse discharge switch[a)]



K. H. Schoenbach, G. Schaefer, M. Kristiansen, H. Krompholz, H. C. Harjes, and D. Skaggs
*Department of Electrical Engineering, Texas Tech University, Lubbock, Texas 79409*

(Received 18 September 1984; accepted for publication 30 October 1984)

The performance of externally controlled, high-pressure, diffuse discharges as switching elements in pulse power systems is strongly determined by the recombination and attachment processes in the fill gas. To obtain high control efficiency and fast response of the diffuse discharge switch the discharge must be attachment dominated with the attachment rate coefficient increasing with field strength. An electron-beam controlled diffuse discharge system was constructed to study the behavior of pulsed discharges in the submicrosecond range in gas mixtures containing $N_2$ as a buffer gas and small additives of electronegative gases. The results of experiments in $N_2$ plus $N_2O$ were compared with values obtained with a Monte Carlo code and a rate equation calculation.

## INTRODUCTION

Inductive energy storage is attractive in pulsed power applications because of its intrinsic high energy density compared to capacitive storage systems. The key technological problem in developing inductive energy discharge systems, especially for repetitive operation (repetition rates greater than one kilopulse per second) is the development of opening switches. Promising candidates for repetitive opening switches are *e*-beam or laser controlled diffuse discharges.[1] The schematic diagram of an electron-beam controlled opening switch as part of an inductive storage system is shown in Fig. 1. The switch chamber is filled with a gas of pressures of 1 atm and above. The gas between th electrodes conducts and allows charging of the inductor, when an ionizing *e* beam is injected into the gas (usually through one of the electrodes which might be a mesh or a foil). The switch voltage remains below the self-breakdown voltage, so that avalanche ionization is negligible. Thus, the discharge is completely sustained by the *e* beam. When the *e* beam is turned off, electron attachment and recombination processes in the gas cause the conductivity to decrease and the switch opens. Consequently the current through the inductor is commutated into the load.

## EXPERIMENTAL SETUP

For the investigation of *e*-beam controlled conductivity in a high-pressure diffuse plasma a discharge system was constructed with an *e*-beam tetrode as the control element.[2] A schematic cross section of the discharge chamber and e-beam tetrode is shown in Fig. 2. The *e*-beam cathode is located in an evacuated Pyrex cylinder between the two plates of a stripline. The anode consists of a grid of molybdenum wires at a distance of 7 cm from the cathode. The anode grid covers the entrance of a 13-cm-long drift tube which is terminated by a 25-$\mu$m titanium foil. The foil is supported by an array of titanium bars. The *e*-beam voltage is applied to the anode by a two-stage Marx generator. The generator (Physics International Co. FRP-250) can deliver a maximum voltage of 250 kV with a 10 ns rise time and with an exponential decay time constant of about 2.5 $\mu$s into a 300-$\Omega$ load.

The electron source is an electrically heated array of 375-$\mu$m-diameter thoriated tungsten filaments. At a filament temperature of about 2100 K, the *e*-beam current density is about 4 A/cm$^2$ over the 100 cm$^2$ cross-sectional area of the beam. The current density can be varied independently of the accelerating voltage by adjusting the filament temperature. The control grid, which is located 0.4 cm above the filament array, is negatively biased to hold the *e* beam off, even when the accelerating voltage is applied to the plate. The *e* beam is turned on by applying a positive voltage pulse of typically $V = +4$ kV to the grid. The control grid is driven by a pulser which provides a train of pulses with variable amplitude, pulse duration and pulse separation.[2] A second grid, 0.6 cm above the control grid, shields the control system electrostatically.

Measurements of the electron beam current at the cathode and at the anode—after passing through the titanium foil—were performed with transmission line current transformers.[3] Figure 3 shows the *e*-beam current pulses, evaluated from current transformer signals. The decay in amplitude is caused by the exponential plate voltage decay. Because of the reduced transmission of electrons through the foil at lower electron energies the effective time of operation is limited

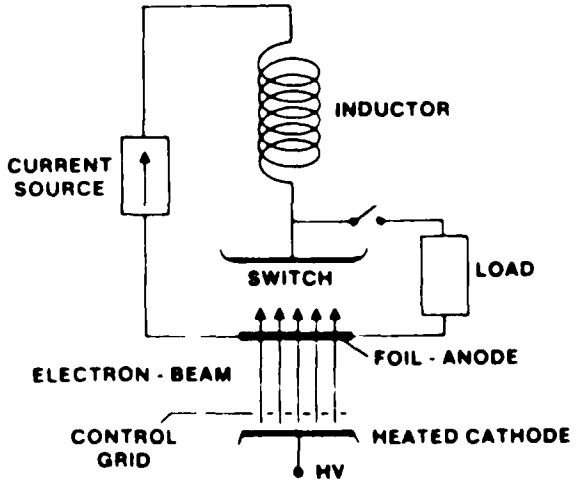


FIG. 1. Schematic of an *e*-beam controlled diffuse discharge opening switch

[a)] Supported by Air Force Office of Scientific Research and Army Research Office

 0021-8979/85/051618-05$02.40 

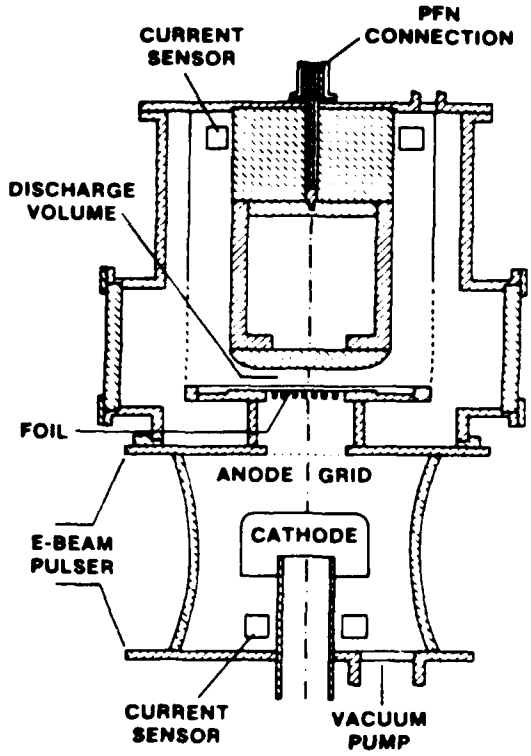


FIG 2 Cross section of *e*-beam tetrode and switch chamber

to approximately 1 $\mu$s with the voltage generator used in this experiment.

After passing through the titanium foil and a 12.5 $\mu$m aluminum foil, which serves as an electrode in the diffuse discharge switch, the *e*-beam generates diffuse plasma between the electrodes in the stainless steel discharge chamber. The current through the plasma is provided by a 2-$\Omega$ pulse-forming network (PFN), which delivers a flat top current pulse of 1 $\mu$s duration and an amplitude of up to 12.5 kA.

## SWITCH-GAS PROPERTIES

The switch opening time, after *e*-beam turn-off, is determined by the electron loss processes in the diffuse discharge: recombination and attachment. In order to achieve opening times of less than a microsecond at initial electron densities $< 10^{14}\,\mathrm{cm}^{-3}$, the dominant loss process must be attachment, which means that the switch gas mixture must contain an electronegative gas. On the other hand, additives of attachers increase the power losses during conduction. Both

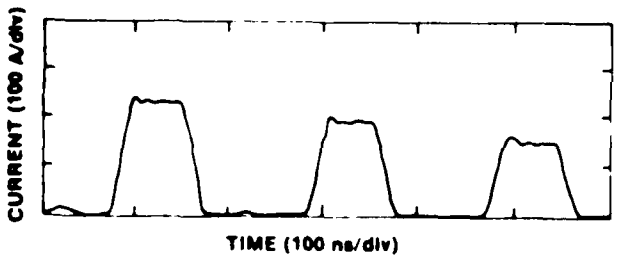


FIG 3 *e*-beam current pulses measured at the cathode

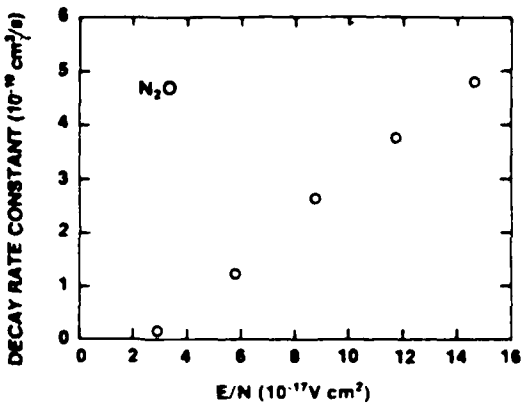


FIG 4 Decay rate constants of the electron conduction current by adding $N_2O$ in 350 Torr of $N_2$ at various $E/N$ (see Ref. 7).

low forward voltage drop and fast opening can only be obtained by choosing gases or gas mixtures which satisfy the following conditions[1,4,5]:

(1) For low values of the reduced field strength $E/N$ (conduction phase) the gas mixture should have a high drift velocity $v_d$ and low attachment rate coefficient $k_a$.

(2) For high $E/N$ values (opening phase) the gas mixture should have lower drift velocities and high attachment rate coefficients.

(3) To avoid the onset of the attachment instability during conduction, the switch should be operated at $E/N$ values where the attachment rate coefficient has a minimum or a negative slope.

Along with these considerations, several gas mixtures have been proposed for diffuse discharge opening switches.[4] For our theoretical investigations $N_2$ was chosen as a buffer gas with $N_2O$ as the added attacher. The $N_2$ was used since a complete set of cross sections is available[6] and the plasma chemistry in a mixture of $N_2$ and $N_2O$ appears to be relatively simple. Furthermore, $N_2O$ in an $N_2$ buffer gas exhibits an $E/N$ dependent electron decay rate which increases by more than a factor of 20 in the $E/N$ range from 3 to 15 Td, as shown in Fig. 4. It should be noted that $N_2$ has an electron drift velocity which increases with $E/N$ and therefore is not the optimum buffer gas in diffuse discharge opening switches. However, for gas mixtures which show a strong attachment rate increase, the drift velocity condition at high $E/N$ is generally of minor importance.

## DISCHARGE ANALYSIS

To calculate the current-voltage characteristics of a diffuse plasma sustained by an electron beam, as well as to evaluate the time dependent impedance of an externally controlled discharge in a given circuit, a computer model has been developed that enables fast calculations for a variety of conditions.[5] It does not, however, provide for spatial analysis of the discharge. The code uses two independent programs. In a first computation, all rate constants of the significant processes are calculated as a function of $E/N$ for a representative gas mixture. These calculations use the $E/N$ dependent electron energy distribution functions that have been previously compiled using a separate Monte Carlo

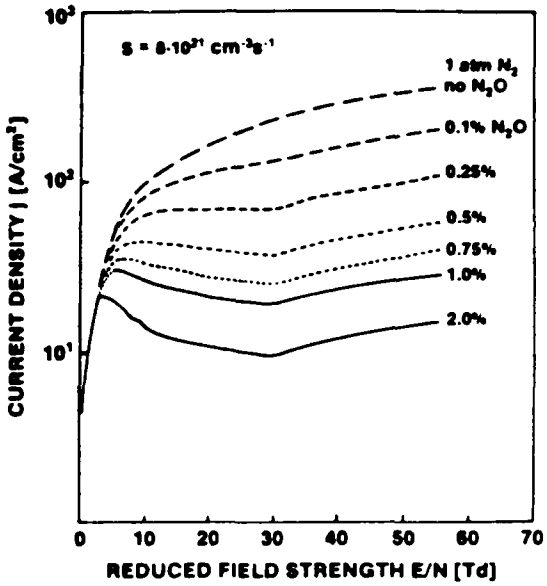


FIG. 5. Calculated steady-state $j$ vs $E/N$ characteristics for an $e$-beam sustained discharge in $N_2$ with admixtures of $N_2O$. The electron generation rate is $8 \times 10^{21}$ cm$^{-3}$ s$^{-1}$. The parameter is the $N_2O$ fraction in percent (see Ref. 5).

code. In a second step, a system of circuit equations and rate equations has been solved, where we used the previously calculated $E/N$ dependence of the rate constants, assuming that they do not change significantly for small variations of the gas mixture.

The transient behavior of the discharge as part of a discharge circuit is discussed in Ref. 5. The calculation of the steady-state behavior of the diffuse discharge does not require information about the circuit. Calculations of the steady-state discharge characteristics were performed with the relative attacher concentration in the buffer gas as the parameter. Figure 5 shows the current density $j$ versus reduced field strength $E/N$ characteristics for different $N_2O$ concentrations in an $N_2$ buffer gas. The total pressure is 1 atm. At small $E/N$, below 4 Td, the electron loss is due to recombination only. At about 4 Td the attachment rate coefficient rises steeply. This means that, for reasonably high attacher concentrations in the buffer gas, the losses increase drastically, causing a negative slope in the current-voltage characteristics. At 30 Td, where the attachment rate coefficient is assumed to level off, recombination becomes more important again, as demonstrated by the change in the slope of $j$ vs $E/N$, at this value.

## EXPERIMENTAL RESULTS

Diffuse discharge experiments were performed in $N_2O$, $SO_2$, and $CO_2$ with $N_2$ as the buffer gas. The e-beam tetrode was for these experiments mostly used in the single pulse mode. The source term, the number of electrons produced per cm$^3$ and per second, was in the range of $10^{20}$ cm$^{-3}$ s$^{-1}$ to $10^{21}$ cm$^{-3}$ s$^{-1}$. The voltage applied at the PFN was varied between 2 and 20 kV. The switch electrode gap was kept constant at 3.5 cm.

Figure 6 shows the influence of attacher concentration ($N_2O$) on the switch current. For high $N_2O$ concentrations

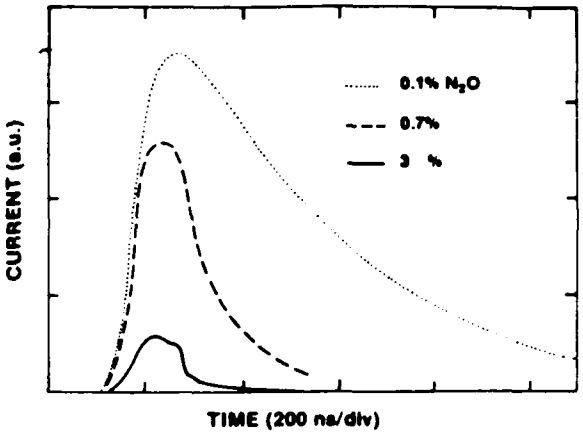


FIG. 6. Time dependence of switch current with $N_2O$ concentration as the variable parameter.

(3%) the switch current pulse replicates the $e$-beam current pulse, except for the tail. The tail may be caused by the current carried by positive and negative ions. The current gain (switch current/electron beam current) is about 2 for this high attachment concentration. For concentrations of 0.7%, the fall time ($1/e$-time) increases to approximately 100 ns. For 0.1% it is on the order of 500 ns. The gain increases to values of 9 and 12 for 0.7% and 0.1% $N_2O$, respectively.

Figure 7 shows the $j$ vs $E/N$ characteristics of the $e$-beam sustained discharge under steady-state condition in 1 atm $N_2$ with 0.7% $N_2O$. The curve represents the calculated values, circles the experimental results. The experimental values at higher $E/N$ correspond well to the theoretical curve. However, the measured discharge characteristics do not exhibit the predicted current maximum at $E/N$ values of approximately 4 Td. These results seem to indicate that attachment is dominant even at $E/N < 4$ Td, where, according to the measured values of the decay rate (see Fig. 4), attachment should be negligible. This assumption is confirmed by results of recently performed attachment rate coefficient measurements[8] and by Monte Carlo calculations of the attachment rate coefficient[9] based on experimentally obtained

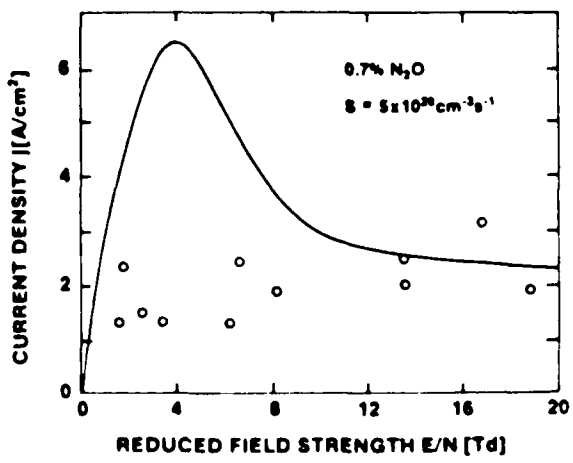


FIG. 7. Current density $j$ vs reduced strength $E/N$ for a discharge in $N_2$:$N_2O$ (calculated curve and experimental data points).

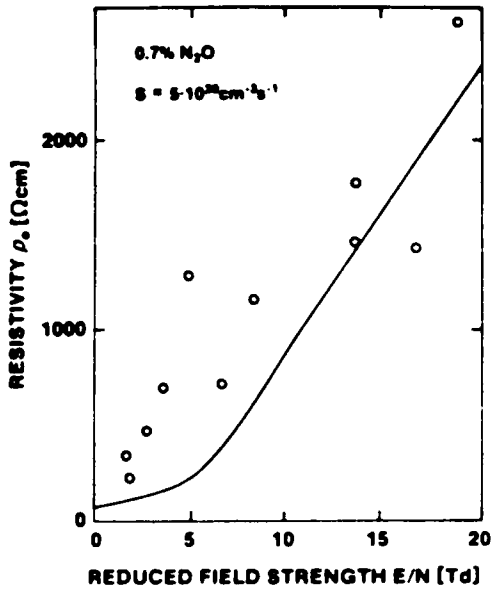


FIG 8 Discharge resistivity $\rho_0$ as a function of reduced field strength $E/N$ for a discharge in $N_2$:$N_2O$ (calculated curve and experimental data points

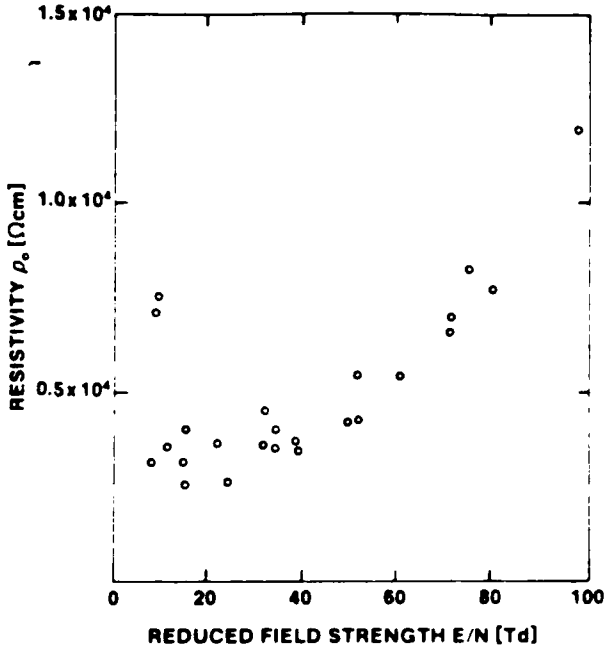


FIG 9 Discharge resistivity $\rho_0$ as a function of reduced field strength $E/N$ for a discharge in $N_2$:$SO_2$ (250 Torr).

attachment cross-sections.[10] The loss of initially high energy secondary electrons by attachment as they lose energy by inelastic collisions could also, at least partially, account for the absence of the current density maximum in the experimental values at low $E/N$. Monte Carlo calculations are under way to gain a quantitative understanding of this effect.

Even with the attachment onset at $E/N < 4$ Td, that means with an attachment dominated discharge during conduction, the $N_2O$:$N_2$ mixture seems to work fairly well as an *opening switch gas*. It satisfies the requirement of having low resistance at low $E/N$ and high resistance at large $E/N$, as seen on Fig. 8, where the results of current-voltage measurements (Fig. 7) are plotted in a resistivity versus reduced field strength diagram. It shows an increase in resistivity of almost two orders of magnitude in an $E/N$ range of 3 to 20 Td.

### $N_2$:$SO_2$

Another gas which has the required $E/N$ dependence of the attachment rate coefficient is $SO_2$ (Ref. 11). The $SO_2$ has a lower attachment rate and an onset of attachment at higher values of $E/N$, compared to $N_2O$. In order to get opening times similar to those in the 0.7% $N_2O$:$N_2$ mixture, the concentration of $SO_2$ in $N_2$ as the buffer gas had to be increased to 20%. The total gas pressure was reduced to 250 Torr, to cover a wider range of $E/N$ with the given switch voltage.

Figure 9 shows the resistivity versus $E/N$ of an $SO_2$:$N_2$, $e$-beam sustained discharge with $S = 3 \times 10^{20}$ cm$^{-3}$ s$^{-1}$. The resistivity rises above an $E/N$ of 50 Td, indicating an increase in attachment at this value. This rise is in agreement with measured attachment characteristics in pure $SO_2$.[11] An increased discharge impedance is also observed at low reduced field strength, as indicated by two high resistivity values shown in Fig. 9, below an $E/N$ of 10 Td. This increase might be caused by strong three-body attachment processes at near thermal electron energies[12,13] and $SO_2^-$ formation via the radiative stabilization process.[11] Both the increased discharge impedance at low $E/N$ and the relatively high overall resistivity make the $SO_2$:$N_2$ mixture not a good gas mixture for switching. The $N_2O$:$N_2$ mixture, under the same conditions (gas pressure, $e$-beam source term, and opening time), has a much lower resistivity at low $E/N$, which means that the Joule losses during conduction can be kept lower for this gas mixture.

### $N_2$:$CO_2$

Like $N_2O$ and $SO_2$, $CO_2$ has an increasing attachment rate coefficient with $E/N$. The disadvantage of $CO_2$ for use as an opening switch gas is its relatively low ionization energy. The field strength range where the attachment coefficient $\eta$ exceeds the ionization coefficient $\alpha$ reaches only up to approximately 60 Td.[11] This value determines the hold-off field strength in this gas. For $E/N > 60$ Td the current rises again, which means that the switch closes further instead of opens after $e$-beam turn-off.

This effect was demonstrated by operating the diffuse discharge at different values of $E/N$ about the crossing point of the attachment and ionization curves (Fig. 10). The discontinuities in the switch current curves represent the stepwise increase in electron concentration in the switch gas due to three successive, ionizing, $e$-beam pulses. The applied field $E/N$ is given by the upper values at each picture. $E/N$ drops to the lower value at the maximum of the switch current after approximately 1$\mu$s. In the range of $E/N$ below 60 Td the net ionization coefficient $(\alpha - \eta)$ is negative, thus electron attachment losses outweigh the ionization gain. The switch current decreases after $e$-beam turn-off (Fig. 10, top i.e., this means the switch opens. However, because of the small attachment coefficient of $CO_2$ compared to $SO_2$ and $N_2O$, the switch opening time (even for the high concentration of 20% in $N_2$ as buffer gas) is much longer than for the

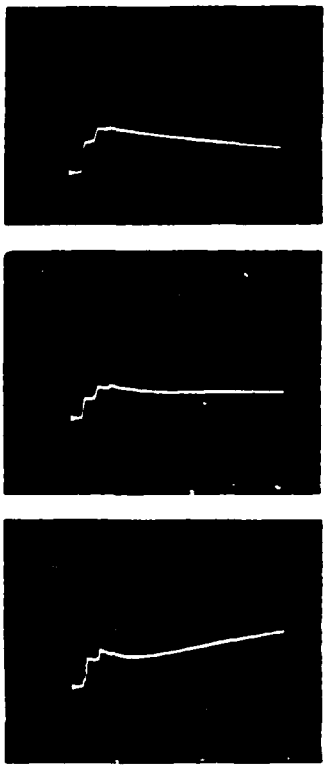


FIG 10 Time dependence of switch current in a discharge in $N_2$:$CO_2$ with reduced field strength $E/N$ as the variable parameter

other gases In the $E/N$ range above 60 Td, $(\alpha - \eta)$ is positive, consequently ionization dominates over attachment, and the switch current increases (Fig 10 bottom) until the field strength in the switch gas drops to a value where the net ionization is zero Operation in an $E/N$ range close to this value is demonstrated in Fig 10, center. After turn-off of the *e* beam, the current stays constant because the ionization and attachment processes balance each other.

## SUMMARY

Diffuse discharge investigations were performed in the gas mixtures $N_2$:$N_2O$, $N_2$:$SO_2$, and $N_2$:$CO_2$. The experimentally obtained current-voltage characteristic for $N_2$:$N_2O$ agrees with previously obtained theoretical results at high $E/N$. The discrepancy in theoretical and experimental data at low $E/N$ reflects the uncertainty in basic data for $N_2O$. With respect to the criteria for optimum switch gases [low losses during conduction (at low $E/N$), large losses during and after opening (at high $E/N$)], $N_2O$ in $N_2$ is superior to the other investigated gases. For opening times of $\sim 100$ ns, the current gain was in the order of 10. With better utilization of the *e*-beam energy in our system, a gain of 100 can be achieved. Shorter opening times, down to $\sim 10$ ns, are possible with higher attacher concentrations, however, at the expense of reduced current gain.

[1] K H Schoenbach, G Schaefer, M Kristiansen, L L Hatfield, and A H Guenther, IEEE Trans Plasma Sci PS-10, 246 (1982)
[2] C H Harjes, K H Schoenbach, G Schaefer, M Kristiansen, H Krompholz, and D Skaggs, Rev Sci Instrum 55, 1684 (1984)
[3] H Krompolz, J Doggett, K H Schoenbach, J Gahl, C Harjes, G Schaefer, and M Kristiansen, Rev Sci Instrum 55, 127 (1984)
[4] L L Christophorou, S R Hunter, J A Carter, and R A Mathis, Appl Phys Lett 41, 147 (1982)
[5] G Schaefer, K H Schoenbach, H Krompholz, M Kristiansen, and A H Guenther, Lasers Part Beams 2, 273 (1984)
[6] A V Phelps (private communication)
[7] L C Lee, C C Chiang, K Y Tang, D L Huestis, and D C Lorents, Second Annual Report on Coord Res Progr in Pulsed Power Physics, Department of Electrical Engineering, Texas Tech University, Lubbock, TX (1981)
[8] L C Lee and F Li, J Appl Phys 56, 3169 (1984)
[9] G Schaefer, K H Schoenbach, and J -S Wang (unpublished)
[10] P J Chantry, J Chem Phys 51, 3369 (1969)
[11] J W Gallagher, E C Beaty, J Dutton, and L C Pitchford, J Chem Phys Ref Data 12, 109 (1983)
[12] V K Lakdawala and J L Moruzzi, J Phys D 14, 2015 (1981)
[13] J Rademacher, L G Christophorou, and R P Blaunstein, J Chem Soc Faraday Trans 2 71, 1212 (1975)

# STREAK PHOTOGRAPHIC STUDIES OF TRIGATRON-TRIGGERED BREAKDOWN*

M.R. Wages, G. Schaefer, and K.H. Schoenbach
Department of Electrical Engineering
Texas Tech University
Lubbock, TX 79407

and

P.F. Williams
Department of Electrical Engineering
University of Nebraska
Lincoln, NE 68588-0511

## ABSTRACT

We present the results of a systematic streak photographic study of trigatron triggering which clearly demonstrates the role of streamers in initiating breakdown of these gaps under conditions of interest for practical switches. These results show that the initiating conditions for these streamers strongly affect their properties and, therefore, the switching characteristics of the gap, and they underscore the importance of the heating phase to the breakdown and overall switching characteristics of these devices.

Trigatron spark gaps are commonly used for high voltage, triggered switching applications. Although a substantial volume of engineering information concerning the design of such gaps has accumulated, there is controversy regarding the physical mechanisms responsible for triggering breakdown in these gaps. We discuss events in the breakdown of these gaps which clearly establishes the role of streamers in the triggering of trigatrons, and which provides new, and in some cases puzzling, information about these streamers.

Fig. 1 shows a schematic drawing of the trigatron gap used in this study. To specify the polarity configuration of a specific experiment, we use the short hand notation +- for example, where the first sign indicates the polarity of the main gap electrode without the trigger pin and the second indicates the polarity of the voltage pulse on the trigger pin, both relative to the main gap electrode with the trigger pin in it. In operation, a voltage less than the static breakdown voltage, $V_{sb}$, is applied across the main gap, which is triggered to breakdown by the application of a high voltage pulse to the trigger pin. Good switching operation generally requires that the main gap voltage be close to static breakdown, but triggering is commonly observed for applied voltages below 60% of $V_{sb}$. Consistent with the findings of other workers, we find the most consistent triggering to occur when the polarity of the trigger pulse is opposite to that of the more distant main gap electrode (-+ or +-), and we find the lowest delay to switch closure in the -+ configuration. In this paper we discuss results for all four possible polarity configurations and for a range of main gap charging voltages.

Several mechanisms for trigatron triggering have been suggested.[1-5] Of most relevance to the work we discuss here is the model of Shkuropat.[6,7] This model is based primarily on the observation that trigatron triggering depends on the polarity of the pulse applied to the trigger pin. The model proposes that triggering is the result of the formation of one or more streamers starting at the tip of the trigger pin, and that these streamers appear and propagate across the main gap independent of and before the appearance of the spark in the trigger gap. The arc channel then forms through an ohmic heating process. The terminus of the arc channel is the trigger pin tip, and the trigger spark between this tip and the adjacent main gap electrode forms only to complete the circuit. This model was supported by voltage and current measurements, by time-resolved photographs of the breakdown, and by the traces of photomultipliers recording the light emission intensity from the gap.

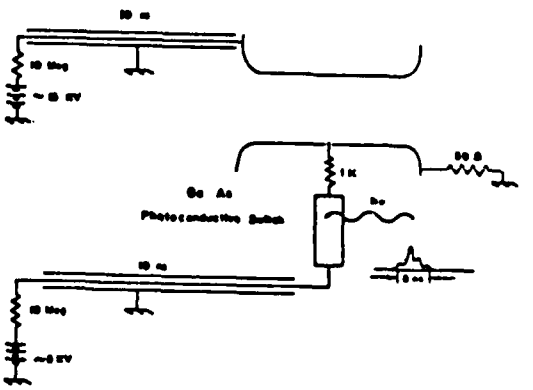

Figure 1. Schematic Drawing of the experimental setup.

## A. EXPERIMENTAL SETUP

We have carried out a systematic study of the physical mechanisms responsible for trigatron triggering using high speed streak photography to resolve directly the initial events leading to breakdown. The experimental setup used in these studies is shown in Fig. 1. A trigatron of essentially standard design was enclosed in a vacuum enclosure which can be evacuated and then backfilled with any desired fill gas. Voltage was applied to the main gap through a charged coaxial cable system. To minimize the intense optical emission from the fully formed spark channel a short (10 ns) charging cable was used. The trigger pin was insulated from the adjacent electrode by a Macor ceramic sleeve, and the position of the pin tip was adjustable. The pin was machined to a sharp, off-center point in order to encourage the trigger spark to form at the same position each time. The main gap electrode separation was 8 mm and

there was a 4 mm diameter hole in one electrode to accommodate the trigger pin and insulating sleeve.

In order to provide a fast rise time, reproducible voltage pulse to the trigger pin, a photoconductive switch was used in the trigger circuit. The switch consisted of a 1x4x15 mm bar of high resistivity GaAs with conductive epoxy electrical contacts on each end. The switch was excited with the 1.06μm output of a Q-switched Nd:YAG laser which provided 50 mJ in a 8 ns FWHM, 3 ns rise time pulse. The switch connected a short length of RG58/U coaxial cable, charged through a large resistor, to the trigger pin of the trigatron. There was a 1kΩ resistor between the switch and the trigger pin to minimize the energy deposited into the trigger spark, and to ensure that the voltage on the trigger pin fell rapidly to zero upon breakdown of the trigger gap. The output voltage of the switch, before the 1 kΩ resistor, was monitored with a Tektronix high voltage probe and displayed on a Tektronix 7831 storage oscilloscope.

## B. EXPERIMENTAL RESULTS

Streak photographs of the early stages of breakdown in pure $N_2$ with the polarity configurations +- and -+ respectively are shown in Fig. 2. The positions of the main gap electrodes and the trigger pin are indicated to the side. The bright region on the lower electrode is from the trigger spark and the corresponding bright region on the upper electrode is a reflection of this spark. In both cases, a weak luminous front is seen to propagate from the trigger spark across the gap. These photographs were obtained by digitizing and storing the output of the streak camera, and the relatively low spatial resolution of the digitization process is evident in the photos. Although the shot noise in these photographs makes precise determination of the characteristics of the front difficult, the behavior is similar in the two cases, and the propagation velocity is $1x10^8$ cm/sec. The delay to main gap breakdown, defined as the time between the fall of the trigger pin voltage and the onset of the current rise in the main gap, was 20 and <5 ns for the +- and -+ configurations, respectively.

The observation that the -+ configuration produced a shorter delay than did the +- was consistently observed in our experiments, is in agreement with the findings of most other workers, and underscores the importance to switch closure of the second, or heating, phase of breakdown in which the resistive streamer channel is converted into a highly conductive spark channel.

Fig. 3 shows the velocity of these fronts as a function of main gap charging voltage for pure $N_2$ for the polarity configurations -+ and +-. The notation e beside some points indicates that the point was obtained with the tip of the trigger pin extending past the plane of the main electrode, into the gap. All other points were obtained with the tip still inside the hole in the main electrode. The determination of the velocity of the front is somewhat subjective due to shot noise. The error bars in Fig. 3 indicate the largest and smallest reasonable values for this velocity.

We also investigated the ++ and -- polarity configurations, and found that triggering was significantly inferior in both cases to the -+ and +- configurations. With the -- configuration triggering was sporadic. We observed a very weak luminous front with the ++ configuration at charging voltages above about 75% of $V_{sb}$, but in no case did we observe a front with the -- configuration. Further the velocity of the front was much slower in the ++ configuration than in the -+ or +-. At a charging voltage of 95% of $V_{sb}$, corresponding to a uniform field $E/N = 1x10^{-15}$ V-cm$^2$, the velocity is approximately

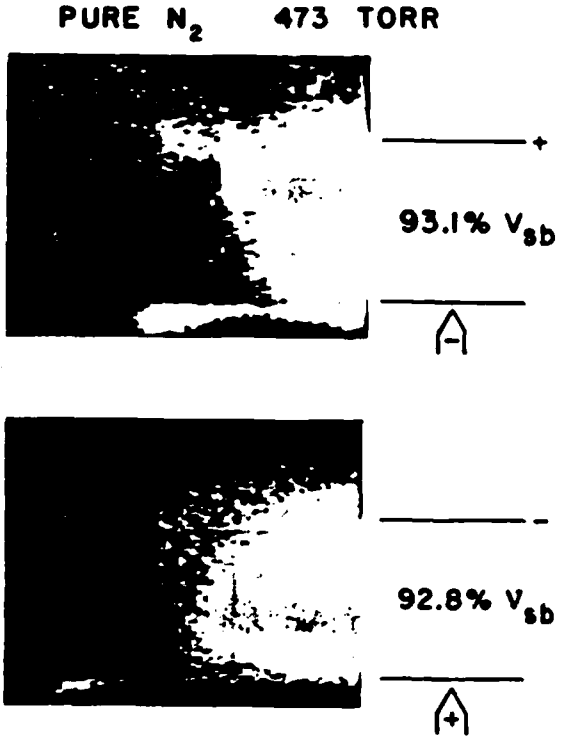


Figure 2. Streak photographs of the initial stages of breakdown in the two hetero-polar configurations. Positions of the electrodes are indicated in the drawings at the right.

$1.8x10^7$ cm/sec, comparable with the electron drift velocity at this E/N of $1x10^7$ cm/sec.[8]

We have also studied streamers in gas mixtures of $N_2$ containing 2.5 and 20% $O_2$. The results observed in these cases were generally similar to those with a pure $N_2$ fill, except that in the -+ configuration with $O_2$, the luminous front clearly started from the tip of the trigger pin instead of from the trigger spark in several cases. Fig. 4 shows streak photographs obtained in the -+ configuration with the trigger pin extending into the gap as shown. The upper photo was taken with a $N_2/O_2$ fill, whereas the lower resulted from a pure $N_2$ fill. In the upper photo the luminous front clearly starts from the tip of the trigger pin, and propagates very rapidly for a distance of 2 mm, starting at the same time as the appearance of the trigger spark. It is unclear whether the agent responsible for the luminous front actually propagates in this manner, or if it started before the trigger spark and propagated more slowly, but only became visible due to photoionization from the trigger spark. After this point, the front travels with more or less constant speed across the gap. This behavior is not seen in the streak photograph taken with pure $N_2$ fill.

Further evidence that the luminous front starts from the tip of the trigger pin instead of from the trigger spark in $O_2$-containing mixtures is seen in Fig. 5, which shows a streak photograph obtained with the trigger pin recessed into the main electrode, at a higher charging voltage than with Fig. 5, and with the -+ polarity configuration. In this case, the luminous front clearly starts before the appearance of the trigger spark. Consistent with the findings with the trigger pin extending into the gap, this

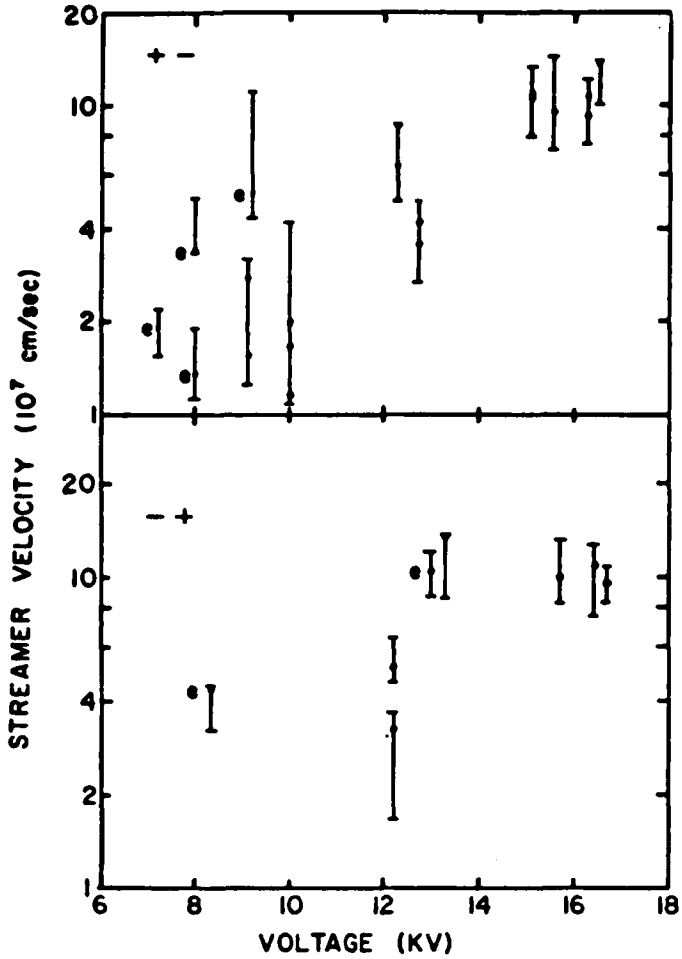


Figure 3. Plots of the dependence of the streamer velocities on applied voltage for the two hetero-polar configurations. Due to shot noise in the streak photos the determination of this velocity is somewhat subjective in many cases, and the error bars give estimates of the largest and smallest velocities which could be reasonable inferred from these photos.

behavior was observed only with fills containing $O_2$, and only in the −+ configuration.

C. DISCUSSION

We associate the luminous fronts such as in Fig. 2 with streamer. For the higher charging voltages, and in the hetero-polar −+ and +− configurations, the velocity of these fronts is more than an order of magnitude too large to result from the propagation of an electron swarm under non-enhanced field conditions. Surprisingly the propagation velocity is the same for both main gap charging polarities. Particularly at lower applied fields, it is generally accepted that under otherwise identical conditions, a cathode-directed streamer propagates slower than an anode-directed streamer. In our numerical simulations of streamer propagation, however, we found that quasi-stable propagation was possible for a wide range of streamer head shapes and sizes, and that the propagation velocity varied significantly with head shape and size.[9,10] We conclude, therefore, that the sizes and other characteristics of the cathode and anode-directed streamers seen in Fig. 2 must differ. This conclusion is supported by the data on main gap breakdown in which the main gap current was observed to start to rise within 5 ns of the appearance

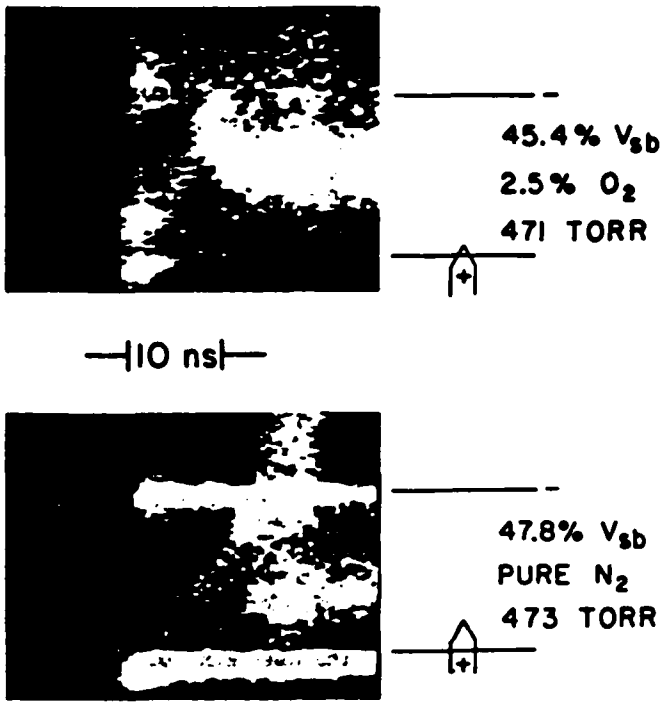


Figure 4. Streak photographs obtained with the trigger pin extending into the gap region. The upper photo was with a $N_2/O_2$ fill, and the lower with pure $N_2$. Note that the luminous front clearly starts from the tip of the trigger pin in the upper photo.

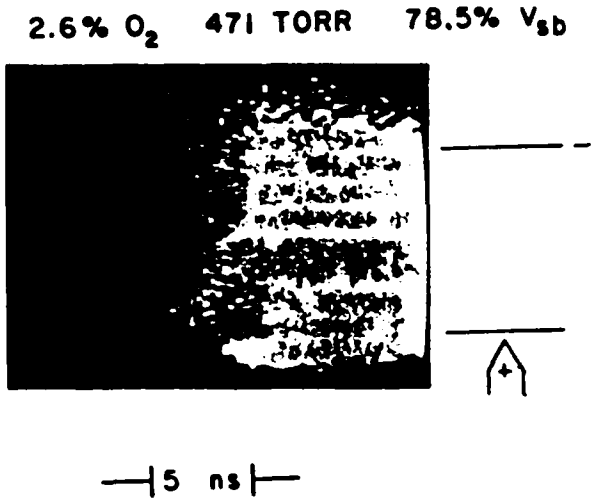


Figure 5. Streak photo obtained with the trigger pin recessed inside the main electrode, with an $O_2$-containing fill mixture.

of the trigger gap spark for the −+ configuration, whereas in the +− case there was a delay of ~ 20 ns before significant current rise was observed.

The strong dependence of the streamer characteristics on the relative polarity of the trigger voltage pulse is surprising. If the streamer propagated while the trigger pin was still charged such behavior would be expected, since for the hetero-polar configuration the charged trigger pin enhances the electric field between the pin and the distant electrode, whereas in the homo-polar configurtion the field

is reduced. Indeed, the observation of substantial differences in triggering characteristics in the hetero- and homo-polar configurations led Shkuropat to suggest that the streamer originated from the tip of the trigger pin and propagated across the main gap prior to the breakdown of the trigger gap.[6,7] In our results with pure $N_2$ fills, however, the streamer is initiated by the appearance of the trigger spark, and, because of the 1 kΩ resistor in the trigger circuit, the trigger pin voltage certainly drops to a negligible value at this time. We conclude, therefore, that the initiating conditions for the streamer play a dominant role in the subsequent behavior of the streamer. This conclusion is consistent with a similar observation discussed above reached on the basis of the similar velocities of cathode and anode-directed streamer, and it is expected on the basis of our numerical simulation results for overvolted streamers.[9,10]

The observation of the very low propagation velocities for fronts with the ++ configuration, and the absence of luminous fronts for the -- configuration suggest that streamers are, in fact, not even formed in these homo-polar configurations. It appears that in the ++ configuration the luminous fronts we observe are associated with electron swarms drifting across the gap, perhaps with the aid of weakly space-charge-enhanced fields. The absence of a visible propagating front for the -- configuration is then expected since the polarity is such as to push any free electrons back into the trigger spark. Breakdown in this case must be the result of ohmic heating occurring after the creation by the trigger spark of substantial free electron density in the main gap region either through photoionization of the fill gas, or the emission of photoelectrons from the cathode.

Our observations with the trigger pin extending into the main gap further support the importance of the initiating conditions on streamer characteristics. Although the experimental error bars are large, it appears that for both hetero-polar configurations faster streamer velocities are observed with the pin extending into the gap than with it recessed inside the main electrode. Greater field enhancements in the region of the tip are expected for the exterior case, and in view of the results discussed above for the ++ configuation, we would expect the propagation velocity to be faster when initiated with the larger field enhancement, as observed.

Finally, we consider the conditions leading to the appearance of a streamer prior to the trigger spark. We observed this behavior only with an $O_2$-containing fill mixture, with the -+ polarity configuration, for main gap charging voltages greater than about 75% of $V_{sb}$, and with the trigger pin inside the main electrode. This last restriction is probably the result of the fact that we were only able to reach charging voltages of 60% of the uniform field $V_{sb}$ with the extended pin due to the reduction in the D.C. holdoff voltage of the gap in this case. Our finding is in agreement with the model of Shkuropat for long, air-filled trigatron gaps in which breakdown triggering results from the formation of a streamer at the trigger pin tip, independent of and before the breakdown of the trigger gap.[6,7] It is curious that we do not observe this behavior with a pure $N_2$ fill. We speculate that the enhanced field at the trigger pin tip is more important in gaps containing $O_2$ because of the finite attachment cross section of $O_2$ at low fields. Perhaps larger fields are needed to reach a regime where impact ionization exceeds attachment in order to initiate a viable streamer. A similar requirement would appear to be necessary for the opposite polarity configuration, +-, however, but we see no evidence for the appearance of a streamer before the trigger spark, or even of the formation of a streamer from the trigger pin tip instead of the spark, in this case.

We thank A. Bushnell and W. Nunnally for helpful discussions of trigatrons and photoconductive switches respectively. The work was supported by AFOSR Grant No. AFOSR-84-0032.

## REFERENCES


* Work sponsored by AFOSR.

† Work conducted at Texas Tech University.

[1] J.D. Craggs, M.E. Haine, and J.M. Meek, J. Inst. Elect. Eng. 93, 963 (1946).

[2] T.E. Broadbent, Brit. J. Appl. Phys. 8, 37 (1957).

[3] T.E. Broadbent and A.H.A. Slash, Brit. J. Appl. Phys. 14, 687 (1983).

[4] A.M. Sletten and T.J. Lewis, Proc. IEE 104C, 54 (1957).

[5] Y. Yoshida, J. Phys. Soc. Japan 42, 1404 (1977).

[6] P.I. Shkuropat, Zh. Tekh. Fiz. 30, 954, (1960) [Sov. Phys. Tech. Phys. 5, 895 (1961)].

[7] P.I. Shkuropat, Zh. Tekh. Fiz. 39, 1256, (1969). [Sov. Phys. Tech. Phys. 14, 943 (1970)].

[8] J. Dutton, J. Phys. Chem. Ref. Data 4, 599 (1975).

[9] S.K. Dahli and P.F. Williams, Phys. Rev. A 31, 1219 (1985).

[10] "2-D Numerical Simulation of Streamers in Atmospheric Pressure $N_2$," S.K. Dahli and P.F. Williams, this conference.

# PHYSICAL TRIGGERING MECHANISMS OF TRIGATRON SPARK GAPS

M.R. Wages, G. Schaefer, and K.H. Schoenbach
Department of Electrical Engineering
Texas Tech University
Lubbock, TX 79409

and

P.F. Williams
Department of Electrical Engineering
University of Nebraska
Lincoln, NE 68588-0511

In a trigatron a main spark gap is triggered to break down by applying a voltage pulse to a smaller, auxiliary gap placed coaxial with and inside one of the main gap electrodes. The main gap is generally D.C. charged to a voltage somewhat less than the static breakdown voltage. Triggering delay and jitter are reduced with increasing charging voltage, but reliable triggering has been reported with charging voltages lower than 50% of static breakdown.[1] Considering the widespread use of trigatrons in pulse power switching applications, the physical mechanism responsible for triggering is of considerable interest. We report the results of an experimental study, utilizing primarily high sensitivity streak photography, of the breakdown of a trigatron gap.

A schematic drawing of the experimental apparatus used in this study is shown in Fig. 1. The spark gap was placed in a vacuum enclosure. Total fill gas pressure was generally 450 Torr, and experiments were carried out with both a pure $N_2$ fill and a mixture of $N_2$ and 1 Torr of $O_2$. The gap spacing was 2 cm and the static breakdown voltage for pure $N_2$ fill was approximately 17.6 KV. Voltage was supplied to the main gap through a 50 Ω coaxial cable charged with a regulated power supply. The main gap discharged into a matched 50 Ω load equipped with a resistive divider current monitor. The auxiliary, triggering gap consisted of a steel rod inside a Macor ceramic sleeve in the main gap electrode. An off-axis knife edge was machined on the rod tip to encourage the trigger spark to form at the same place on each shot. The ceramic sleeve was flush with the surface of the main electrode and the position of the steel rod was adjustable.

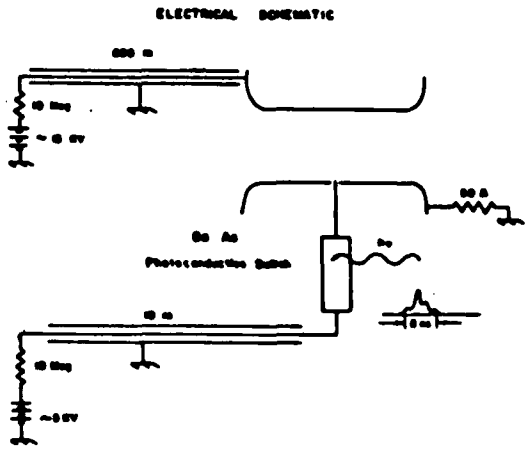


Fig. 1. Electrical schematic of trigatron circuit.

Voltage was applied to the rod through a GaAs photoconductive switch controlled by the ~10 ns wide, 1.06μm output pulse of a Nd:YAG laser. With

this system an essentially jitter-free voltage pulse of several KV amplitude was applied to the trigger gap. Triggering could be accomplished with main gap charging voltages as low as 50% of the static breakdown voltage (VSB), and delay and jitter varied from about 20 ± 1 ns for charging voltages near VSB to several hundred ns for voltages near the lower limit.

The early stages of the breakdown were monitored with a high sensitivity streak camera system consisting of a Hamamatsu Model C979 Temporal Disperser, and associated control electronics. Open shutter photographs were obtained with a 35 mm camera, and spark gap current and voltage were monitored. In most cases, a short charging cable, corresponding to a pulse length of ~10 ns, was used in order to minimize the light intensity from the main spark which could swamp the electron optics of the streak camera.

Three mechanisms for trigatron triggering have been suggested. In the first, field distortion around the trigger pin launches a streamer which crosses the main gap, eventually causing gap closure.[1,2] In the second, the ionizing radiation from the trigger spark creates a broad conducting channel which finally constricts under ohmic heating to form the spark. In the third, the plasma of the trigger spark launches a streamer which crosses the gap, eventually resulting in switch closure.[3-5] Propagation of this streamer may be aided by photoionization produced by radiation from the trigger spark.

In all streak photographs we have obtained, the trigger spark appeared before any visible activity in the main gap, precluding the first mechanism in our experiments. In streak photos of gaps with $N_2/O_2$ mixtures we see clearly a luminous front propagating across the gap, starting from the trigger spark. In gaps with pure $N_2$ this front, if present, is very much weaker. Instead, emission appears roughly simultaneously and uniformly across the gap. Further, using a short (~10 ns) charging cable, in open shutter photographs we observe a large diameter, diffuse glow of roughly uniform intensity for pure $N_2$ fills, and a similar diffuse glow but with intense channels originating from both main gap electrodes for $N_2/O_2$ mixtures. These observations suggest that the second, or photoconductive, mechanism is dominant with pure $N_2$ fill, and that the addition of small amounts of $O_2$ strengthens streamer formation, probably through supression of the photoconductive mechanism.

This work was supported by the U.S. Air Force Office of Scientific Research, Grant No. AFOSR-84-0032.

## REFERENCES

1. P.I. Shkuropat, Zh. Tek. Fiz 30, 954 (1960) [Sov. Phys. Tech. Phys 5, 895 (1961)].
2. P.I. Shkuropat, Zh. Tek. Fiz. 39, 1256 (1969) [Sov. Phys. Tech. Phys. 14, 943 (1970)].
3. T.E. Broadben and A.H.A. Shlash, Brit. J. Appl. Phys. 14, 687 (1963).
4. Y. Toshida, J. Phys. Soc. Japan 42, 1404 (1977).
5. R.A. Dougal and P.F. Williams, J. Phys. D 17, 903 (1984).

# ARC CURRENT, VOLTAGE, AND RESISTANCE IN A HIGH ENERGY, GAS FILLED SPARK GAP

B. Maas, H. Krompholz, M. Kristiansen, and M. Hagler
Department of Electrical Engineering/Computer Science
Texas Tech University
Lubbock, TX 79409

## Abstract

A spark gap was designed and constructed to measure its time dependent arc resistance. The arc current was measured and the resistance calculated using the current waveform and the circuit parameters. Operating parameters were: Unipolar pulses, breakdown voltage 35 kV, peak current 30 kA, total energy per shot 1 kJ. The energy dissipated in the arc was found to be 5 % to 10 % of the total energy. Arc resistance vs. time curves were obtained for the electrode materials Stainless Steel, Copper-Tungsten, and Graphite; for the gases air, Nitrogen, and $SF_6$; and the gas pressures 1, 2, and 3 atm. Statistical analysis was performed on the resultant data. Essential results are: Within the statistical and measurement errors, the resistance is independent of the electrode material. For each gas, the resistance, R, is proportional to pd (p-pressure, d-gap distance). The constants of proportionality for the temporal minimum value of the resistance are: $31\pm7$ m Ω/cm-bar (air), $47\pm14$ m Ω/cm-bar ($N_2$), and $76\pm16$ m Ω/cm-bar ($SF_6$).

## Introduction

In relation to spark gap erosion studies it is important to obtain information about the energy or power dissipated in an arc discharge. The main energy sources for electrode erosion are Joule-heating of the electrodes and the power dissipated in the arc itself. In order to investigate the dependence of the erosion rate on physical parameters, such as the power dissipated in the arc, it is desirable to have information on the arc current and voltage as a function of time, with the voltage separated into resistive and inductive components. Whereas current measurements are straightforward, the measurement of the arc voltage, and especially the separation into resistive and inductive parts, is difficult at best. The first problem in measuring the voltage is the neccessarily high dynamic range of the sensor and recorder, from 10's of kilovolts before breakdown to several 10's V during current maximum. Furthermore, direct measurements at the arc (i.e. voltage measurement at the electrode tips) are virtually impossible.

Several authors have reported arc voltage measurements in the past. Barannik et al. [1] used capacitive dividers in a coaxial arrangement, Braudo and Craggs [2] used a resistive divider and a biased diode to overcome the problem of the high initial voltage. Common problems for these arrangements are, among others, stray capacitances of the probes, use of nonlinear elements, and the impossibility to distinguish beween resistive and inductive voltage drops. Measurements of the spark gap resistance has also been reported by Sorenson and Ristic [3] and by Ristic and Dubois [4] for very short pulses ($\tau < 2$ ns) where the arc drop is relatively large and predominantly resistive in nature.

In the present paper a pragmatic approach was chosen to overcome the mentioned difficulties. In the circuit equation

$$V_0 = \frac{1}{C}\int i\,dt + Ri + \frac{d}{dt}(Li), \qquad (1)$$

with $R = R_0 + R_e(t) + R_a(t)$, $L = L_0 + L_e(t) + L_a(t)$ ($R_0$, $L_0$ circuit parameters, $R_e$, $L_e$ electrode parameters, $R_a$, $L_a$ arc parameters, and $V_0$ breakdown voltage), the essential unknown quantities are the arc resistance, $R_a$, and the arc inductance, $L_a$. All the other parameters or functions can be either measured easily ( i(t), C, $L_0$, $R_0$ ) or estimated within a sufficient accuracy ($R_e$, $L_e$ using the geometry of the device and equations describing the time dependent skin effect [5]). If the arc inductance $L_a(t)$ is known within reasonable accuracy, Eq. (1) can be solved for the arc resistance $R_a(t)$ obviating the need for making explicit arc voltage measurements.

## Experimental Set-Up

The spark gap arrangement is sketched in Fig. 1. It was designed to facilitate changing of electrodes (electrode materials used were Graphite, Stainless Steel, and Copper-Tungsten), to withstand up to three atmospheres of gas pressure, and to provide easy access for diagnostics. In order to obtain a unipolar pulse in accordance to other experiments on electrode erosion conducted at Texas Tech University, the current was overcritically damped, using a load resistor of 0.8 Ohm.

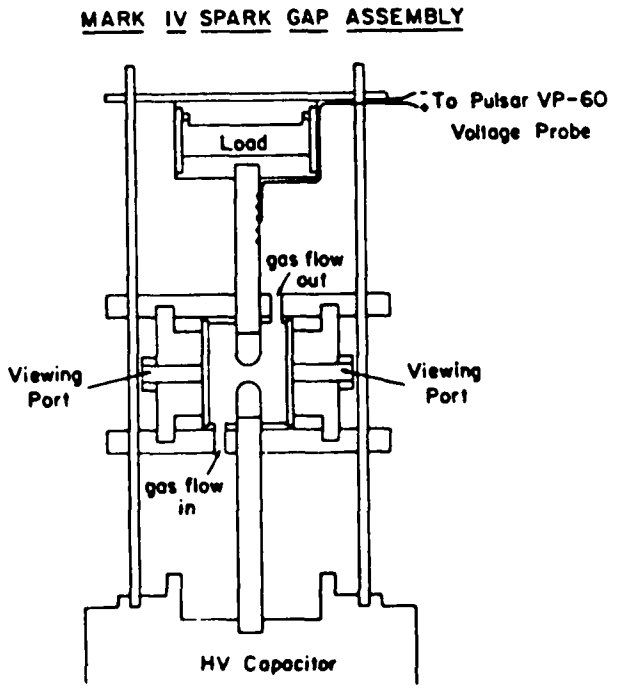


Fig. 1 Experimental Arrangement

The current has been measured using a Pearson Coil (model 110) around one of the eight current return rods of the system. In order to increase the accuracy of the current measurement, the dI/dt signal

was also measured with a calibrated pick-up coil. Output signals were registered with a transient digitizer and stored in a computer.

For estimation of the arc inductance, $L_a(t)$, the self luminance of the arc channel was recorded simultaneously at three axial positions with a streak camera. The arc inductance was calculated from the channel radius as a function of time, taking a homogeneous current distribution within the luminous channel as basis for the maximum inductance value and a surface current distribution as basis for the minimum value. Both values have been considered to estimate the total error for the final calculation of the arc resistance.

## Results

Figure 2 shows, as an example, the arc current, resistance, and resistive arc voltage, including the range of uncertainty for the resistance. Inductive

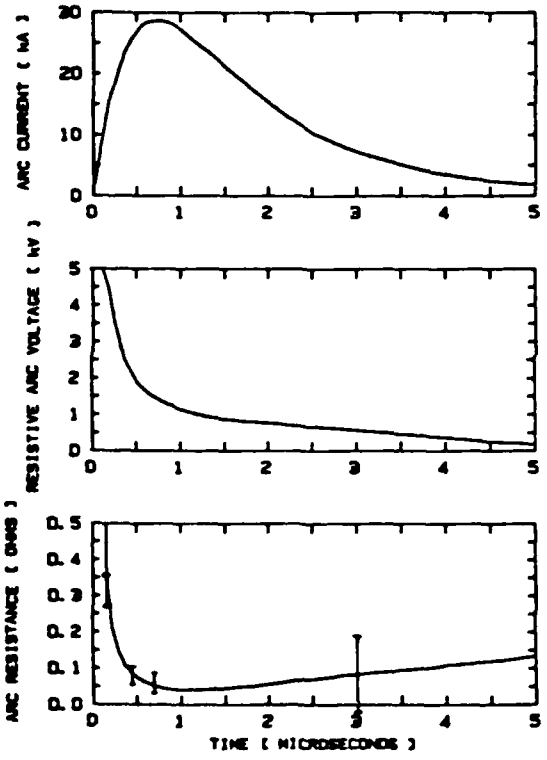


Fig. 2 Arc Current, Voltage, and Resistance for Graphite Electrodes in $N_2$ at 1 Atmosphere.

parts of the arc voltage are in the same order of magnitude during the current maximum (Fig. 3). Measurements have been performed for all combinations of electrode material (stainless steel 304, Graphite AFC-100, Copper-Tungsten 3W3), gases (air, $N_2$, $SF_6$), and pressures (1, 2, and 3 atm). The breakdown voltage has been kept fixed for all cases to 35 kV in order to provide comparable peak current amplitudes of approximately 30 kA by adjusting the gap distance.

Within the measurement and statistical errors, no dependence of the resistance on the electrode material has been found. The value of the resistance at its temporal minimum depends on the gas type, pressure, and gap distance according to

$$R_{a,min} = C_g p d$$

where $C_g$ describes the dependence on the gas. This constant has the values $31 \pm 7$ for air, $47 \pm 14$ for $N_2$, and $76 \pm 16$ m$\Omega$/cm bar for $SF_6$. Due to the measurement errors, a dependence on pressure as proportional to $p^{1/2}$, as mentioned by Mesyats [6], cannot be excluded.

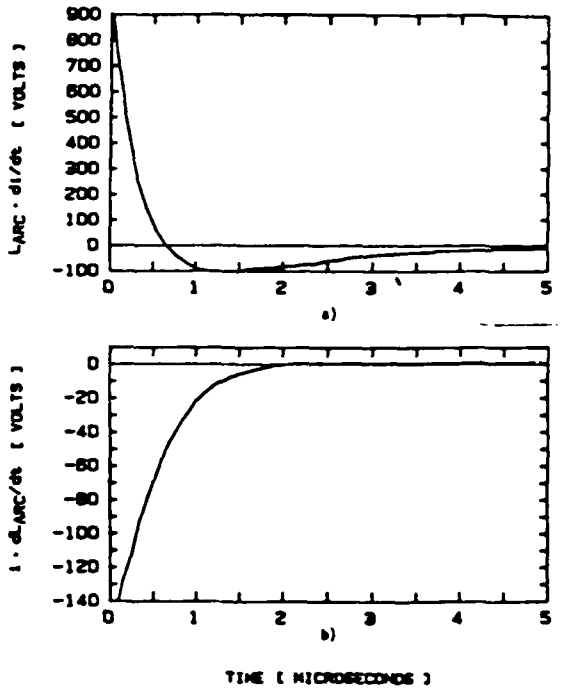


Fig. 3 Inductive Arc Voltage Drops
a) $L_{arc} \cdot di/dt$, b) $i \cdot dL_{arc}/dt$

The time dependence of the measured arc resistance has been compared with different models for the case of the filling gas being air. Whereas the older models of Toepler [7] and Weizel/Rompe [8] show discrepancies of up to a factor of 10, excellent agreement is found with the model of Mesyats [6] and Vlastos [9] for times up to the current maximum (Fig. 4).

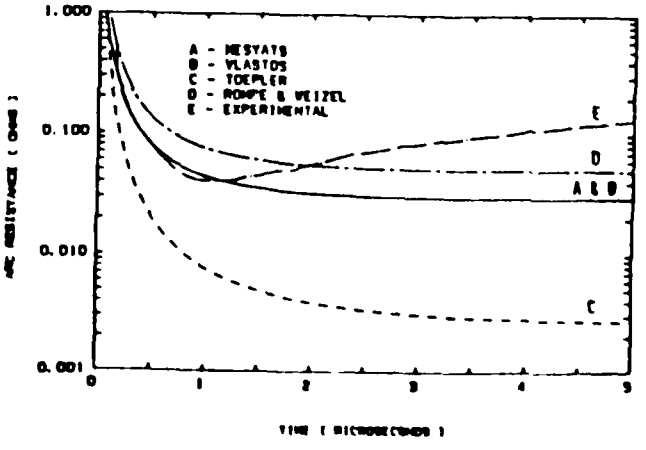


Fig. 4 Comparative Arc Resistance Plot

## Discussion

By careful design and analysis of a spark gap and its circuit geometry, it is possible to find the power dissipated in the arc (including the electrode fall regions) within reasonable accuracy without performing an explicit voltage measurement. Relatively simple diagnostical methods, such as current measurements and optical diagnostics using a streak camera to determine the arc radius as a function of time, reveal sufficient information to determine the arc resistance and the power dissipated in the arc with an accuracy of approximately 20 %.

## References


[1] Barannik, S.I., et al., "Resistance and Inductance of a Gas Arc," Sov. Phys. Tech. Phys., Vol. 19, No. 11, pp. 1449-1453 (May 1975).

[2] Braudo, C. and Cragga, J.D. "Some Properties of High Current Spark Channels," Int. J. Electronics, Vol. 22, No. 4 pp. 329-353 (1967).

[3] Sorensen, T.P. and Ristic, V.M., "Risetime and time-dependent Spark-gap resistance in nitrogen and helium", Journal of Applied Physics, Vol. 48, pp. 114-117, (1977).

[4] Ristic, V.M. and G.R. Dubois, "Time-Dependent Spark-Gap Resistance in Short-Duration arcs with semimetallic Cathodes", IEEE Trans. Plasma Sci. Vol. PS-6, pp. 550-551 (1978).

[5] Knoepfel, H., Pulsed High Magnetic Fields, New York: American Elsevier Publishing Company, pp. 46-72 (1970).

[6] Mesyats, G.A., "Techniques of Shaping High Voltage Nanosecond Pulses," FTD-HC-23-643-70, Foreign Technology Division, Wright Patterson Air Force Base (March 1971).

[7] Toepler, M., "Zur Bestimmung der Funkenkonstante," Archiv Fur Elektrotechnik, Vol. XVIII, p. 549 (1927).

[8] Weizel, W. and Rompe, R., Theorie Elektrischer Lichtbogen und Funken, Leipzig Johann Ambrosius Barth Verlag (1949).

[9] Vlastos, A.E. "The Channel Resistance of Sparks," IEE Gas Discharges Conference Proceedings, pp. 31-34 (Sept. 1970).


## Acknowledgment

This work was supported by the Air Force Office of Scientific Research and the Army Research Office.

END

4-87

DTIC